Sugar Research Australia

FINAL REPORT 2016/952

Understanding interactions between basecutters and other forward-feed components with the cane stalk and determining practical strategies to minimise damage as harvester speed increases

FINAL REPORT PREPARED BY	Chris Norris and Floren Plaza
CHIEF INVESTIGATOR(S)	Chris Norris (NorrisECT) and Floren Plaza (QUT)
RESEARCH ORGANISATIONS	Norris Energy Crop Technology, Queensland University of Technology
CO-FUNDER	Australian Department of Agriculture, Water and the Environment
DATE	2 April 2020
KEY FOCUS AREA (KFA)	4. Farming systems and harvesting

NORRIS Energy Crop Technology

QUT

Sugar Research Australia

Australian Government
Department of Agriculture, Water and the Environment

Please cite as: Norris, C. and Plaza, F. (2020) Understanding interactions between basecutters and other forward-feed components with the cane stalk and determining practical strategies to minimise damage as harvester speed increases: Final Report Project 2016/952. Sugar Research Australia Limited, Brisbane.

ABSTRACT

To constrain Industry costs, harvesting speed has continually increased, made possible by increases in harvester throughput. Despite this, there is little understanding of the interactions between the harvester's 'front end' components and the cane plant. Ratoon damage is now a widely identified challenge associated with machine harvesting of sugarcane. The original project hypothesis was that it would be possible to reduce ratoon damage by optimising and matching harvester component speeds to ground speed. This would then also facilitate developments in machine component design.

Multi-factorial field observation trials were conducted with five modified harvesters at six trial sites and multiple treatments over 3 years. Computational modelling was conducted in parallel. The project demonstrated that damage to the crop stool by the harvester is substantial, and this can be anticipated to adversely impact on ratooning. Gathering, feeding and basecutting functions all contribute to this damage. Matching speeds of gathering and cutting components did not significantly reduce damage, but did qualitatively improve machine performance, particularly in heavier crops. Outputs of the parallel Finite Element Modelling and analysis proved beneficial in gaining an understanding of the mechanisms by which the observed damage was occurring.

Modifications to reduce aggressiveness of knockdown appeared to significantly reduce damage (improve ratoon yields), however significant further work is required to arrive at a commercially viable industry solution.

Assuming a conservative 10% potential ratoon yield increase by reducing knockdown damage, the potential benefit to the Australian industry could be readily expected to exceed 2 million tonnes of cane per year, or in the order of $100 million annually in total industry value at current sugar prices.

EXECUTIVE SUMMARY

Issue and objectives:

Increasing harvesting speed has been necessary to facilitate the large increases in productivity required by the harvesting fleet to manage sugarcane industry cost pressures. Whilst the power and processing throughput of the harvesters has been able to easily meet this requirement, the design of the 'front end' of the harvesters has undergone relatively little functional change since the initial development over 50 years ago. There has been little attempt to improve the interactions between harvester front-end components and the cane plant with respect to damage caused by the gathering, knockdown and basecutting operations. This is a contributor to poor ratoon performance often seen through the industry, impacting on ratoon cycle economics.

Linking rotational speeds of basecutters and gathering/forward feed components to groundspeed was hypothesised to improve machine performance and minimise damage over a much wider operating speed range than with current machines. Additional gains could then also be achieved by the active optimisation of the design of the front end of the harvester, through the modelling of the interactions between the cane stalk and machine components.

R&D methodology:

Five harvesters, operating between Ingham and Condong, were modified to link forward component tip speeds to groundspeed. A multi-factorial replicated trial program was then undertaken to assess the impact of machine operating parameters on damage to the cane stalk (billet damage), damage to the cane stool, ratoon crop emergence and subsequent crop yield. Simultaneously, a modelling program was commenced to develop an understanding of the dynamic structure of the sugarcane stalk, to allow assessment of changing machine parameters on stalk damage.

The field trial layout was three replicates of four randomised treatments. Each plot was typically four rows wide and the area harvested per treatment was 0.3 to 0.5 ha, or 3.6 to 6 ha for the whole trial. Stalk damage was assessed by sorting of harvested billets, with particular attention to assess the characteristics of the observed damage to allow the primary source of the damage/mutilation to be identified and recorded. Damage to the plant stool was assessed by establishing semi-permanent sub-plots immediately after the first harvest. Protocols developed in previous research were utilised. After crop emergence, plant counts, plant height assessment and biomass assessment were typically undertaken. Prior to the subsequent harvest, stalk numbers in the sub-plots were assessed.

This work involved active collaboration with the grower, the harvesting team, and the mill, as well as local extension staff.

Project outputs:

The project has clearly illustrated that the design of the front end of current harvesters is resulting in very high levels of damage to the crop being harvested, reducing the yield potential for ratoon crops, and harming Industry profitability. Across the thirteen field trials conducted, over 75% and up to 100% of the cane stumps had suffered clearly identifiable damage, with major damage sometimes exceeding 60%.

The field trial program was modified to include sub-treatments which allowed the separation of the impact of the full harvesting process from "basecutting only". This demonstrated that approximately half of the total damage occurs before the basecutters contact the cane stalk. Eliminating the initial forward-feeding damage resulted in reduced ratoon shoot numbers, but improved ratoon growth

(biomass production) and an average yield increase of greater than 12% over the 60 paired sub-plots.

Whilst the modifications undertaken to the machines for the trials to match forward speed and rotational speed of key components did improve machine operational performance, particularly in larger crops, only limited positive impact on damage and subsequent yield was noted. More significant machine modifications reduced damage but further development is necessary before such modifications could be commercialised.

Processes, practices, products and/or technology

The project directly led to the development of functional guidelines for the technology for linking the rotational speed of key components to groundspeed. The field experience with the machines showed that active feedback on the rotational speed of all components, rather than "open loop" control, is necessary to achieve satisfactory speed control because of the high variability in load.

The development of the matched component speed in conjunction with gathering fronts of optimised design resulted in very significant improvements in observed performance of machines in very large crops. Modifications of a commercial machine to reduce the aggressiveness of the pre-basecutting knockdown demonstrated very much reduced damage to the cane stalk relative to a standard commercial machine.

The modelling component of the project introduced the LS-DYNA structural analysis software into the Australian sugar industry in a first application. The software has capabilities not seen before in other structural software, and in a single well-integrated package. In particular, it has the ability to model in real time a relatively fast process in which there are large strains, damage, failure, contact and friction, in geometrically complicated moving and rotating equipment.

The project has identified significant deficiencies in the geometry of the current feeding system and proposed detailed geometry design modifications to the cane harvester. A capability tool has been developed using the LS-DYNA software to combine modifications and predict likely results, minimizing the need for physical manufacture of prototypes.

The outcomes and implications of the project findings on the sugar industry and the Australian community.

The project has demonstrated that front-end damage is a real issue for the Industry, with potential gains from reduced front-end damage to the harvested crop being in the order of 15% in ratoon yield. This demonstrably also impacts on economic ratoon cycle life, with financial and environmental implications.

The project also Identified that "slowing down" alone is not a viable solution to stool damage with standard harvester configurations, as little benefit accrued, however lower harvesting speeds in conjunction with component speeds matched to groundspeed both improved machine functionality in larger crops and reduced damage to the crop stool. Modifications to gathering spiral design in conjunction with matching of component speeds to groundspeed in an optimal relationship offers both capacity to harvest larger crops unburned at commercially viable speeds and reduce billet damage.

By demonstrating the magnitude of the issues, appropriate strategies can be developed to minimise this very significant source of losses. The combination of further development of modelling of machine-cane interactions and physical trials with modified machines offers the potential to be able

to develop retro-fit modifications to machines which can both significantly reduce the current damage levels to the crop and improve machine functional performance.

The project also facilitated the introduction of powerful new software for analysis of machine /cane interactions. This can potentially be used in a range of harvester /crop interaction applications.

TABLE OF CONTENTS

TABLE OF TABLES

TABLE OF FIGURES

1. BACKGROUND

1.1. Harvester Technology Development

The technological breakthrough that allowed the successful development of the chopper harvester was the aligning and pushing over of the cane stalk prior to the basecutting operation, allowing the cane to then be fed base-first into the harvester feedtrain (Spargo & Baxter, 1974). This led to levels of machine operational functionality that facilitated the widespread adoption of chopper harvesting as the preferred method of mechanically harvesting sugar cane. Since this initial development of modern chopper harvesters around 60 years ago, machine performance and harvesting speeds have continually increased to facilitate ever-increasing machine productivity.

Whilst the decline in the value of the Australian Dollar boosts the value of the Australian crop to growers, harvesters and tractors are fully imported and their prices are rising. The cost of a new harvester has increased by more than 60% relative to the time of the high Australian Dollar, and this continues to drive the harvesting sector to maximise machine productivity in the field conditions presented. Harvesting speed is one of few available strategies to manage increasing harvesting costs in Australia, as there is little potential to increase productivity by increasing effective machine operating width. This is because of machinery width restrictions associated with travel on public roads.

Over the past two decades, the number of harvesters operating in some areas of the Australian industry has decreased by 50% (Anon, 2014), driving a significant increase in area harvested per machine per day, and an associated increase in harvesting speed. Unless current harvester speed can be maintained or ideally, further increased, harvesting costs will have to significantly increase to maintain viability of the harvesting sector.

Guidance and steering technologies such as GPS Autosteer have facilitated higher harvesting speeds whilst maintaining aspects of the 'quality of job' by maintaining correct positioning of the harvester over the crop row and allowing the operator to give greater focus to aspects such as basecutter height setting, topping and bin filling. This has reduced these factors as limitations on potential harvesting speeds but exacerbated the issue of machine-crop interactions during gathering, feeding and basecutting, as well as increasing probable damage associated with errant haulout traffic damage.

GPS guidance systems on both crop production machinery and harvesters mean that optimum placement of the machine with respect to the crop row profile is possible at the high operating speeds common in today's industry. Similarly, both major manufacturers are continually upgrading the performance of their respective Automatic Basecutter Height Control systems. The Industry has largely adopted GPS guidance technology for crop cultural operations, a pre-requisite for effective use of the systems on harvesters. Industry adoption of GPS on haulage units has been miniscule, despite the damage caused by these units during harvest.

1.1.1. Past Research

The impact of harvester 'front end' (gathering, feeding and basecutting) design on the quality of product produced and the damage caused by the harvesting operation on the ratooning crop in different field conditions is of significant interest to the industry. Fuelling (1980) noted that crop presentation impacted on the damage levels of harvested billets, as well as soil in cane. Schembri

and Garson (1996) noted that, as crop presentation became more lodged, the evenness of feed through the machine deteriorated. Norris *et al.* (1998) compared two harvesters with different 'front-end' configurations in lodged crops ranging from 100 t/ha to 185 t/ha at sites from Mulgrave to the Burdekin. As crop size increased, the evenness of feed deteriorated and the proportion of sound billets off the 'standard' harvester (a near-new Austoft 7000) fell from 40-45% in the lightest crop to 25-30% in the heaviest crop. The alternative harvester, a prototype machine that had been developed by Massey Ferguson prior to their closing, showed a similar trend; however, much lower levels of billet damage were observed under all conditions. This indicated that the design of the harvester front end significantly impacts on harvesting performance and damage to the harvested crop, particularly as the crop becomes more lodged. No formal assessment was done of stool damage or ratooning, although limited counts indicated fewer larger ratoon shoots in the MF-harvested plots (Davis & Norris, 2000). In the light of subsequent findings, this effect was consistent with less stool damage being caused by the prototype machine.

Further work (Davis & Norris, 2002) discussed the performance of a harvester which had been modified to accept interchangeable front-end modules. The front-end geometry of this machine complied with the recommendations of Kroes and Harris (1996) with respect to the maximum cane stalk deflection by the harvester knockdown system prior to basecutting, and all front-end systems had rotational speed linked to groundspeed. The modules developed demonstrated both exceptional gathering and feeding performance and low levels of stalk damage. Despite this, there was little commercial interest in the development, primarily because the design "moved away" from common norms and would have required significant re-engineering of the machine designs. There was little pressure from customers to address a problem which they, at that stage, were not aware existed.

Some of the earliest work by Kroes and Harris (1994) identified that several different modes of damage occur during the severing of cane stalks by the basecutters. The resulting losses are impacted differently by the relationship between basecutter rotational speed and groundspeed, although, even at the optimum operating point, losses are significant.

Work by others indicated that changes to blade geometry can reduce these losses (Harris & da Cunah Mello, 1999); however, the maximum benefit can be strongly argued to be achieved when basecutter speed and machine forward speed are matched. To date, the increase in cost and reduced operating life expectancy of proposed blade shapes meant that little commercial interest has developed.

At typical current harvesting speeds, the interactions between the basecutter components and the cane stool are well outside the optimum range. The impact of harvester speed and harvester pour rate on subsequent block yield has been analysed by Sefton (Anon, 2014) using large datasets from both Ingham and Burdekin areas. This data strongly correlated decreasing ratoon yield with increasing harvesting speed, but more significant was the relationship between harvester pour rate and yield depression. This implies crop size and gathering effects are important with respect to outcomes, confirming both the gathering & feeding processes and the basecutters inflict substantial stalk damage. This then impacts on both immediate losses (juice losses, increased extractor losses of damaged/part billets) and increased deterioration, as well as on stool damage and losses in the subsequent crop.

Kroes and Harris (1997) developed guidelines for minimising basecutter damage by defining the optimum rotational speed and basecutter configuration at a nominated forward speed. Whiteing and Kingston (2008), utilising a harvester in which the basecutters and front-end components were

linked to groundspeed, achieved good results. That research focused on reducing damage and losses at speeds significantly lower than current operations.

More recently, trials have been conducted looking at the impact of harvesting speed on ratoon performance using standard commercial machines. In the Burdekin, Milla (2017) found no correlation between harvesting speed and ratoon performance. McBean and Rose (2017) in northern New South Wales also found minimal effect. The results of these trials indicate the complexity of the issues, particularly compared with the results of large data-set analysis of Sefton.

1.1.2.Significance to Industry

As previously noted, the kinematics of the harvester basecutters has not significantly changed over the past 45 years. Kroes (1996) identified that several different modes of damage occur during the severing of cane stalks by the basecutters during normal machine operation, and all modes of damage are observable in the field (Hurney, et al., 2005) The type of damage is impacted on differently by the relationship between basecutter rotational speed and groundspeed although, even at the optimum operating point, damage is still significant. Kroes estimated that additional direct and indirect losses from basecutter damage to the stalk through reduced billet quality and increased chopper and extractor losses to be up to 7%.

Significantly, damage observed to the above-ground cane stalk components can be anticipated to be reflected in below-ground damage. Hurney *et al.* (2005) reviewed trials on the impact of basecutter damage on ratoon growth and subsequent yield and found this to be a significant issue. Observations by Australian farmers are that sections of fields harvested at low speed with harvesters setup for cutting plants then ratoon significantly more aggressively than adjacent sections of the same field harvested commercially. This occurs even if both operations are undertaken within a similar time frame. “Wholestalk” plant cutters hold the cane stalk erect during the basecutting process and there is little opportunity for stool damage. Seedcane chopper harvesters, apart from typically operating at low forward speed, usually have the forward feeding rollers re-configured to give much less aggressive feed into the throat of the harvester.

Norris *et al.* (2015) reported that a significant component of their international consulting relates to the higher rate of ratoon yield decline in machine-harvested fields relative to manually harvested fields, with many clients observing the rate of yield decline with machine harvesting being over twice that observed with manual harvesting.

Many trials have been conducted to assess the impact of basecutter blade parameters on crop ratooning. Hurney *et al.* (2005) observed that much of the reduction in ratoon stand associated with basecutter damage was caused by pathogens which utilised the physical damage of the stool as an entry point. Irrespective of the process, yield loss associated with the harvesting process is often highly variable but can be severe. In one trial reviewed, there was a 34 t/ha difference in yield between plots cut with new v’s worn blades. Hurney also reported on a trial which identified harvester speed as a factor in ratooning performance, with minimum damage being recorded at a speed of 6 km/hr (matching the standard basecutter speed of 640 rpm under Kroes’ relationship (1997)) and damage increasing above and below this speed. This is consistent with expectations relating to damage, both with respect to the interactions between gathering components and the cane stalk and the basecutters and the cane stalk and stool. The magnitude of the observed effect on yield in these trials indicates that disease pressure must have been high for the observed changes in damage to be exploited (by pathogens) and result in the measured yield changes. Whilst damage was therefore not the ultimate cause of the yield reduction, it enabled the outcome.

1.1.3. Developments on previous research

Kroes (1997) developed guidelines for minimising basecutter damage by defining the optimum rotational speed and basecutter configuration at a nominated forward speed. This research indicated that at lower groundspeeds the basecutter rotational speed on harvesters was too high, and this resulted in higher than necessary levels of stool damage. Conversely, as harvesting speeds increased the mode of damage changed, and again damage increased. Kroes hypothesised that, for then-current basecutters, there was a minimum basecutter speed which should be utilised up to a set forward speed, and, as forward speed increased above this, basecutter RPM should increase proportionally. The actual optimum relationships depended on a number of parameters including number and length of basecutter blades and cane stalk diameter. Research by Whiteing and Kingston (2008), utilising a harvester in which the basecutter RPM was were linked to groundspeed according to Kroes's guidelines, achieved good results, however this research focused on reducing damage and losses at speeds significantly lower than current operations.

The shape of basecutter blades and mounting configuration can also be argued to be sub-optimal, particularly at higher speeds. The current design, which has been in use for over 45 years, was developed on the basis of cost and durability, not the machine-crop interactions. Interestingly, the early harvesters utilised a basecutter blade design which, when new, would have been clearly superior to current designs. Harris and da Cunah Mello (1999) undertook an investigation into basecutter blade shape and in trials demonstrated benefit from alternative designs, however Industry interest was limited at the time.

More recently, the issue of the impact of the harvesting process on crop ratooning has become recognized as a major issue, primarily because of the availability of data from the harvester logging systems being adopted across the Industry (Anon, 2014). These systems allow harvesting speed to be logged as the harvesting operation progresses throughout the field. The magnitude of the decline in yield of the field in the following year can be correlated against average harvesting speed and derived parameters such as pour rate (the product of crop size and harvesting speed). Analysis of data from several mill areas by Sefton, as reported in Anon (2014) has demonstrated a very strong trend linking both harvesting pour rate and harvesting speed with accelerated yield decline. Data trends indicate either harvesting speeds in the range of 10-12 km/hr or harvester pour rates greater than 140 t/hr can result in yield depression of over 40% relative to lower harvesting speeds. These performance points are now well within the common envelope of harvester operation. This very strong observed relationship between pour rate and accelerated yield decline can be seen to relate strongly to gathering and aligning damage in addition to the basecutter damage effects which could be anticipated to be primarily forward-speed related. The impact of forward speed on gathering and aligning damage relates to the momentum effects related to change in alignment and also the forces associated with anchoring the stalk in the stool whilst this alignment occurs.

1.1.4. Machine design considerations

Both gathering and aligning the crop and basecutting are physical operations, which can be achieved with minimal damage over a potentially wide range of forward speeds, assuming appropriate machine design. Significantly, both the basecutters and forward-feed components have evolved into designs which can be argued to function moderately well operationally over a moderate speed range. There is clear evidence that damage and losses are higher than necessary across the entire operating range, with the most dramatic effects being at the higher harvesting speeds now deemed necessary by the industry for commercial reasons. Damage and losses do increase, however at lower harvesting speeds in large crops.

Analysis of the interactions between the gathering spirals and the cane, for example, indicates that aspects of the current front end design are optimised for widely disparate harvesting forward speeds (Davis & Norris, 2000). The wrap of the spirals is optimised for low forward speeds, consequently, as harvesting speed increases, non-optimum spiral geometry and speed are likely to hold back the cane as it is fed into the throat of the harvester. Typical spiral diameters and rotational speed are inappropriate at lower harvesting speeds. Components such as knockdown rollers tend to operate at excessively high tip speeds at low forward speed, resulting in unnecessary stalk damage by "force feeding" the cane stalk before basecutting. The linking of forward feed components of the harvester to groundspeed would allow a systematic process of optimisation of component speeds and component design.

Similarly, the design of the basecutters has evolved slowly, with manufacturers increasing rotational speed to partially compensate for increasing forward speeds. This, however, adversely impacts on losses and stool damage at lower groundspeeds (Kroes, 1997). Trials at Tully (Di Bella, et al., 1997), using a harvester with adjustable base-cutter speed, demonstrated a reduction in soil in cane of approximately 50% where basecutter RPM was matched to groundspeed within the Kroes guidelines relative to the "standard" RPM setting.

The matching of the basecutter and the gathering and forward-feed components to groundspeed is an essential development to facilitate the capacity of harvesters to operate at higher speeds to manage harvesting costs. With appropriate engineering, it is anticipated that actual machine performance will improve across the full operating speed range.

Davis and Norris (2002) demonstrated that improvements in front end configuration of the harvester improved both feeding performance (and evenness of material flow through the feedtrain of the harvester) and billet quality in lodged crops. The linking of forward-feed component RPM to harvesting speed will allow further significant development. Similarly, work by other researchers (Harris & da Cunah Mello, 1999) indicated that changes to blade geometry can reduce these losses, however the maximum benefit is only achieved when basecutter speed and machine forward speed are matched. To date, the increase in cost and reduced operating life expectancy of proposed blade shapes meant that little commercial interest has developed. The increase in harvesting speeds means that this is now an area where further research, based on the assumption of basecutter speed being linked to forward speed, is appropriate.

1.1.5. Modelling machine cane interface and impact on damage

Whilst measured cane damage has been linked to basecutter kinematics (Kroes & Harris, 1994, 1997; Harris & da Cunah Mello, 1999) and blade geometry (Harris & da Cunah Mello, 1999), it has not yet been adequately linked to the measured cutting forces (Kroes, 1997) and cane material properties to understand how cane will respond to changes in the design of front end components, including basecutters.

One of the main barriers to the use of FEM has in the past been the simulation time associated with the modelling of multiple interacting particles. DEM and FEM techniques and computer speed have advanced significantly in the last ten years to the extent that proprietary modelling software is able to provide a full dynamic simulation of the interaction in the basecutter region between the harvester components and cane material. Such a model would provide critical insights into the mechanisms of cane damage associated with current basecutter design as well as providing a powerful engineering tool for the development of improved low cane loss technology.

1.2. Linkages to past research

This project aimed to draw heavily on the previous research into harvester front end design, including the research on basecutter operating parameters and blade design in several ways.

Machines have previously been designed to comply with the Kroes recommendations and have demonstrated the ability to successfully feed large crops. An example of this was the Massey Ferguson 405 prototype machine, developed in the early 1980s. Whilst pre-dating the work of Kroes, the designers recognised the need to minimise knockdown prior to basecutting to minimise damage to the cane stool. The R&D documents including technical argument for the radical machine layout were able to be accessed by Norris & Davis (2000), who noted "the machine was designed to give a ground-job similar to hand cutting. The front-end layout for that machine is shown in Figure 1.

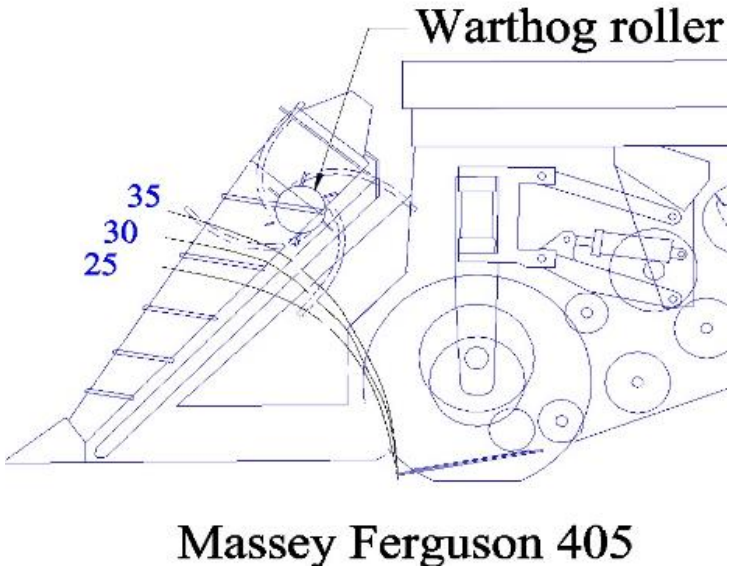

Figure 1: Forward feed configuration of the MF 405 prototype.

The 405 had a large diameter feeding roller on top of the basecutters to achieve aggressive feed after the stalk had been cut. Comparative trials with this machine and an Austoft 7000 harvester indicated fewer but larger emerging shoots after harvest. The comparative treatments were not followed through to subsequent yield, however based on the findings of the current project, it is anticipated that the ratooning crop would have had higher biomass, flowing through to increased subsequent yields.

Further work (Davis & Norris, 2002) was used in the development of the "BSES High Density Harvester" (Figure 2) and the harvesters which were developed after it in the "Enhanced Feeding of Green Cane" project suite deliberately complied with the Kroes recommendations. These harvesters also had additional aggressive feed over the basecutters and achieved noticeably low levels of stool damage whilst also having impressive gathering and feeding performance.

Davis and Schembri (2004) developed initial models to look at the behaviour of cane stalks as they crossed the basecutters and entered the throat of the harvester.

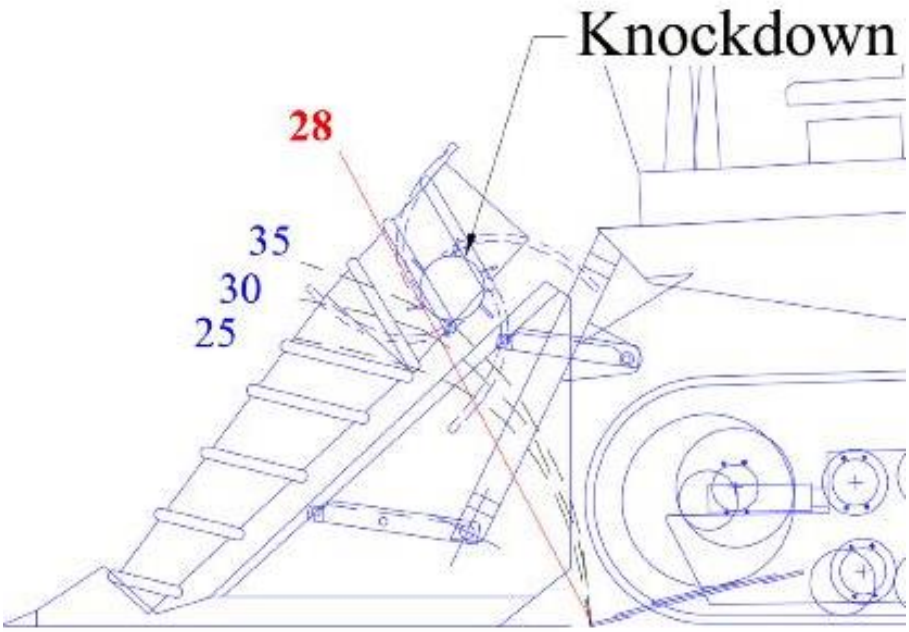

Figure 2: The BSES "high density" harvester and the "front end" developed under subsequent programs also complied with the Kroes recommendations.

The MF 405 prototype (Figure 1) developed in the late 1970s had very moderate knockdown and the cane stalk deflection was within the (yet to be developed) Kroes recommendations.

1.2.1. Linking component speeds to groundspeed

During the research into “Improved Feeding of Green Cane” and follow-on research, the BSES-developed “Modular Front End” Harvester was set up to have the rotational speed of the spirals, forward feed components and basecutters linked to groundspeed.

To achieve this, the basecutters were driven on a dedicated closed loop system, allowing speed to be modulated. A speed sensor was fitted to the basecutter gearbox to allow speed to be monitored and controlled.

The rotational speed of the spirals and the forward feed rollers were controlled as individual groups of components. The oil control strategy utilised was to control the oil flow to the circuit with high flow solenoid-controlled valve blocks. Because of the magnitude of oil flow through this system, high power solenoids were required and an associated modulated power supply system. The system was initially problematic but was able to be developed to be fully functional. Whilst the system worked well, a major disadvantage was that any failure in the system resulted in the closedown of that harvesting function. It was considered that a better strategy would be “fail safe” at maximum component speeds.

1.2.2. Field trials of linked component speeds

The field trialling on a commercial scale of linking basecutter rotational speed and gathering and feeding component rotational speed to harvester forward speed was the adoption of specific recommendations of previous research.

The impact of this machine modification on cane and stool damage was assessed in a series of field trials by Whiteing and Kingston (2008). The focus of their work was harvesting speeds which were

much slower than typical current harvesting speeds. They found statistically significant improvements in crop regrowth and yield, however the magnitude of the gains was relatively small (<10%)

1.2.3. Development of machine components for matched groundspeed operation

The linking of forward feed and basecutter components was argued to allow further optimisation of speeds and design configuration of key machine elements. The aim was to draw heavily on the research of Davis & Norris (2000, 2002).

1.2.4. Modelling of the fundamental machine -cane interactions

The review of the fundamental interactions between the cane plant and the basecutter system was also planned to draw heavily on the work of Kroes and da Cuna Mello. In conjunction with the application of the technology to link harvester component speeds, significant advances in blade configuration were seen as viable.

2. PROJECT OBJECTIVES

2.1. Project Organisation

The project was organised to incorporate two research streams, with a common goal.

2.1.1. Stream 1

Stream 1 was the field-based components of the project. It aimed to develop and install equipment on commercial harvesters to facilitate and evaluate the benefits of adoption of currently adoptable knowledge relating to reduced crop damage during gathering, feeding and basecutting by:

- Modifying hydraulic and electric systems to allow linking of both basecutter speed and the rotational speed of forward-feed components (knockdown and finned rollers) to groundspeed, based on currently understood guidelines for minimum damage;
- Undertaking field trials where the impact of this variable speed system on harvesting losses, cane quality and crop ratooning performance can be quantified under different harvesting and field conditions; and
- Determining the robustness of the current machine components (e.g. basecutter box) for handling increased speeds and determine modifications needed to retain an economic life from the unit.

This component of the project was undertaken by NorrisECT, with assistance from co-operating harvesting groups and growers.

2.1.2.Stream 2

Stream 2 of the project aimed to use computational modelling to develop an improved design of the harvester basecutter to minimise damage to the cane stool, including, but not be limited to:

- changes in number of blades, blade shape/design and blade mounting configuration to optimise the actual cutting action and minimise stool and stalk damage when operating within optimised speed parameters; and
- further develop optimisation guidelines relating to the relationships between harvesting groundspeed and components (gathering system and basecutter component rotational speeds).

This component of the project was undertaken by QUT.

3. Outputs, Outcomes and Implications

3.1. Outputs

The ultimate output of this project has been a greater understanding and initial quantification of the sources and associated magnitude of harvester-related ratoon yield depression. The project established that there are multiple mechanisms by which modern harvesters lead to depressed ratoon yields through damage to the standing stool at the time of harvest, and that there also exist promising strategies (design changes) to overcome these mechanisms and ultimately realise better ratoon yield performance than the industry currently experiences.

The developments that have contributed to this overall output include:

- Computational modelling (FEM) that has facilitated a greater understanding of the exact mechanisms that cause the damage observed in field trials; and

- A series of field trials over multiple ratoons with modified harvesters that have generated a significant body of data on the impact of modern harvester components on future yields.

3.2. Outcomes and Implications

The project has identified opportunities to improve ratoon yields by significant margins, conservatively greater than 10% annually over the ratoon cycle, although further work is required in order to arrive at readily adoptable solutions.

Based on prior experience of the project team, it is likely that the solutions that will allow the industry to realise these gains are able to be developed, deployed and adopted within the Australian industry (i.e. modifications to existing commercial machines), without the requirement to engage with the international harvester manufacturers. The anticipated cost of the solution to a harvesting group in Australia would be readily covered by the reduction in yield decline experienced by that group, and as such the outcome of this project is of high value to the Australian industry.

Assuming a conservative 10% potential ratoon yield increase by reducing knockdown damage, the potential benefit to the Australian industry could be readily expected to exceed 2 million tonnes of cane per year, or in the order of $100 million annually in total industry value at current sugar prices

4. INDUSTRY COMMUNICATION AND ENGAGEMENT

4.1. Industry engagement during course of project

Industry engagement during the course of the project was regular feedback to the Research Management Group (RMG), regular communication with the SRA Harvesting Adoption group, and annual attendances at the SRA Harvesting forums. Further, the project itself required ongoing collaboration with a number of industry participants (growers, mills and harvesters), who had ongoing visibility of project developments.

4.2. Industry communication messages

The key industry messages from this project are that:

- The interactions between the gathering, feeding and basecutting components in a modern sugarcane harvester are responsible for significant levels of damage to both the harvested stalk and the crop stool, under all harvesting scenarios investigated.
- Adjusting the rotational speed of these machine components had limited impact on the level of damage to both billets and the stool, although some benefits were noted relating to evenness of feed and ability to harvest larger crops.
- The high levels of damage are primarily associated with the configuration of the key harvester components, as approximately half of the observed damage related to the aggressive manipulation of the crop prior to the basecutting function.
- Changing operating parameters alone had little impact on observed damage, or on subsequent yield.
- Reducing stool loss and stool damage by eliminating the damage associated with the gathering and knockdown functions resulted in lower ratoon shoot numbers but higher total biomass accumulation, higher pre-harvest counts of millable stool and higher yield.
- The re-design of the “front end” of the harvester to minimise damage during the harvesting operation appears likely to offer potential ratoon yield increases of > 10%. Such a modification is a one-off, not a recurring cost.

While it is understood that the front end design of modern harvesters has evolved as it has to allow reliable harvesting of large crops, the side effect of this evolution is high levels of damage both to the harvested crop and the remaining stool. This damage then has a negative impact on ratoon yields.

Previous work by others as well as the findings of this project suggest that reliable feeding of large crops can be achieved with much lower levels of damage by designing the harvester front end with greater attention to optimising machine/crop interaction. Key aspects of the findings of this project would facilitate this.

5. METHODOLOGY

5.1. Overview

The project was carried out in two parallel steams over a number of distinct phases, commencing with the execution of the funding agreement between NorrisECT, QUT and SRA in July 2016 (Milestone 1).

The two streams were:

- **Steam 1** – Machine modifications and field trials. This stream consisted of a series of field trials designed to allow the observation of the actual impact of various changes in harvester operation and configuration; and
- **Stream 2** – Modelling. This steam focussed on developing computer models of the cane stalk and machinery in order to allow the plant/machine interaction to be simulated and the impact of changes in this interaction due to changes in machine configuration or operation to be predicted.

The methodology of the two streams is described below.

5.2. Stream 1 – Machine modifications and field trials

5.2.1. Development of a database relating to key geometries and tip speeds of harvester components.

Key dimensions and rotational speeds of the relevant gathering, feeding and basecutting components were measured and recorded for the most common machines in use in the Australian sugar Industry. The machines for which the data was collected included:

- "Series 1" Case 7000/7700 harvesters (pre-1996 manufacture);
- "Series 2" Case 7000/7700 harvesters (post-1996 manufacture);
- Case 8000/8800 harvesters;
- Cameco 2500 harvesters, wheeled and tracked;
- John Deere 3520 harvesters, wheeled and tracked;
- John Deere CH 570 harvesters, wheeled and tracked.

This library of data was essential to allow initial modelling of the interactions between these components and the cane crop, and an understanding of the associated velocity relationships. This was to facilitate the development of the models for Stream 2 of the project. The information on speeds and geometry was also utilised to select the target relationships between component RPM and harvester groundspeed.

5.3. Current Harvester Component Speed Configurations.

5.3.1. JD 3520 Harvester Hydraulic System

The 'ex-factory' relationship between component speed and groundspeed for the JD machines is illustrated in Figure 3. This indicates that the forward feed components generally have tip speeds in the range of seven km/hr to nine km/hr. Simple spreadsheet analysis allows the relationship to be described between component tip speed and the velocity at which the cane stalk moved past the roller surface as the harvester moves forward. This analysis indicates that the optimum tip speeds of forward feed rollers should generally be below groundspeed, and the spirals' tip speed at approximately groundspeed. In the absence of further information, the relationships between

component tip speed and groundspeed, as indicated in Figure 3, were targeted in the modification to the harvester hydraulic systems, as shown in Figure 4.

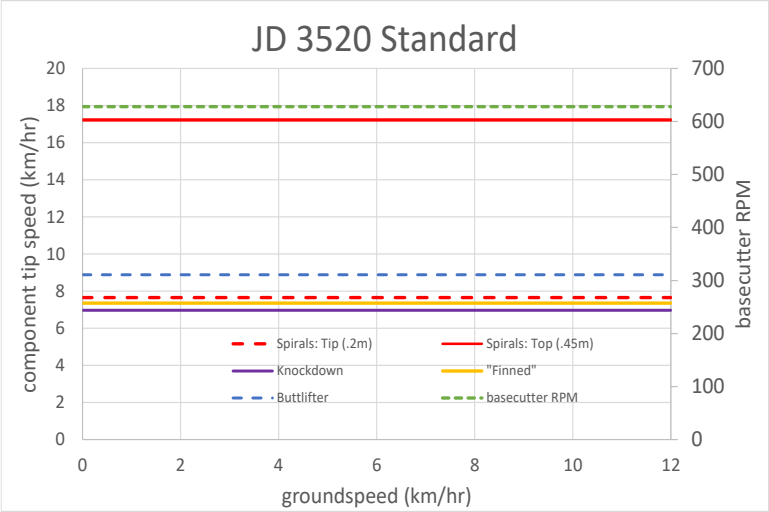

Figure 3: Component tip speeds for JD 3520 harvester in standard configuration.

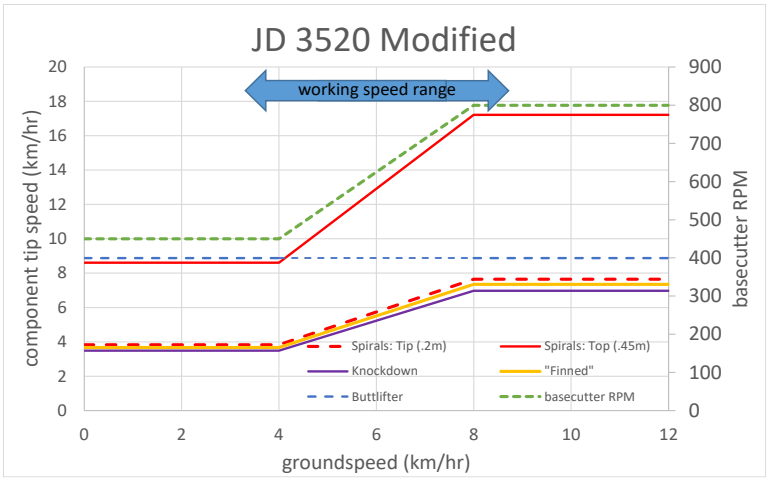

Figure 4: Target component tip speeds and basecutter RPM for the modified machines.

5.4. Design of Harvester Modifications.

5.4.1. Overview of JD 3520 Harvester Hydraulic System

The engine-driven hydraulic power pack on the JD 3520 harvesters utilises:

- Two variable displacement pumps for the machine traction,
- Three variable displacement pumps supplying oil for the choppers, basecutter and primary extractor. The variable displacement function is used for the primary extractor, however the basecutter and chopper units are configured to operate at maximum flow, with electrical activation of the control module to achieve component reverse to clear machine chokes.
- Eight fixed displacement pumps which drive the remaining machine functions such as gathering, forward feed, feedtrain, elevator etc. These units are controlled by a servo-controlled valve banks. All functions are fixed speed, with a reversing function incorporated into the valve banks. The flow from each of these pumps was in the range of 122 to 76 l/min (32 to 20 US gpm).

5.4.2. System design to control Basecutter and Forward Feed Component Speeds: JD 3520 Harvesters.

Childers Machine (Central Harvesting)

Prior to the project, two of the harvesters operated by Central Harvesting at Childers had been modified to increase basecutter speed. The 100^{cc} motor fitted to drive the basecutters was replaced with a 71^{cc} unit, as used on later model machines. Whilst the standard basecutter speed is approximately 620 RPM, the changed motor specification gave a maximum basecutter speed of 880 rpm, an increase of 42%.

To control the basecutter speed, a simple electrical circuit using a potentiometer to vary the current supply to the controller on the pump was fitted, allowing the speed to be varied from zero to maximum. This control system was however “open loop” so as load changed on the basecutters, speed also varied.

“Standard practice” by operators was to run at maximum basecutter speed, irrespective of the actual harvesting speed.

After consultation with different hydraulic suppliers, a control system for basecutter speed utilising a Hydraforce ECDR-0506A controller was selected (Figure 5). Initial programming was undertaken by the technical support group in New Zealand of the Brisbane branch of *Hyspecs*. Several difficulties were encountered in the fitting and commissioning of the unit, involving a degree of re-programming. During the project, the control system allowed:

- The ratio between groundspeed and basecutter RPM to be selected via an external potentiometer, and
- A minimum basecutter speed, to allow effective basecutting during initial end of row harvesting and when harvesting at low forward speeds. This was also set via an external potentiometer.

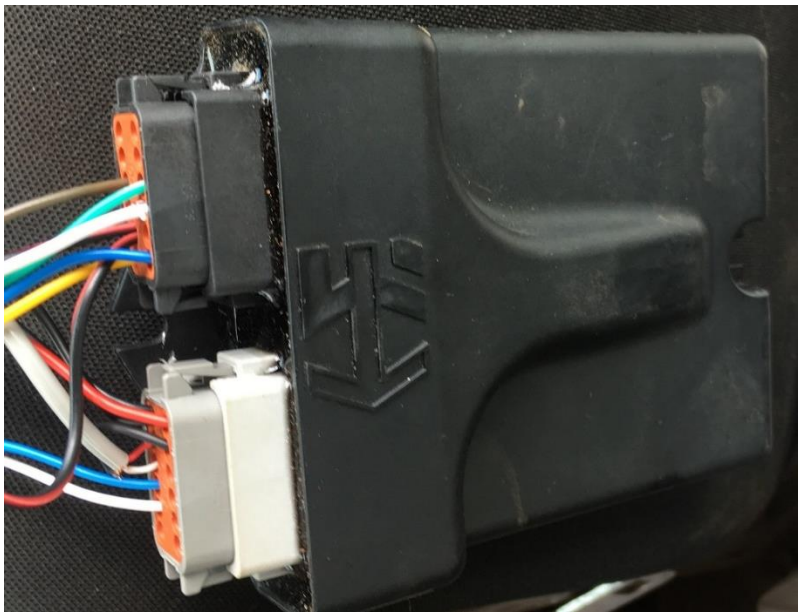

Figure 5: Electronic control unit (Hydraforce ECDR-0506) installed to control basecutter speed, spiral speed, and forward feed roller speed.

Several modifications were made to the control circuit and program to better integrate the unit and make operation “user friendly”.

Hyspecs also assisted in the initial design of the hydraulic and electrical circuits to control the speed of gathering and forward feed components. Each of these are on individual hydraulic circuits. The operational requirements of hydraulic circuits on a sugarcane harvester are different to most industrial applications, and different but cost-effective and stable control strategies are required, along with appropriate failsafe mechanisms. The design of the system required failsafe mechanisms to ensure that basecutters would operate at maximum speed in the event the control system failed. The range of RPM over which stable speed control is required significantly impacts on the circuit design. As the hydraulic systems are “open circuit architecture” heat generation is also an issue.

The initial concepts compared included:

- Manufacturing new manifold blocks to allow the inclusion of pressure-compensated bleed-off of the oil supply to the hydraulic motors. RPM of the motors was measured and used as the feedback input; This was the strategy utilised on the BSES modular harvester.
- Controlling the spool position of the main control valve, again with feedback being component RPM. This strategy is made more complex because the spool in the main control valve is pilot-operated.
- Controlling only the driver current to a pressure-compensated oil bleed-off, and using predictive algorithms to achieve component RPM settings within the target range; and
- Fitting external pressure-compensated bleed-off valves and using measured component RPM as feedback to the control circuit.

Consideration of a range of factors, including the required circuit stability and relative cost, the option of an external pressure-compensated bleed off valve was utilised as the “Mark 1” option. An additional consideration was the requirement for the system to “failsafe” so that if the electronic control system or hydraulic components failed, the system must continue to operate, albeit without speed control.

The Childers harvester was then fitted with bleed-off proportional flow control valves on both the spirals and forward feed circuits, and the controller software updated to control these valves. The control logic being utilized for these circuits did not incorporate direct feedback, as it is anticipated that the speed control achieved would be appropriate for the task. The characteristic of the valve is shown in Figure 6. It indicates that whilst the valve is a high-performance pressure-compensated valve, operating pressure still impacts on oil flow rate. This effect had to be taken into consideration with the control program. To achieve this, pressure in the circuit was also measured by the controller and incorporated into the algorithm.

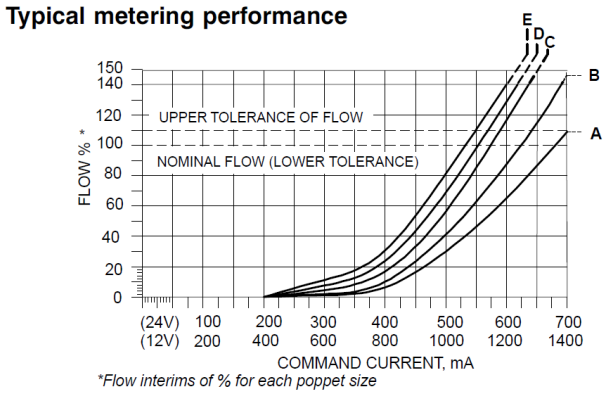

Pressure Differential		
A –	10 bar	145 psi
B –	20 bar	290 psi
C –	50 bar	725 psi
D –	100 bar	1450 psi
E –	200 bar	2900 psi

Figure 6: Typical metering performance of Valvistor pressure-compensated control valve used to control the bleed-off of oil from the spirals and KD/Finned rollers. Despite being "pressure compensated" pressure differential vary significantly impacts on flow through the valve at any command current.

After initial operation of the machine during the 2016 harvest, further modifications were made to the wiring harness and controller software and the circuit architecture to eliminate the start-up sequence issues initially encountered.

Condong Machine (Central Tweed Harvesting) and Ingham Machine (SJC Harvesting):

On the basis of the knowledge gained from the Childers machine, the modifications to the John Deere 3520 harvesters operated by Central Tweed Harvesting at Condong and SJC Harvesting in Ingham included:

- The replacement of the original (100 cc/rev) basecutter motor with a 71 cc/rev motor (as used on the latest model CH 570 harvesters). This increases maximum basecutter speed from 620 RPM to 880 rpm;
- Fitting of "Valvistor" pressure-compensated flow control valves to control component speed by controlled bleed oil from the oil supply to both the spirals and the KD/lower forward feed rollers, both of which are on separate circuits. Pressure transducers were also fitted to monitor pressure for control purposes; and
- Fitting an ECDR-0506 controller with a wiring harness developed after experience with the Childers machine. Similarly, the software control programs have been developed based on experience with the machine at Childers, with increased focus on "failsafe" attributes if part of the system suffers damage.

Rocky Point (Rocky Point Harvesting)

Based on the experience of the previous machines, considerable difficulty was experienced in achieving reliable speed control on the KD and finned rollers. The Rocky Point machine was also fitted with modified spirals developed by EHS Manufacturing in Mackay, as shown in Photograph 1 and Photograph 2. The spirals had a "double start" design of the flights, with the pitch modified to give a design rotational speed of 16 rpm/kph forward speed. To accurately maintain this relationship, it was decided to fit one spiral with a hydraulic motor which incorporated a speed encoder. The signal was used for direct feedback on instantaneous speed of the spirals. Because of the additional input, the controller had to be changed to a higher specification Hydraforce ECU-0809

controller. New software was required, with the basic algorithms being derived from the 0506 programs.

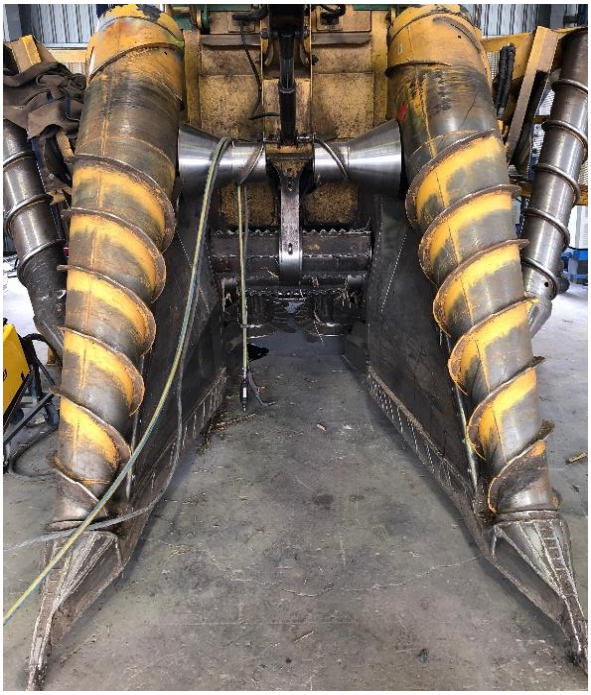

Photograph 1: Spirals with modified flights fitted to a JD 3520 harvester. The flights have a design rotational speed of 16 rpm/km/hr.

Photograph 2: Modified fronts with more aggressive flighting height and double start pitch dramatically improves harvester performance in large lodged crops when linked to groundspeed.

Initial setup and calibration was undertaken on this machine.

5.4.3. System design to control Basecutter and Forward Feed Component Speeds: Case 8000 Harvesters.

The hydraulic system design philosophy and therefore the configuration of the hydraulic circuits of the Case 8000 harvester is radically different to the John Deere machines. Apart from the traction circuits, the Case 8000 utilises lower pressure “open-centre” hydraulic circuits on all harvesting related functions, including the basecutters. The gathering spirals, butt lifter and second bottom feed roller are supplied with oil from sections of the basecutter motor. Oil for the Knockdown and Finned rollers is supplied from a different hydraulic circuit. The oil for the feed rollers is supplied from three separate circuits. A summary of the main harvesting function oil flows and the systems they supply is given in Table 1.

The complexity of the circuits and their use meant the development of the hydraulic configuration circuits for Case 8000 harvesters was hydraulically very much more complex than on the John Deere machines, but electronically simpler to control. As the spirals and butt lifter are driven from the basecutters, controlling basecutter speed then controls the oil flow in these circuits.

Table 1: Hydraulic Configuration, Case 8000

Pump	Oil Flow (l/min)	
Flow Divider	170	Topper, side knives, auxiliaries
Basecutter	313	Basecutter: Spirals, butt lifter, 2nd bottom roller
Primary Extractor	170	Primary Extractor
Elevator	115	Elevator, Secondary Extractor, Cooling Fan
Chopper	383	Chopper, Upper feedrollers, KD & Finned Rollers, Lower feedrollers

The layout of the basecutter circuit is shown in Figure 7. In the standard machine configuration, the Knockdown and Finned rollers received oil supply from a flow divider in the Chopper circuit.

When the feedtrain/chopper system on Case 8000 machines is "optimised" the hydraulic circuits are modified so that, with the exception of the butt lifter, all the feed rollers are on the same hydraulic circuit. This includes moving the "1st fixed roller after the butt lifter" from the basecutter circuit to the feed roller circuit. The modified basecutter circuit is shown in Figure 8. The standard basecutter motor was exchanged for a custom manufactured unit in which the 2.5" sector which returned directly to the control valve was split into two 1.25" sectors. One of these sectors then powered the Knockdown and Finned rollers, the other returned directly to the valve. These modifications then allowed the basecutters, knockdown & Finned rollers and the spirals all to be controlled together by the same oil supply.

To modulate the speed of the "front-end" components, the flow of oil to the basecutters then had to be both increased and decreased relative to standard flows. Flow reduction could be achieved by controlled dumping of oil via a pressure-compensated control valve. Increasing system speed above factory speed involved supplying the circuit with additional oil. The options were:

- Fit a higher capacity basecutter pump, or
- Divert un-used oil from other circuits.

To achieve target maximum component speed of over 800 RPM, the oil flow to the basecutter motor would have had to increase to greater than 400 L/min. To achieve 283 L/min to the choppers, a double pump would need to be utilised. Given space and other constraints, this was not a possible option.

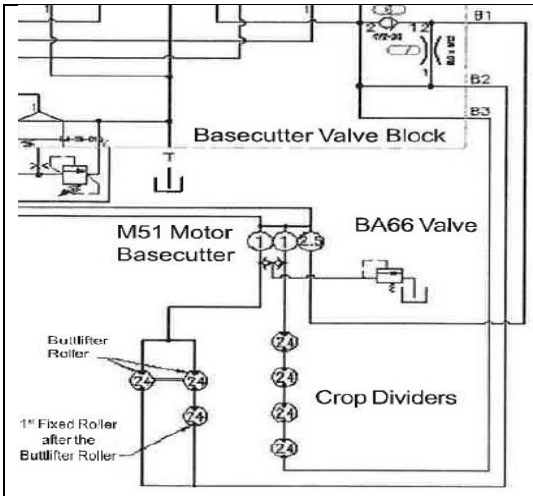

Figure 7: Standard configuration of the hydraulic circuit of the basecutter motor, butt lifter and gathering spirals on Case 8000 harvesters.

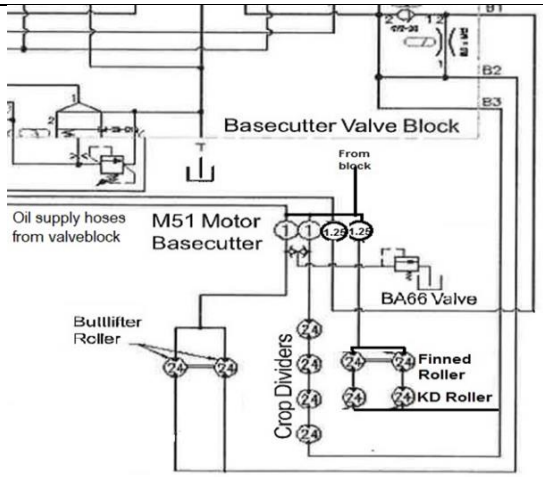

Figure 8: Modified basecutter motor configuration, with Finned & KD rollers on the basecutter circuit.

The option of diverting oil from other circuits was considered the best option. Analysis of the different circuits on the harvester indicated that oil was potentially available from the flow divider downstream from the chopper motors. In the standard configuration, this flow divider supplies the oil to the upper feed rollers (using a pressure-compensated flow control valve to bleed off oil to control motor speed) and the knockdown and finned rollers, and sequentially the first and second top feed rollers. Because all feed rollers were moved onto one circuit, it was possible to re-configure the flow divider to a four segment unit, as indicated in Figure 9. The two 1" segments could then be utilised to sequentially supply additional oil to the basecutter circuit.

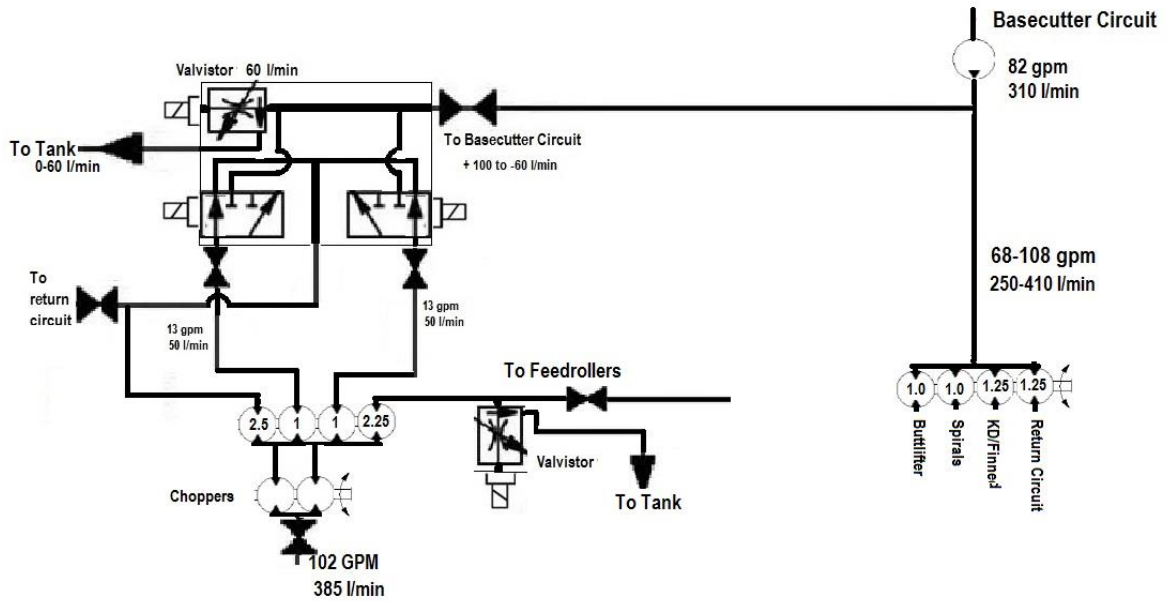

Figure 9: Overview of circuit, showing control valve block.

The valve block was configured to:

- At basecutter speeds below the standard speed, no additional oil is supplied to the basecutter circuit, and speeds lower than standard speed are achieved by bleed-off of oil from the basecutter circuit.

- At speeds above standard speed, initially one additional oil supply was added and flow modulated by the Valvistor valve. At higher speeds the second additional oil supply is introduced and the increased flow then further “trimmed “by the Valvistor valve.

This arrangement aimed to minimise oil being dumped at any time, thus minimising heat generation.

Photograph 3 shows the control block and the modified flow divider fitted to the harvester.

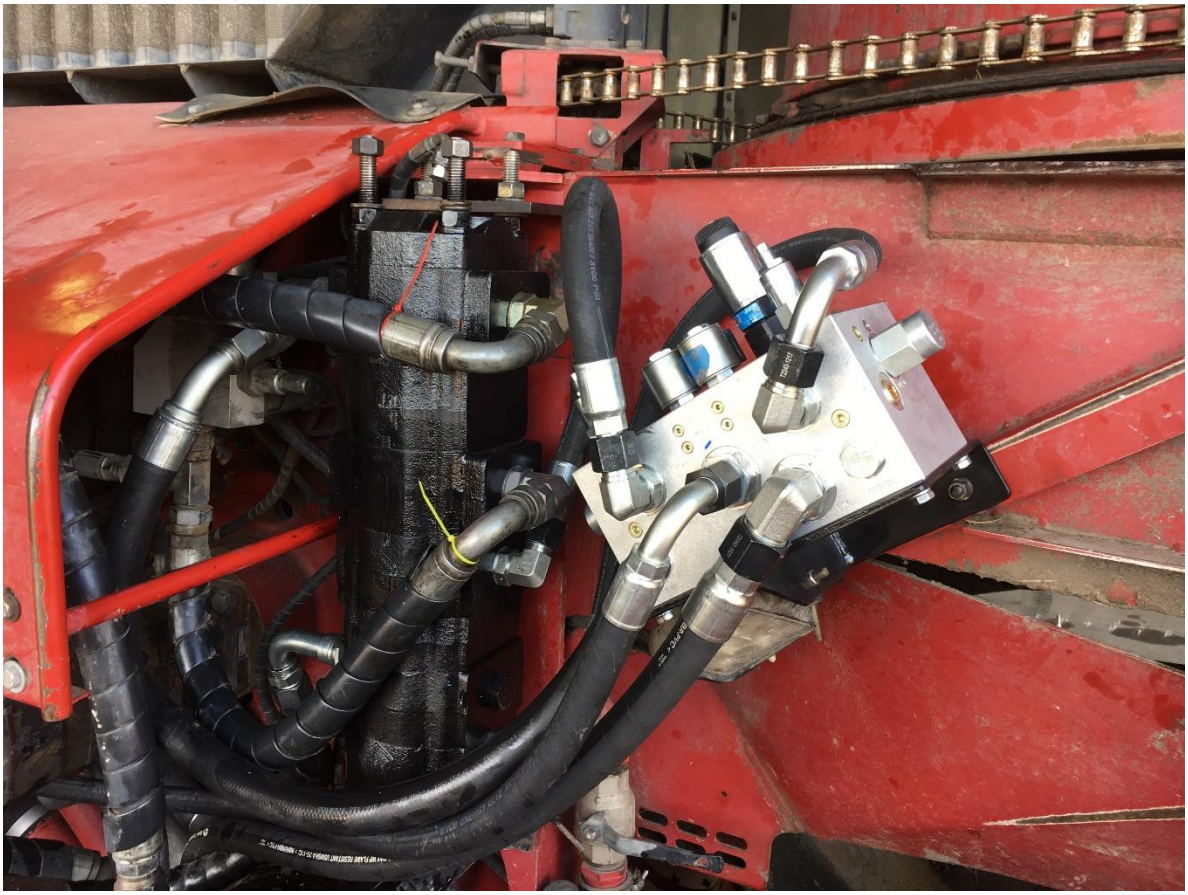

Photograph 3: The control block, which was designed and manufactured to allow oil flow to the basecutter motor to be modulated, is shown here after fitting to the harvester. The modified flow divider is also shown.

In addition, a CAMBUT^{R} “Sat-Speed” receiver had to be fitted to supply a groundspeed signal to the controller, as the speed signal generated by the integrated GPS receivers on Case 8000 harvesters could not readily be accessed.

The control methodology being utilized has limited maximum potential heat generation in the circuit to approximately 20 kW, with typical heat generation significantly lower than this. Less sophisticated strategies would have more than doubled the potential heat build-up and increased the likelihood of machine reliability problems.

The control system developed was based on a Hydraforce EcDR-0506 controller, with inputs of groundspeed and basecutter speed. The control system had three modes:

Off: Basecutters and forward feed components operating in standard configuration, allowing normal RPM “droop” under load;

Manual: Basecutter speed can be set and controlled manually, with the controller maintaining the nominated speed irrespective of load or forward speed;

Auto: Full automatic control linking component speed to groundspeed, with the relationships being software adjustable.

Whilst the concept development, specialist hydraulic component design and manufacture and initial implementation of the modifications was relatively straight-forward, the machine was been problematic for several reasons:

- The Case 8000 machine hydraulic design generally utilizes higher “no-load” system pressures at working engine speed. This means that the margin between no load and maximum load is less in these machines than the machines which utilize higher pressure closed-loop systems. This causes maximum net power available for harvesting functions to reduce at higher basecutter operating speeds. Whilst this was a consequence which was anticipated, the magnitude of the issue was greater than anticipated.
- Intermittent electronic problems with the harvester basecutter speed sensor caused major delays and very significant cost increases in achieving reliable system operation. Much of this additional cost and lost time was unnecessary but was not identified despite manufacturer-recommended trouble-shooting protocols being utilized.
- A problem in the design of the oil control block, requiring re-manufacture of some parts of the block, initially also caused major operating functionality problems.
- Internal leakage through the built-to-order basecutter motor caused speed loss and functionality problems. The unit was replaced with a unit designed and manufactured by the OEM supplier.
- Further issues related to the requirement for the machine to be able to be utilized as a seed cane harvester, with the associated requirement of being able to vary the feedtrain roller speed to well outside the original design speed range.
- “Unhelpful” input behind the scenes by the local Case dealer also exacerbated issues.

Most significant, however has been the limitations caused by the design of the hydraulic circuits:

- For a given oil flow, the Case harvester utilizes smaller hydraulic hoses than the other machines. As a result, in “ex-factory” configuration, the high idle (no-load, full engine RPM) pressures are significantly higher than for the John Deere machines. This is compounded by lower maximum operating pressures in key circuits meaning that the “working range” is much narrower.
- A significant proportion of the no-load pressure drop in hydraulic circuits is generated by the flow in hoses and fittings, and this pressure drop is proportional to the square of oil flow velocity. When oil flow is increased to increase component speeds, the “no load” pressures are increased. This further reduced the available working pressure range.

Whilst in lighter crops these factors were less significant, as the crop size and harvesting rates increased, the reduction in working pressure range became a more significant issue. At the harvesting rates targeted in large burned crops in the Burdekin area, the reduced working pressure range became unworkable.

The most significant of these issues which impact on the longer-term viability of matching forward feed component speed to forward speed is the “under-sizing” of the hydraulic plumbing and components, and the subsequent high parasitic losses at higher groundspeeds.

5.4.4. Harvester Modification:

After the end of the 2018 harvest, the JD 3520 harvester at Condong was replaced for commercial harvesting with a CH 570. The 3520 was then used for seed cane harvesting. Based on the previous knowledge bought to the project relating to “front end” layout, the “front end” of the 3520 harvester was modified to reduce the knockdown effect. A schematic of the standard layout and the modified layout is shown in Figure 10, along with the maximum deflection curves derived by Kroes and now being utilised in the modelling component of this project.

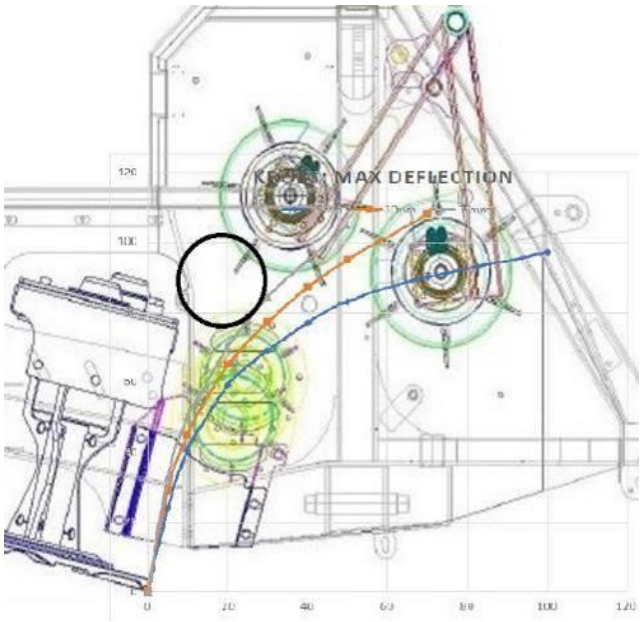

Figure 10: The Kroes maximum deflection curves superimposed on the component layout of a standard JD 3520, with the modified lower feed roller position also shown.

The modifications to the machine are illustrated in Photograph 4. The spirals and forward feed rollers were also fitted with hydraulic motors incorporating speed encoders, to allow speed to be actively controlled under varying field conditions.

Photograph 4: The final layout of components on the modified 3520 harvester.

The speed signals from the spirals, forward feed rollers and basecutters were then fed into a EcDR-0506 controller mounted in the engine bay of the harvester and a Wachendorff Opus A3 Display fitted in the cab as a driver interface. The machine driver was able to vary component speeds through this interface.

5.5. Field Trial Protocols.

The protocols for project field trials are outlined below.

5.5.1. Harvesting treatments

The initial aim of the field component of the project was to assess the impact on stool damage, ratoon emergence and subsequent crop yield of different harvesting speeds with standard harvester component speed configuration, and compare the impact of matching optimised component speeds with groundspeed.

The early trials contained treatments of matched component speed with standard machine configuration (620 basecutter r/min) at high and low harvesting speed, as indicated in Table 2**Error! Reference source not found.**. Subsequent trials would incorporate both machine modifications and changes to the field protocols to capitalise on knowledge gained.

In the first year of trials, in treatment 3 & 4, the high and low operating speed were linked with "standard" component speed settings. However, in the later trials, the trial protocol was modified to accentuate differences between component speeds and groundspeed: the unmatched treatments were changed so the low basecutter/front end speed was utilised with the high harvesting speed and the inverse was also utilised.

Table 2: Harvester and basecutter speed settings by treatment.

Treatment	Basecutter speed (r/min)	Harvesting speed (r/min)	Comment
1	450	4.5	Matched, low harvesting speeds
2	800	8.0	Matched, high harvesting speed
3	620/800	4.5	Unmatched, low harvesting speed
4	620/450	8.0	Unmatched, high harvesting speed

The first harvest event was undertaken at Plath Rd, Childers, in 2016. In 2017, trials were initiated at two sites in the Condong area, an additional site in Childers and a site in the Burdekin region. A further additional trial site was initiated in 2018 at Ingham. The machine at Rocky Point was used for equipment development and field observations, but no formal trials were undertaken.

5.5.2. Initial field protocols.

Initial trial protocols developed

The trial protocol at each site consisted of 12 plots, with three replicates and each of the four treatments randomised within the replicate. Each plot was either four or six rows depending on row length, giving the area per plot of typically 0.3 to 0.5 ha, with the total harvested area per trial in the range of 3.6 to 6 ha for each trial.

In all districts except the Burdekin, the sites chosen had row spacing matched to equipment width to minimise impact of wheel traffic on the damage/ratooning result. Where possible, the harvester utilised GPS Autosteer. Details of the trial sites are presented in Table 3**Error! Reference source not found.**.

Table 3: Project trial sites.

District	Farm	First harvest	Crop and plot configuration		Notes
Condong	Colonial Drive	2017	Q240 Plant	4 x 1.9 m dual row	Harvester and haulouts on GPS
	BZ Farms (S2)	2017	Q208 1R	4 x 1.9 m dual row	Harvester and haulouts on GPS
Childers	Plath Rd	2016	Q208[A] 1R	4 x 1.83 m single row	GPS not used
	Bouchards Rd	2017	Q240 Plant	6 x 1.83 m single row	Harvester only on GPS
Burdekin	Mona Park	2017	Q208 1R	4 x 1.65 m single row	GPS not used 2017, used 2018
Ingham	Bambaroo	2018	Q208 1R	4 x 1.9 m dual row	Harvester only on GPS

At harvest, extraneous matter (EM) samples were typically taken from each treatment and the total product harvested off each plot was consigned separately for weights and mill analysis. Where practical, individual row weights were noted when haul-outs with load cells were utilised in the harvesting operation, or where it was practical to assign one row to a transport unit.

Billet Quality

Billet quality is an indicator of a number of factors in the machine-crop interactions, with analysis of the type of damage on the billets being an indicator of the source of damage. Photograph 5 illustrates damage which is caused by the basecutting action of the harvester, with multiple splitting of the cane stalk. This effect is exacerbated by blade wear.

Photograph 5: Damage typical of that caused by the basecutting action.

Photograph 6 illustrates damage to the cane stalk during the gathering and aligning process. This type of damage to the cane stalk results in mutilated billets & billet parts in the final product.

Photograph 6: Stalks split and damaged during the gathering/aligning process result in damaged and mutilated billets.

Additional sources of damage occur when the high tip speed of the forward feed rollers in conjunction with aggressive design of the "teeth" on these rollers result in axial compression of the stalk and failure prior to basecutting. This effect is shown in Photograph 7.

Photograph 7: Stalk damage at ground level and at 15-20 cm above ground level associated with aggressive forward feeding. The stalk is forced into the throat of the machine and buckles under compression failure

The source of billet damage was determined by analysing the type of damage on the billets delivered by the harvester. Photograph 8 is of a sample of billets from a harvester operating in a heavily lodged crop, with the probable sources of damage identified.

Photograph 8: Billet sample from harvester illustrating the probable source of damage (Gathering, Basecutting or Chopper) observed on billets.

In this sample, a high proportion of the billets had suffered significant damage, with the gathering/aligning process being the most probable cause of damage associated with the cane stalk splitting or “buckling”.

In each of the trials, a damage assessment was undertaken on billets from each treatment. The billet damage was categorized according to the most probable source of the damage, i.e. gathering, basecutters and other/choppers.

At the first harvest, extracted trash weight was also measured on tarpaulins, however the value of the data was perceived as limited and the process discontinued.

The trial protocols developed for assessment of damage caused by the harvesting operation were developed based on the protocols developed by Whiteing and Kingston (2008) for similar work in 2002-2003. Key aspects of the protocol are explained in the section below.

The guidelines initially developed by Kroes and Harris (1994) to assess damage caused by the basecutting operation are presented in Figure 11. These categories were further refined by Davis and Whiteing (pers. comm.), who included a category for “snapped” stalk (where the stalk has characteristics of a clean stress failure below the depth setting of the basecutters) and “loose” where the stool is still attached into the soil by surface roots but is loose in the soil.

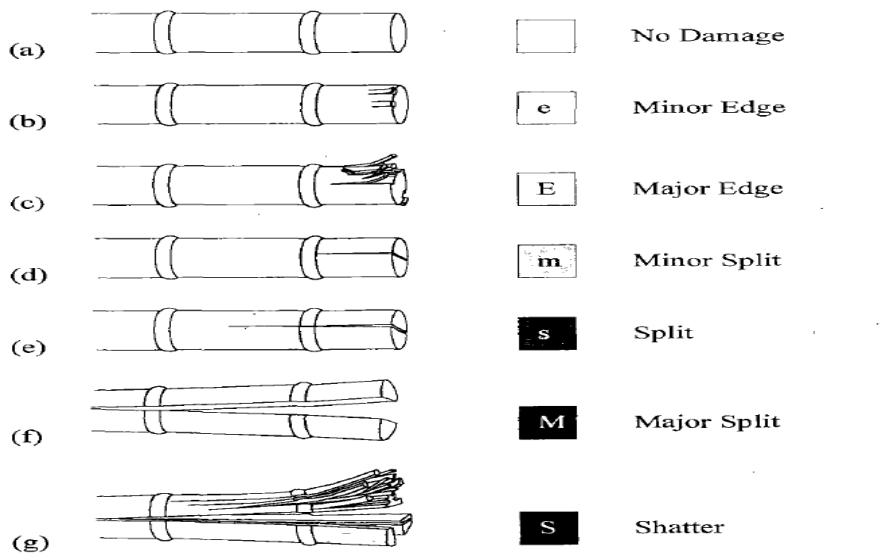

Figure 11: Criteria developed by Kroes and Harris (1994) to assess damage caused by the basecutting operation. Upper or lower case on the associated box indicates if the damage level is considered major or minor.

Stool Damage

After the harvesting operation, an assessment of stool damage was undertaken. The damage to the stool was categorized based on the guidelines developed by Kroes and Harris (1994)) and later used by other researchers. The classifications and a short description are presented in Table 4**Error! Reference source not found.**. The criteria are based on assessments of the possible impact of the different modes of damage on the ability of the remaining stool to ratoon successfully. The actual level of ratoon emergence which occurs can be argued to depend not only on the level of damage associated with the harvesting operation, but also on many factors affecting the crop after harvest. Similar levels of stool damage can be anticipated to give different outcomes under different field conditions.

Table 4: Cane Stool Damage Classification, based on the work of Kroes and Harris (1994).

Stool/Stalk Classification	*Type of Damage*	*Comment*
Sound	Minimal	Predominantly clean cut by blade, some limited "edge" damage acceptable.
Minor Damage	Edge damage	More significant edge damage
	Surface shatter or shallow split	Superficial shatter of cut surface or shallow split
Major Damage	Split	Split down through at least one node below cutting depth
	Deep Shatter	Multiple splits down through one or more nodes
	Snapped (below cutting depth)	Clear break below the typical cutting depth of the blades
	Loose in ground	Loose in ground associated with fracture of stalk from the root mass.

After harvest, sub-plot sections were marked out, typically 50 m from the field edge, to ensure that the plot locations represented 'steady state' harvesting, free from any end of row influences. The

treatment plots were either of four or six rows, depending on the row length, and the stool damage assessment was typically undertaken on the second row of the treatment plot. Consistency in this measurement is essential because of the “up and back” harvesting operation, and to avoid complications relating to direction of harvest. In crops with single row planting configuration, the stool damage assessment was undertaken on a 10 m length of plot which was then split into 20 x 0.5m sub-plots. For dual row configuration plots, the two rows were assessed separately over a 7.5m length, effectively giving 15m of row length assessment.

Semi-permanent markers were installed to allow the same reference point to be utilised for all subsequent activities in the plot. The trash was raked off the row in these sections and loose soil removed with a low-pressure air blower (Photograph 9), typically down to the basecutter operating depth (Photograph 10).

Photograph 9: Cleaning-off trash and loose soil to allow assessment of stool damage.

Photograph 10: Typical row section with trash and loose soil cleared down to the operating level of the basecutters, and ready to be assessed.

Photograph 11 shows examples of the types of stool damage observed after harvest.

Photograph 11: Illustration of different types of damage in the exposed stool.

5.6. Stream 2 – Modelling

5.6.1. Compilation of database of properties of sugarcane plant for Discrete Element Modelling (DEM), or Finite Element Analysis (FEA)

Although it was initially intended that DEM methods be adopted, the recent advances made in FEM methods prompted a more extensive assessment of the latter. Due to the varying input requirements, the material and mechanical properties of the harvester, cane and soil components are reported (where available) with the different modelling software (DEM and FEM) platforms. The review identified sufficient (but not extensive) sugarcane plant property data for both DEM and FEM analyses to be undertaken.

Primary input data for the preliminary model development and demonstration is given in Table 5.

Table 5: Constitutive properties of sugarcane stalk used in the preliminary FEM model development

Density (kg/m^3)	Young's Modulus (MPa)	Poisson's ratio	Yield stress (MPa)
1200	1250	0.3	25.3

5.6.2. Development of initial single cane stalk FEM model.

A preliminary time dependant (dynamic) model of a cane stalk embedded in soil and impacted sideways by a knockdown roller (rod) was developed using LS-DYNA's FEM capability. The soil was modelled as a cylinder 500 mm diameter and 500 mm high. A partial stalk was modelled as a 30 mm diameter and 1000 mm high cylinder with half of its length embedded in the soil. The knockdown roller was represented in these early simulations as a simple 50 mm diameter and 540 mm long rod.

The simulation showed that the maximum bending stress (adjacent to the soil surface) was equivalent to the elastic limit of the cane (25 MPa) when the knockdown roller had pushed the point of contact on the stalk horizontally forward by 0.3 m. Any further horizontal forward displacement of the knockdown roller will result in progressive failure of the stalk near the soil, if the soil holds firm. Any loosening of the soil will allow further movement of the stalk without failure. The Von

Mises stress distribution in the cane stalk at this displacement of the knock down roller is shown in Figure 12.

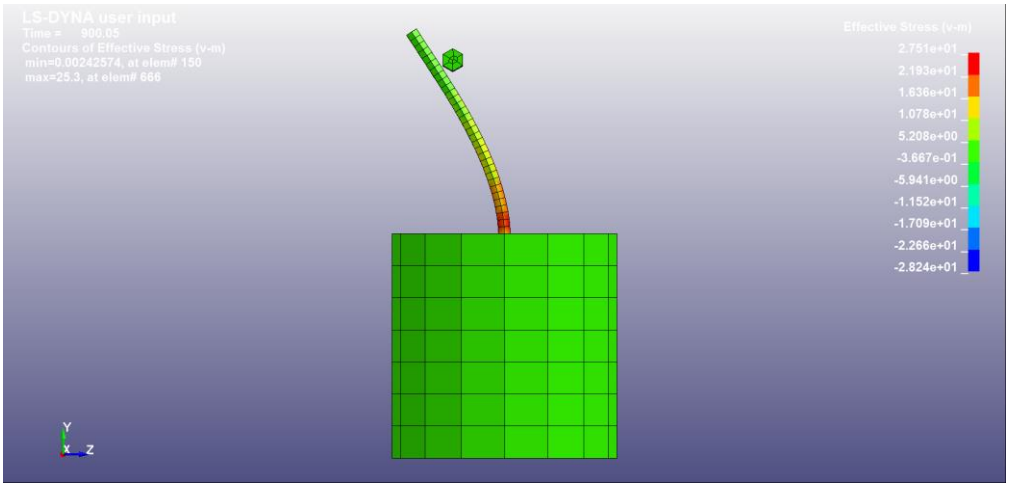

Figure 12: Von Mises stress distribution at knockdown conditions close to the elastic limit of the cane stalk.

5.6.3. Development of DEM model and simulation of initial field trial scenarios

The decision to develop a cane stalk model using advanced Finite Element Modelling (FEM) rather than Discrete Element Modelling (DEM) necessitated an expansion of the material property data set. Cane material property data available or derived from the literature suitable for direct use in the FEM model is summarized in

Table 6Error! Reference source not found..

Some material properties relevant to the FEM model which have not been measured for cane were collated from the literature on other crops such as bamboo, energy cane and reed. These additional properties included compressive strength, tensile strength and breaking strength. Material property values for these other crops are summarized in **Table 7Error! Reference source not found.**.

Modelling was progressed at two levels. At a macro level, model development involved the use of solid modelling of the basecutter geometries and kinematics using the dimensions and operating conditions of the harvester currently being used in Stream 1 field trials in the Burdekin.

Table 6: Sugarcane material property data.

Property	Units	Value	Reference	Notes
Bending strength	MPa	9.58	Taghijarah et al, 2012	Iran - cane variety L310, diameter = 19.07 mm, length = 77.63 mm
Bending strength	MPa	9.2	Taghijarah et al, 2012	Iran - cane variety L820, diameter = 17.21 mm, length = 83.17 mm
Crushing force	kN	0.75	Bastian and Shridar, 2014	India - most common cane variety CO-86032, top of stalk
Crushing force	kN	1.53	Bastian and Shridar, 2014	India - most common cane variety CO-86032, bottom of stalk
Fracture energy	J/m^2	5530	Kroes, 1997	Cane variety CP65-357
Fracture energy	J/m^2	5200	Kroes, 1997	Cane variety NCo-310
Fracture energy	J/m^2	5760	Kroes, 1997	Cane variety L60-25
Fracture energy	J/m^2	4990	Kroes, 1997	Cane variety CP70-321
Fracture energy	J/m^2	7110	Kroes, 1997	Cane variety L79-1003
Modulus of rupture	MPa	13	Kroes, 1997	Cane variety CP65-357
Modulus of rupture	MPa	10.8	Kroes, 1997	Cane variety NCo-310
Modulus of rupture	MPa	12.2	Kroes, 1997	Cane variety L60-25
Modulus of rupture	MPa	12	Kroes, 1997	Cane variety CP70-321
Modulus of rupture	MPa	16.5	Kroes, 1997	Cane variety L79-1003
Penetration resistance	$kN\ m^{-2}$	29.74	Bastian and Shridar, 2014	India - most common cane variety CO-86032, top of stalk
Penetration resistance	$kN\ m^{-2}$	56.33	Bastian and Shridar, 2014	India - most common cane variety CO-86032, bottom of stalk
Shear strength	MPa	4.92	Taghijarah et al, 2012	Iran - cane variety L310, diameter = 19.07 mm, length = 77.63 mm
Shear strength	MPa	5.25	Taghijarah et al, 2012	Iran - cane variety L820, diameter = 17.21 mm, length = 83.17 mm
Shear strength	MPa	3.482	Hemmatian et al, 2012	Iran - random cane stalks from Ahwaz farm, mositure 78%
Specific cutting resistance	$kN\ m^{-2}$	957.48	Bastian and Shridar, 2014	India - most common cane variety CO-86032, top of stalk
Specific cutting resistance	$kN\ m^{-2}$	1764.56	Bastian and Shridar, 2014	India - most common cane variety CO-86032, bottom of stalk
Specific shearing energy	$mJ\ mm^{-2}$	53.36	Taghijarah et al, 2012	Iran - cane variety L310, diameter = 19.07 mm, length = 77.63 mm
Specific shearing energy	$mJ\ mm^{-2}$	57.35	Taghijarah et al, 2012	Iran - cane variety L820, diameter = 17.21 mm, length = 83.17 mm
Specific shearing energy	$mJ\ mm^{-2}$	107.477	Hemmatian et al, 2012	Iran - random cane stalks from Ahwaz farm, mositure 78%
Toughness	kPa	302	Kroes, 1997	Cane variety CP65-357
Toughness	kPa	346	Kroes, 1997	Cane variety NCo-310
Toughness	kPa	263	Kroes, 1997	Cane variety L60-25
Toughness	kPa	409	Kroes, 1997	Cane variety CP70-321
Toughness	kPa	401	Kroes, 1997	Cane variety L79-1003
Ultimate strength	MPa	6.7	Yin et al, 2013	Australia - most popular cane variety Q183 (Burdekin region), diameter = 30 mm, leng
Yield strength	MPa	5.3	Yin et al, 2013	Australia - most popular cane variety Q183 (Burdekin region), diameter = 30 mm, leng
Youngs modulus	MPa	86	Bastian and Shridar, 2014	India - most common cane variety CO-86032
Young's Modulus	MPa	18.81	Taghijarah et al, 2012	Iran - cane variety L310, diameter = 19.07 mm, length = 77.63 mm
Young's Modulus	MPa	24.5	Taghijarah et al, 2012	Iran - cane variety L820, diameter = 17.21 mm, length = 83.17 mm
Young's Modulus	MPa	325	Yin et al, 2013	Australia - most popular cane variety Q183 (Burdekin region), diameter = 30 mm, leng
Young's Modulus	MPa	76.2	Kroes, 1997	Cane variety CP65-357
Young's Modulus	MPa	58.4	Kroes, 1997	Cane variety NCo-310
Young's Modulus	MPa	63.7	Kroes, 1997	Cane variety L60-25
Young's Modulus	MPa	59.6	Kroes, 1997	Cane variety CP70-321
Young's Modulus	MPa	105.6	Kroes, 1997	Cane variety L79-1003

Table 7: Material properties for crops other than sugarcane.

Material	Property	Units	Value	Reference	Notes
Reed stalk	Bending strength	MPa	152.42	Zhen et al, 2011	China
Reed stalk	Breaking strength	MPa	148.65	Zhen et al, 2011	China
Bamboo stalk	Compressive strength	MPa	47	Li, 2004	Bottom - 1 yr old bamboo
Bamboo stalk	Compressive strength	MPa	50.9	Li, 2004	Middle - 1 yr old bamboo
Bamboo stalk	Compressive strength	MPa	55.7	Li, 2004	Top - 1 yr old bamboo
Bamboo stalk	Compressive strength	MPa	86.8	Li, 2004	Bottom - 3 yr old bamboo
Bamboo stalk	Compressive strength	MPa	83.9	Li, 2004	Middle - 3 yr old bamboo
Bamboo stalk	Compressive strength	MPa	84	Li, 2004	Top - 3 yr old bamboo
Bamboo stalk	Compressive strength	MPa	93.6	Li, 2004	Bottom - 5 yr old bamboo
Bamboo stalk	Compressive strength	MPa	86.6	Li, 2004	Middle - 5 yr old bamboo
Bamboo stalk	Compressive strength	MPa	85.8	Li, 2004	Top - 5 yr old bamboo
Bamboo stalk	Compressive strength	MPa	14.8	Li, 2004	Bottom - 1 yr old bamboo
Bamboo stalk	Compressive strength	MPa	16	Li, 2004	Middle - 1 yr old bamboo
Bamboo stalk	Compressive strength	MPa	17.4	Li, 2004	Top - 1 yr old bamboo
Bamboo stalk	Compressive strength	MPa	33	Li, 2004	Bottom - 3 yr old bamboo
Bamboo stalk	Compressive strength	MPa	29.8	Li, 2004	Middle - 3 yr old bamboo
Bamboo stalk	Compressive strength	MPa	33.8	Li, 2004	Top - 3 yr old bamboo
Bamboo stalk	Compressive strength	MPa	34.1	Li, 2004	Bottom - 5 yr old bamboo
Bamboo stalk	Compressive strength	MPa	33.6	Li, 2004	Middle - 5 yr old bamboo
Bamboo stalk	Compressive strength	MPa	35.3	Li, 2004	Top - 5 yr old bamboo
Bamboo stalk	Modulus of elasticity	Mpa	7770	Li, 2004	Bottom - 1 yr old bamboo
Bamboo stalk	Modulus of elasticity	Mpa	8680	Li, 2004	Middle - 1 yr old bamboo
Bamboo stalk	Modulus of elasticity	Mpa	8929	Li, 2004	Top - 1 yr old bamboo
Bamboo stalk	Modulus of elasticity	Mpa	10039	Li, 2004	Bottom - 3 yr old bamboo
Bamboo stalk	Modulus of elasticity	Mpa	10122	Li, 2004	Middle - 3 yr old bamboo
Bamboo stalk	Modulus of elasticity	Mpa	10397	Li, 2004	Top - 3 yr old bamboo
Bamboo stalk	Modulus of elasticity	Mpa	13162	Li, 2004	Bottom - 5 yr old bamboo
Bamboo stalk	Modulus of elasticity	Mpa	13410	Li, 2004	Middle - 5 yr old bamboo
Bamboo stalk	Modulus of elasticity	Mpa	13307	Li, 2004	Top - 5 yr old bamboo
Bamboo stalk	Modulus of rupture	Mpa	110.3	Li, 2004	Bottom - 1 yr old bamboo
Bamboo stalk	Modulus of rupture	Mpa	119.3	Li, 2004	Middle - 1 yr old bamboo
Bamboo stalk	Modulus of rupture	Mpa	117.2	Li, 2004	Top - 1 yr old bamboo
Bamboo stalk	Modulus of rupture	Mpa	151	Li, 2004	Bottom - 3 yr old bamboo
Bamboo stalk	Modulus of rupture	Mpa	151.7	Li, 2004	Middle - 3 yr old bamboo
Bamboo stalk	Modulus of rupture	Mpa	160.6	Li, 2004	Top - 3 yr old bamboo
Bamboo stalk	Modulus of rupture	Mpa	186.2	Li, 2004	Bottom - 5 yr old bamboo
Bamboo stalk	Modulus of rupture	Mpa	184.8	Li, 2004	Middle - 5 yr old bamboo
Bamboo stalk	Modulus of rupture	Mpa	183.4	Li, 2004	Top - 5 yr old bamboo
Reed stalk	Shearing strength	MPa	22.41	Zhen et al, 2011	China
Bamboo stalk	Tensile strength	Gpa	0.55	Li, 2011	
Reed stalk	Yield strength	MPa	5.42	Zhen et al, 2011	China
Bamboo stalk	Youngs modulus	MPa	2067	Li, 2004	Bottom - 1 yr old bamboo
Bamboo stalk	Youngs modulus	MPa	2776	Li, 2004	Middle - 1 yr old bamboo
Bamboo stalk	Youngs modulus	MPa	3658	Li, 2004	Top - 1 yr old bamboo
Bamboo stalk	Youngs modulus	MPa	4426	Li, 2004	Bottom - 3 yr old bamboo
Bamboo stalk	Youngs modulus	MPa	4428	Li, 2004	Middle - 3 yr old bamboo
Bamboo stalk	Youngs modulus	MPa	4660	Li, 2004	Top - 3 yr old bamboo
Bamboo stalk	Youngs modulus	MPa	4896	Li, 2004	Bottom - 5 yr old bamboo
Bamboo stalk	Youngs modulus	MPa	4980	Li, 2004	Middle - 5 yr old bamboo
Bamboo stalk	Youngs modulus	MPa	5185	Li, 2004	Top - 5 yr old bamboo
Bamboo stalk	Youngs modulus	MPa	277	Li, 2004	Bottom - 1 yr old bamboo
Bamboo stalk	Youngs modulus	MPa	254	Li, 2004	Middle - 1 yr old bamboo
Bamboo stalk	Youngs modulus	MPa	359	Li, 2004	Top - 1 yr old bamboo
Bamboo stalk	Youngs modulus	MPa	535	Li, 2004	Bottom - 3 yr old bamboo
Bamboo stalk	Youngs modulus	MPa	456	Li, 2004	Middle - 3 yr old bamboo
Bamboo stalk	Youngs modulus	MPa	606	Li, 2004	Top - 3 yr old bamboo
Bamboo stalk	Youngs modulus	MPa	533	Li, 2004	Bottom - 5 yr old bamboo
Bamboo stalk	Youngs modulus	MPa	527	Li, 2004	Middle - 5 yr old bamboo
Bamboo stalk	Youngs modulus	MPa	552	Li, 2004	Top - 5 yr old bamboo
Energy cane stalk				Mathanker et al, 2015	USA

The initial model was further developed to incorporate features in the LS-DYNA software to allow high levels of material deformation to produce fracturing of the cane causing splitting and

potentially chipping as a result of interactions with the knockdown roller and basecutter blades. This stage of the modelling was problematic and although there were no technical barriers encountered, the implementation of these effects and the lack of appropriate material properties caused delays.

Two examples of the predicted effect of sugarcane material properties on outcomes resulting from the interaction between the harvester knockdown roller and a single cane stalk are given below. In both cases the stalk was modelled as a cylinder penetrating into and being bonded to the soil. The soil was represented as a vertical cylinder 0.5 m long and 0.5 m diameter. The stalk was 0.03 m diameter and projected 0.5 m above the surface of the soil. The knockdown roller made contact with the stalk at a height of 0.382 m above ground. Figure 13 gives a perspective of the geometry used in the simulations (top view).

Using material properties reported for relatively soft cane (low Young's modulus) planted in firm soil, Figure 14 shows initial bending of the cane stalk by the knockdown roller followed by cane failure and damage after the harvester has passed over the cane (Figure 15). It is interesting to note that for these cane properties, the cane failed (snapped off) just below ground level. This phenomenon was also observed during the NSW harvester trials in Q240, a thicker cane variety.

At the other end of the scale, experimentally measured material properties data reported by Kroes (1996) for hard, brittle cane (Young's Modulus of 60 MPa, ultimate bending strength of 25 MPa) planted in loose/ weak soil (Young's Modulus of 1.2 MPa) were implemented in the model.

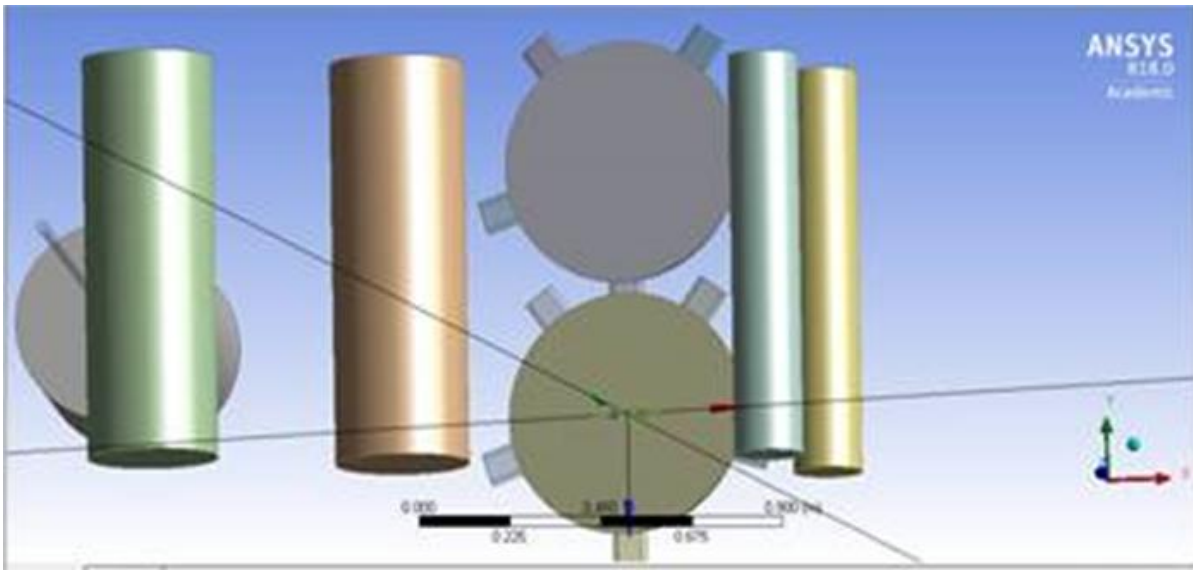

Figure 13: Solid modelling of cane (far left), feed components, harvester basecutters and kinematics.

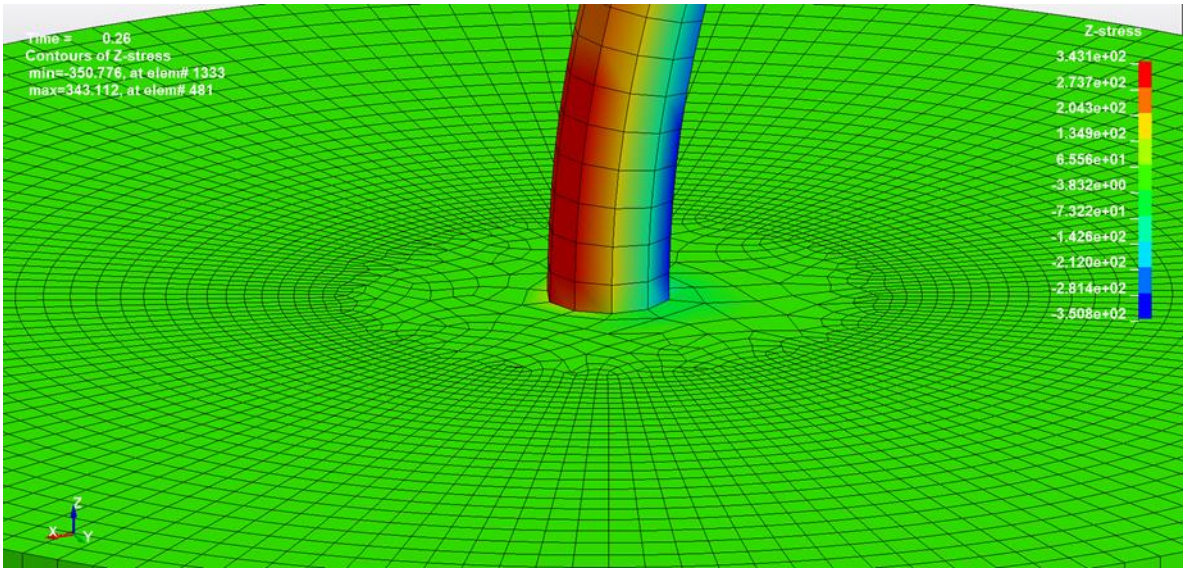

Figure 14: Von Mises bending stress predicted during initial elastic deflection f relatively soft (low Young's modulus) cane by the knockdown roller (closeup of stalk at ground level.

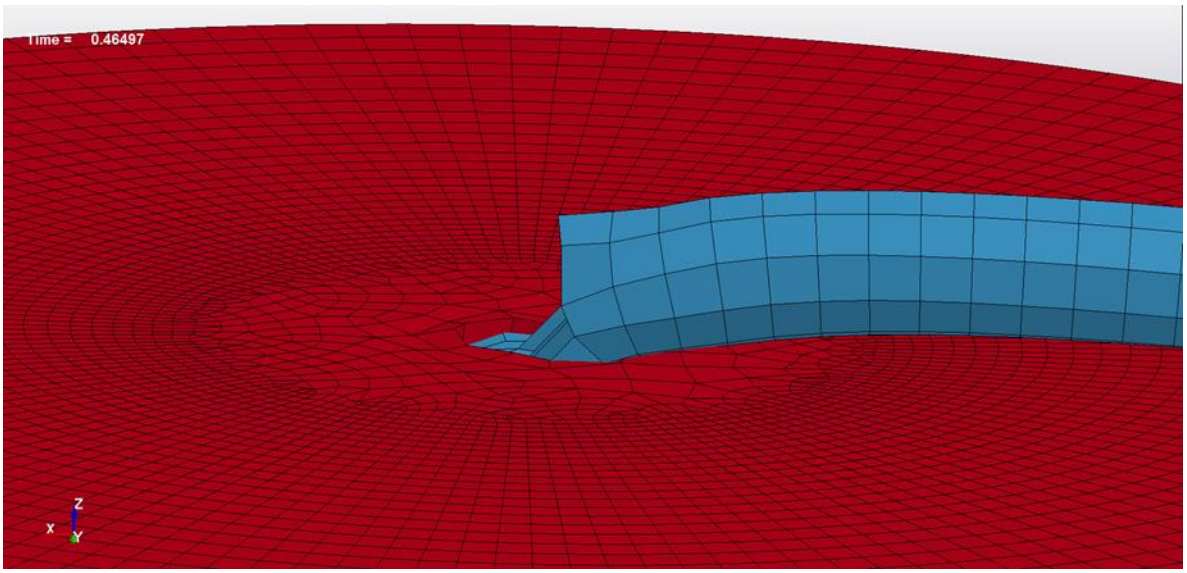

Figure 15: Eventual failure and damage of soft cane by the knockdown roller. Failure is predicted to occur just below ground level.

Figure 16 shows the predicted initial flexing and Figure 17 the eventual failure of the brittle cane as it is impacted by the knockdown roller. In this case failure of the cane occurred well above ground level and in the vicinity of the point of impact with the knockdown roller.

Close inspection of the edges of the cylindrical soil element (Figure 16, Figure 17) shows breakup of the (soft) soil caused by both the bulk deflection and the propagation of a wave up and down the cane stalk after impact with the knockdown roller. Action of this type would facilitate uprooting of the cane during harvest.

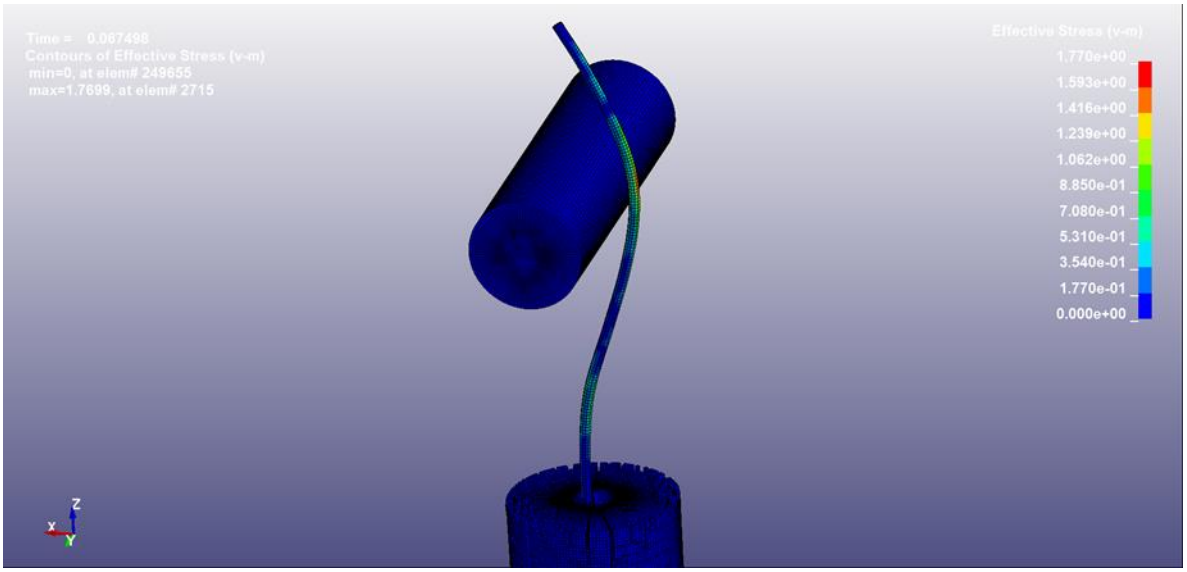

Figure 16: Von Mises bending stress predicted during initial elastic deflection of relatively hard and brittle cane when impacted by the knockdown roller.

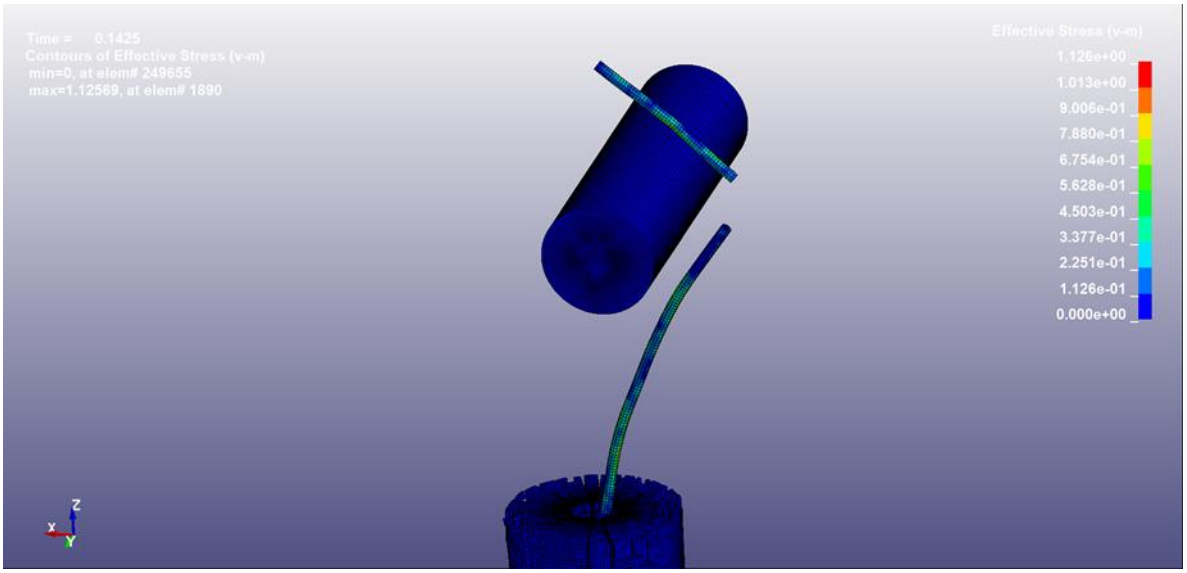

Figure 17: Predicted eventual failure and damage of hard cane; failure occurs at the point of impact with the knockdown roller

5.6.4. Validation of FEM model against field trial observations

A validation of the FEM model was undertaken although this exercise was limited to the effects of the knockdown roller on stool damage. The single stalk FEM model was set up to simulate the range of harvester speeds (4.5 to 8.5 km.h^{-1}) trialled in the Burdekin, Childers and Condong regions as

detailed in the above Stream 1 activities. Material property data for Q183[1] was used in the initial validation[2].

Results and Discussion

The model clearly demonstrated cane failure and fracture (snapping off) at or below ground level as a result of interaction with the knockdown roller. This mode of failure has been shown to contribute to the high levels of major damage (34% to 63% of total damage) to the cane stool observed in the field trials and indicated in Figure 93, Figure 97 and Figure 101. Three stages of deformation of the cane stalk were observed as the stalk was progressively pushed forward by the knockdown roller:

1. a high buildup of stress in the leading and trailing surface layers of the stalk causing elastic and eventually plastic deformation (Figure 18);
2. elastic and plastic deformation with partial fracture (Figure 19) and;
3. fracture resulting in release of stress with residual stool and billet damage (Figure 20)

This phenomenon was found to be largely independent of harvester ground speed. To what extent this result is dependent on cane variety is not possible to say at this stage except to note that at the lower Young's Modulus reported for some of the older varieties of Australian cane, *e.g.* cane variety NC0-310[3], failure of the cane stalk occurred but fracture did not.

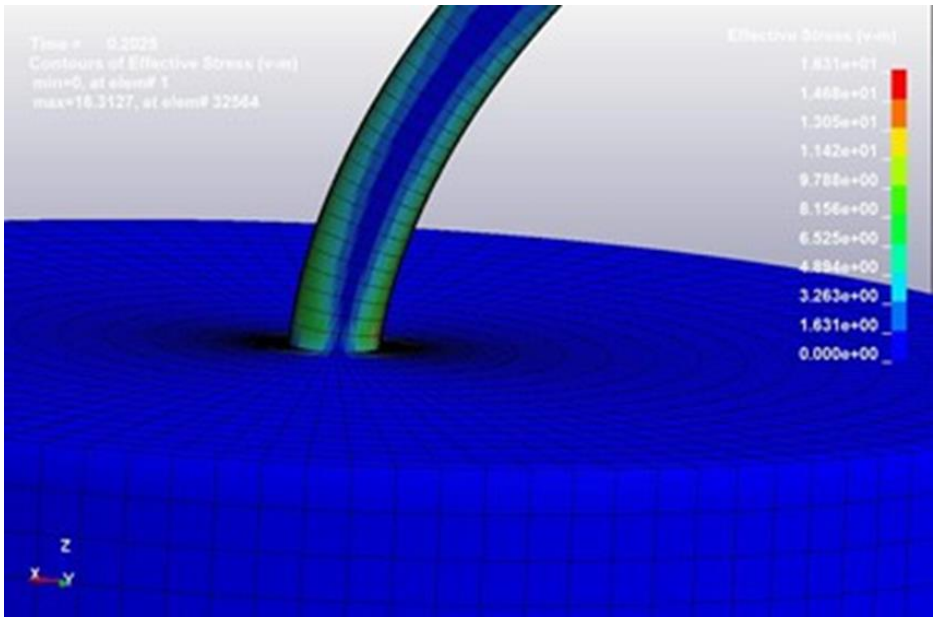

Figure 18: Stage 1 deformation - elastic and eventually plastic deformation.

[1] This cane variety was simulated as detailed material properties data are available and it is a variety which is widely used in the Burdekin, Childers and Condong regions. Material properties data for Q240 and Q208 are not available.

[2] Yin et al. (2013) Experimental and simulation approaches: Effect of microwave energy on mechanical strength in sugarcane. Australian Journal of Multi-Disciplinary Engineering, Vol 10, No 2, 120-128.

[3] The Young's Modulus for NC0-310 was reported as 58 MPa compared to a Young's modulus of 325 MPa for Q183.

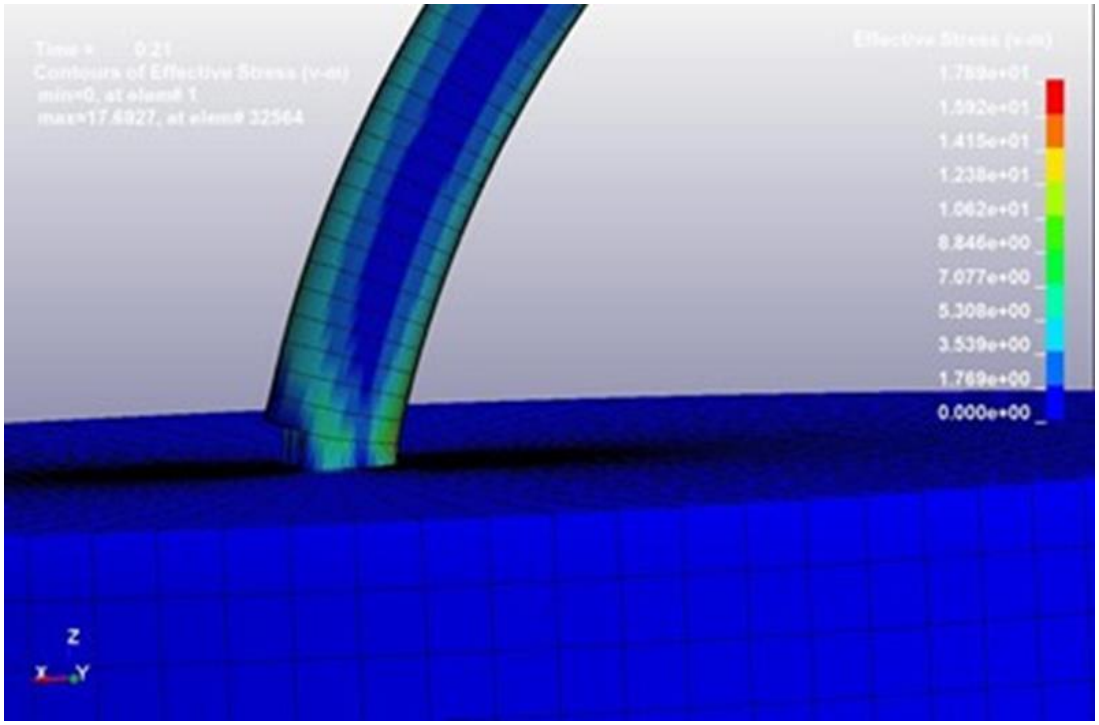

Figure 19: Stage 2 deformation - elastic and plastic deformation with partial fracture.

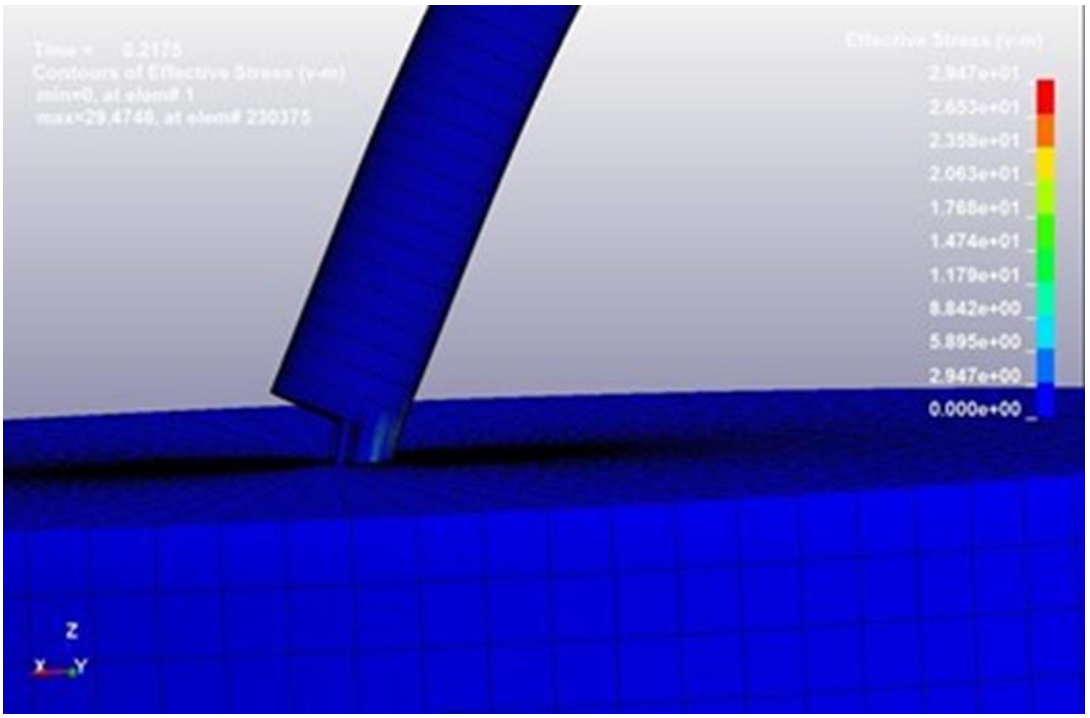

Figure 20: Stage 3 deformation - fracture resulting in release of stress

The FEM model was unable to duplicate the longitudinal splitting damage to the stool and stalk observed during the trials despite a significant 'flexing' of the model material property inputs. Although the longitudinal splitting observed in the field trial (Photograph 5) were ascribed primarily to basecutter action (which the current model does not simulate), work by Kroes has shown that such splitting can also occur due to the action of the knockdown roller alone.

In discussions with Dr Jindong Yang (Technical Director, LEAP Australia Pty Ltd) it was suggested that longitudinal splitting would be initiated by modelling the cane stalk as a cylinder with a thin hard shell (rind) and a softer (predominantly pith) interior section. Limited data available from a single study by Handong *et al.* (2011) that the material properties of cane are both heterogeneous and anisotropic. The results of a FEM simulation exercise was reported by Handong *et al.* using the data in **Table 8 Error! Reference source not found.**to simulate the cutting of cane. However the cutting mechanism being simulated by Handong *et al.* (2011) did not include lateral forces (such as would be produced by the knockdown roller) and so the suitability of heterogeneous anisotropic material properties in predicting splitting damage could not be assessed.

Table 8: Axial and radial material properties of cane billet components (Handong *et al.* (2011)).

Mechanical index	Cane pith (MPa)	Cane rind (MPa)
Axial tensile strength	6.7	47.0
Radial tensile strength	1.3	2.6
Axial compressive strength	14.5	101.4
Radial compressive strength	2.3	4.5
In-plane shear strength	0.5	2.3
Axial elastic modulus	1515	10615
Radial elastic modulus	613	1175
Shear modulus of elasticity	11	54
Poisson's ratio	0.47	0.34

5.6.5. Further development and validation of FEM modelling

An FEM model of the cane stem, forward-moving harvester knockdown roller and the two counter-rotating basecutter disc-mounted blades has been completed. The model has been run to duplicate the harvester operating conditions associated with the most recent Childers field trials and qualitative comparisons made between the predicted and observed cane damage.

Key simplifying assumptions in the current model are:

- a solid stalk with isotropic, homogeneous material properties;
- the bottom 100 mm of the stalk is simply ‘clamped’ to represent a non-deforming soil;
- all harvester components are non-deforming;
- the knockdown and feed rollers are smooth non-rotating cylinders; and
- friction between all components is neglected.

The configuration and dimensions of the modelled components are shown in Figure 21.

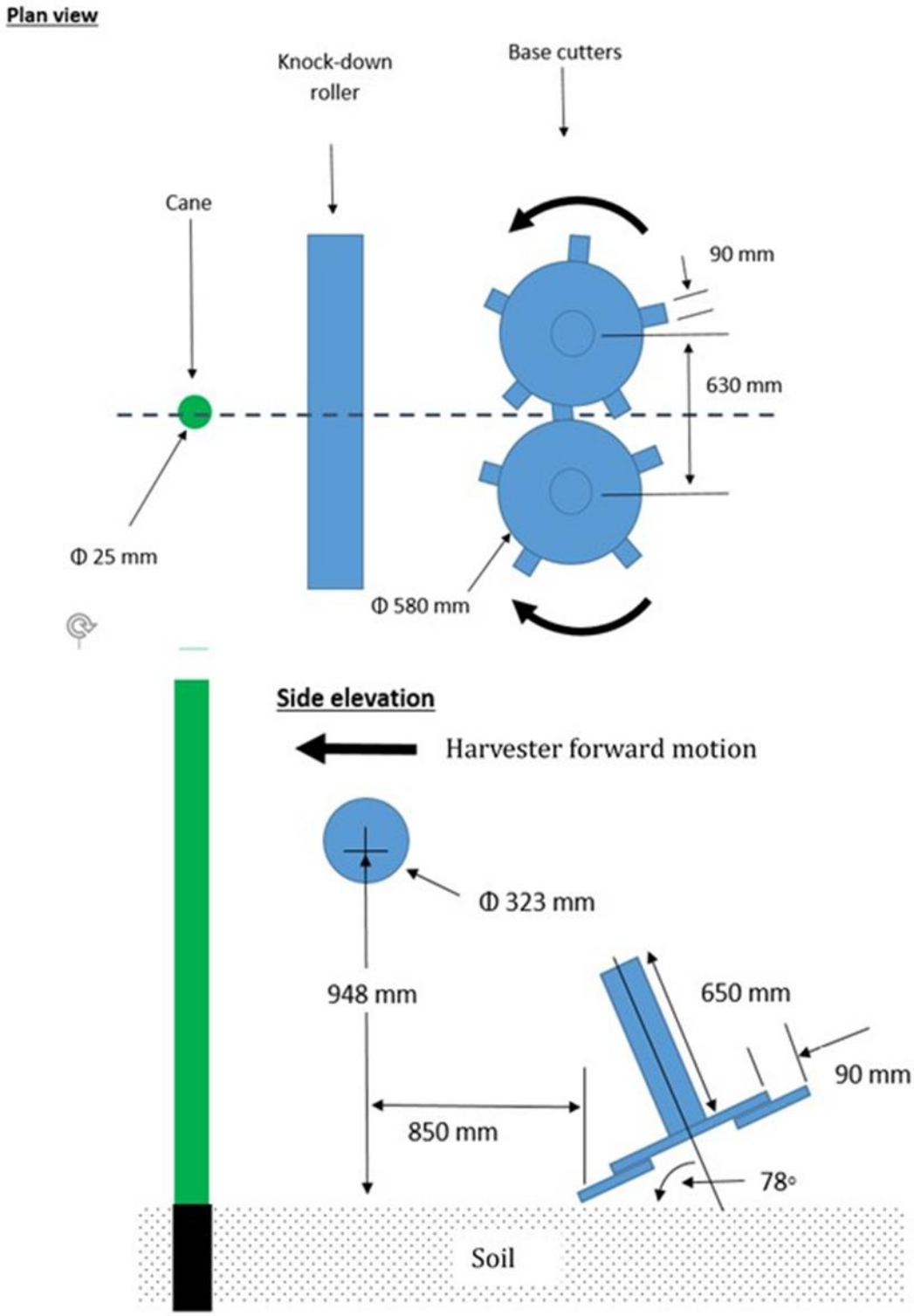

Figure 21: Configuration and dimensions of the modelled components.

The model was created in ANSYS DesignModeller and ANSYS workbench LS-DYNA. A non-uniform FEM mesh was developed and applied such that cells were clustered more closely in regions of expected high stress gradients (Figure 22).

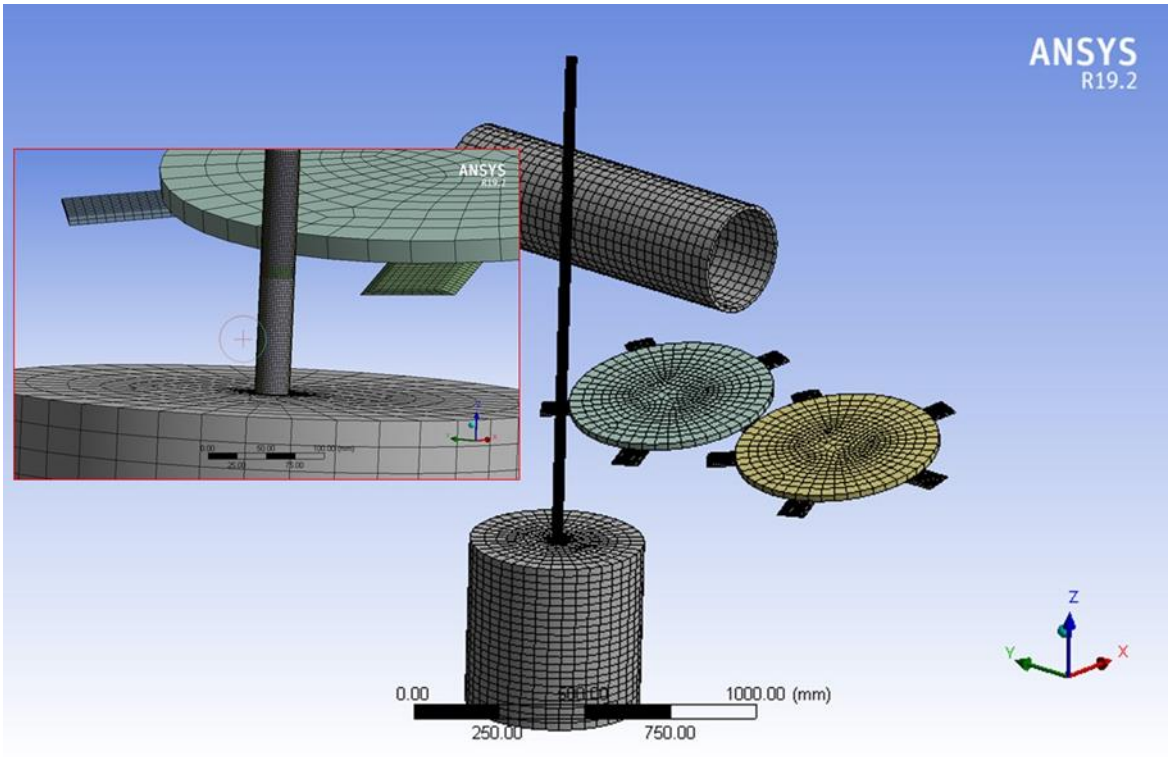

Figure 22: Non-uniform FEA mesh developed in LS-DYNA model (inset shows increased clustering of cells in the above-ground stalk and base cutter blade regions where high stress gradients develop).

A wood-based model was utilised with material properties adjusted (where available) to more closely represent those of cane stalk. The material properties used are given in Table 9**Error! Reference source not found.**.

The model has been run to duplicate the harvester operating conditions associated with the most recent Childers field trials using the harvester forward and basecutter rotational speeds shown in **Error! Reference source not found.**Table 10. For the 'pre-cut' harvester trials (carried out to determine the impact of the forward feeding components on cane damage) the knockdown rollers were removed from the model.

Results and Discussion

The results of the harvester field trials are reported (qualitatively) in terms of damage to the cane stool. Although non-uniform failure of the cane stalk was predicted by the model the degree of damage was more readily inferred from the results by the observed nature of failure and cane loss. Major damage was assumed when small but whole sections of cane were separated from the main stalk while minor damage was assumed when only small cane particles (arising for example from the gouging out of the cane caused by a partial cut) were predicted (Figure 23). If both minor and major damage occurred then this was deemed to be simply major damage.

Table 9: Material properties and factors used in the LS-DYNA cane stalk model.

Property	Value
Parallel normal modulus (MPa)	80
Perpendicular normal modulus (MPa)	80
Parallel shear modulus (MPa)	80
Perpendicular shear modulus (MPa)	47.5
Parallel major Poisson's ratio	0.157
Parallel tensile strength(MPa)	10
Parallel compressive strength(MPa)	10
Perpendicular tensile strength(MPa)	2.05
Perpendicular compressive strength(MPa)	4.08
Parallel shear strength(MPa)	5
Perpendicular shear strength(MPa)	5
Parallel fracture energy in tension (N.mm/mm^2)	2.7
Parallel fracture energy in shear (N.mm/mm^2)	8.3
Parallel softening parameter	30
Parallel maximum damage	0.9999
Perpendicular fracture energy in tension	0.4
Perpendicular fracture energy in shear	0.83
Perpendicular softening parameter	30
Perpendicular maximum damage	0.999
Parallel hardening initiation.	0.5
Parallel hardening rate	400
Perpendicular hardening initiation	0.4
Perpendicular hardening rate	100

Table 10: Harvester basecutter rotation and forward speeds used in simulating the Childers field trials.

Knock-down rollers	No knock-down rollers
450 rpm (4.5 km.h^{-1})	450 rpm (4.5 km.h^{-1})
850 rpm (4.5 km.h^{-1})	850 rpm (4.5 km.h^{-1})
450 rpm (8.5 km.h^{-1})	450 rpm (8.5 km.h^{-1})
850 rpm (8.5 km.h^{-1})	850 rpm (8.5 km.h^{-1})

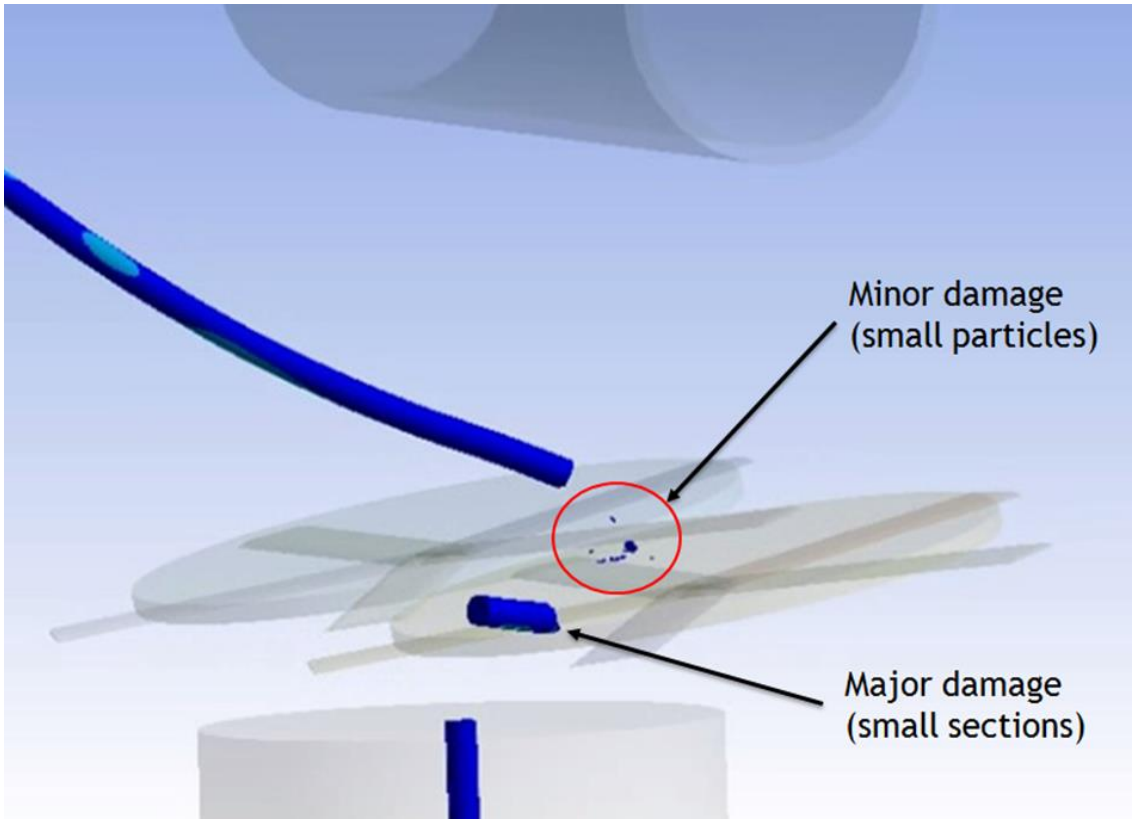

Figure 23: Simulation output showing minor and major loss/ damage.

Comparing predicted damage across the range of harvester conditions associated with the Childers trials it was found that for the given knockdown roller position, the slower blade speed (450 rpm) would produce high levels of damage. Conversely the higher blade speed (850 rpm) would result in only minor damage regardless of the forward speed of the harvester (shown in Figure 23, Figure 24 and Figure 25 respectively).

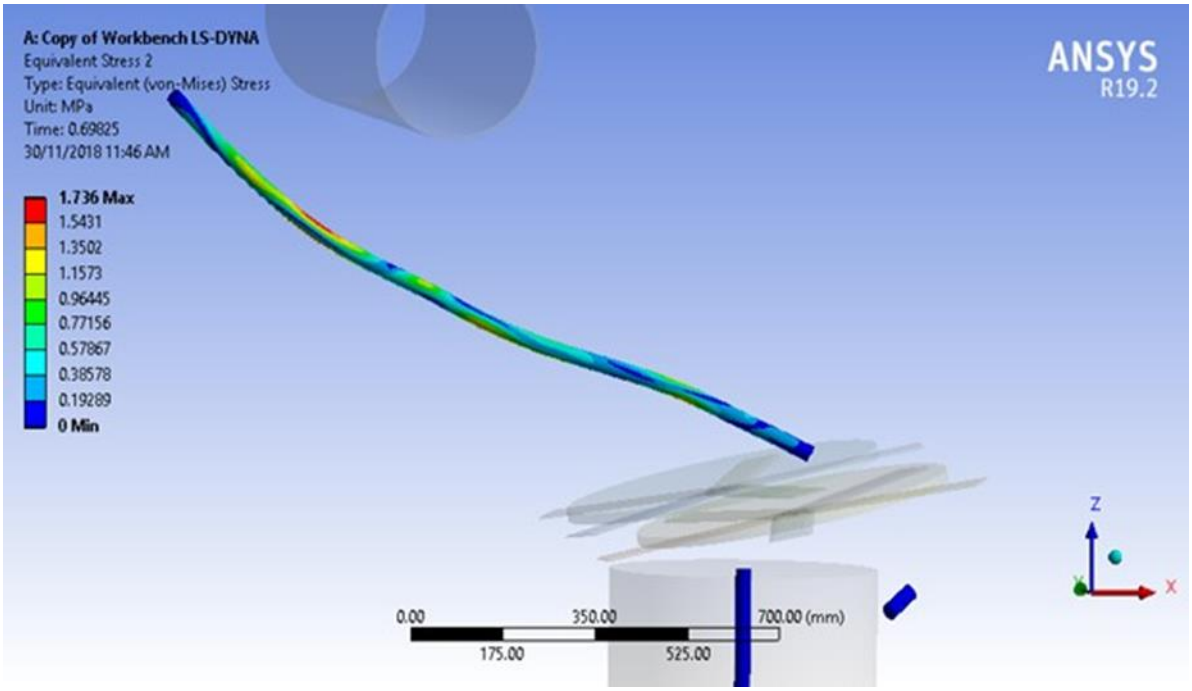

Figure 24: Major damage and cane loss incurred at a low basecutter speed of 450 rpm (standard knockdown roller fitted, harvester forward speed is 4.5 km.h^{-1})

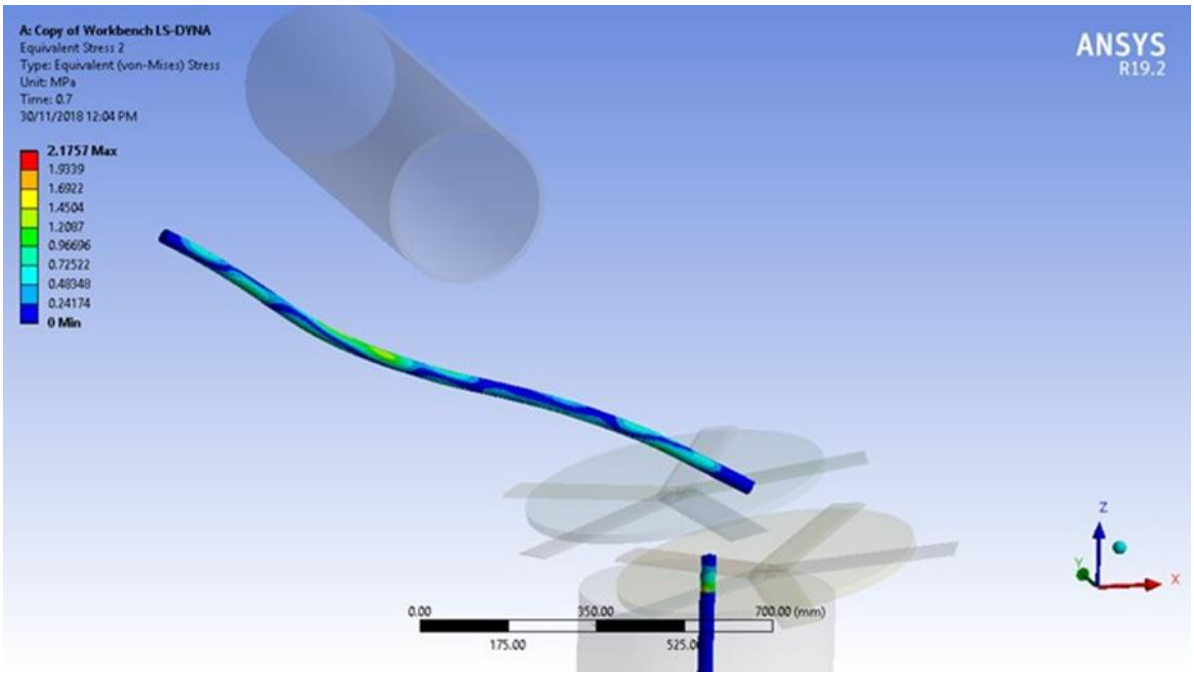

Figure 25: Minor damage and cane loss incurred at a high basecutter speed of 850 rpm (standard knockdown roller fitted, harvester forward speed is 4.5 km.h^{-1})

Minor damage only was predicted for all harvester forward and basecutter speeds for the simulations where the knockdown rollers are removed (corresponding to the 'pre-cut' Childers trials). Figure 26 shows the lack of cane damage predicted at low basecutter speeds as a result of removing the knockdown rollers.

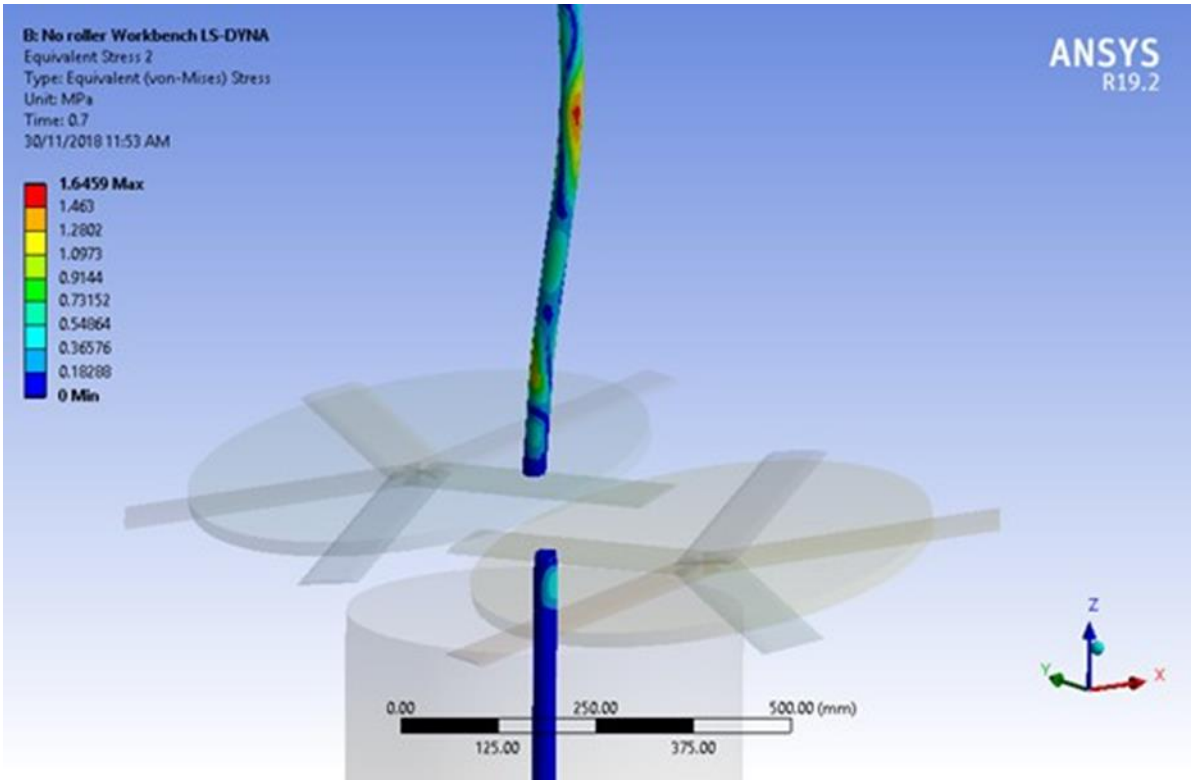

Figure 26: Minor damage and cane loss incurred at a low basecutter speed of 450 rpm as a result of removing the knockdown roller (harvester forward speed is 4.5 km.h^{-1}).

The above simulation results broadly mirror the relative damage levels observed after the Stream 1 Childers field trials, shown in Figure 76 later in this document, where the major damage incurred at a basecutter speed of 850 rpm was significantly less than that produced at 450 rpm regardless of the forward speed of the harvester. Also as previously noted, the major damage at all harvester operating conditions was lower for the 'pre-cut' trials relative to the 'non-pre-cut' field trials; an outcome reflected by the consistently low losses predicted when the knockdown roller is removed.

For the simulations where major damage was predicted (i.e. at the low basecutter speed) if the first blade cut was such that the cane was severed at say 20 mm above the ground (due to the forward tilt of the basecutters), then the acoustic wave (produced by the impacting blade) travelling down into the ground was sufficient to cause the remaining 'stump' to snap off at ground level. This would result in the release and loss of a small section from the base of the stalk thereby causing relatively major cane loss and damage (Figure 24). This rather than multiple cuts appears to be the mechanism for the release of large cane particles (sections). This phenomenon did not occur at the higher basecutter speed and if the first blade cut was above the ground level then the cane would be severed cleanly at the point of impact and the remaining 'stump' left intact and attached to the roots. In a sense this is also cane loss but the cleaner cut (rather than a snapping off at ground level) may result in improved ratooning.

The model at this stage was capable of predicting cane damage (as indicated by cane loss) in broad agreement with the results of the field trials undertaken at Childers. The predictions confirm that higher cane loss and therefore damage occur at relatively lower basecutter speeds regardless of forward harvester speed. These relatively larger losses are caused by the acoustic forces incurred by the impact of the blade rather than multiple cuts. The significance of the knockdown roller as a cause of cane loss also confirms the findings of the 'pre-cut' field trials although this significance is lessened at higher basecutter speeds.

5.6.6. Validation of single stalk model against Kroes Data

The PhD investigation by Kroes (1996) showed that too much bending of the stalk, primarily by the knockdown roller, resulted in breakage of the stalk and a large amount of damage to the stalk and the stool. This conclusion was corroborated by field trials carried out by NorrisECT in stream 1 of this project.

Previous modelling using the finite element code LS-Dyna showed qualitative agreement with the damage measured in the field with and without bending. However, it was judged that it was particularly important that relatively good quantitative agreement of the bending behaviour was required before the interactions of a number of stalks with the front of a harvester could be modelled. As noted, the bending behaviour is particularly important: the shape of the bend stalk, the location of the failure, and the horizontal displacement of the knockdown roller when failure of the stalk occurs. It is noted that the Kroes (1996) experimental data did include some assumptions such as the bending of a metal strip being equivalent to the bending of a cane stalk. This may not be quite right, for example, when localized failure is close to occurring. However, it is judged that the Kroes (1996) data presents the best available information in terms of the theory and calibrations for the test equipment, the experimental program and the detail provided. The base experimental conditions presented were used to calculate properties, calibrate the modelling and should also be used in the future if any further modelling is performed as a check to ensure that no errors are introduced when changes are made.

Bending Behaviour

The bending force / stress / deflection behaviour of interest is described in chapters 7 and 8, including Figure 8.19 of Kroes (Kroes, 1996). The ultimate bending moment allows the calculation of the ultimate bending stress. The data is summarized in Table 11**Error! Reference source not found.**

Table 11: Bending data for a cane stalk (derived from Kroes, 1996).

Key parameters	Intermediate parameters	Parameter values	Units / comments
	bending stress = M y / I		
	cane stalk		
	fibre content (%)	14	
	diameter (mm)	**30**	**c in mm**
	2nd Moment of area (I, mm4)	39761	
	distance from neutral axis to extreme fibre (y, mm)	15	
	Ultimate bending moment (M, Nm)	67	thesis page 8-26, Figure 8.19
	Ultimate bending moment (M, Nmm)	67000	
Ultimate bending stress	**Ultimate bending stress**	**25.3**	**MPa**
	Table 8.2 summary for calibrating deflection		
	Constant of proportionality Ki	7.31	
	Constant of proportionality Ku	5.78	
Initial stiffness	Equation 8.25 EIinitial = 7.31 (c-17)	95.03	where c in mm and EI in Nm^2
	Determine E	**2390**	**MPa**
Final (ultimate) stiffness	Equation 8.26 EIult = 5.78 (c-17.1)	74.56	
	Determine E	**1875**	**MPa**
Final stiffness in terms of initial stiffness	EIult = 0.8 x EIinitial (Equation 8.28)	76.02	
	Figure 8.45 Mu / f = .507 c - 8.12		c in mm, f in %, Mu in Nm
Ultimate bending moment range	Mu = (0.507 c -8.12) f	99.26	(N.m), for the node
	Mu = (0.286 c - 3.49) f	71.26	(N.m), for the internode
Ultimate fibre strain for cane stalks (failure at the nodes)			
Fibre strain for less than 15% of stalks to fail		1.62	(%) Kroes and Harris, 1996 ASSCT
		1.57	(%), p13-7 of thesis, **adopted**

The instrumented steel beam used as a cantilever by Kroes (1996) is shown in Figure 27. The distance P between a support and a 'knockdown roller' is shown. Two values for P (250 mm and 1000 mm) were chosen to represent the range of situations in the field. Using the determined value

of fibre strain for less than 15% of stalks to fail, 1.57%, the acceptable horizontal deflection limits for the knockdown roller were calculated and are shown in Table 12.

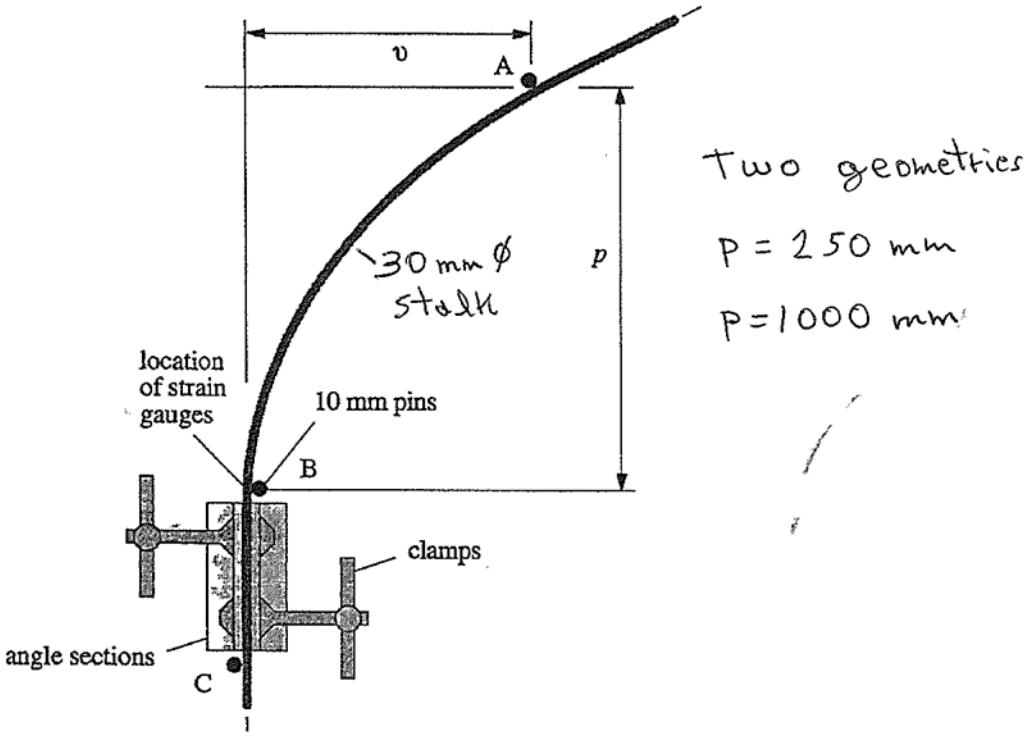

Figure 27: Instrumented steel beam used as a cantilever by Kroes (1996) showing deflection geometry.

Table 12: Acceptable horizontal deflection limits for the knockdown roller (derived from Kroes, 1996).

P (mm)	Horizontal deflection limit for 'knock down roller' (mm)
250	31
1000	588

Notes of significance from Kroes (1996):

1. Page 8-25: "as discussed in chapter 7 the stalks remain almost elastic until rupture, though as the deflection increases they progressively reduce in stiffness".
2. Page 13-2: "The stalks tend to fail at a node in the field".
3. Page 13-2: "Supported by the previous arguments it is assumed that the ultimate strains determined for the nodes during the bending experiments are indicative of stalks in the field. The mean ultimate strain for sugarcane stalks is therefore 1.77%".
4. Sect 8.10: "Strain rate (rate of applied deflection) did not change the models of failure or the damage sustained by the stool or stalk to a noticeable degree. This held true for all failure locations investigated".

The wood material model (model number 143) in the LS-Dyna documentation (Anon., 2005) (Anon., 2007) was used to model the behaviour of the cane stalk. The stalk did not include nodes with different material properties as the provided material property values are those calculated from failure at the nodes. Starting with the derived Kroes (1996) values, a range of simulations was

carried out with changes to material parameters to reproduce the deflections at 1.57% fibre strain. The two ranges of input data are given in Table 13. It is noted that there are a significant number of material parameters which have not been measured for cane stalks and the values given are those from the wood model. Some values have been modified in the second column to achieve better agreement with the measurements, using guidance from the LS-DYNA literature. The achieved agreement with the measurements is also shown in Table 13. It is concluded that modification of the values of the fracture energy and softening parameter between the values in the two columns will result in an adequate representation of the bending behaviour in the harvesting process.

Plots of the predicted bending stress and strain just before failure are shown in Figure 28 and Figure 29 respectively, while Figure 30 shows the predicted bending stress during failure for the material parameters in the second column in Table 13 for P=250 mm.

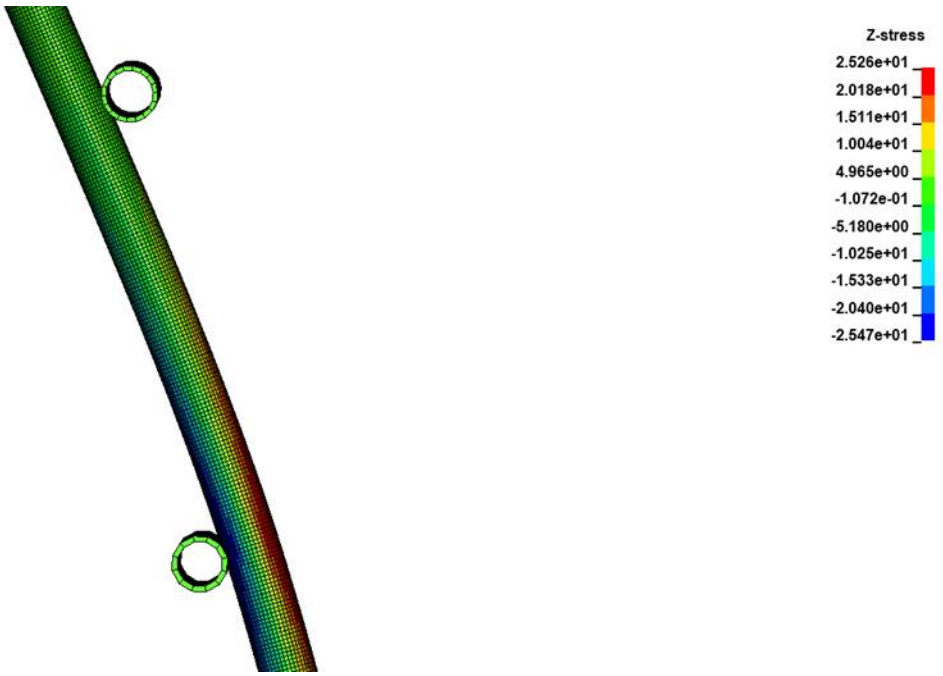

Figure 28: Predicted bending stress (MPa) just before failure.

Table 13: Range of input data for wood model and predictions of bending.

Parameter	Limit 1 values	Limit 2 values
Density (kg/m^3)	573	573
Parallel normal modulus (MPa)	2390	3158
Perpendicular normal modulus (MPa)	2390	3158
Parallel shear modulus (MPa)	2390	3158
Perpendicular shear modulus (MPa)	2390	3158
Parallel major Poisson's ratio	0.157	0.157
Parallel tensile strength (MPa)	25.3	25.3
Parallel compressive strength (MPa)	25.3	25.3
Perpendicular tensile strength (MPa)	25.3	25.3
Perpendicular compressive strength (MPa)	25.3	25.3
Parallel shear strength (MPa)	25.3	25.3
Perpendicular shear strength (MPa)	25.3	25.3
Parallel fracture energy in tension (N.mm/mm^2)	15.3	2
Parallel fracture energy in shear (N.mm/mm^2)	15.3	2
Parallel softening parameter	30	10
Parallel maximum damage	0.9999	0.9999
Perpendicular fracture energy in tension (N.mm/mm^2)	15.3	2
Perpendicular fracture energy in shear (N.mm/mm^2)	15.3	2
Perpendicular softening parameter	30	10
Perpendicular maximum damage	0.99	0.99
Parallel hardening initiation.	0.5	0.5
Parallel hardening rate	400	400
Perpendicular hardening initiation	0.4	0.4
Perpendicular hardening rate	100	100
Objectives – knockdown roller horizontal displacement		
31 mm for P=250 mm		
displacement when yield stress reached	37	31.9
displacement at failure	80	39.8
588 mm for P=1000 mm		
displacement when yield stress reached	380	286
displacement at failure	>850	359

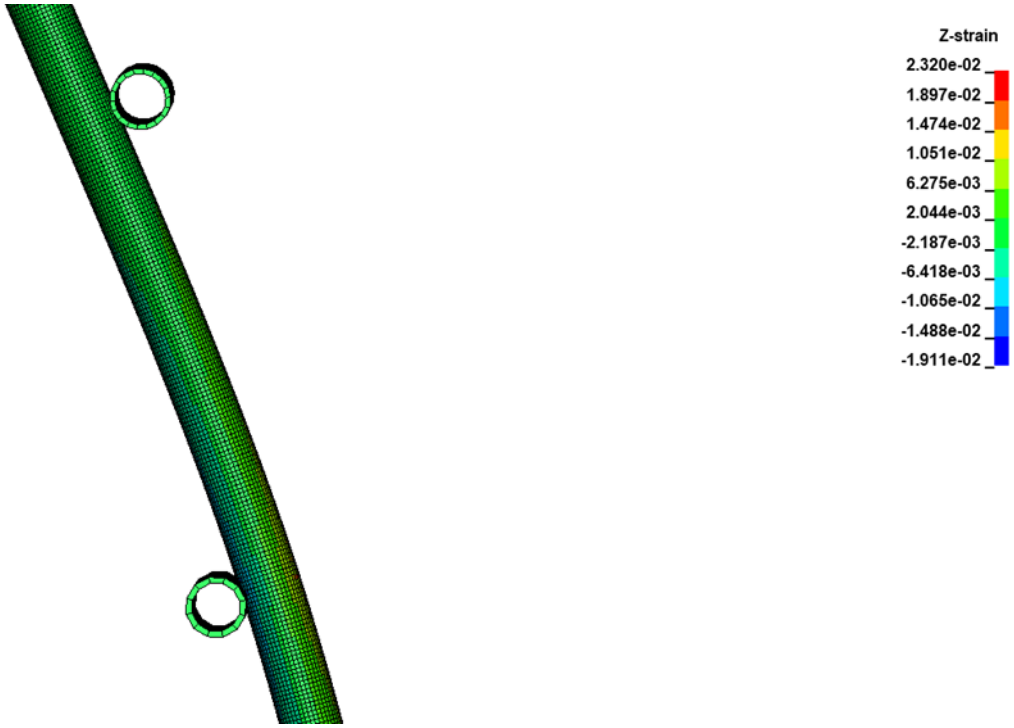

Figure 29: Predicted bending strain just before failure.

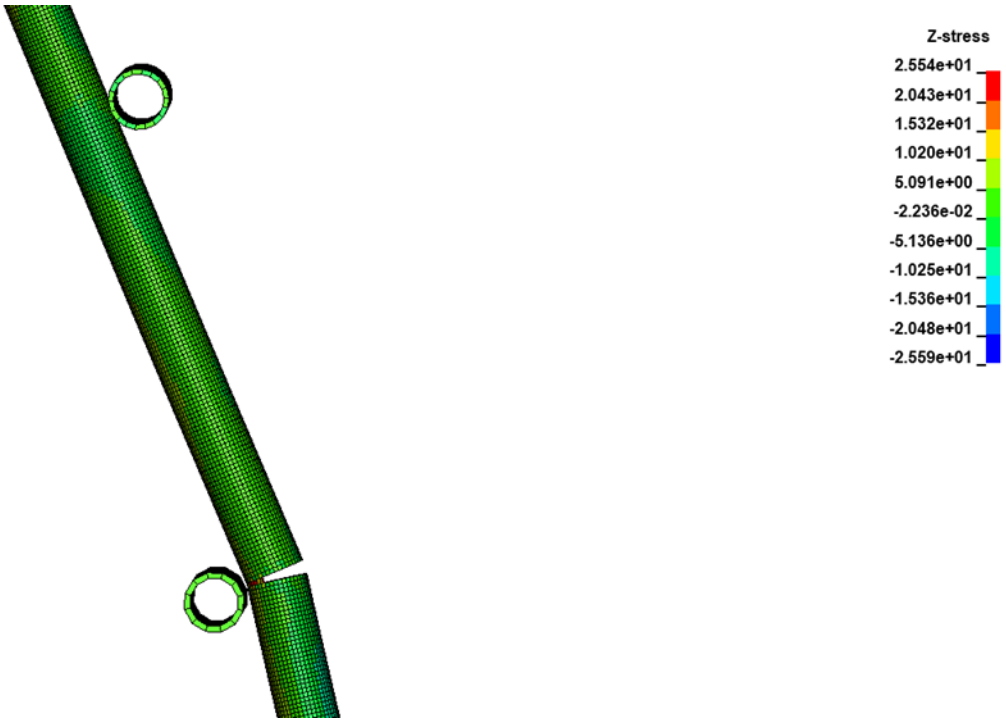

Figure 30: Predicted bending stress during failure.

Cutting Behaviour

Cutting behaviour is considered secondary to the bending behaviour to model the overall behaviour of the front of the harvester with the objective of feeding while reducing the damage due to bending of the stalks. However, it is still important for determining the forces involved in the cutting process and the predicted damage to the stalk and stool with changed geometry and operating parameters.

The description of the experimental equipment, test procedure and range data for the cutting by a single blade of a single stalk is given in chapters 10 and 11 of Kroes (1996). The equipment is shown in his Figure 10.4, Figure 10.5c, and also Figure 3 from Kroes and Harris (1996), reproduced here in Figure 31, Figure 32 and Figure 33 respectively. The data chosen for comparison was that given in Chapter 11 of Kroes (1996), with p=35 mm and q=310 mm, and with no knockdown. An example of the force trace is given in Kroes' Figure 11.2, with a peak force measured of approximately 400 N.

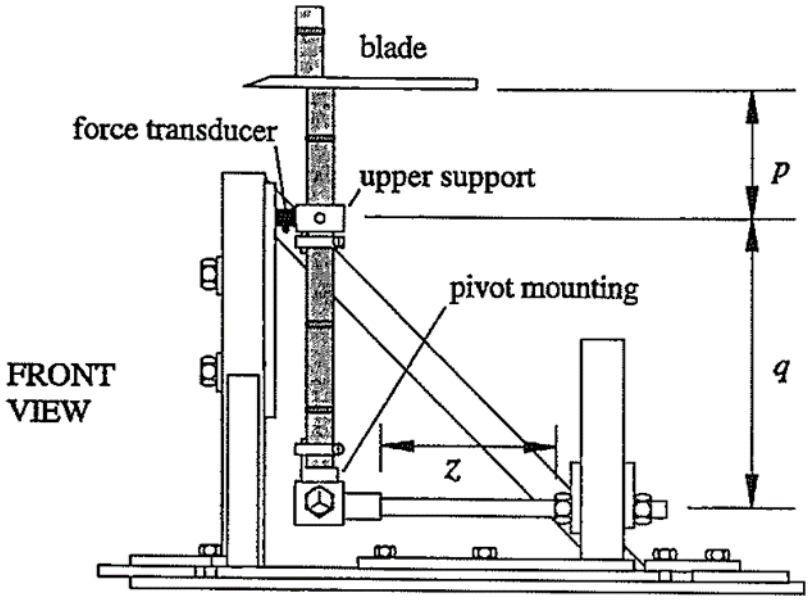

Figure 31: Cutting equipment by a single blade of a single stalk in Kroes (1996).

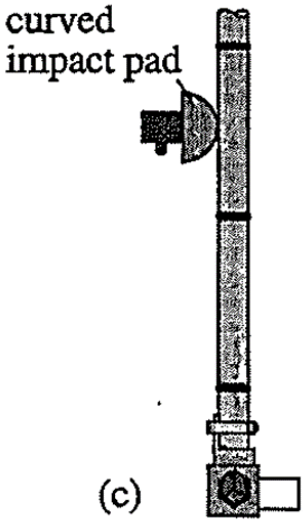

Figure 32: Cutting equipment by a single blade of a single stalk in Kroes (1996) – stalk support.

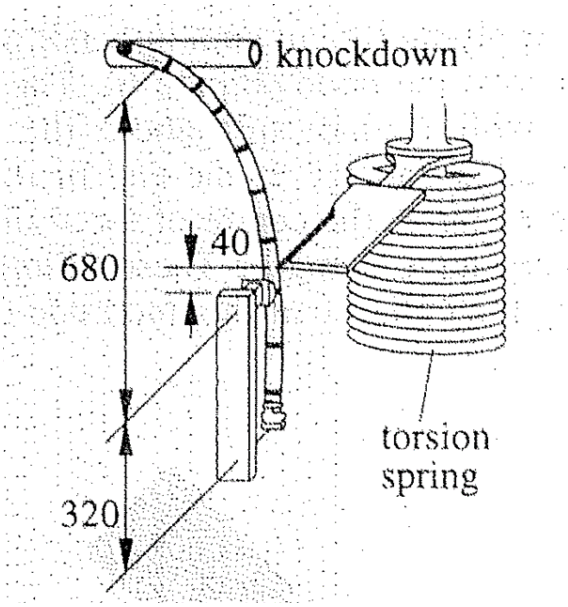

Figure 33: Cutting equipment by a single blade of a single stalk in Kroes (1996) – sample dimensions.

An LS-DYNA model for reproducing the Kroes (1996) cutting rig is shown in Figure 36. The model adopted the curved impact pad support as shown in Figure 32. In order to progress towards an acceptable prediction of cutting, the modelling started with the material properties shown in Table 14, which achieved a relatively good reproduction for bending.

The next step was to adopt Table 1 from Handong *et al.* (2011), reproduced here as Table 14. The ratio of the radial to axial properties was calculated, and then averaged between the cane core and the cane skin. These ratios were applied to the axial values given in Table 13 to calculate the radial properties and those values are shown in

Table 15: Adopted input data for wood model and predictions for cutting.

Parameter	Adopted values
Density (kg/m^3)	573
Parallel normal modulus (MPa)	3390
Perpendicular normal modulus (MPa)	615
Parallel shear modulus (MPa)	680
Perpendicular shear modulus (MPa)	175
Parallel major Poisson's ratio	0.4055
Parallel tensile strength (MPa)	25.3
Parallel compressive strength (MPa)	25.3
Perpendicular tensile strength (MPa)	3.2
Perpendicular compressive strength (MPa)	3.2
Parallel shear strength (MPa)	5.0
Perpendicular shear strength (MPa)	5.0
Parallel fracture energy in tension (N.mm/mm^2)	12.7
Parallel fracture energy in shear (N.mm/mm^2)	18.3
Parallel softening parameter	30

Parallel maximum damage	0.9999
Perpendicular fracture energy in tension	0.4
Perpendicular fracture energy in shear	0.83
Perpendicular softening parameter	30
Perpendicular maximum damage	0.99
Parallel hardening initiation.	0.5
Parallel hardening rate	400
Perpendicular hardening initiation	0.4
Perpendicular hardening rate	100
Objective 31 mm for P=250 mm	
displacement when yield stress reached	41
displacement at failure	44
Objective 588 mm for P=1000 mm	
displacement when yield stress reached	400
displacement at failure	435

. The average of Poisson's ratio between the core and the skin was calculated and adopted. The calculation was not completely consistent as, after inspection of the previous bending modelling results, the Parallel Normal Modulus (the bending Young's Modulus) was increased from 2390 to 3390 MPa. However, the adopted updated material properties are shown in

Table 15: Adopted input data for wood model and predictions for cutting.

Parameter	Adopted values
Density (kg/m^3)	573
Parallel normal modulus (MPa)	3390
Perpendicular normal modulus (MPa)	615
Parallel shear modulus (MPa)	680
Perpendicular shear modulus (MPa)	175
Parallel major Poisson's ratio	0.4055
Parallel tensile strength (MPa)	25.3
Parallel compressive strength (MPa)	25.3
Perpendicular tensile strength (MPa)	3.2
Perpendicular compressive strength (MPa)	3.2
Parallel shear strength (MPa)	5.0
Perpendicular shear strength (MPa)	5.0
Parallel fracture energy in tension (N.mm/mm^2)	12.7
Parallel fracture energy in shear (N.mm/mm^2)	18.3
Parallel softening parameter	30
Parallel maximum damage	0.9999
Perpendicular fracture energy in tension	0.4
Perpendicular fracture energy in shear	0.83
Perpendicular softening parameter	30
Perpendicular maximum damage	0.99
Parallel hardening initiation.	0.5
Parallel hardening rate	400

Perpendicular hardening initiation	0.4
Perpendicular hardening rate	100
Objective 31 mm for P=250 mm	
displacement when yield stress reached	41
displacement at failure	44
Objective 588 mm for P=1000 mm	
displacement when yield stress reached	400
displacement at failure	435

. The updated values for the horizontal movement of the 'knockdown roller' are also provided in

Table 15: Adopted input data for wood model and predictions for cutting.

Parameter	Adopted values
Density (kg/m^3)	573
Parallel normal modulus (MPa)	3390
Perpendicular normal modulus (MPa)	615
Parallel shear modulus (MPa)	680
Perpendicular shear modulus (MPa)	175
Parallel major Poisson's ratio	0.4055
Parallel tensile strength (MPa)	25.3
Parallel compressive strength (MPa)	25.3
Perpendicular tensile strength (MPa)	3.2
Perpendicular compressive strength (MPa)	3.2
Parallel shear strength (MPa)	5.0
Perpendicular shear strength (MPa)	5.0
Parallel fracture energy in tension (N.mm/mm^2)	12.7
Parallel fracture energy in shear (N.mm/mm^2)	18.3
Parallel softening parameter	30
Parallel maximum damage	0.9999
Perpendicular fracture energy in tension	0.4
Perpendicular fracture energy in shear	0.83
Perpendicular softening parameter	30
Perpendicular maximum damage	0.99
Parallel hardening initiation.	0.5
Parallel hardening rate	400
Perpendicular hardening initiation	0.4
Perpendicular hardening rate	100
Objective 31 mm for P=250 mm	
displacement when yield stress reached	41
displacement at failure	44
Objective 588 mm for P=1000 mm	
displacement when yield stress reached	400
displacement at failure	435

. A significantly improved prediction in bending was achieved.

Table 14: Mechanical properties of the stubble of sugarcane stalk (reproduced Table 1 from Handong *et al.* (2011)).

Mechanical Index	Cane core/MPa	Cane skin/MPa
Axial tensile strength	6.71	47.02
Radial tensile strength	1.34	2.57
Axial compressive strength	14.47	101.40
Radial compressive strength	2.32	4.45
In-plane shear strength	0.45	2.25
Axial elastic modulus	1514.8	10614.89
Radial elastic modulus	612.5	1174.72
Shear modulus of elasticity	10.82	54.1
Poisson's ratio	0.467	0.344

Table 15: Adopted input data for wood model and predictions for cutting.

Parameter	Adopted values
Density (kg/m^3)	573
Parallel normal modulus (MPa)	3390
Perpendicular normal modulus (MPa)	615
Parallel shear modulus (MPa)	680
Perpendicular shear modulus (MPa)	175
Parallel major Poisson's ratio	0.4055
Parallel tensile strength (MPa)	25.3
Parallel compressive strength (MPa)	25.3
Perpendicular tensile strength (MPa)	3.2
Perpendicular compressive strength (MPa)	3.2
Parallel shear strength (MPa)	5.0
Perpendicular shear strength (MPa)	5.0
Parallel fracture energy in tension (N.mm/mm^2)	12.7
Parallel fracture energy in shear (N.mm/mm^2)	18.3
Parallel softening parameter	30
Parallel maximum damage	0.9999
Perpendicular fracture energy in tension	0.4
Perpendicular fracture energy in shear	0.83
Perpendicular softening parameter	30
Perpendicular maximum damage	0.99
Parallel hardening initiation.	0.5
Parallel hardening rate	400
Perpendicular hardening initiation	0.4
Perpendicular hardening rate	100
Objective 31 mm for P=250 mm	
displacement when yield stress reached	41
displacement at failure	44
Objective 588 mm for P=1000 mm	
displacement when yield stress reached	400

displacement at failure	435

Following the updating of the material parameters, the next step was to carry out calculations, predictions and comparison with the Kroes (1996) force measurement. The modelled geometry is shown in Figure 34 and Figure 35. The detail of the geometry is shown in Table 16. A blunt edge of 1 mm was built into the basecutter blade. For a model in which the stalk mesh is greater than 1 mm, it was expected that the 1 mm blunt edge would make little difference to the prediction. However, the edge was added as an option that could be modified in future modelling. The modelled rotational speed of the blade was 496 rpm. Further model views are shown in Figure 36 and Figure 37.

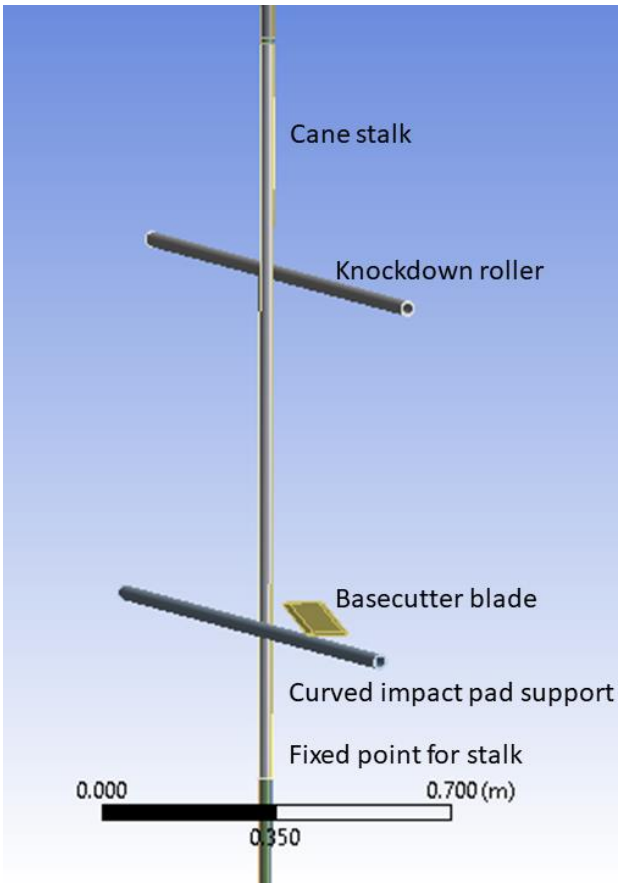

Figure 34: Geometry for reproducing Kroes (1996) cutting rig (dimensions in Table 16**).**

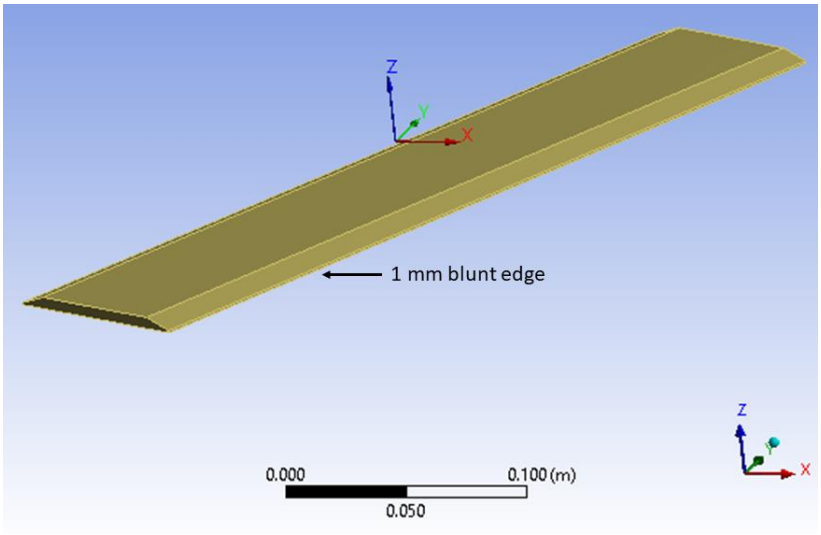

Figure 35: Geometry of the modelled basecutter blade (dimensions in Table 16 **)**

Table 16: Geometry dimensions for reproducing Kroes (1996) cutting rig for P = 715 mm.

Parameter	(mm)
Distance from fixed point of stalk to centreline of impact pad support	310
Distance from fixed point of stalk to top surface of basecutter blade	345
Distance from fixed point of stalk to centreline of knockdown roller	1025
Basecutter blade thickness	5
Basecutter blade bottom surface width	84
Basecutter top surface width	60
Basecutter blade blunt edge height	1
Basecutter blade length	384

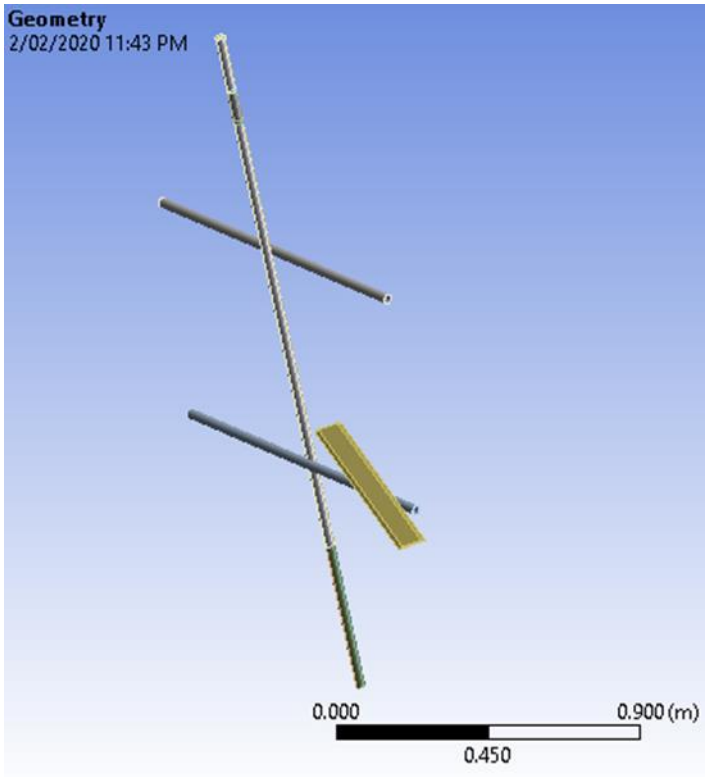

Figure 36: LS-DYNA Model for reproducing Kroes (1996) cutting rig.

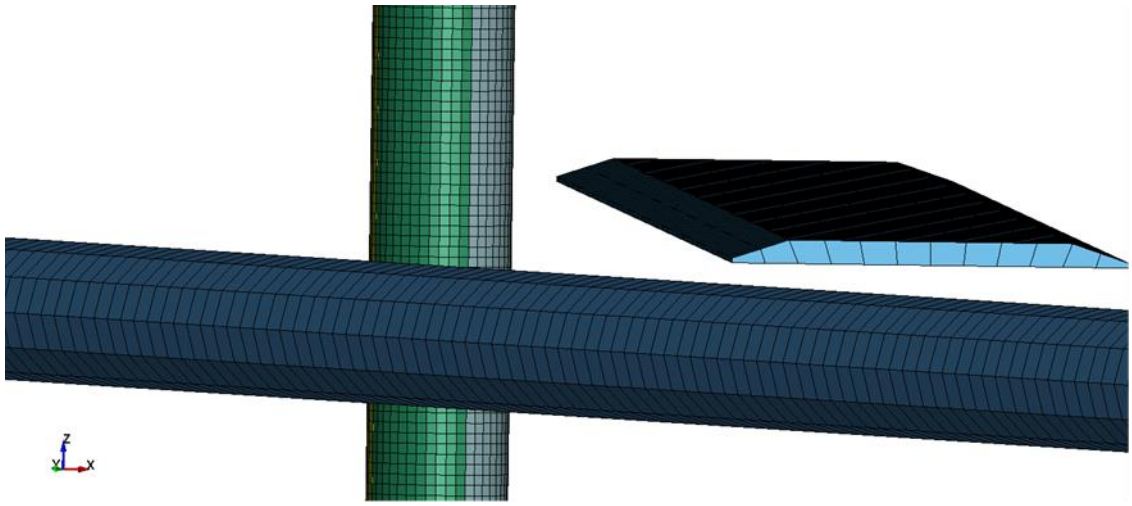

Figure 37: LS-DYNA Model for reproducing Kroes (1996) cutting rig (close-up at cutting plane).

A shear area calculation was also carried out. It was determined that, if a single failure plane formed in the stalk due to cutting, the shear strength would be 0.7 MPa. The Parallel Shear Strength and Perpendicular Shear Strength values were changed to 0.7 MPa. It is noted that, if a slice was removed by the blade, two shear areas would form and the shear strength value for the stalk would actually be 0.35 MPa.

The modelling of the cutting mechanism required more than just the material parameters. An additional command in LS-Dyna called MAT_ADD_EROSION had to be activated. This option allows the input into the model of additional failure criteria. After some significant work, it was determined that a plastic strain of 0.2 and an average strength of 5 MPa would combine with the material

parameters in the Wood model to provide prediction of cutting behaviour similar to that measured by Kroes (1996). The cutting prediction (with Von Mises stress) is shown in Figure 38 and a predicted trace of the cutting force is shown in Figure 39.

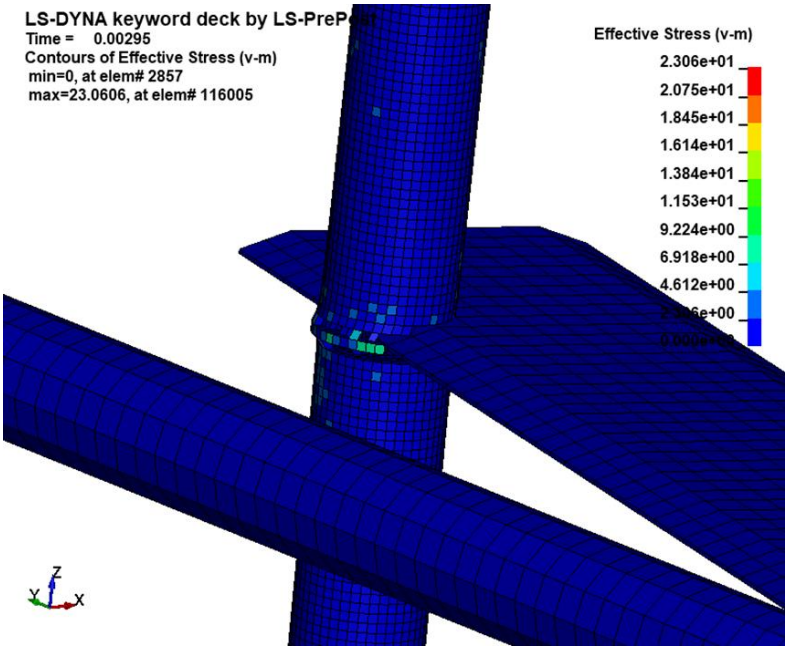

Figure 38: Cutting prediction for cane stalk without bending.

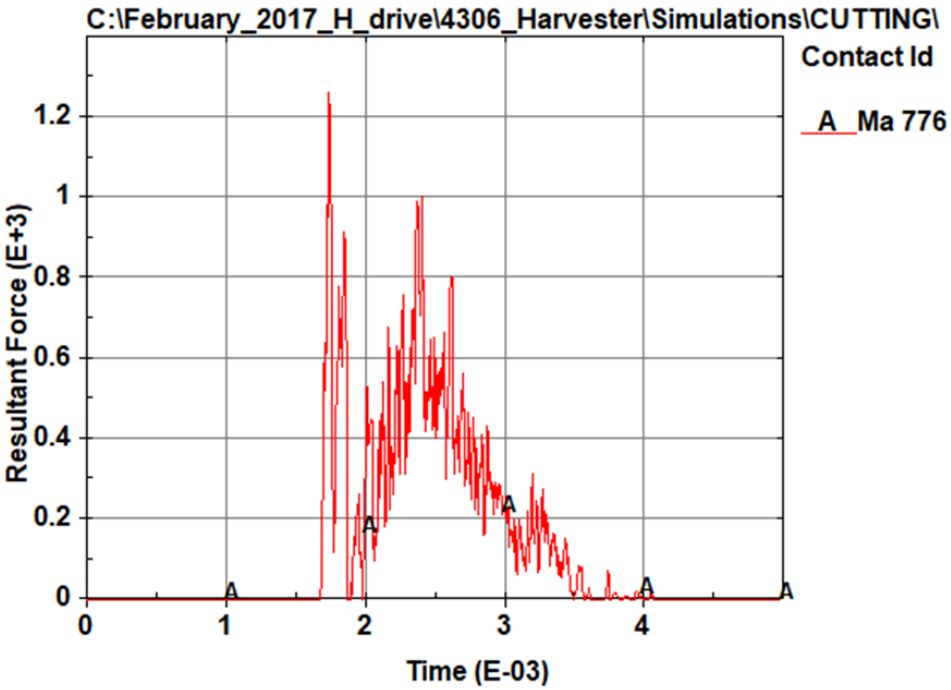

Figure 39: Predicted trace for the cutting prediction for cane stalk without bending.

Combined Bending and Cutting Behaviour

It was judged that it was important for the stalk model to be able to simulate combined bending and cutting behaviour (with the bending behaviour taking priority). However, there is a complication in that the bending of a stalk induces both bending stress and shear stress in the stalk. This is a different shear stress than the shear stress caused by the impact of the basecutter blade. A calculation of both the bending moment diagram and the shear stress diagram was carried out for an approximated simply supported beam 500 mm long and loaded by a point load in the middle. It was calculated that the shear stress caused by the 'knockdown roller' bending the stalk, when the stalk reaches the bending stress at which it fails, is actually somewhat higher than the cutting action shear strength calculated previously. The repercussion of this is that, if shear strengths of either 0.35 MPa or 0.7 MPa, as determined in page 72 above, are input into the Wood model as described in Table 15 **Table 14Error! Reference source not found.**, the stalk would fail in shear while it was undergoing bending by the knockdown roller. This behaviour is not realistic as shown by Kroes (1996) in his bending tests.

To ensure a realistic bending and cutting behaviour, the shear strengths for the stalk were changed to 1.0 MPa, somewhat higher than the shear stress induced during bending. The average strength in the MAT_ADD_EROSION additional command was changed to 20 MPa. This combination was found to provide a relatively realistic force prediction, although higher than that measured. The cutting prediction is shown in Figure 40. Interestingly the simulation predicted the removal of a slice of cane from the stalk. The force trace is shown in Figure 41 while Figure 42 shows a filtered force trace through a 60 Hz filter. It was judged that the predictions were adequate to progress to a more complicated model of the actual harvester.

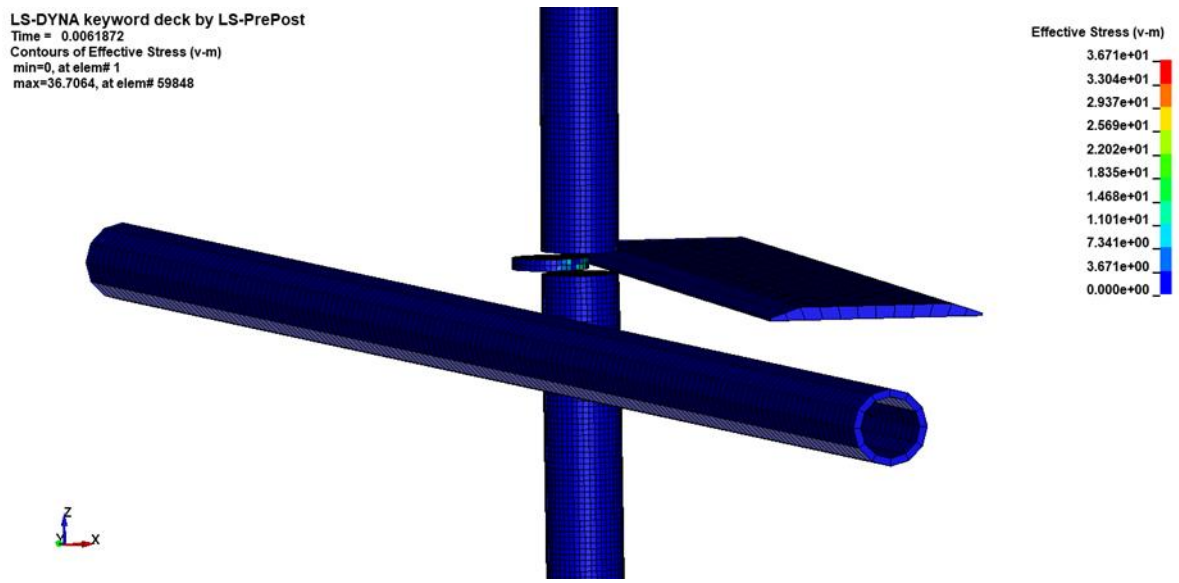

Figure 40: Cutting prediction for cane stalk without bending for modified parameters.

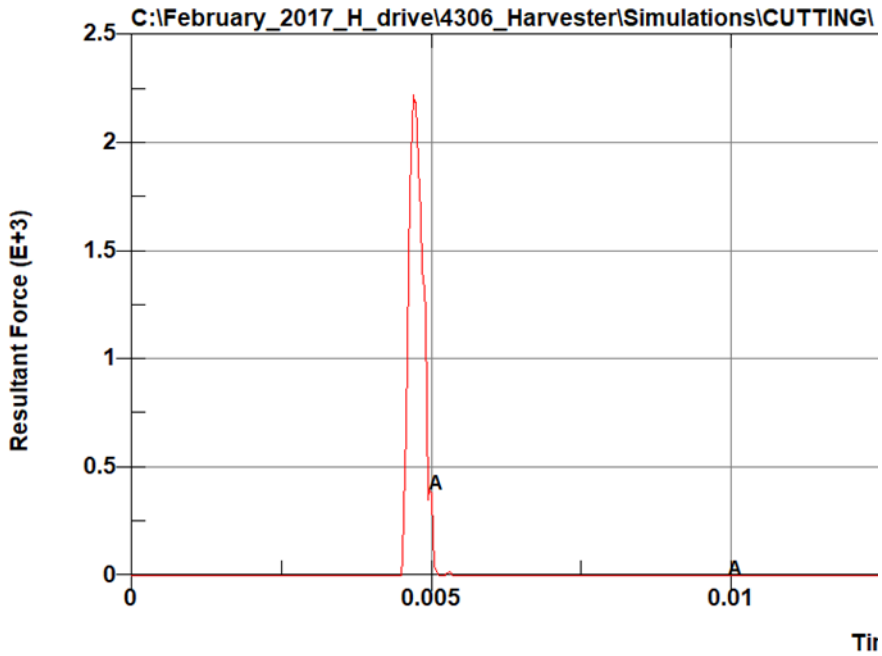

Figure 41: Predicted trace for the cutting prediction for cane stalk without bending for modified parameters.

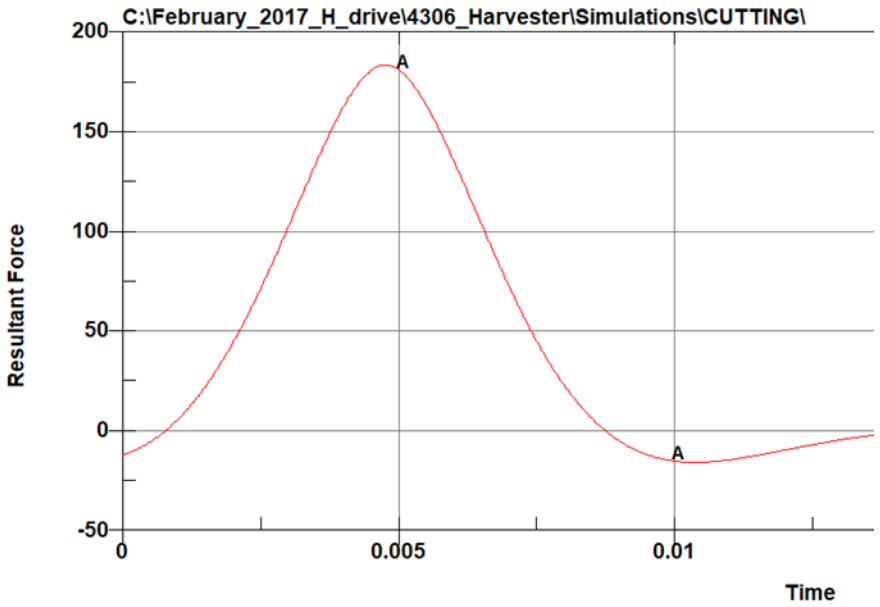

Figure 42: Predicted trace for the cutting prediction for cane stalk without bending for modified parameters.

The calculations and modelling for simulating bending of the stalk by the knockdown roller, and cutting by the basecutter blade, with the same set of material parameters, took a large amount of time and resources. It was judged that it was important for further modelling that this capability be developed, as well as resulting in a significantly improved understanding of the physical processes involved and the capabilities and limitations of LS-DYNA.

Extension of single stalk model to include environmental factors, including soil and trash energy damping, the root system and soil, and heterogeneous and non-isotropic cane properties, including nodes.

Soil Models

LS-Dyna has many models for modelling the behaviour of soil including:

1. Model 025, Geologic Cap model (Anon., 2017)
2. Model 145, Schwer-Murray Cap geological model, which is an extension of model 025 (Geologic Cap model) (Anon., 2017)
3. Model 159 a Continuous Surface Cap model (CSCM) which is an extension of Model 145, (Schwer-Murray Cap geological model) (Anon., 2017)
4. Model 147, The Federal Highway Administration's (FHWA) soil model (Anon., 2004)

The original aim for the development of Model 147 was to model soil under low or no confinement. Specifically, it was developed to predict the dynamic performance of the foundation soil in which roadside safety structures are mounted when undergoing a collision by a motor vehicle. It is therefore relevant to modelling the soil directly underneath sugarcane as large forces are imparted to the sugarcane by the harvester's knockdown roller and other components. The model is a modified Drucker-Prager plasticity model, and includes pre-peak hardening, post-peak strain softening (damage occurring), strain rate effects (strength enhancement), pore-water effects (moisture effects), and erosion capability (for example, particles or parts of the soil being pushed aside or breaking off main body of soil. These enhancements to the standard soil material models were made to increase the accuracy, robustness, and ease of use for roadside safety applications (Anon., 2004). It is an isotropic material with damage and has a modified Mohr-Coulomb surface.

Model 159 has a smooth (continuous) surface and is a concrete model primarily developed to simulate the deformation and failure of concrete on roadside safety structures impacted by vehicles. Although it is noted to be developed for concrete, the LS-DYNA manual (2004) notes that it is recommended to be used instead of model 145 (the Schwer-Murray Cap geological model). Model 145 was developed for geomaterials including soils, concrete and rocks. Model 159 has a Cap surface which can change in size and this feature distinguishes Model 159 from model 147.

Model 147 has been adopted for the soil model for the cane stalk support modelling. Model 159 can easily be substituted in its place.

The key material parameters for model 147 are shown in Table 17. The material model has been initially exercised. A deformed soil pushed by the bending stalk is shown in Figure 43. The deformation of the soil absorbs energy and therefore provides damping to the stalk.

Table 17: Key input data for soil material model 147 (FHWA) and predictions.

Parameter	Values
Density (kg/m^3)	2350
Bulk modulus (MPa)	3250
Shear modulus (MPa)	1300
Maximum friction angle (degrees)	20 (loose) to 50 (dense)
Residual friction angle (degrees)	5 (low) to 10 (high)
Cohesion (kPa)	5 (low compaction) to 90 (high compaction)

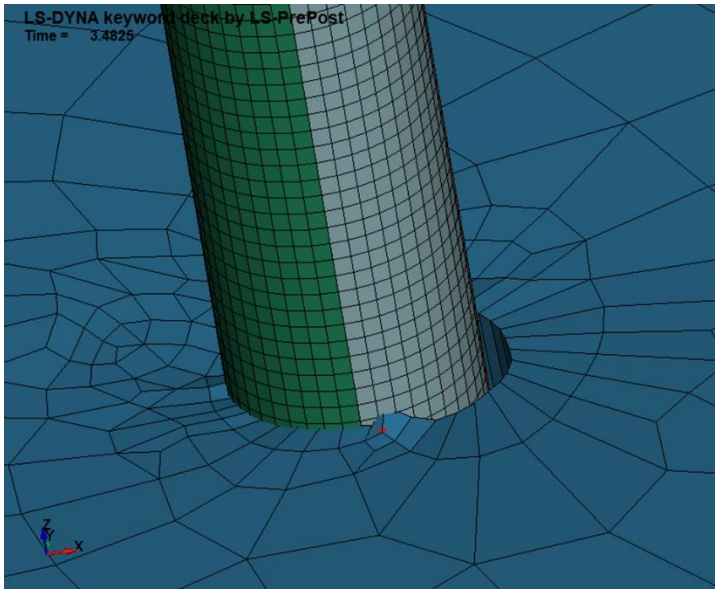

Figure 43: Deformation of soil by bending stalk.

Addition of root system

It was judged that the geometry of the root system should be relatively simple while allowing the soil to deform and provide a range of supports to the stalk by adjusting its bulk and shear moduli, cohesion strength and shear strength. There would be little gain in a complicated root system for modelling the cane stalk behaviour and harvester performance, and a complicated root system would result in a heavy computing load. The geometry adopted was a hollow cone with vertical sides at the bottom, as shown in Figure 44 with the dimensions shown in Figure 45.

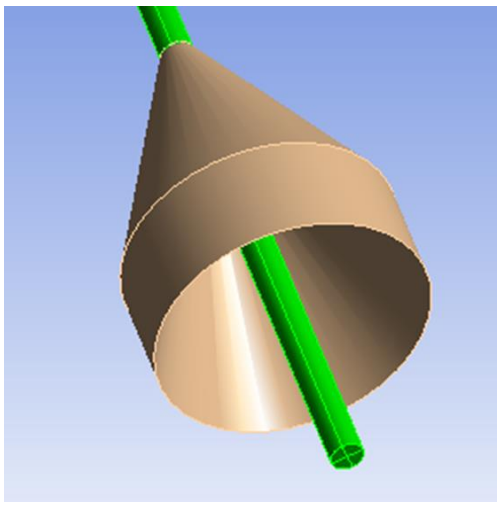

Figure 44: Root cone model.

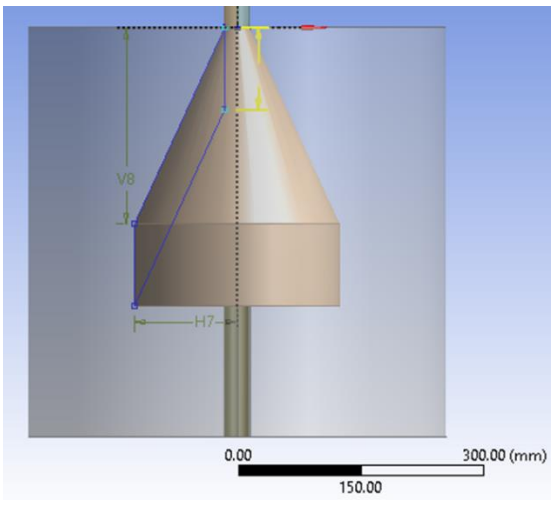

Figure 45: Root cone geometry dimensions.

H5=15mm, H7=125mm, V6=100mm, V8=240mm,

The model for the root was a simple elasto-plastic model similar to that for steel. A bonded contact option was adopted to connect the root surfaces to the soil surfaces. The cone was made of solid elements. The model was exercised and shown to solve. However, use of shell elements for the cone would be preferable and this is a minor modification to the existing model.

Addition of leaves to the stalk

Leaves were added to the cane stalk to represent damping and also provide interaction with the harvester components in the future. The leaf properties are shown in Table 18. Young's Modulus was calculated following G = E / (2 x (1+v)) (Popov, 1978). The tensile strength and shear strength were adopted from MacAdam and Mayland (2003). The leaves were built as 1 mm thick using shell elements with the wood material model as per the stalk. Nodes were included at the location where the leaves attach. A sketch of the dimensions is shown in Figure 46. A close-up of the detail of the stalk with nodes and leaves is shown in Figure 47. Figure 48 to Figure 50 show a progression of the predicted bending. The wood model for the cane stalk and the leaves has the capability of applying heterogeneous and non-isotropic cane properties, including at the nodes.

Table 18: Leaf properties (Plaza & Hobson, 2011) [a].

Parameter	Value
Poisson's ratio [a]	0.1
Shear modulus (kPa) [a]	6000
Density (kg/m^3) [a]	1023
Young's Modulus (kPa)	13200
Tensile strength (kPa)	8000
Shear strength (kPa)	8000

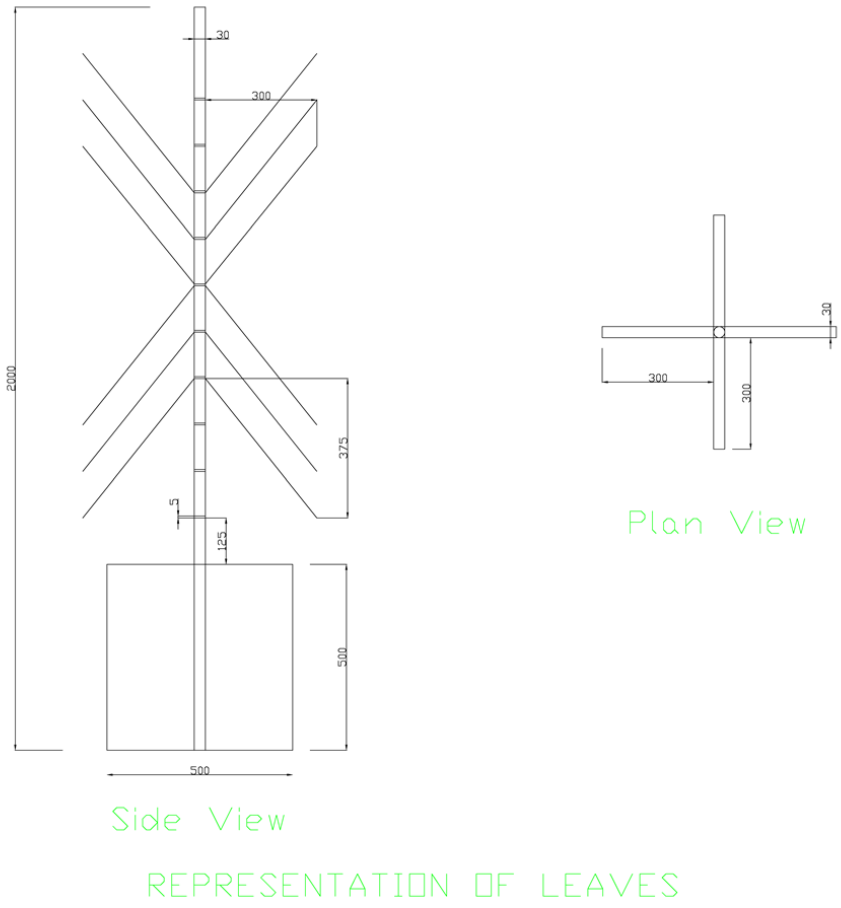

Figure 46: Dimensions for stalk with leaves and nodes.

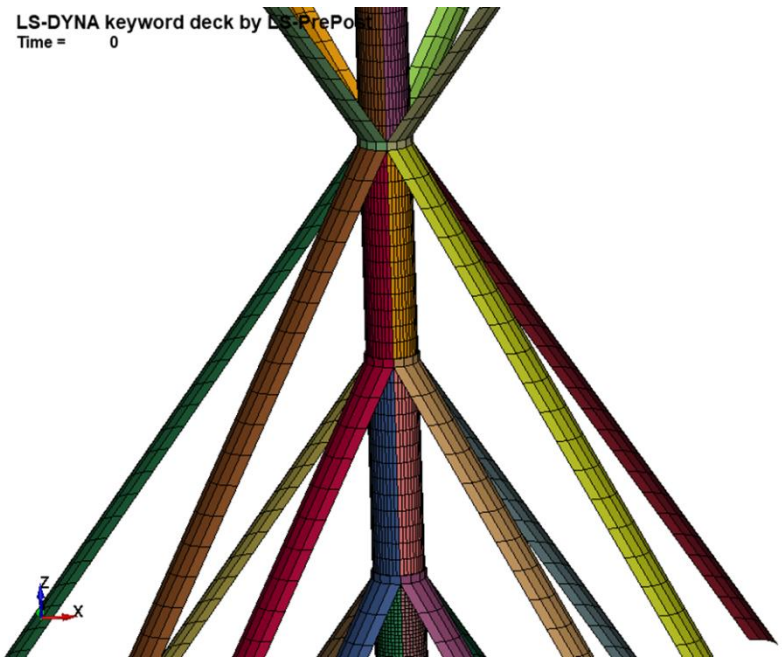

Figure 47: Close-up detail of the model of stalk, nodes and leaves.

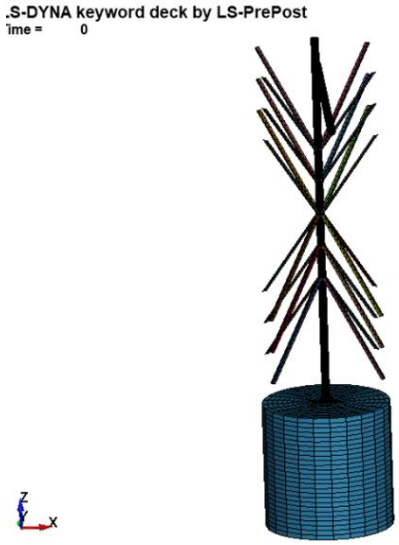

Figure 48: Progression of bending of stalk with leaves and nodes (1 of 3).

Figure 49: Progression of bending of stalk with leaves and nodes (2 of 3).

Figure 50: Progression of bending of stalk with leaves and nodes (3 of 3).

5.6.7. Modelling the harvester front and basecutter components

A series of preliminary simulations were carried out with the aim of simulating most of the feeding and cutting components of the cane harvester working together. These simulations are not described here as they would not add significantly to the information provided in the report. The simulation provided valuable information on the capability of LS-Dyna to produce and solve larger and more complicated models, and the QUT high performance computer Lyra to solve them in a reasonable time. Previous simulation work with different software in other areas of the factory process, such as boilers and clarifiers, concluded that a solution time of 12 to 24 hours per simulation provided viable information for research projects. It was found that a total of 16 CPUs per simulation were optimal within the existing operating restrictions of Lyra.

The geometry for the single stalk with leaves developed previously in the project, together with a version of the mechanical components of the A8000 harvester, is shown in Figure 51 to Figure 55. The single stalk, plus the spirals, sidewall, knockdown roller, finned roller, basecutters, butt lifter

roller and one feed roller are shown. The finite element mesh of the model is on display. The sidewall on one side has been hidden in order to see the internal components. The detail of the knockdown roller and finned roller are shown in Figure 56 and Figure 57. The geometry is designated model A.

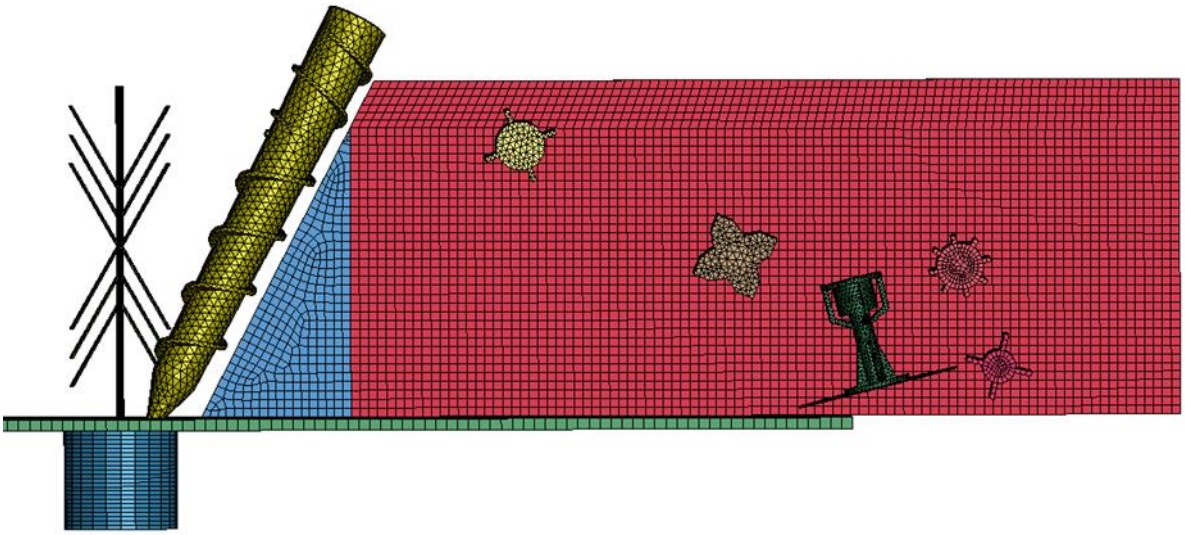

Figure 51: Side view of single stalk and harvester components as modelled.

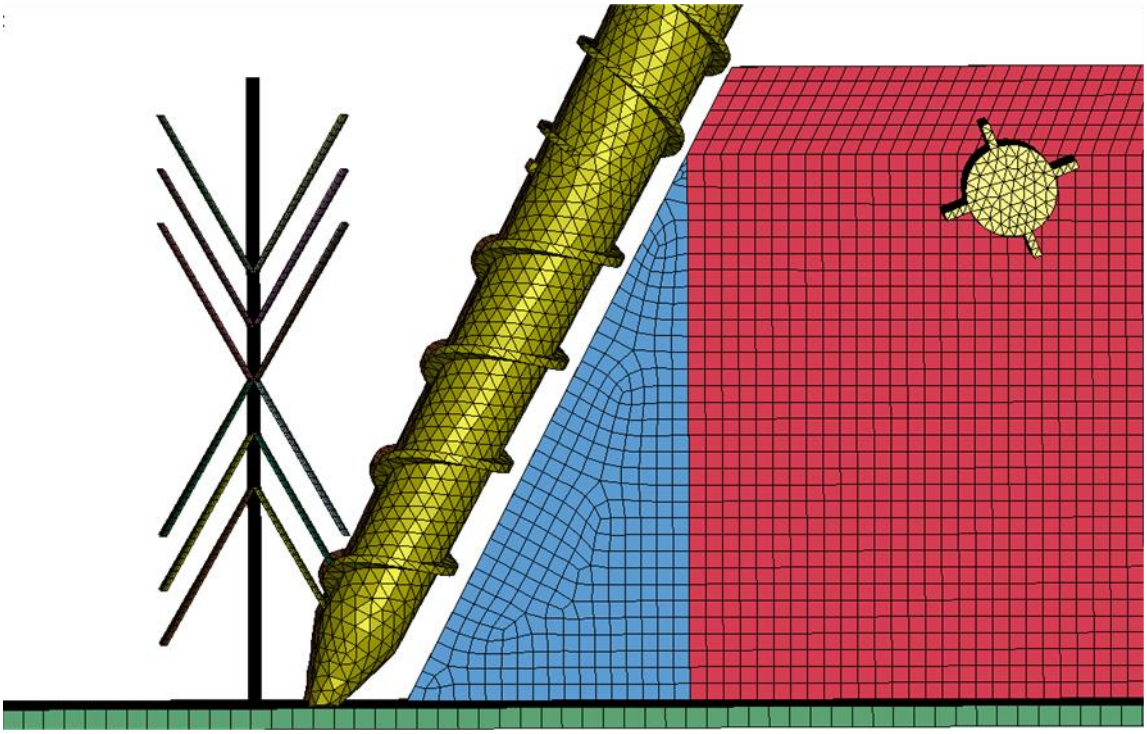

Figure 52: Closeup of side view of front part of harvester.

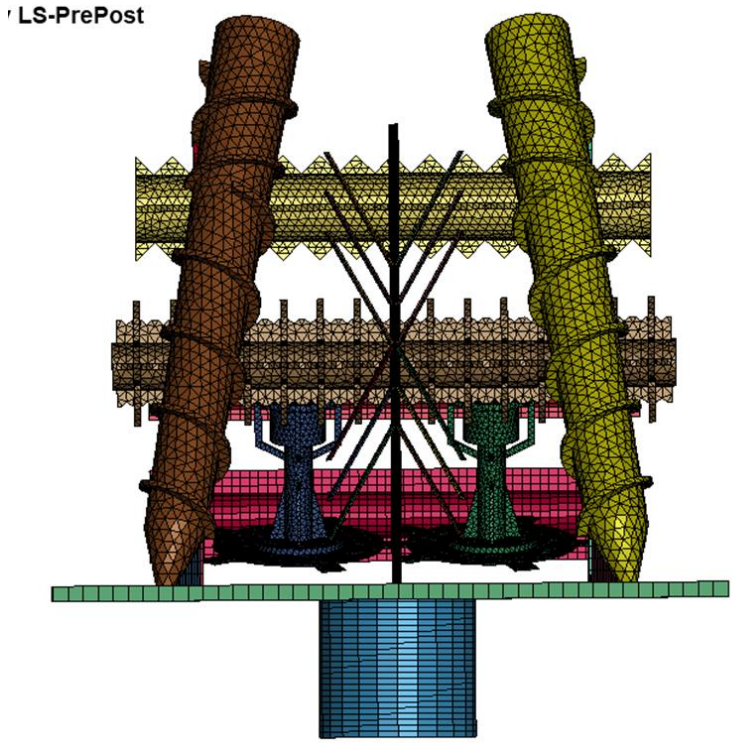

Figure 53: Front view of single stalk and harvester components.

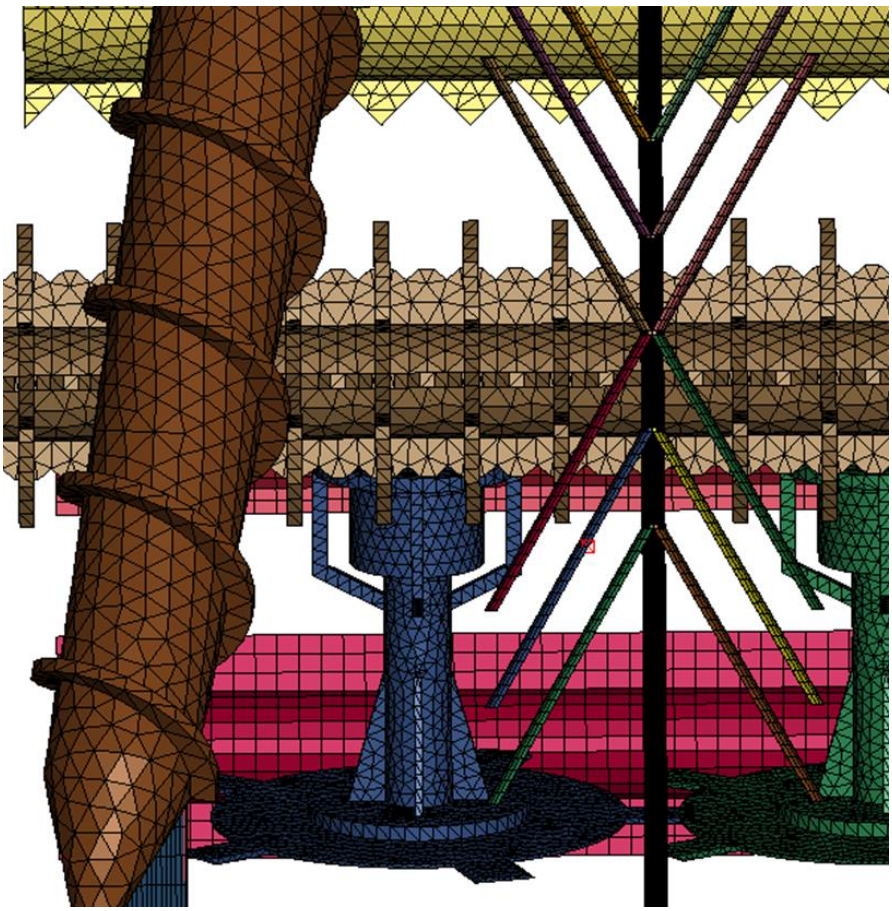

Figure 54: Closeup of front view of single stalk and harvester components

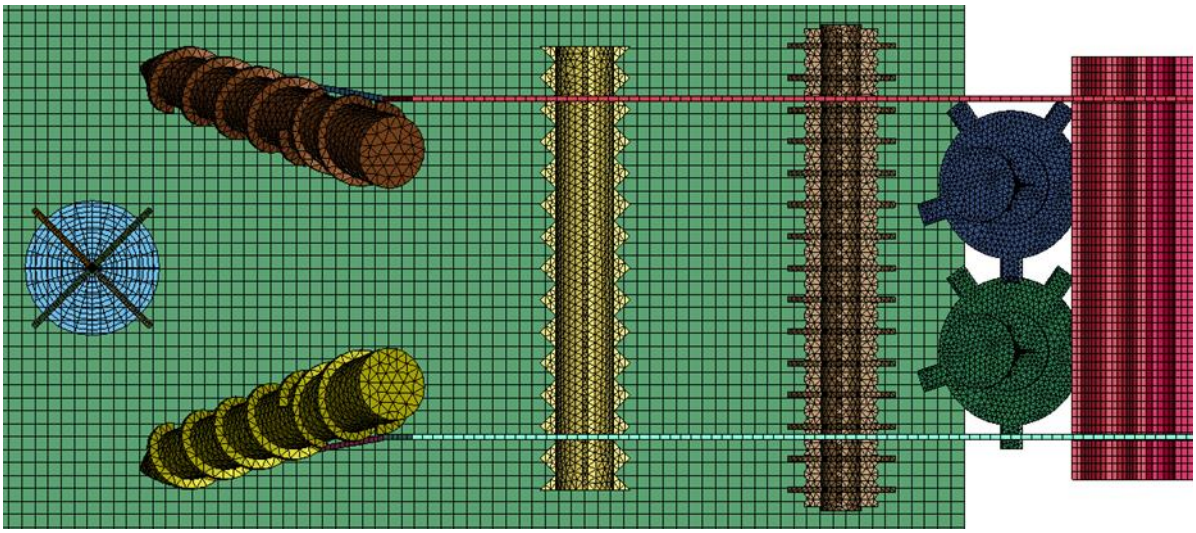

Figure 55: Closeup of front view of single stalk and harvester components.

The detail of the geometry and operating conditions is shown in Table 19.

Table 19: Modelled harvester geometry and operating conditions.

PARAMETERS	DIMENSION
DISTANCE BETWEEN TIPS OF SPIRALS (MM)	1460
SIDEWALL SPACING AT THROAT (MM)	1260
LENGTH OF SPIRALS (MM)	1540
SPIRALS ANGLE FROM VERTICAL (LOOKING FROM FRONT) (°)	10
SPIRALS ANGLE WITH GROUND (LOOKING FROM SIDE) (°)	45
SPIRALS CYLINDER DIAMETER AT TOP (MM)	285
SPIRALS CYLINDER DIAMETER AT BOTTOM (MM)	200
SPIRALS PITCH (MM)	225
KNOCKDOWN ROLLER DIAMETER (MM)	340
FIN ROLLER DIAMETER (MM)	280
BASECUTTER DISCS DIAMETER (MM)	580
BASECUTTER CENTRE TO CENTRE (MM)	630
NUMBER OF BASECUTTER BLADES PER DISC	5
BUTT LIFTER DIAMETER (MM)	300
FEED ROLLER DIAMETER (MM)	210
HARVESTER FORWARD SPEED (KM/H)	8.5
SPIRALS. ROTATION (REV/MIN)	136
KNOCK DOWN ROLLER (REV/MIN)	185.4
FIN ROLLER (REV/MIN)	144.5
BASECUTTER'S ROTATION (REV/MIN)	496.0
TOP FEED ROLLER (REV/MIN)	185.4
BUT LIFTER (REV/MIN)	185.4

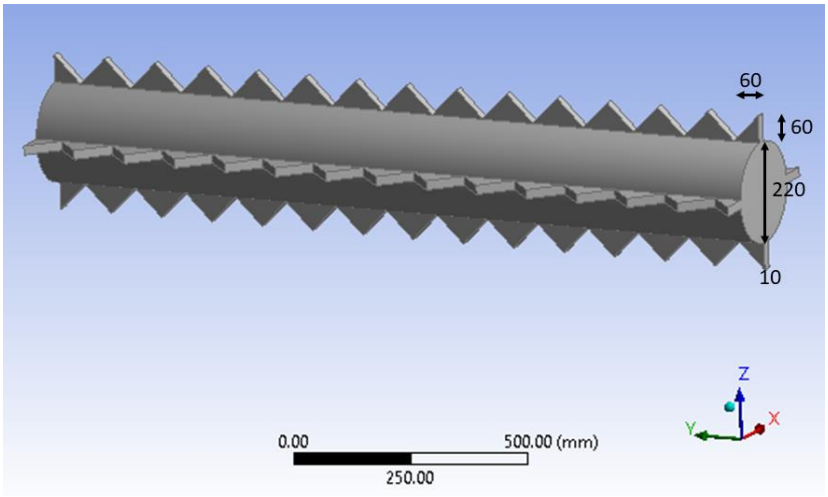

Figure 56: Knockdown roller geometry (dimensions in mm).

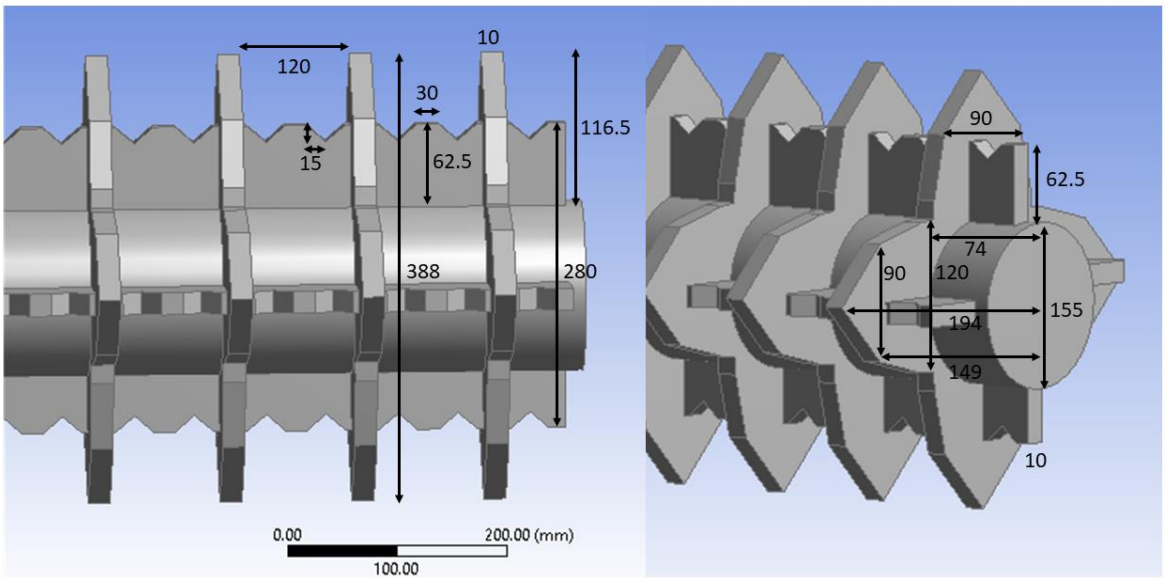

Figure 57: Finned roller geometry (dimensions in mm).

5.6.8. Simulation of alternative harvesting scenarios

The next step in the simulations was to increase the number of stalks with leaves at the entry to the harvester. The objective was to make the simulations more realistic, including making the spirals become involved in the feeding process. There is a compromise between increasing complexity and the capability of the LS-DYNA software and the QUT high performance computer system to achieve simulation results in an adequate time period (say 24 hrs). Shown in Figure 58 and Figure 59 is a model with three stalks while Figure 60 and Figure 61 show a model with five stalks.

An option that has not been carried to possibly make the model more realistic, but remains a possibility, is to increase the interaction between the cane stalks, leaves and harvester components by increasing the stiffness and strength of the leaves (i.e. this would model a situation where there were more leaves present, without increasing the complexity, model size and solution time).

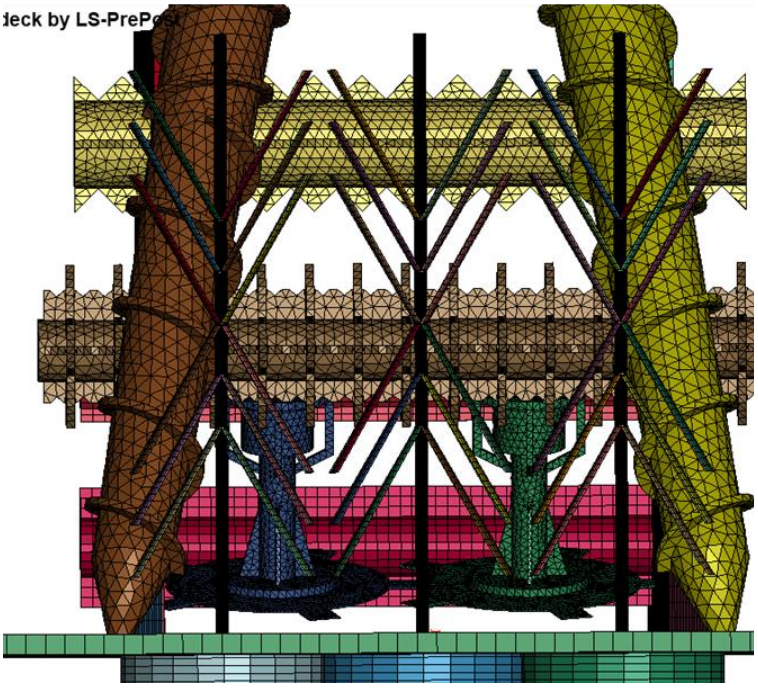

Figure 58: Front view of three stalk harvester model.

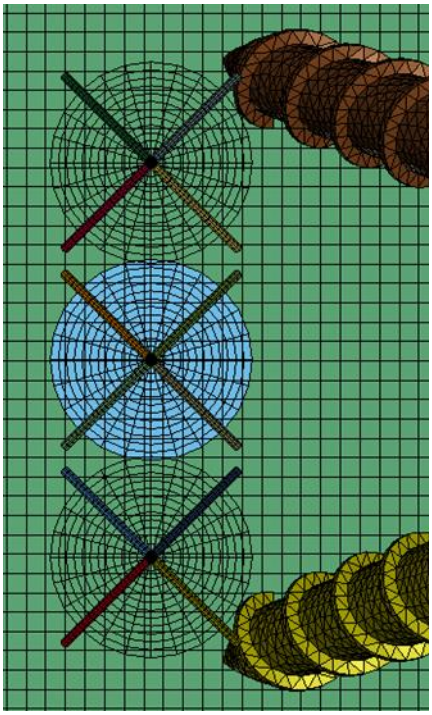

Figure 59: Plan view of three stalk harvester model.

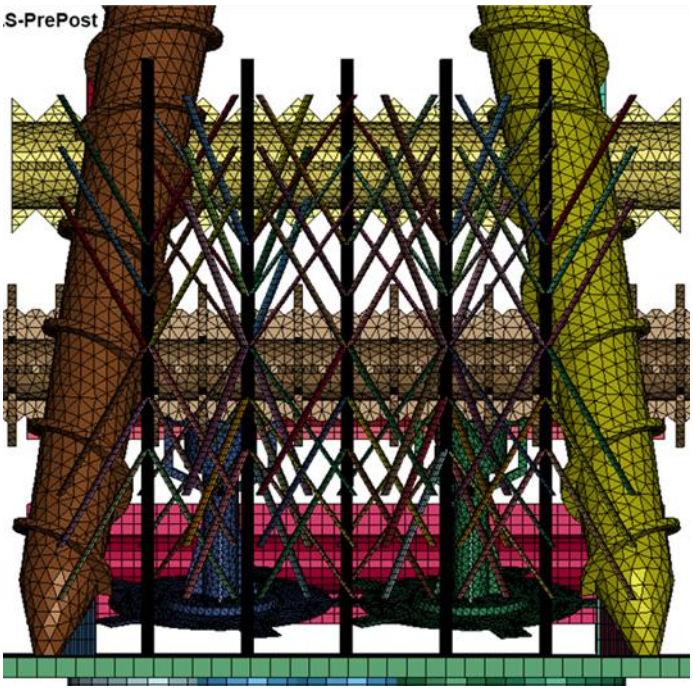

Figure 60: Front view of five stalk harvester model.

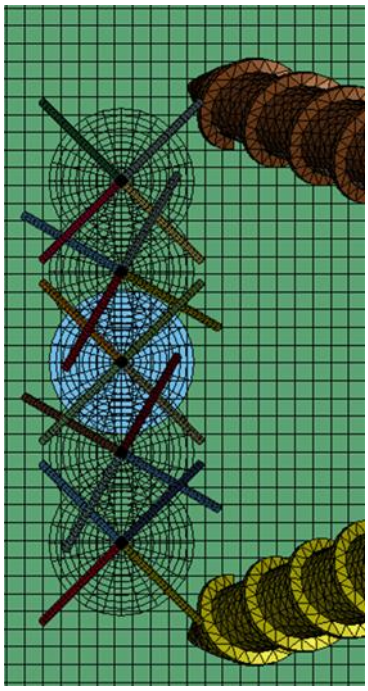

Figure 61: Plan view of five stalk harvester model.

The following models were built:

1. Model B: spirals pitch increased to 280 mm.
2. Model C: sideways spiral angle with the ground changed from 63.5° to 45°.
3. Model D: move the knockdown roller horizontally towards the finned roller.
4. Model E: sideways spiral angle with the ground changed from 63.5° degrees to 45° and move the knockdown roller horizontally towards the finned roller.
5. Model F: sideways spiral angle with the ground changed from 63.5° degrees to 45°, move the knockdown roller horizontally towards the finned roller, and shorten the harvester in the horizontal direction.

The models are shown in Figure 62 to Figure 66.

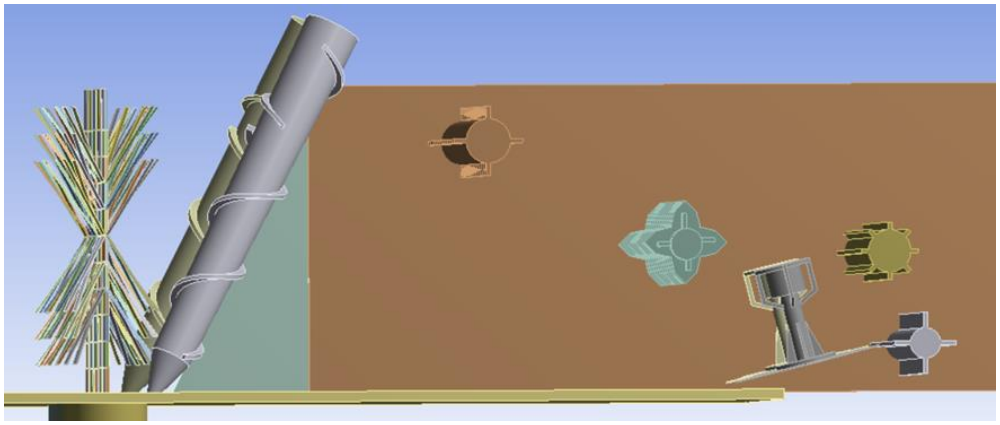

Figure 62: Model B: spirals pitch increased to 280 mm.

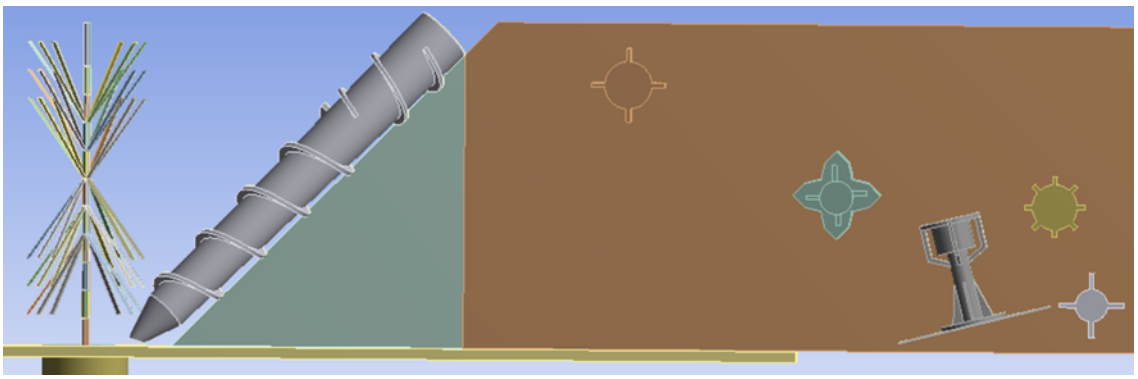

Figure 63: Model C - sideways spiral angle with the ground changed from 63.5° degrees to 45°.

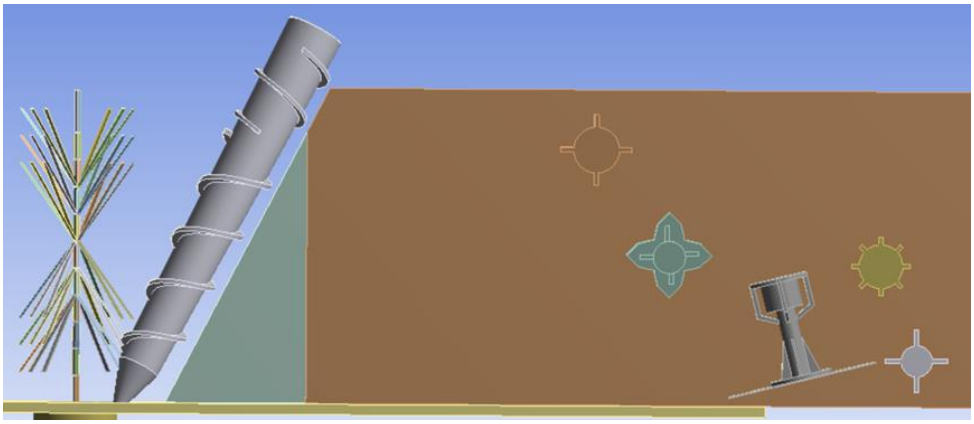

Figure 64: Model D - move the knockdown roller horizontally towards the finned roller.

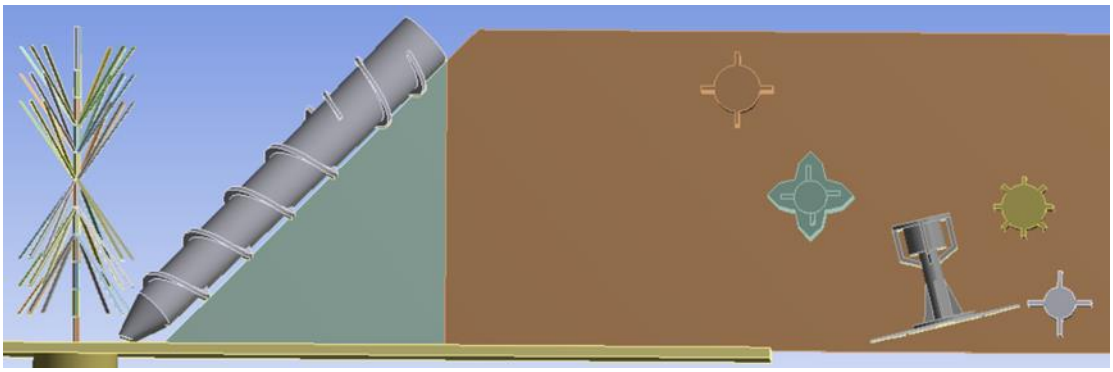

Figure 65: Model E - sideways spiral angle with the ground changed from 63.5° degrees to 45° and move the knockdown roller horizontally towards the finned roller.

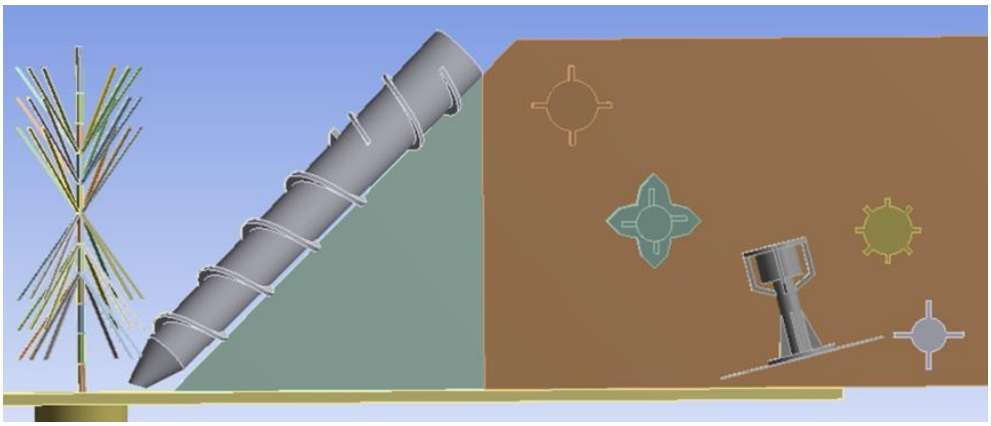

Figure 66: Model F - sideways spiral angle with the ground changed from 63.5° degrees to 45°, move the knockdown roller horizontally towards the finned roller, and shorten the harvester in the horizontal direction.

6. RESULTS AND DISCUSSION

6.1. General comments on statistical significance of trial results

The results of the core (4 Treatment, ground and basecutter speed variations) field trials did not generally show statistically significant differences, although there were generally trends in the data. Where a robust trend was observed, this is discussed, even if it was not statistically significant, as this lack of significance is thought to be attributable to uncontrolled factors or variability, or small sample sizes. Unless noted otherwise, results were not found to be statistically significant at P=0.05 or better.

Some statistically significant results were observed in the 'non-core' trials and measurements, the significance of these is discussed in the relevant sections.

6.2. Field Trial Results: 2016 Harvest

The first trial conducted at Childers was undertaken primarily to refine protocols and test the machine, however the site was maintained as part of the trial program.

6.2.1. Trial Results: 2016 Harvest Childers.

The first trial was conducted at the farm of Mr M Mamino, Plaths Rd Childers. The details are presented in Table 20. The initial harvest was planned to give information on the variability of the block, setup the trial treatments and assess initial impacts of different treatments.

Table 20: Details of trial block at the Plaths Rd trial block.

Parameter	*Descriptor*
Farming Area	Horton (Plaths Rd)
Farm Number	5581 (Mamino)
Block	3A & 4A
Variety and Crop Class	Q 208 1R
Harvest Date	16/11/16
Anticipated yield	90 t/ha
Row Spacing	1.83m single row
Row Length	600m
Rows/plot	4
Plot area	0.439 ha
GPS Utilization:	Fitted to harvesters only: Signal problems & seldom used at this farm

6.2.2. Childers Trial: Cane quality, Yield and EM levels.

Block Yield.

The rail wagons filled with each plot were separately consigned so that mass and other parameters such as ash levels could be assessed. Recovered yield and EM component composition across the trial are indicated in Figure 67. EM was determined by taking 16-20 kg samples from one tramway wagon from each treatment and sorting the billets from other plant components. This indicates that the cane yield varied across the block, with the yield of the first treatments in replicate one being approximately 100 t/ha (clean billets) and the clean billet yield of the last treatments of replicate three being approximately 120 t/ha. The most significant variation was across replicate three. Up to the last two treatments, there was a consistent trend in the proportion of stool in the sample, generally increasing as crop yield increased. The last two treatments were an anomaly to the trend.

Leaf EM% did not show a consistent trend, however an increasing leaf% would have been expected with increasing yield.

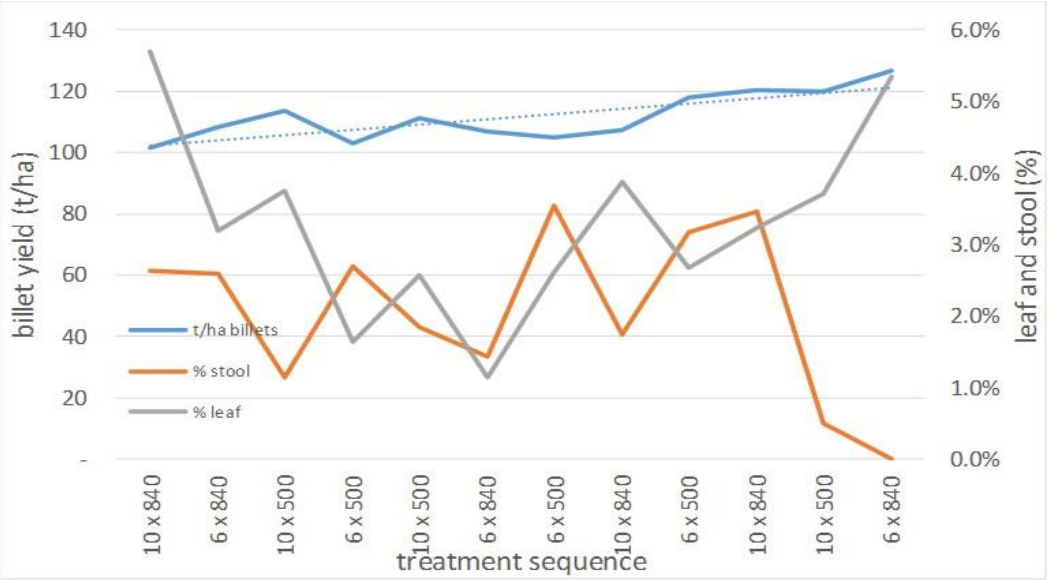

Figure 67: Billet yield across trial and leaf and stool content of delivered product.

Whilst the differences between treatments are large, no consistent trends are visible. Trash & dirt levels do not consistently change with harvesting speed, and stool levels are also inconsistent.

Trash Blanket Yield:

After harvest, the mass of the trash blanket was also estimated, and this is presented in Figure 68. Whilst the crop yield trend across the trial is consistent, the trash blanket effect is less consistent, although a trend is evident.

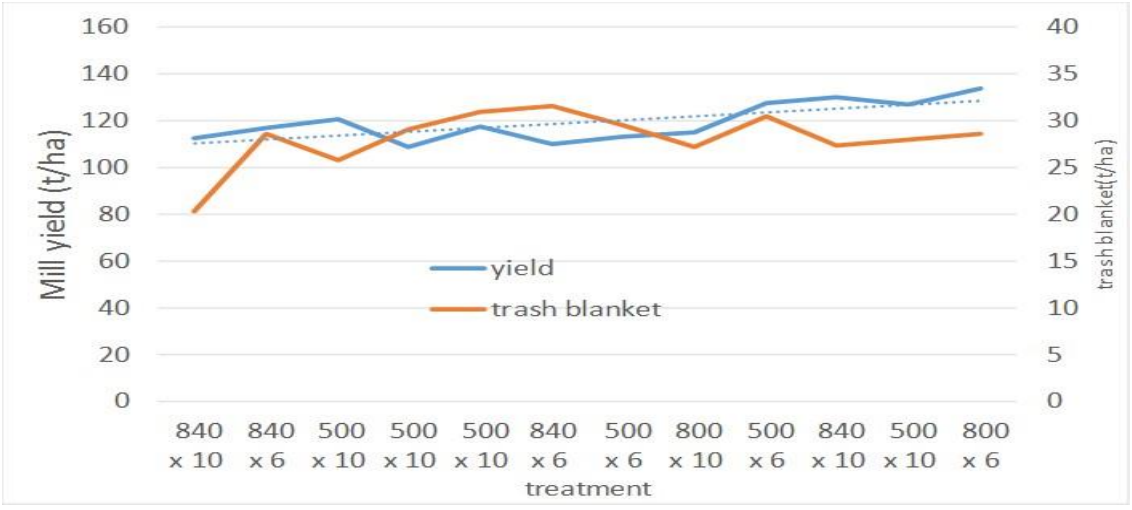

Figure 68: Trend of trash blanket mass across the trial relative to mill yield.

The trash blanket mass increased across the trial, indicating a similar, but more subdued trend than cane yield. This is anticipated as trash yield is not directly proportional to cane yield.

Billet quality.

The samples which were taken for EM assessment were also sorted for billet quality. The results relating to billet quality and damage are indicated in Figure 69.

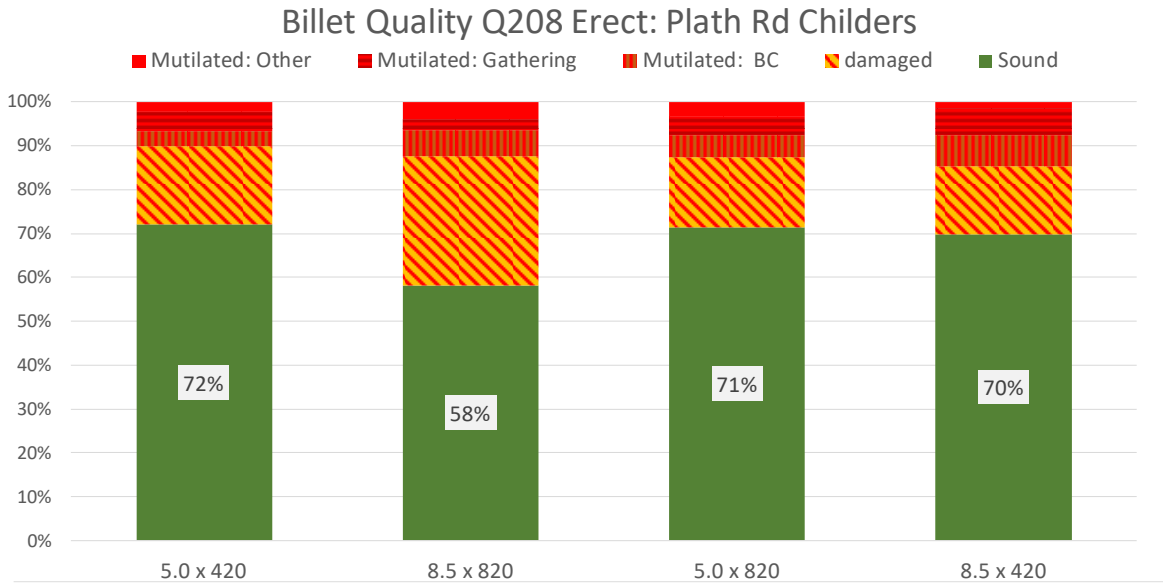

Figure 69: Impact of different treatments on billet damage.

Overall, the levels of damage and mutilation observed were similar to expectations, however the breakdown of indicated sources of damage and mutilation is informative. Gathering damage and mutilation tended to be highest at the higher groundspeed treatments while basecutter damage and basecutter mutilation were generally low.

This indicates that the type of billet damage which was characterized as being caused by damage by the basecutters to the cane stalk was relatively consistent across the trial, whereas there was an apparent strong relationship between harvesting speed and damage.

Stool Damage

Stool damage caused by the harvesting operation was determined by assessing the visible damage to the cane stalks in each 0.5m section of each marked plot. Typically, the marked plot was in row 3 of the four rows in each treatment. The relative damage across the four different treatments is indicated in Figure 70.

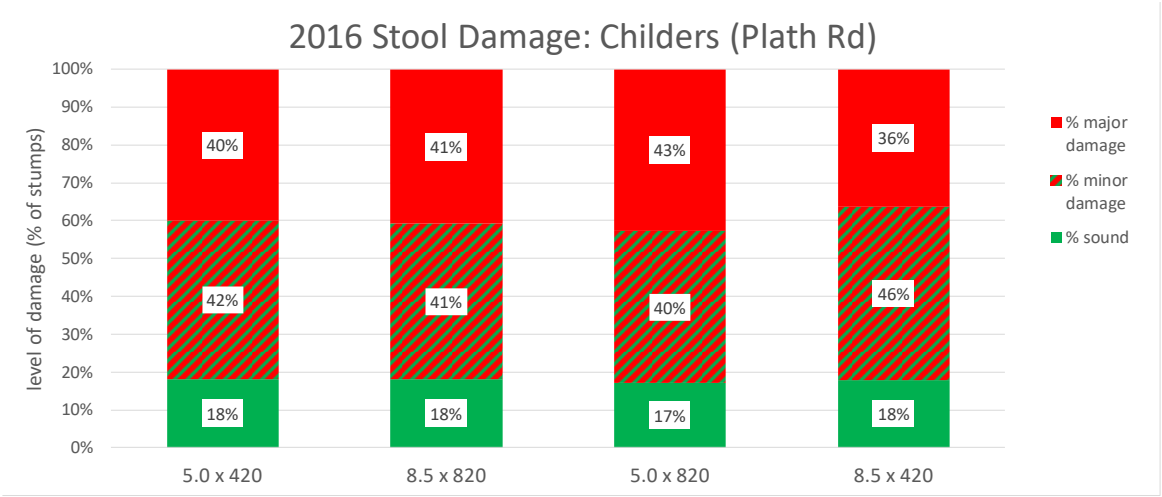

Figure 70: Stool damage noted for the different treatments for the 2016 harvest at Plath Rd.

Key points were:

- Percentage of stalk with minimal damage (sound stalks) was only 17% - 18% across all treatments.
- Major damage was indicated at between 36% and 43% across the treatments.

Further analysis of the raw data for the different sub-plots indicates that the variation across the field is the most significant trend, particularly the total number of stumps counted/treatment. This indicates that in the different treatments in Replicate 1, there were 6-7 visible cut stalks per 0.5 metre section of plot, whereas in the higher yielding Replicate 3, the number of cut stalks was 5-6. Based on the higher yield of Replicate 3, an increase in cut stalk would have been anticipated. This indicates that complete removal of stalk has occurred. This effect is not, however indicated by the measured levels of stool in the product delivered off the harvester.

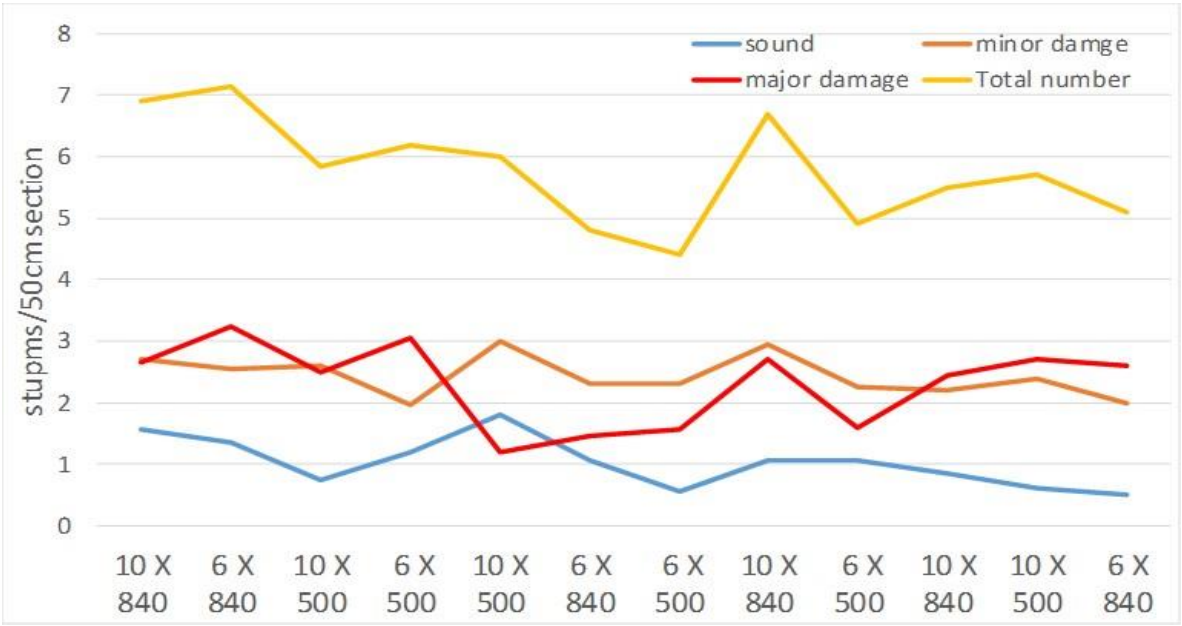

Figure 71: Number of stumps and damage level across trial.

Ratoon Emergence

The trial received a significant rainfall event soon after harvest and did not require further irrigation to establish the ratoon. At 30 days after harvest, the ratooning plots were inspected, and number of plants and plant height were recorded in each plot. A selection of plants in the one-meter section adjacent to the ends of the plots were cut at ground-level and retrieved for weighing and measuring.

Photograph 12: Variation in shoot height from the crop row adjacent to the sub-plots, sorted into height categories.

The plants for each replicate were then sorted into height categories and weighed, as indicated in Photograph 12.

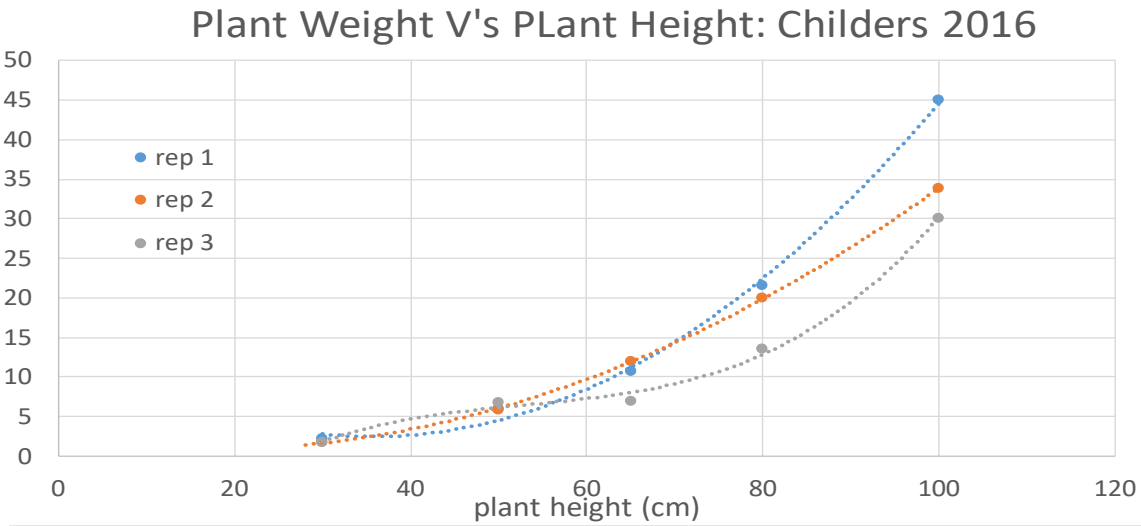

Figure 72: Relationship between plant height and fresh-weight for the three replicates of the trial.

The difference in plant weight relative to height is believed to be associated with the higher levels of damage in Replicate 3. Figure 73 indicates that the most significant factor impacting on biomass yield of the ratoon at 30 days after harvest was original plot yield. The indicated ratoon biomass on the “rep 1” side of the trial was almost double the ratoon biomass of the higher yielding “rep 3” side of the trial. The reduction in biomass was a product of both reduced emerged plant numbers and lower mass per plant.

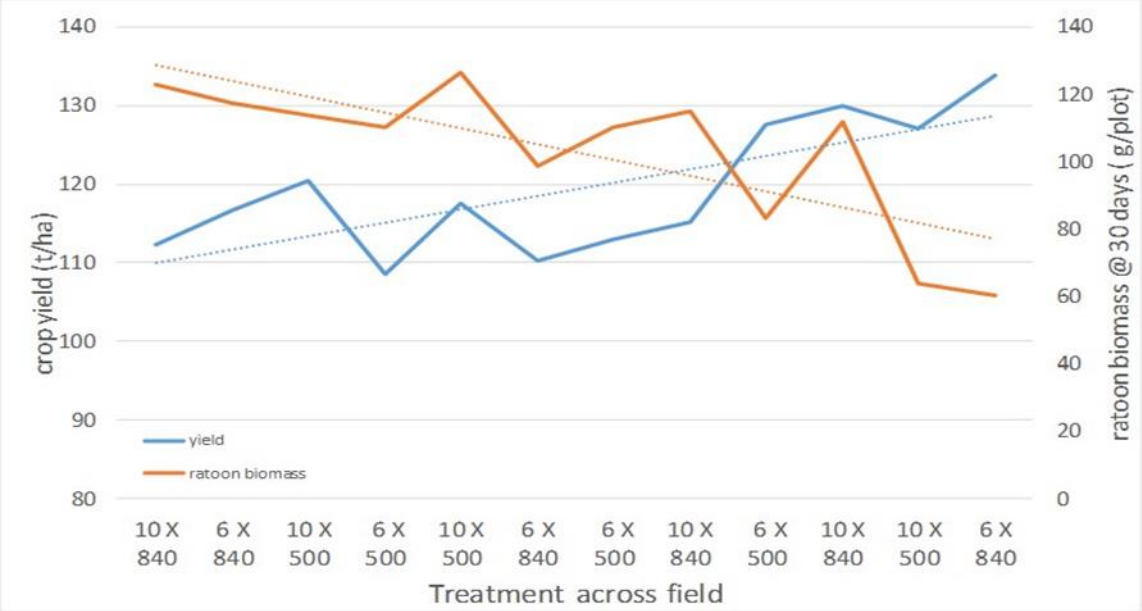

Figure 73: Trend of ratoon biomass at 30 days after harvest and mill yield, for the treatments across the field.

Summary:

The results of the first trial indicated that whilst very significant damage was suffered by the cane stool during the harvesting operation, the differences associated with different harvesting speeds and component speeds were relatively small. Size of the crop being harvested appeared to be a very significant factor in determining damage. This best explains the observed large difference in ratoon biomass across the trial.

Variability in field factors which drive the yield variability are an issue in this research.

6.3. Field Trial Results: 2017 Harvest

The 2017 harvest program consisted of:

- Two trials in the Condong (Northern NSW) area. The harvester modified for the trial was a JD 3520 machine operated by Central Tweed Harvesting.
- Two trials in the Childers / Bundaberg area, with the modified Central Harvesting JD 3520.
- One trial in the Burdekin region, with the harvester supplied by Wilmar International, on whose farm the trial was conducted.

6.3.1.2017 Harvest: Site Details, Yield and Cane Quality.

The trials are detailed below in order of harvest for 2017. Yield results from the initial harvest in 2017 were to “benchmark” each field and to also impose the harvest treatments.

Trial 1: Condong (BZ Farms)

The details of the site are presented in Table 21. The harvester was the Tweed Valley harvesting JD 3520, with both the outer gathering spirals and the “cross half rollers” removed. The machine had been fitted with the modified basecutter motor and flow control valves, and the controller to link these components to groundspeed. The machine was also fitted with aftermarket chopper drums.

Table 21: Crop and Field details for Condong (Bartlett) trial.

Parameter	*Descriptor*
Farming Area	Condong
Farm Number	Zahsviv 6 – 8146 (BZ Farms)
Block	203 & 204
Variety and Crop Class	Q 208 1R (Burned prior to harvest)
Yield	120-125 t/ha
Date of Harvest	2/8/2017
Billet length & Diameter	Length: 180 mm. Diameter 28 mm
Row Spacing	1.90m dual row
Row length	600 m
Rows per Plot	4
Plot Area	0.46 ha
GPS Utilisation	Harvester & haulouts fitted: rigorous use

The harvesting settings associated with the different treatments for each trial were discussed with the harvester operator. The treatments used are indicated in Table 22:

Table 22: Harvesting treatments for Condong first trial on 2nd August 2017 (BZ farms).

Treatment	*Harvesting Speed (km hr^{-1})*	*Basecutter Speed RPM*	*Comment*
T1	5.0	500	Automatic: Low speed
T2	8.5	850	Automatic: High speed
T3	5	620	Standard: Low speed
T4	8.5	620	Standard: High speed

The crop was burned prior to harvest and the yield from the first harvest is presented in Table 23. The harvesting pour rate for the 4.5 km/hr treatment was approximately 103 t/hr, and approximately 182 t/hr for the higher speed treatment.

Table 23: Yield across replicates for BZ Farms trial.

Replicate	*1*	*2*	*3*	*Average*
Yield (t/ha)	126.0	132.1	132.1	130.0

This indicates limited variability across the block, and that the average yield was 130 t/ha. The crop was heavily water stressed at time of harvest. The difference in yield across the different treatments is shown in Table 24. Again, the block was even in yield across the treatments.

Table 24: Yield across different treatments at first harvest, BZ Farms.

Treatment	*4.5 x 450*	*8.0 x 800*	*4.5 x 620*	*8.0 x 620*
Yield	133.0	126.2	131.5	129.4

Trial 2: Bouchards Rd Childers.

The details of the site are presented in Table 25.

Table 25: Crop and Field details for Childers (Bouchards Rd) trial.

Parameter	*Descriptor*
Farming Area	Childers (Fairnsfield), Bouchards Rd
Farm Number	6363 (Petersen Farms)
Block	3A
Variety and Crop Class	Q 240 1R, green cane harvesting.
Date of Harvest	21/8/2017
Yield	105-110 t/ha estimated
Billet length & Diameter	20.1 cm length & 22.3 mm diameter
Row Spacing	1.83m single row
Row length	299-349
Rows/plot	6
Plot area	.33-.38
GPS Utilisation	Harvester only

The harvester used for the trial was the JD 3520, operated by Central Harvesting, in standard configuration except for the modifications to achieve the variable basecutter /forward feed component RPM and aftermarket chopper drums. The settings associated with the different treatments were derived in discussion with the operator.

Table 26: Harvesting treatments for Childers (Bouchards Rd) trial on 21st August.

Treatment	*Harvesting Speed (km hr^{-1})*	*Basecutter Speed RPM*	*Comment*
T1	5.0-5.5	520	Automatic: Low speed
T2	8.5	850	Automatic: High speed
T3	5.0-5.5	620	Standard: Low speed
T4	8.5	620	Standard: High speed

The Bouchards Rd trial was harvested green and the yield data across replicates is presented in Table 27. Lower extractor fan speed was used in the lower groundspeed treatments to maintain similar levels of cane loss across treatments.

Table 27: Yield data across replicates for Bouchards Rd Trial initial Harvest

Replicate	*1*	*2*	*3*	*Average*
Yield (t/ha)	108.82	113.72	102.10	108.2

The average yield for the block was 108.2 t/ha with the middle replicate having higher average yield. This was primarily driven by very high yields in plots 7 & 9 (135 & 137 t/ha). This was believed to be associated with variability in irrigation evenness, given the dry growing conditions and high irrigation usage.

The difference in yield across treatments is presented in Table 28. This again indicates the variability within the field.

Table 28: Average yield data across treatments, Bouchards Rd.

Treatment	*4.5 x 450*	*8.5 x 850*	*4.5 x 850*	*8.5 x 450*
Yield	110.3	100.3	114.5	117.7

At the estimated average yield of 102 t/ha, the harvesting pour rate for the 5 km/hr treatment was 95 t/hr, and 160 t/hr for the higher speed treatment.

Trial 3: Condong (Colonial Drv)

Details for the third trial in 2017 is presented in Table 29. The trial utilised the Tweed Valley Harvesting modified harvester and crew, as utilized for Trial 1. (22/8/2017)

Table 29: Crop and Field details for Condong (Colonial Drive) trial.

Parameter	*Descriptor*
Farming Area	Condong: Colonial Drive
Farm Number	8105 (M North)
Block	201
Variety and Crop Class	Q 240 Plant, green cane harvested.
Date of Harvest	19/09/2017
Yield	105-120 t/ha
Billet Length	175mm
Row Spacing	1.90m dual row
Row length	250 m
Rows /plot	4
Plot area	.285 ha
GPS Utilisation	Harvester & haulouts fitted: rigorous use

The treatments implemented are indicated in Table 30:

Table 30: Harvesting treatments for Condong second trial on 19th September on farm of Mr M North.

Treatment	*Harvesting Speed (km hr^{-1})*	*Basecutter Speed RPM*	*Comment*
T1	5.0	500	Automatic: Lower harvesting speed
T2	5.0	620	Standard: Lower harvesting speed
T3	8.0	800	Automatic: Higher harvesting speed
T4	8.0	620	Standard: Higher harvesting speed

The trial block was harvested green and the yield variability across replicates is presented in Table 31

Table 31: Yield across replicates Condong (North) trial.

Replicate	*1*	*2*	*3*	*Average*
Yield (t/ha)	116.7	117.8	109.6	114.6

The yield variability between replicates indicated moderately low variability across the block, with an average yield of 114.6 t/ha.

Table 32: Yield across treatments at first harvest Condong (North) trial.

Treatment	*5 x 500*	*8 x 800*	*5 x 620*	*8 x 620*
Yield (t/ha)	115.1	118.2	113.0	115.4

The variability across treatments was also small.

Trial 4: Childers Plath Rd.

This trial was the second harvest of the field on Mamino's farm, Plaths Rd, Horton (near Childers), with relevant details given in Table 33. The harvester was the Central Harvesting machine used for the Bouchards Rd Trial.

Table 33: Crop and Field details for Plaths Rd (Childers) trial.

Parameter		*Descriptor*
Farming Area		Horton (Plaths Rd)
Farm Number		5581 (Mamino)
Block		3A & 4A
Variety and Crop Class		Q 208 1R
Date of Harvest (2nd harvest)		11/10/2017
Anticipated yield		90 t/ha
Row Spacing		1.83m single row
Plot Area		.439 ha
GPS Utilisation		Harvester Only: Signal difficulties.

The treatments are detailed in Table 34.

Table 34: Harvesting treatments for the Plaths Rd trial in 2017.

Treatments	*Speed (km/hr)*	*Basecutter RPM*	*Comment*
T1	8.5	820 (Auto)	Auto: higher harvesting speed
T2	5.0	820	High basecutter at low harvesting speed
T3	8.5	420	Low basecutter at high harvesting speed
T4	5.0	420 (Auto)	Auto: low harvesting speed

This was the second harvest for this site. The difference between replicates was associated with variability across the plots as shown in Table 35, with the highest yield being associated with Replicate 1. This was the lowest yielding replicate in the 2016 harvest and suffered the lowest damage at harvest.

Table 35: Yield across different replicates for the second harvest at Plaths Rd Site.

Replicate	1	2	3	Average
Yield (t/ha billets)	77.9	73.5	77.2	76.2

Table 36: Yield across different treatments at Plaths Rd site for second harvest.

Treatment	5.0 x 420	8.5 x 820	5.0 x 820	8.5 x 420
t/ha billets	74.9	73.9	78.4	76.1

The treatment differences (Table 36) were not significant.

Trial 5: Burdekin (Mona Park)

This trial was conducted at the Wilmar Farm in the Mona Park District, BRIA. Details of the block and crop are presented in Table 37.

Table 37: Crop and Field details for Burdekin trial.

Parameter	*Descriptor*
Farming Area	Mona Park
Farm Number	220-8A
Block	34-2
Variety and Crop Class	Q 208 1R
Harvest Date	6/11/2017
Yield	140-145 t/ha (lodged)
Billet Length & Diameter	Billet Length: 165mm. Diameter: 19.6 mm
Row Spacing	1.65m
Row Length	4 x 410 m
Plot Area	.271 ha
GPS Utilisation	Harvester only 2018 & 2019 harvests.

The machine was the Case 8000 harvester which was modified for the trial. The treatments for the trial are presented in Table 38.

Table 38: Harvesting treatments for the Mona Park trial.

	5.5	135	620
	5.5	135	550
	7 - 7.5	185	620
	7 - 7.5	185	750

The crop was burned prior to harvest and the yield from the first harvest is presented in Table 39. The variability across the block ranged from 137t/ha to 149 t/ha, which is low for the Burdekin.

Table 39 Yield across different replicates for Mona Park Site.

Replicate	1	2	3	Average
Yield (t/ha)	139.7	144.0	143.7	142.5

Treatment average yield is presented in **Error! Reference source not found.**. It demonstrates a high level of evenness across the treatments.

Table 40: Treatment yield for Mona Park site.

Treatment	**5.5 x 550**	**7.5 x 850**	**7.5 x 620**	**7.5 x 620**
Yield	142.1	142.2	142.7	142.9

6.3.2. Billet Damage Results 2017 Trials

Billet damage can be assessed as “by harvester” as harvester setup did not significantly change between trials.

Trial 1 & Trial 3:

The observed billet damage for the BZ farms trial harvested by the Central Tweed harvester (Condong) is presented in **Figure 74**. The crop was burned, sprawled at time of harvest and average crop yield was 130 t/ha.

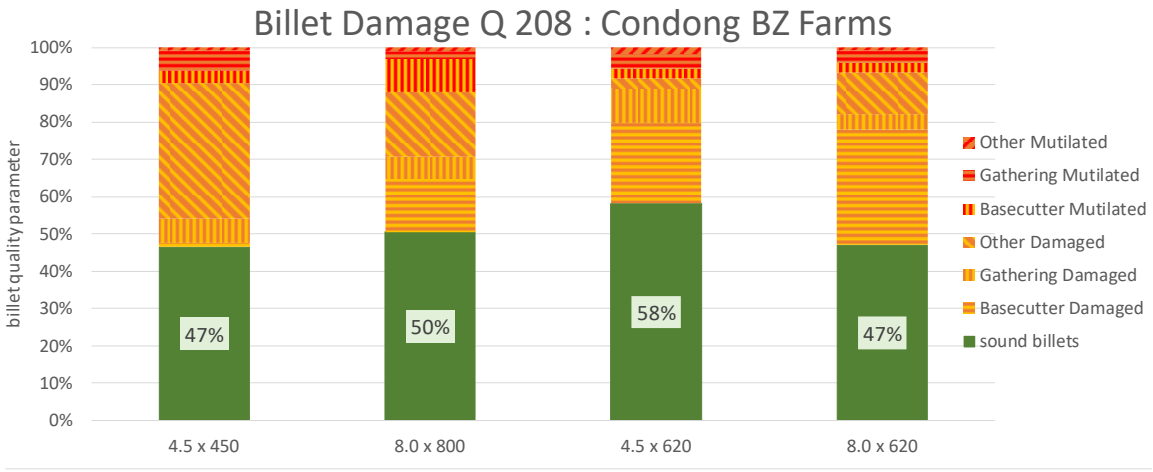

Figure 74:Billet quality for Trial 1 at BZ Farms in variety Q 208.

The damage is within expectations, however apparent basecutter damage is high for the 8.0 x 620 treatment. The billet damage in the product harvested by the same harvester at the trial on the Colonial Drive trial site is presented in Figure 75.

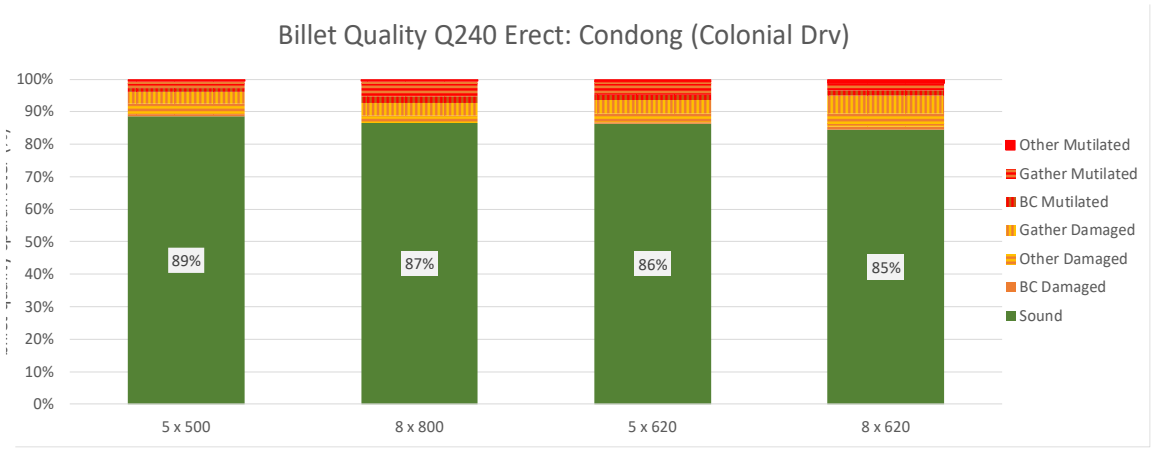

Figure 75: Billet quality for Trial at North's Farm in variety Q240.

The harvester was fitted with EHS chopper drums and the outer spirals and cross half-rollers had been removed in an attempt to minimise stalk damage when harvesting lodged crops. The levels of mutilated billets in the lodged crop in Trial 1 is considered within expectations. The damage recorded for the erect crop in Trial 3 is very low by commercial harvesting standards. The levels of billet mutilation at both sites was very low.

Trial 2 & Trial 4:

Trial 2 & Trial 4 were harvested by the Central Harvesting JD 3520 machine. The billet quality data for the 2017 harvest is presented in **Figure 76**. The levels of billet damage observed were consistent with expectations.

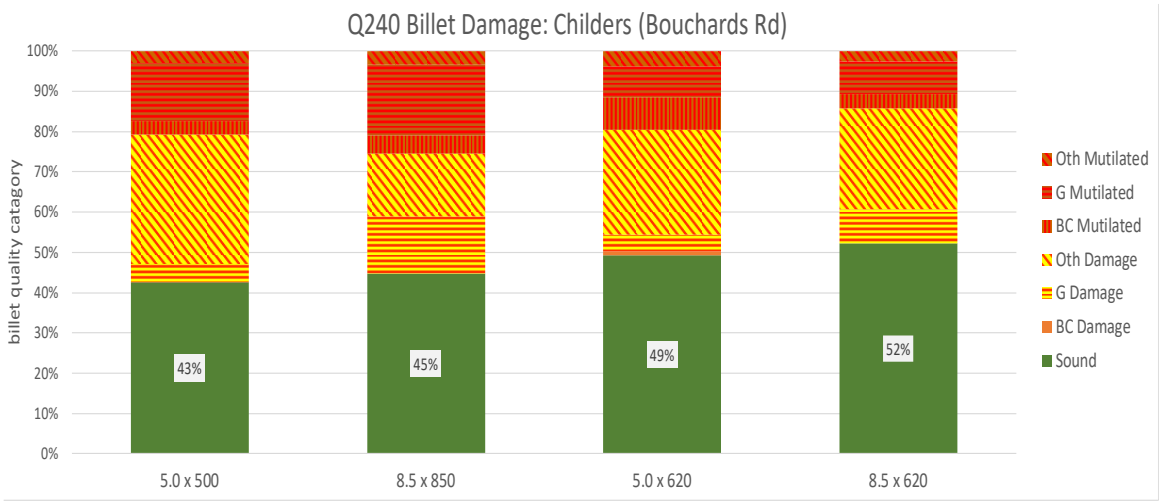

Figure 76: Billet quality for different treatments at Blouchard's Rd trial in an erect crop of variety Q240.

Trial 4 was the second harvest of the plots on Mamino's farm, with the crop being erect at time of harvest.

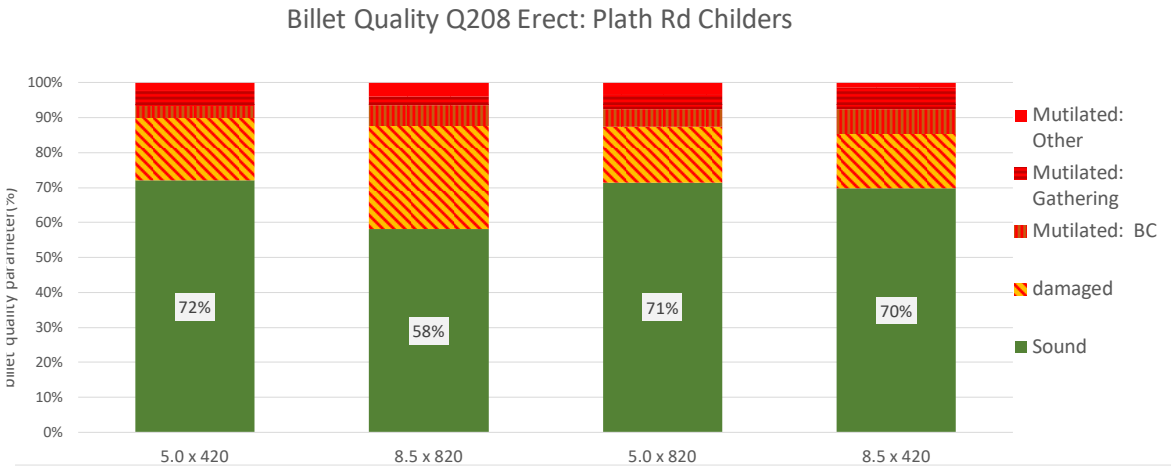

Figure 77: Billet quality for different treatments at Mamino Trial in an erect crop of Q208.

The billet quality at both sites was generally within expectations. The levels of billet mutilation in Trial 2 appeared highest in the high speed/high basecutter speed treatment, however the result was not significant. The higher levels of mutilated billets in the erect crop in Trial 3 than were noted in the Condong trial is probably at least partially related to the more aggressive knockdown setting used in this Childers trial.

Trial 5:

Trial 5 was conducted in a field of Q208 at the Mona Park site in the Burdekin region. The harvester was a Case 8000 harvester.

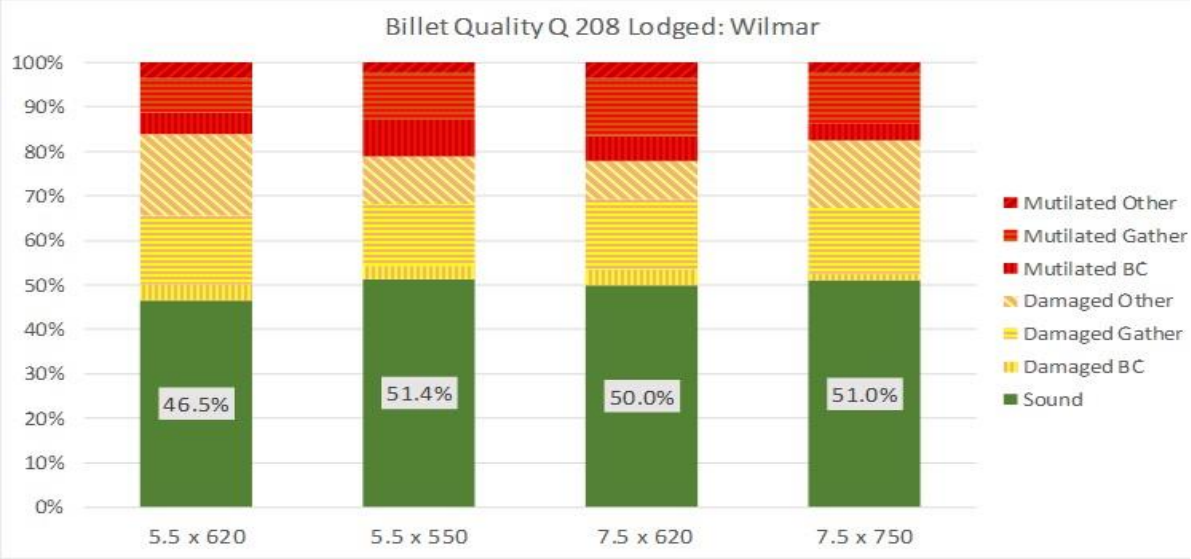

Figure 78: Billet quality data for the Mona Park trial.

Given the thin cane stalk diameter (19.6 mm average billet diameter), the overall levels of mutilated and damaged billets are generally within the expected range. Approximately 15-22% of the billets were mutilated and approximately 50% of billets were "sound" for all treatments. The difference between treatments was minimal and not significant, indicating that the damage was not highly related to the parameters of the trial.

Summary: Billet Damage

Billet damage levels generally followed the expected trend of being higher in lodged crops. The lowest level of billet damage was in the erect crop of Q240 at Condong using with the Central Tweed harvester which was fitted with only single gathering spirals.

The billet damage levels in the crop of Q208 in the Burdekin was somewhat lower than expected, given the configuration of the harvester and the crop size and degree of lodging. The thin billet diameter of <20 mm observed in this crop was undoubtedly a contributing factor to this lower damage.

From an Industry perspective, the levels of billet damage are significant. Trials conducted in Nicaragua by Caldere Dominguez and Norris (2018) indicated that, under the short cut-to-crush delays achieved by the "Just-in-time" truck based transport system utilized at San Antonio Mill, the recoverable sucrose levels were approximately 10% lower than for sound billets.

Larsen *et al* (2017)and Larsen (pers. comm.) observed that both damaged and mutilated billets reduced recoverable sugar across all sites of their survey (burned and green cane harvesting). Larsen also showed the effect was highly related to cut-to-crush delay, and after an extended but "realistic" delay associated with the rail transport system recoverable sugar in mutilated billets approached zero. This then indicates the magnitude of the loss to the Industry of the levels of mutilated billets in the delivered product from the harvesters.

6.3.3.Stool Damage and Ratoon Performance Results 2017 Trials

The post -harvest assessment conducted on each trial illustrated the magnitude of the issue of damage caused by the harvesting operation. Photograph 13 illustrates a typical plot after removal of the covering soil and trash, with the harvesting depth just above ground level. This is demonstrated

by the undisturbed soil surface over much of the plot. Photograph 14 indicates deep stool damage, where at least some of the crop stool has been removed by the harvester.

At all sites, new or near-new basecutter blades had been fitted to the harvesters at the time of harvesting the trials in 2017 and 2018. The levels of damage observed are therefore the 'best case scenario'.

Photograph 13: After harvest, the trash and soil loosened by the basecutters is removed to facilitate clear visual assessment of the harvested stool.

Photograph 14: Removing the residues and loose soil from around the stool allows for the mode of damage to be better assessed.

The 2017 harvest was predominantly very dry and many crops were water stressed at the time of harvest.

Trial 1 BZ Farms: Stool Damage 2017

The stool assessment after harvest is presented in Figure 79. The level of "sound" stumps ranges from 17% to 23%. Similarly, the level of badly damaged stumps ranged from 35% to 39%.

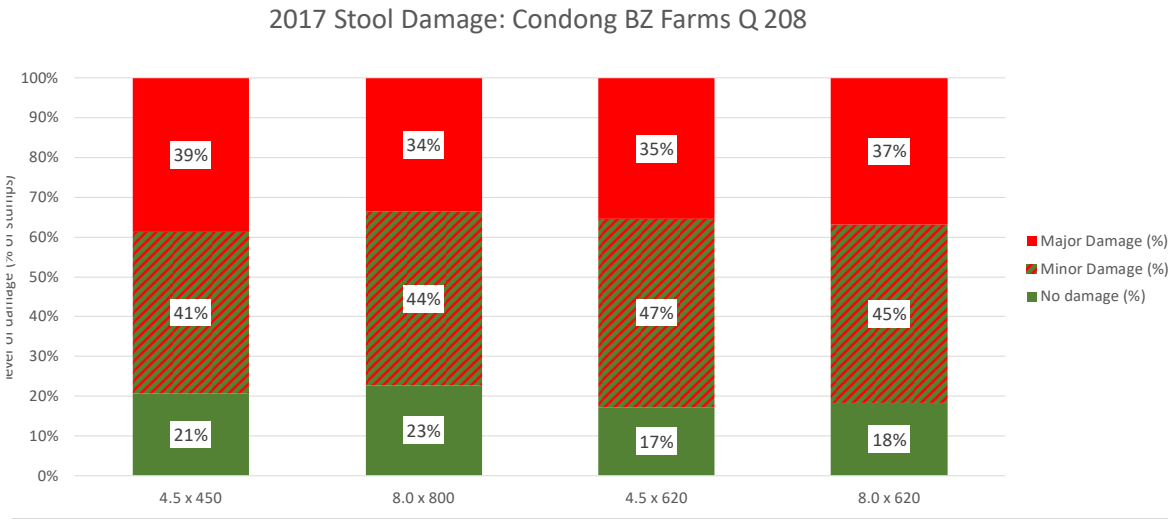

Figure 79: Stubble damage at BZ Farms with Q208A.

Further understanding of the issues can be gained by looking at the raw numbers of cut stalks assessed, as indicated in Figure 80. This indicates that the total number of visible stalks after harvest was highest in the low groundspeed treatment with matched component speeds.

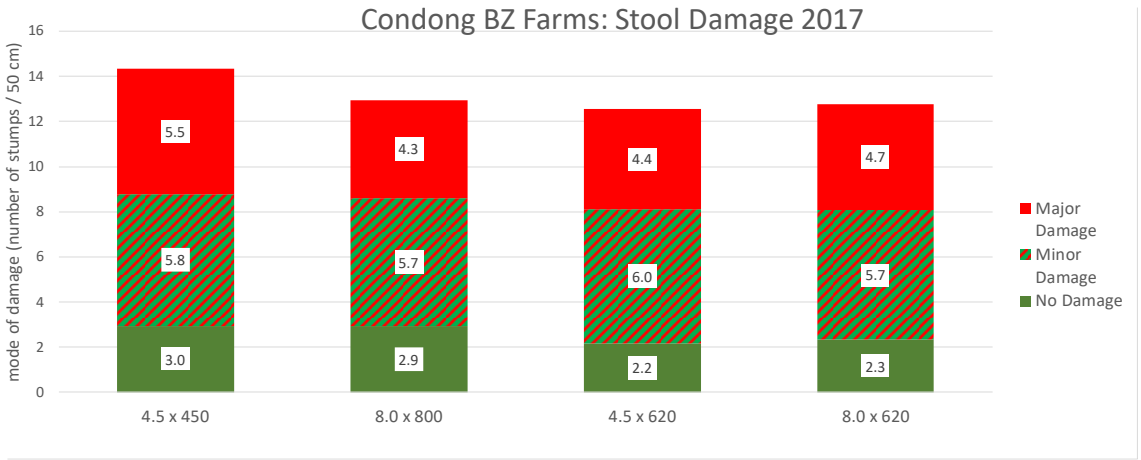

Figure 80: Raw data relating to total stalk numbers after harvest (BZ Farms).

Ratoon Emergence & Early Growth

Ratoon emergence was assessed by at post-harvest shoot counts after crop emergence. At BZ farms, emergence was very slow because of cold dry conditions, and plant counts were done at 9 weeks after harvest and 16 weeks after harvest. An additional 30-50% shoots had emerged at 16 weeks relative to 9 weeks. Photograph 15 shows examples of ratooning behaviour at this site.

Photograph 15: Ratoon emergence at the BZ farms block. Note the shoot emerging vigorously from a relatively shallow node off the undamaged stump, v's the obviously much deeper nodes associated with the split stump.

Significant damage was observed by canegrubs in the plot areas, which impacted on final emergence. As with the observations at Pranges Rd after the 2016 harvest, there was very significant variance in plant size at 16 weeks. The effect of this is shown in Figure 81 where the 4.5 x 620 treatment had a higher number of late emerging shoots. These did not follow through to millable stalks.

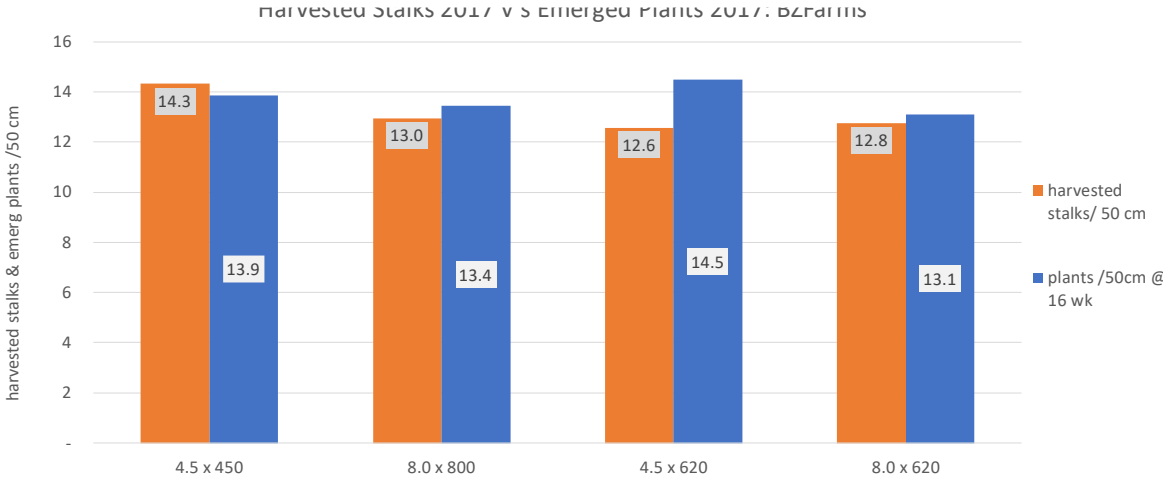

Figure 81: Emerged plants 16 weeks after harvest and millable stalks prior to harvest for the BZ trial plots.

2018 Yield

The yield from the different treatments is presented in Figure 82. There was no significant difference in yield across treatments. Given the millable stalk numbers counts prior to harvest, this was not expected.

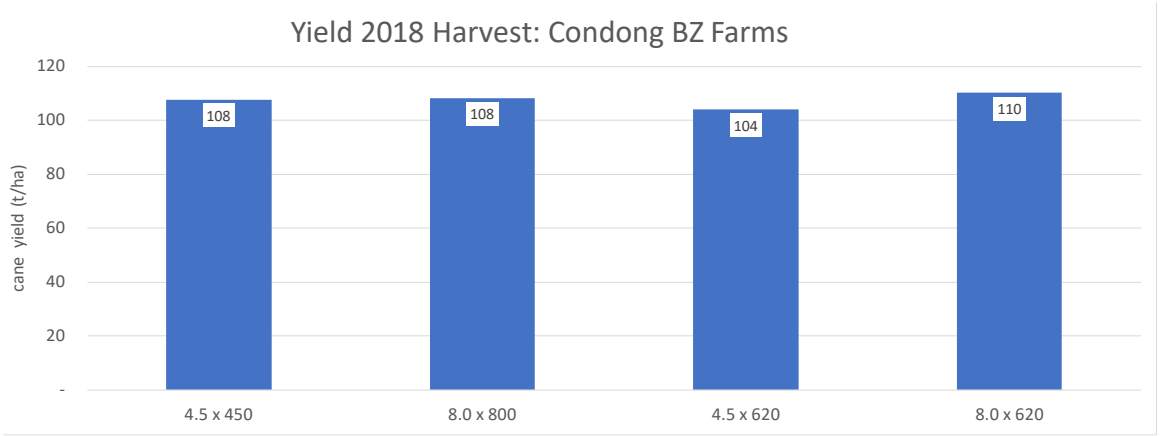

Figure 82: Crop yield BZ Farms trial 2018.

A large area in the centre of the trial block appeared to be badly affected by greyback canegrubs, and this is believed to have created variability in the observed results.

Trial 2: Bouchards Rd Childers.

Stool Damage

The 2018 harvest was the second harvest for this site. The variety is Q240 and the crop configuration is 1.8m "wide" single row. The yield at the 2017 harvest was approximately 110 t/ha across all plots.

Stool damage was assessed after harvest and the raw data is presented in Figure 83. As previously noted, the variety was Q240$^{\Phi}$ and billet diameter was typically 26-28 mm. Q240$^{\Phi}$ is a brittle variety.

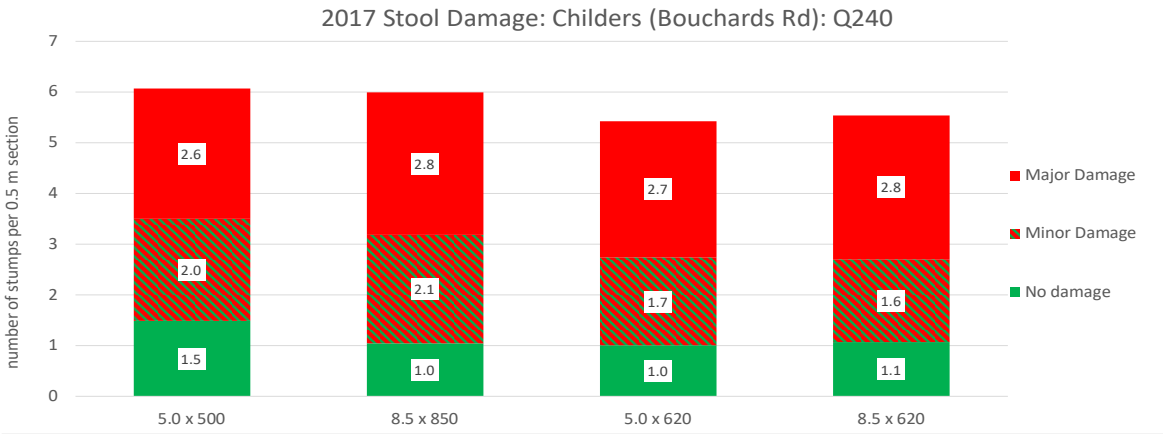

Figure 83: Stool damage assessment after 2017 harvest at Bouchards Rd Site with Q240$^{\Phi}$.

The stool damage assessment indicates the average number of cut stalks which could be assessed was higher for the two matched treatments, and lower for the "standard" high and low harvesting speed settings. Significantly, the low harvesting speed has 50% more undamaged cut stalks than the other treatments. The damage is presented on a percentage basis in Figure 84. This also indicates the lowest damage was associated with the low harvesting speed with linked component speeds.

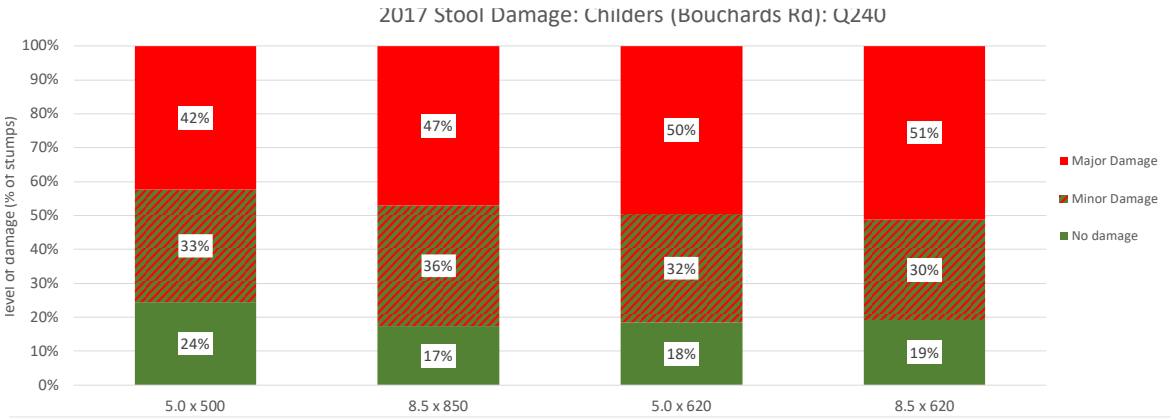

Figure 84: Stool damage assessment expressed as a percentage.

Plant Emergence and Growth

The shoot count was undertaken on 5/10/17, 45 days after harvest. Significant leaf damage to the emerging plants was noted across the trial, with the heaviest damage being noted in Replicate 1. The issue, and the variability of insect attack is illustrated in Photograph 16.

Photograph 16: Plant count being undertaken at trial on Bouchards Rd site. Note the insect damage to the cane leaf from insects, which is particularly apparent from the second visible row.

Figure 85 presents the postharvest emerged plant count and pre-harvest stalk count prior to the 2018 harvest. The post-harvest plant count and the pre-harvest (2018) millable stalk count both indicate some potential benefit in the matched component speeds, however the effect was not significant.

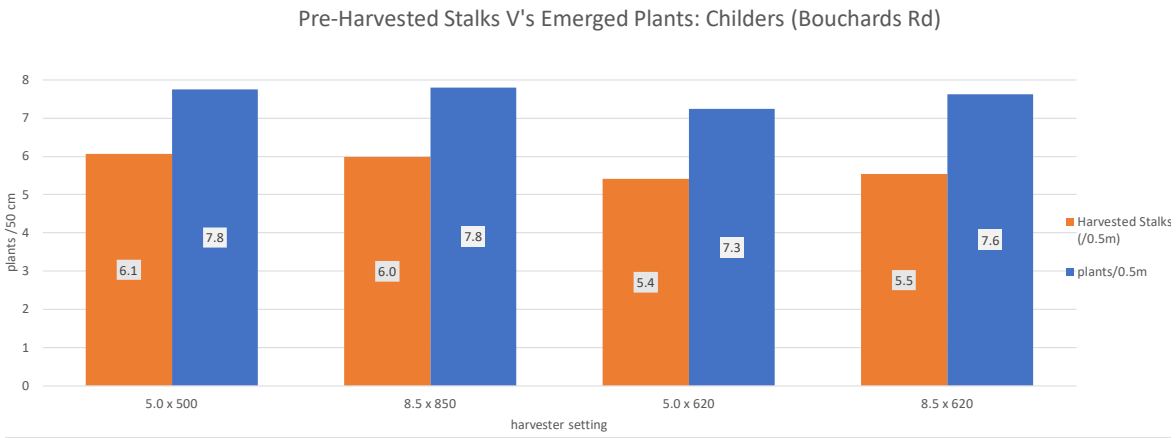

Figure 85: Emerged shoot count and pre harvest stalk count at Pranges Rd site.

Harvested Yield

The yield data for the main plots is presented in Figure 86. The value of difference between treatments 1 and the other treatments was P=0.0054. This indicated differences in yield figures were significant.

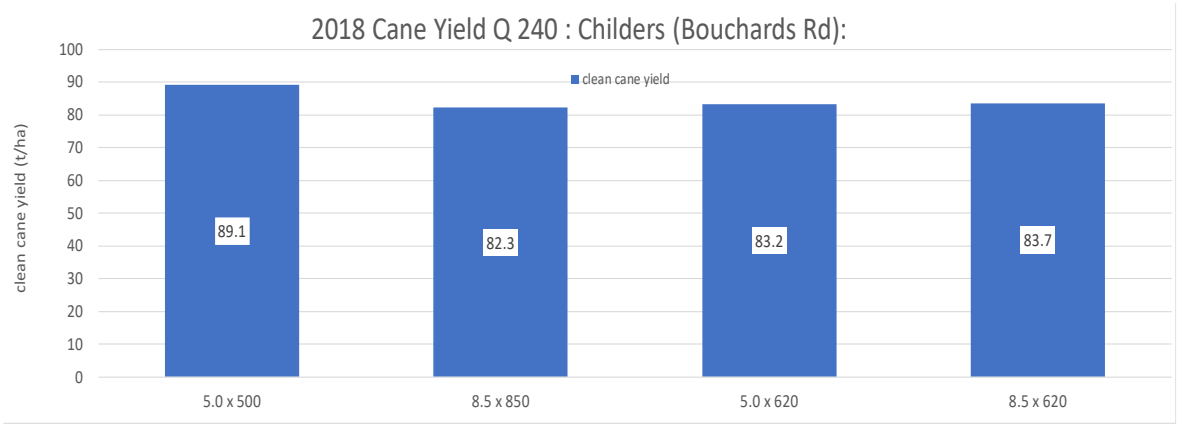

Figure 86: Cane yield at 2018 harvest.

The general trend was that with the low groundspeed and matched front-end speed the lowest stool damage (highest proportion of undamaged stalks) and highest pre-harvest millable stalk count were associated with highest yield. This also followed through to sugar yield, as indicated in Figure 87.

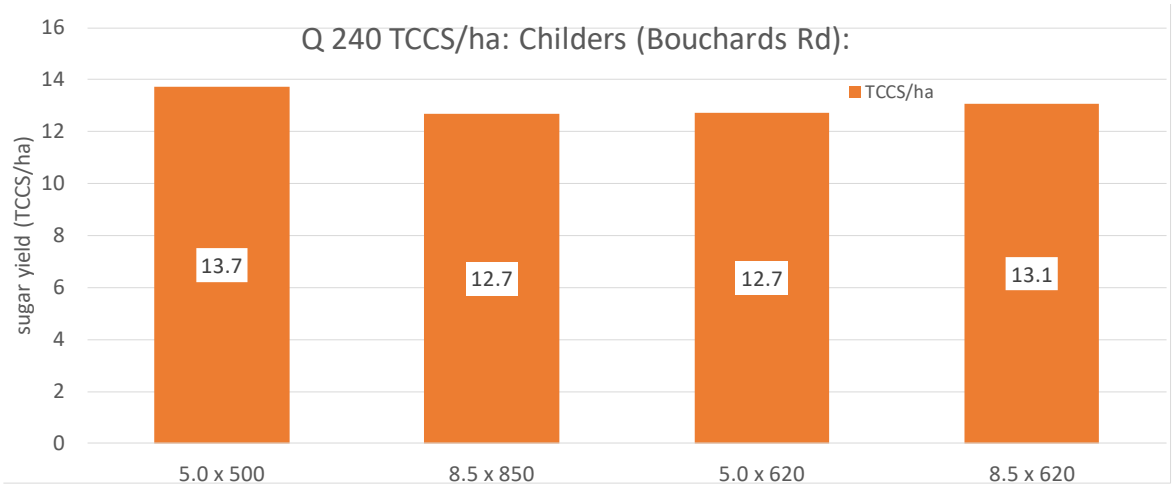

Figure 87: Sugar yield for the different treatments in the 2018 harvest, Bouchards Rd.

Trial 3: Condong Colonial Drive

Stool Damage 2017

Raw data relating to stool damage at Colonial Drive (average cane yield 115 t/ha) is presented in Figure 88. The variety was Q240$^{\Phi}$ in dual row configuration. The data relates to the 15m of row length in the 7.5m plots.

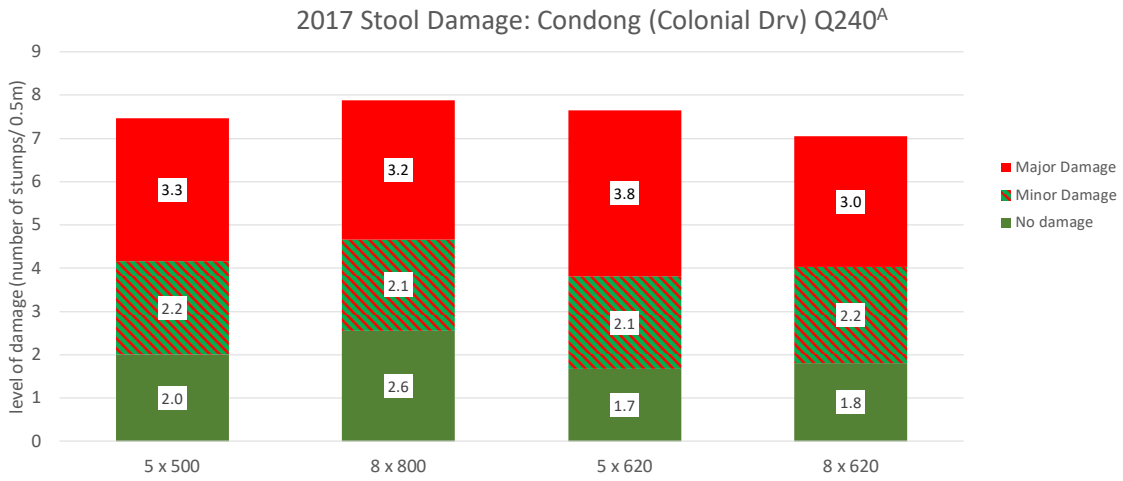

Figure 88: Stubble damage (raw data) at Colonial Drive with Q240

The data indicates highest stalk numbers for all damage levels at the high harvesting speed and matched component speeds. The data is expressed as a percentage in Figure 89.

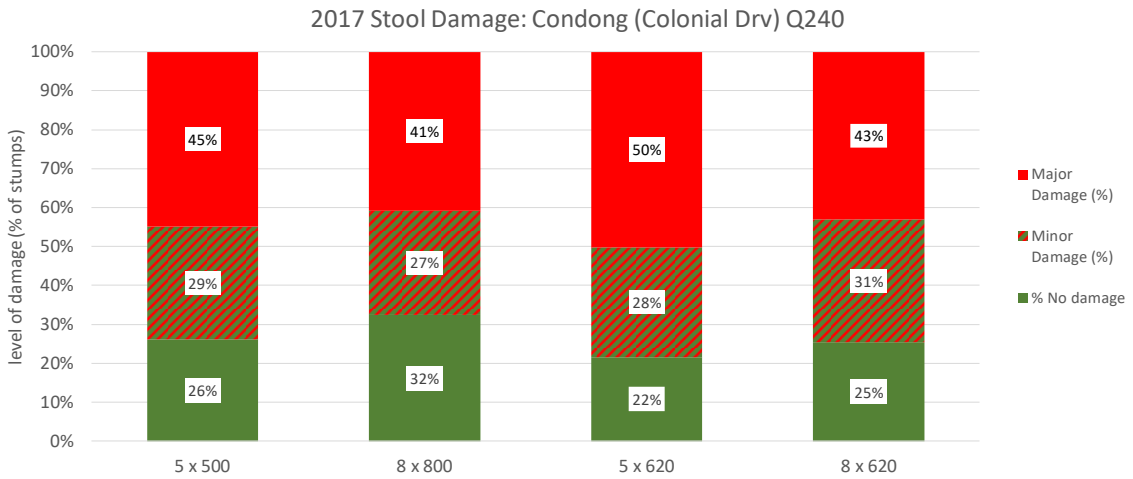

Figure 89: Stubble damage (as %) at Colonial Drive with Q240

Q240$^{\phi}$ is a relatively brittle variety and with a billet diameter of typically 26-28 mm, was considered a candidate for high levels of stool damage. Damage at both this site and the Bouchard's Rd site was moderate, relative to the damage observed to Q208$^{\phi}$ at the other sites. We consider that stalk breakage probably occurred prior to the basecutting operation, and the basecutters then 'trimmed the stool'.

Plant Emergence and Growth

The harvest assessment plant count was undertaken on 6/10/17, 17 days after harvest.

Photograph 17: Crop emergence at the North trial 17 days after harvest.

Photograph 18: High levels of germination and very even plant size was common across most plots.

As indicated in Photograph 17 and Photograph 18, germination and emergence was rapid and the emerged population was generally high and growth even across all plots. This can be attributed to recent rain, giving good soil moisture conditions and the warm weather conditions at the time.

At 45 days after harvest, plant counts and biomass assessments were undertaken, with the findings presented in Figure 90. The plant count was highest for the high speed/matched treatment, which was consistent with the stubble damage observations, however plant biomass was higher for the low speed / matched treatment, because of higher plant growth rate.

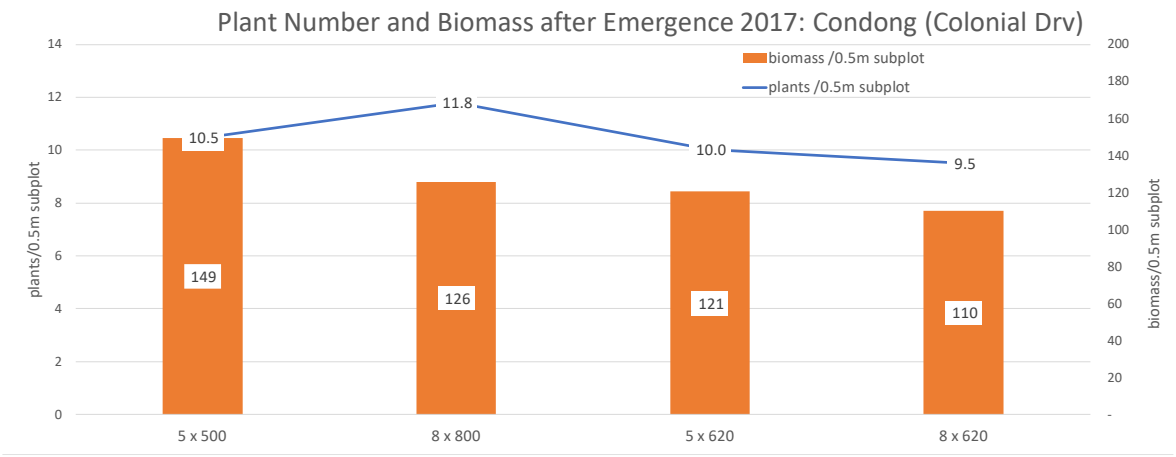

Figure 90: Plant emergence count and biomass.

Harvested Yield

Harvested yield is presented in Figure 91. This indicates that the low harvesting speed and matched compliment speed gave the highest yield, which was consistent with the biomass assessment at 45 days.

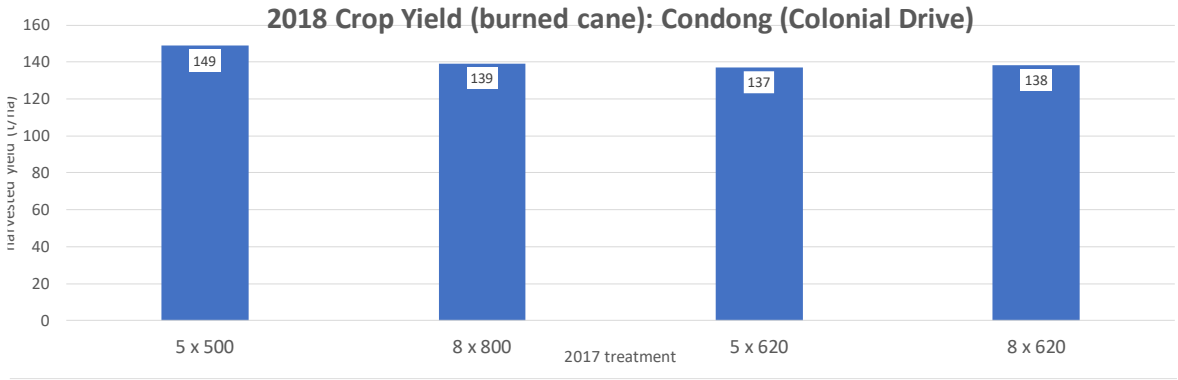

Figure 91: Harvested yield at the Colonial Drv site, 2017

The differences were not significant (P=.15) at normally acceptable statistical levels, however the results were consistent with trends in other trials.

Trial 4: Plath Rd Childers

Stool Damage:

The Plath Rd 2016 harvest and 2017 yield data was primarily used to initiate treatments, establish protocols and observe any yield variability across the block. The 2016 yield data for Plath Rd indicated a gradient of approximately 30% across the trial, which was not evident in the 2017 harvest, however replicate 2 was the lowest yielding replicate in 2017. We consider that unevenness in irrigation application was a major contributor to the initial 2016 variability, however the 2017 yield data is of greater significance, because it is believed that increased stool damage associated with the larger crop size in Replicate 3 was a significant driver of the effect. This limited the usefulness of full plot yield data for this site.

The block was harvested on 11/10/17, the harvesting operation was undertaken utilizing GPS Autosteer on the harvester. Post-harvest stool assessments were undertaken on the following day. A

photo of the row profile indicating typical cutting height is shown in Photograph 19. Of interest is the development of larger “stool clumps” with significant gaps between stools. Observations at this site were similar to the observations at other sites, which indicate that smaller and shallower stools are more prone to damage, complete removal or mortality.

Photograph 19: The row profile at the Plaths Rd trial after the trash and loose soil had been removed.

The averaged stool damage data from the different treatment plots in 2016 was shown in Figure 70. The 2017 data is shown in Figure 92.

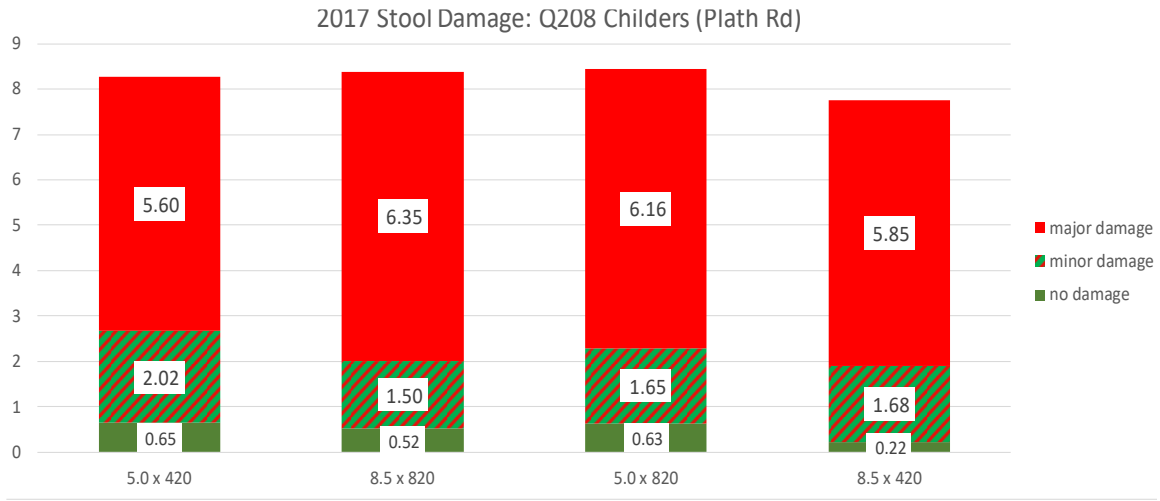

Figure 92: Stubble damage (raw data) after the 2017 harvest at Plath Rd with the same harvester as in 2016

The stool damage data indicates very high levels of stool damage across all harvesting treatments, with minimal difference in the average total number of stumps counted per treatment. Analysis of the data as percentage damage is shown in Figure 93.

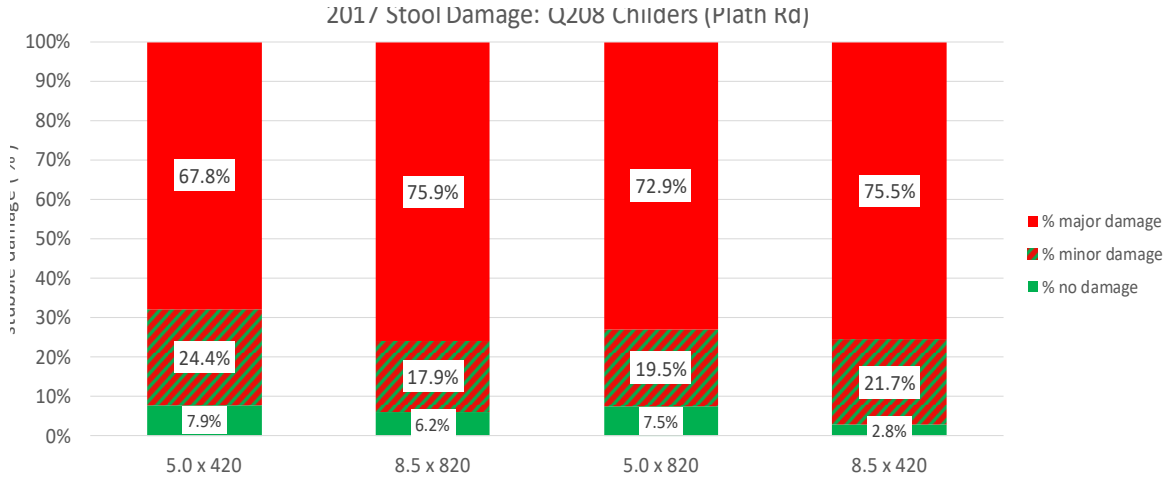

Figure 93: Stubble damage after the 2017 harvest at Plath Rd with the same harvester as in 2016.

The variety was Q208(ϕ) and had a typical billet diameter of <22 mm. Being a moderately thin variety, it was initially anticipated that stool damage would be low. The data shows very high levels of major damage, with total damage across all plots being higher in 2017 than in 2016. Differences among treatments was small, but there was a trend for lower forward speed in conjunction with higher component speeds to give greater damage. The crop was more stressed in 2017, and there was an apparent trend of greater damage in stressed crops. This is consistent with observations from Nicaragua (Caldere Dominguez & Norris, 2018).

Plant Emergence and Growth

At 50 days after harvest, plant counts were conducted, and again prior to the 2018 harvest. The data is presented in Figure 94.

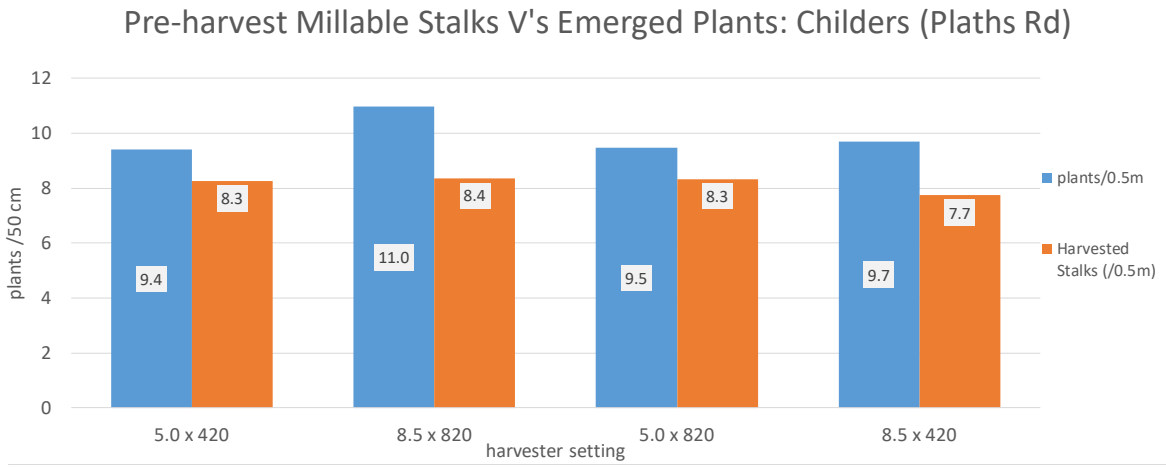

Figure 94: Emerged plant population and pre-harvest millable stalks, Plaths Rd.

The Emerged plants data indicated highest shoot levels associated with the high speed and matched component speed settings. This may be associated with higher levels of damage. With the exception of the 8.5 x 420 treatment which was lower, millable stalk counts for all treatments were similar.

Yield

The harvested yield data for the trial is presented in Figure 95. The data indicates little difference in yield between treatments, and no significant effects.

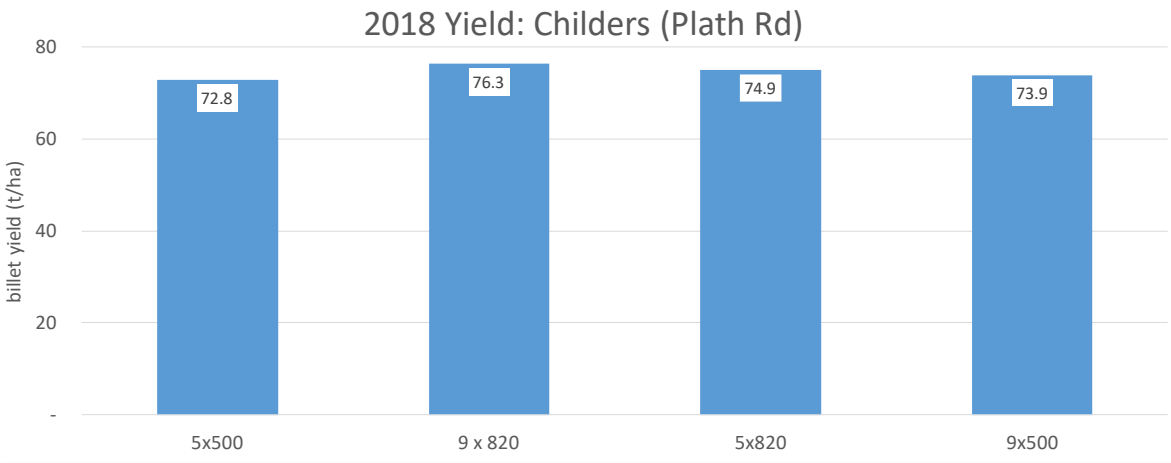

Figure 95: 2018 billet yield for Plaths Rd trial.

Trial 5: Mona Park.

Stool Damage

At Mona Park (average cane yield 140 t/ha) and BZ Farms (average cane yield 115 t/ha) the variety was again Q208(ϕ). Stool damage at Mona Park was extremely high (Figure 96) with the crop appearing to be heavily moisture stressed prior to harvest.

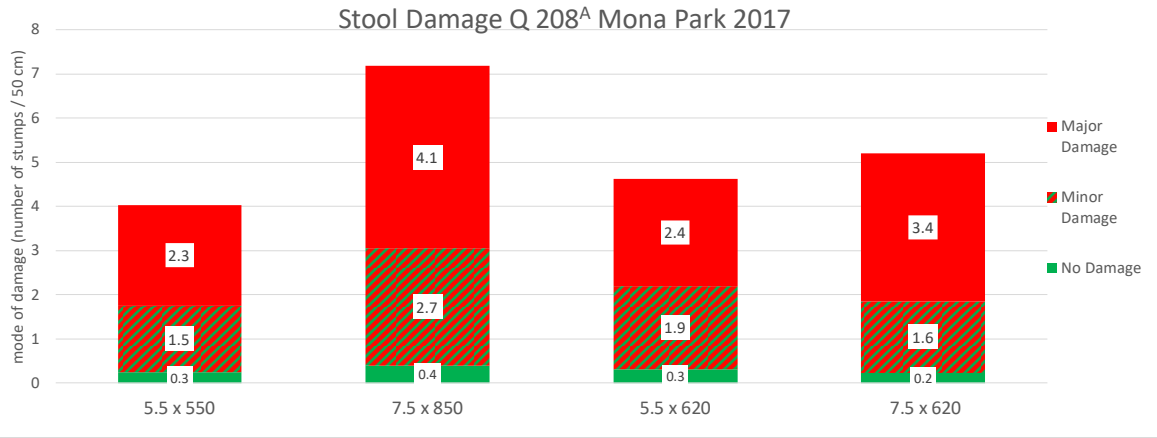

Figure 96: Stubble count data for Mona Park trial after 2017 harvest.

The stubble count data indicates very low levels of "visible" stubble in the sub-plots, and very high levels of damage. The relationship between treatments and damage (Figure 97) does not follow any anticipated patterns. The number of visible stubble pieces is low compared what would have been anticipated.

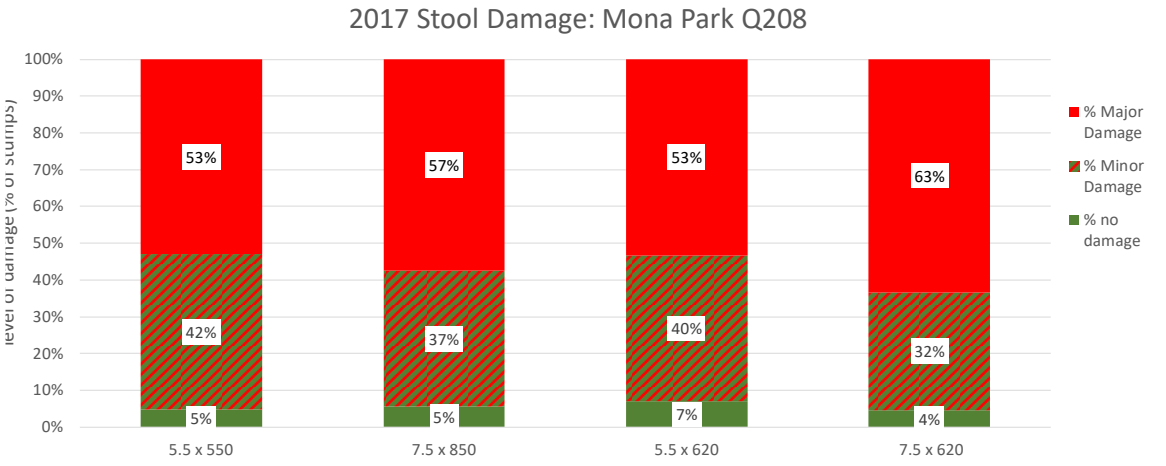

Figure 97: Stubble damage assessment for Mona Park trial after 2017 harvest.

Plant Emergence and Growth

Plant counts were undertaken 37 days after the harvest, and plant weight adjacent to each sub-plot also assessed.

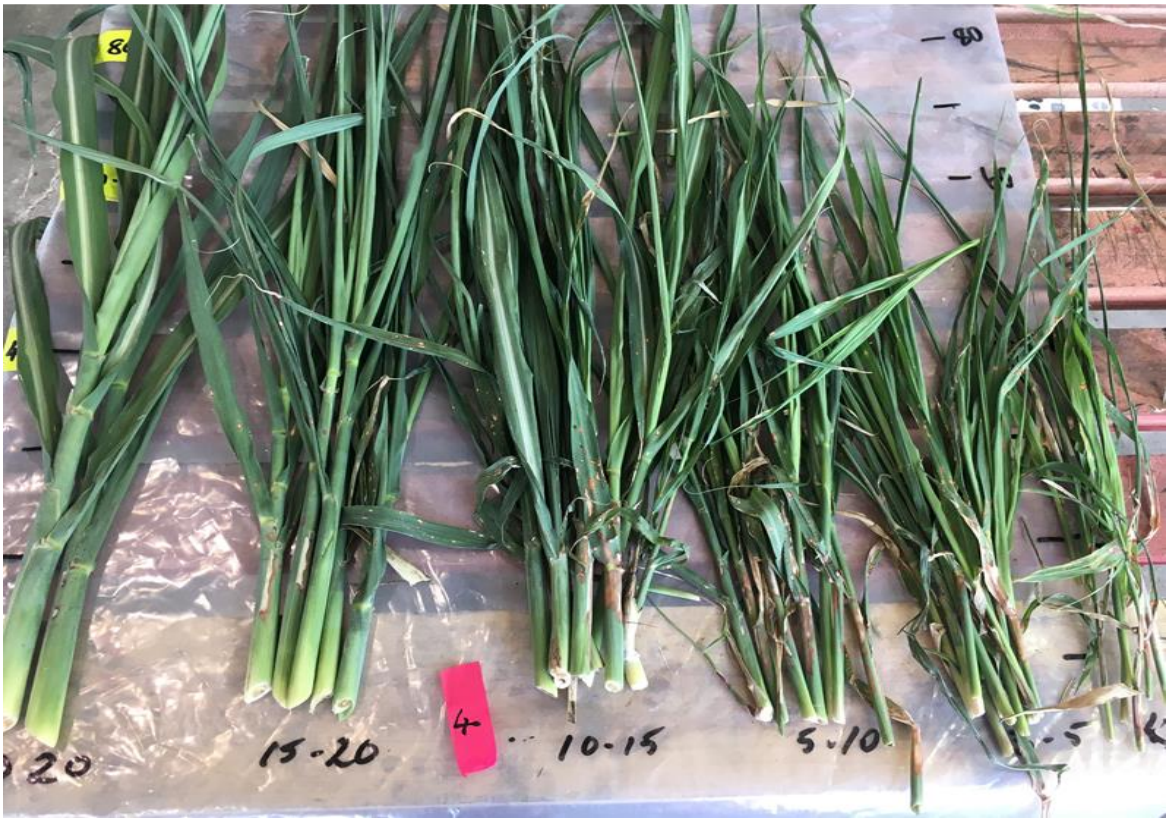

Photograph 20: Range in ratoon shoot size typical in Mona Park trial plots.

The plant numbers and harvested plant biomass from adjacent to the ends of the plots is presented in Figure 98.

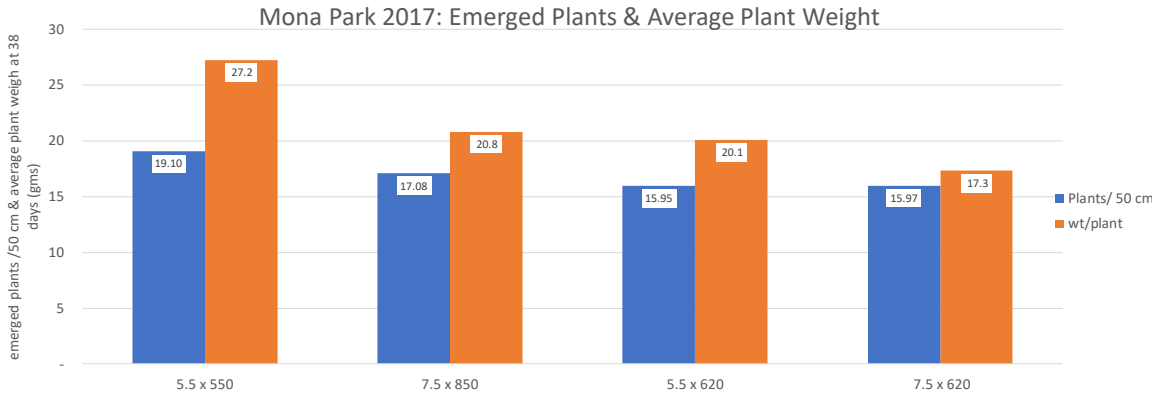

Figure 98: Shoot emergence at 37 days and typical average plant weight, Mona Park.

Despite the low visible stump count, the number of ratoons was relatively high, with the highest shoot count being associated with the low harvesting speed and matched component speeds. This treatment also had the highest observed plant weight, with average plant weight being >30% higher than other treatments.

Yield

The harvested yield of the main plots at the Mona Park site is presented in Figure 99.

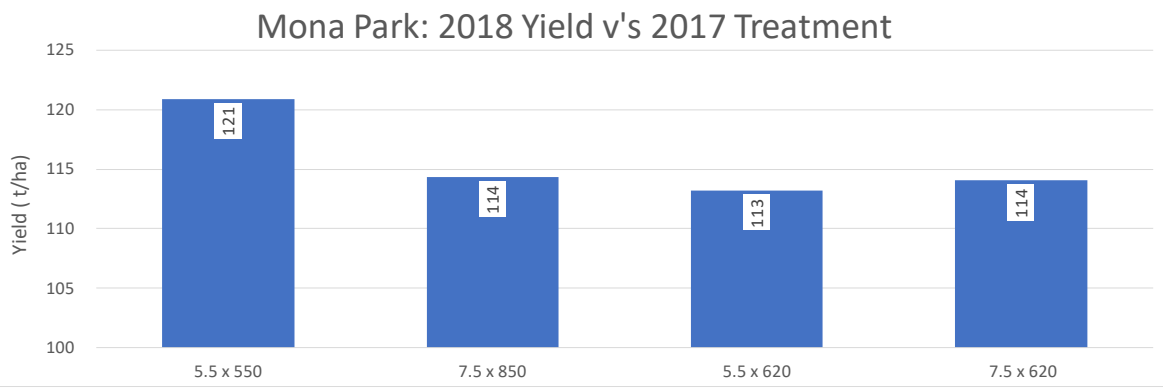

Figure 99: Yield of different treatments in 2018 from 2017 treatments at Mona Park.

Whilst a large difference between yields from different treatments was indicated, with the major effect being the low groundspeed treatment v's the other treatments, high variability between replicates meant that statistical significance was not achieved at typical confidence levels.

6.3.4.2018-19 Trial results.

Based on the observations of the 2016 and 2017 harvest data, damage to the cane stool associated with all harvest treatments was very high, with typically the post-harvest assessments indicating fewer than 20% of the stalks from the cane stool having minimal damage, with severe damage being observed on over 50% of stalk in some instances. Three clear issues needed to be addressed:

- The high levels of stool damage were sustained across all treatments;
- The limited impact of the different harvester setup and operation options meant that alternative strategies to understand damage were necessary; and
- The relatively poor correlation between typical measurements relating to stool damage and crop response.

To address these issues, a decision was made to introduce new treatments to "separate" the damage associated with gathering and knockdown from basecutting damage.

Based on the work of Kroes, significant damage can be anticipated to result from the knockdown and feeding processes, particularly on modern harvesters where these settings are much more aggressive than older machines. Work by Davis and Norris (2002) also indicated that stool damage is likely to be associated with the gathering and aligning processes.

To quantify the relative impact of the gathering and feeding processes relative to basecutter damage per se, an additional sub-plot was incorporated into each trial plot. The treatment protocol was then to:

- Pre-cut additional sub-plots at a height of approximately 200-250 mm above ground level, prior to harvest. The sub-plots were parallel in location to the initial sub-plots, but in the second row across. Whilst the initial sub-plot was in R3 of the main plot, the additional sub-plot was in R1, so that direction of harvest etc was the same.
- The 200-250 mm cutting height was to maximise the length of the uncut stalk but ensure there was no contact between the forward feed components and the cane stalk prior to basecutter contact.

- At the pre-cut sub-plots, the cut cane stalk was laid on top of the cut stumps; this allowed it to be picked up by the harvester but also “anchored” the top of the stalks to better represent the normal cutting process.

This protocol then allows the relative impact of the gathering and feeding and the basecutting to be better isolated.

The process at the trials is illustrated in Photograph 21 and Photograph 22

Photograph 21: Sub-plot manually harvested at approximately 250 mm above ground level at the Childers Plath Rd trial.

Photograph 22: Sub-plot manually harvested at the Mona Park trial. Note the cane is placed to assist feed and support the stumps from horizontal movement.

The visual differences between the levels of damage are illustrated in Photograph 23 and Photograph 24, taken at the North trial site at Condong. The impact of the pre-cutting of the cane stalks prior to the harvesting operation can be seen.

Photograph 23: Cane stool in the "pre-cut" or "no KD" treatment, showing generally lower levels of damage.

Photograph 24: Cane stool showing much higher levels of damage in a "standard" treatment. Note the level of "deep splits".

Trial 1: BZ Farms Condong.

The stool damage associated with the 2018 harvest is presented in Figure 100, with the damage presented on a percentage basis in Figure 101. In the "std" treatments, levels of stool damage were very high, and this is probably associated with both the crop being moisture stressed prior to harvest as well as areas of canegrub damage which effected the field and some of the sub-plot areas.

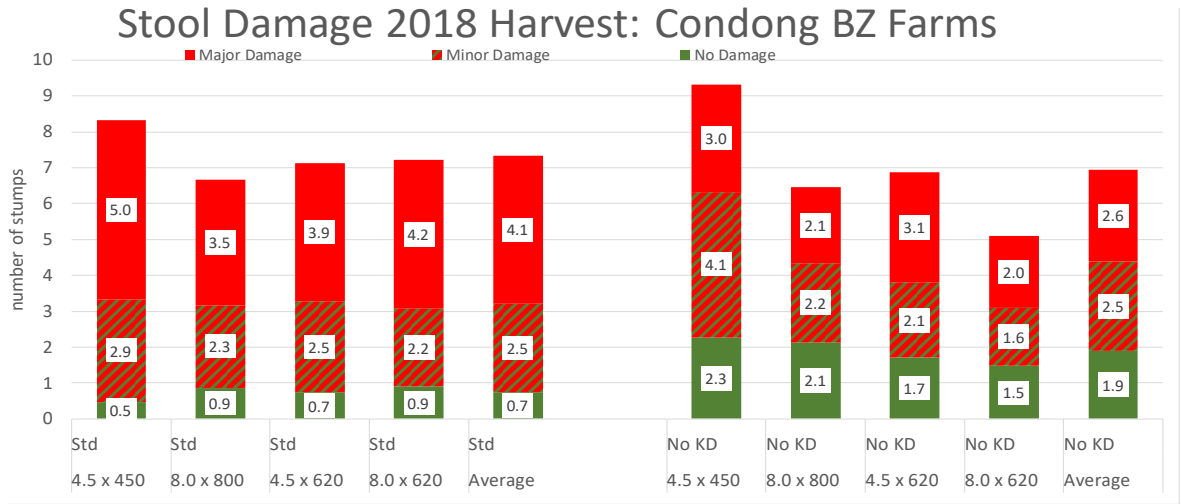

Figure 100: Data relating to stool damage for "standard" and "no-knockdown treatments.

Most significantly, the levels of damage observed in the "no-KD" plots were very significantly less than the damage with the "standard" machine configuration. The average number of stumps

identified for classification were also higher in the “no KD” treatments. In Figure 101, the data is presented as percentage damage.

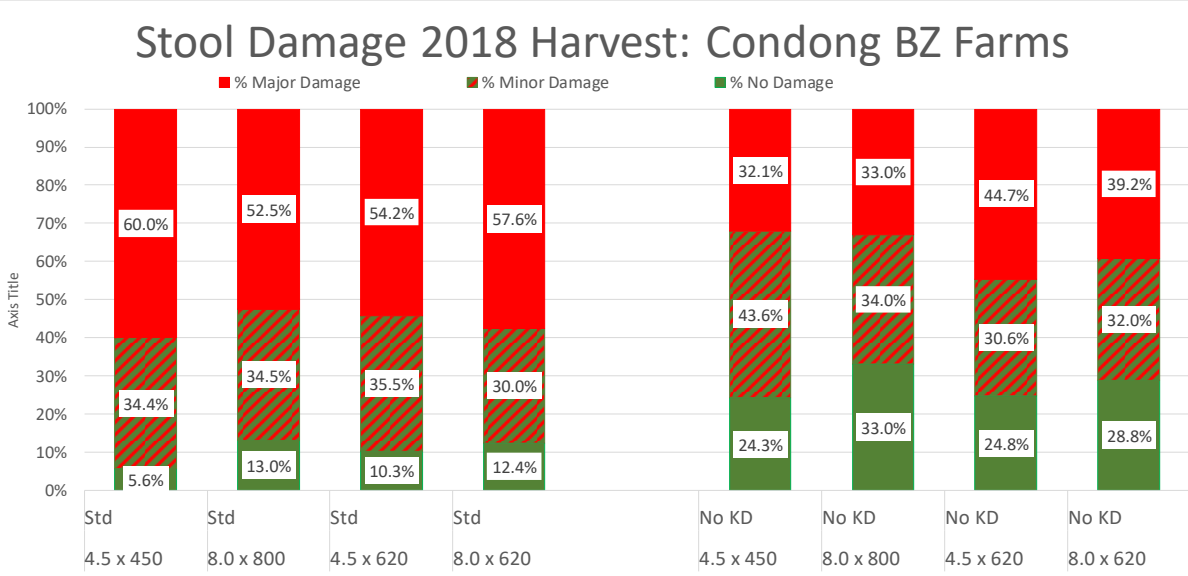

Figure 101: Stool damage assessment after 2018 harvest, expressed as a percentage.

From the data, the damage was high in the “std” low forward speed treatments, with undamaged stumps accounting for less than 13% of stumps, whereas in the “no-KD” treatments, undamaged stumps were as high as 33%. The reasons for higher levels of damage at the low speed “matched” treatments is not understood, however issues with the speed control on the forward feed rollers may have had these units running at maximum speed rather than matched speed.

The crop emergence after the 2018 harvest is presented in Figure 102. This indicated lower shoot numbers for the “no-KD” treatments. Visually, the plants from the no-KD treatments were more vigorous.

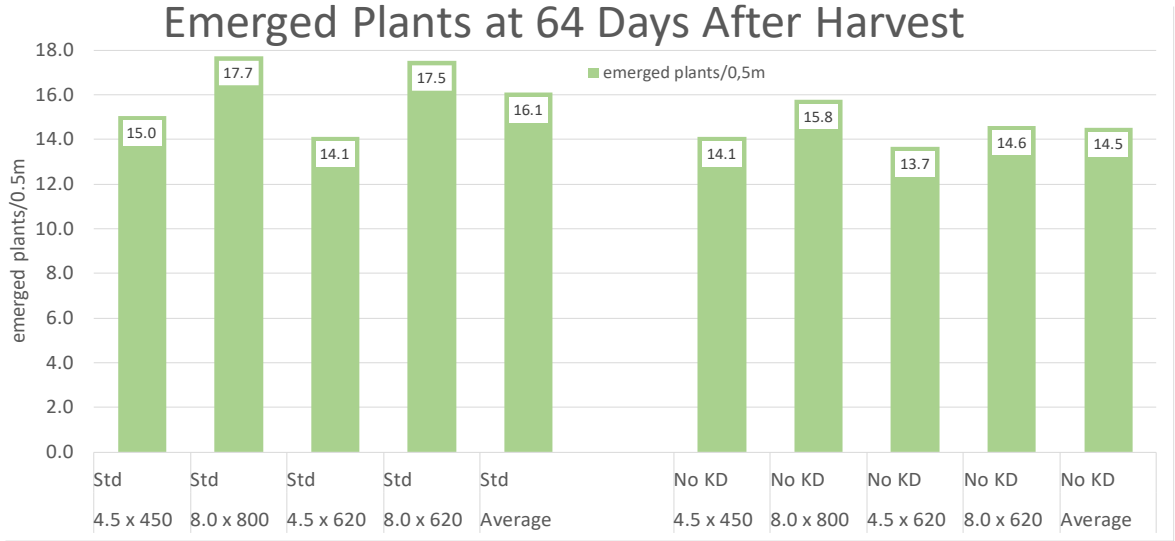

Figure 102: Emerged plants at 64 days after harvest, BZ farms.

The crop was one of the last crops to be harvested in 2019, because the field was to be rejuvenated. A combination of length of growing season and climatic conditions meant that crop yield was high (approx. 126 t/ha). The crop was also very heavily lodged. This meant that, despite major effort, it

was not possible to find and handcut the plots without major disruptions to the harvesting schedule. Conventional yield data was gathered, as was an assessment of stumps in the plot areas after harvest. The stump assessment is shown in Figure 103.

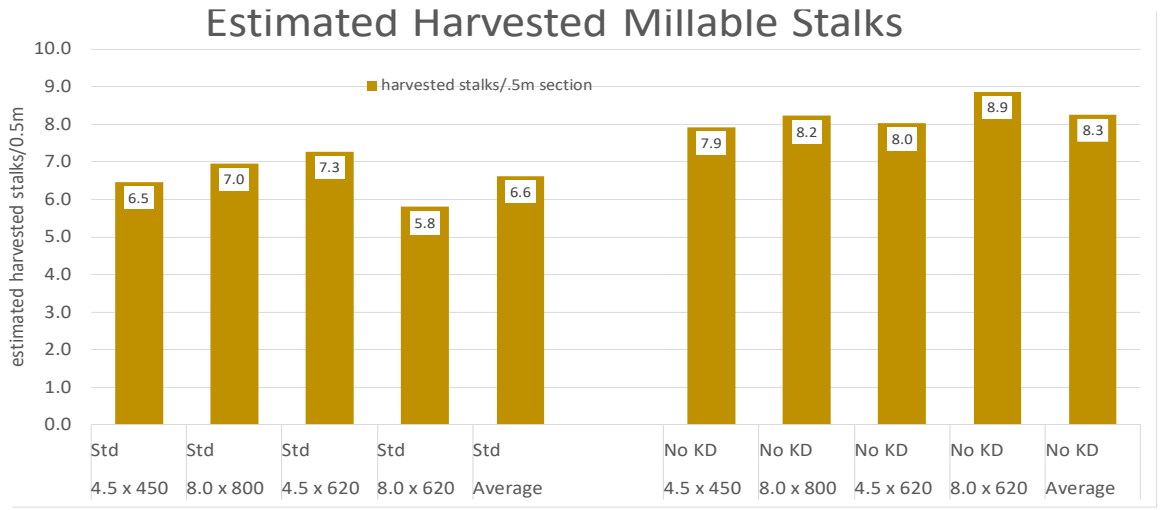

Figure 103: Estimated harvested millable stalks, BZ Farms 2019

The estimated millable stalk data indicates that, on average, the "no KD" treatment had 6.6 stalks/0.5 m of row length and the no-KD treatment averaged 8.3, an increase of 25%.

The yield from the harvest of the full plots is presented in Figure 104.

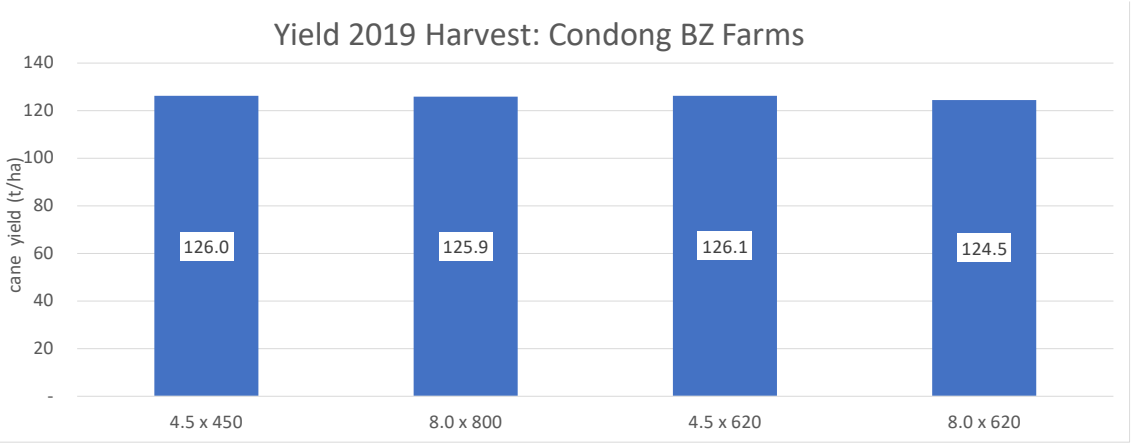

Figure 104: Harvested full plot yield BZ Farms 2019.

This indicated no differences in yields from different main treatments. This was expected given the issue with variability associated with the canegrub issue.

Analysis of the stump population after harvest can be utilised as an indicator of the impact of the harvest process on the number of stools available to re-grow, and the change in spacing regime of the regenerating crop. Figure 105 presents the average stool population (stumps/0.5m for the treatments) and the variability of this population measure, presented as the mean of the Standard deviations in each of the three replicates.

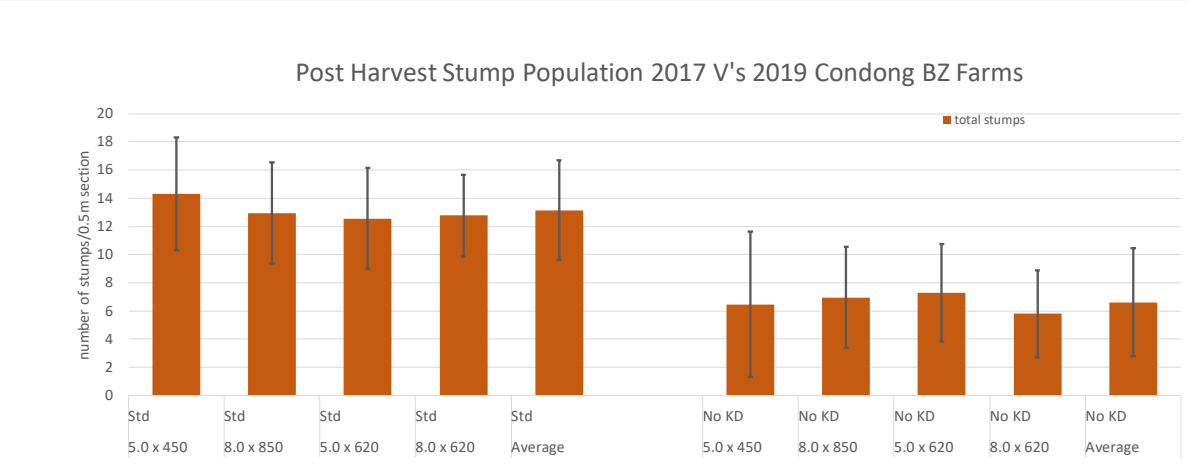

Figure 105: Post harvest stump population and spacing distribution after 2017 and 2019 harvests.

The data indicates that the average number of stumps per 0.5m section declined from approximately 13 after the 2017 harvest to approximately 6.2 after the 2019 harvest. This difference was significant at >99% confidence level. Significantly also the variability in population has increased. Whilst the mean standard deviation has changed by only a small level, the Standard Deviation as a percentage of mean for the two groups increased from 27% to 58%,, with significance again being at > 99%. Typically, viable stools have several well anchored stumps, whereas where stools consisted of a small number of stumps, the damage was higher and viability more questionable. The data indicates that probability of having sections with limited stool viability increased over the time period observed.

Trial 2: Bouchards Rd Childers.

The stool damage assessment at the Bouchards Rd trial site after the 2019 harvest is presented in Figure 106. The average number of stumps assessed in the standard treatment was approximately 3.8, and the number assessed in the no KD treatments averaged 4.6, an increase of 21%.

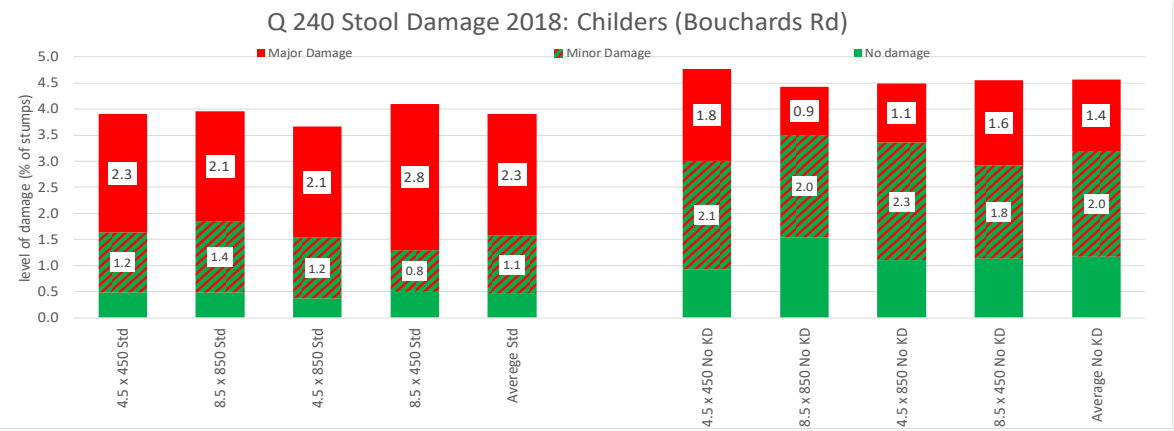

Figure 106: Stool damage raw data Bouchards Rd 2019

The stump assessment expressed as a percentage damage is presented in Figure 107. This indicates that in the standard setup, the percentage undamaged averaged 12%, v's 25% in the treatments with no-KD.

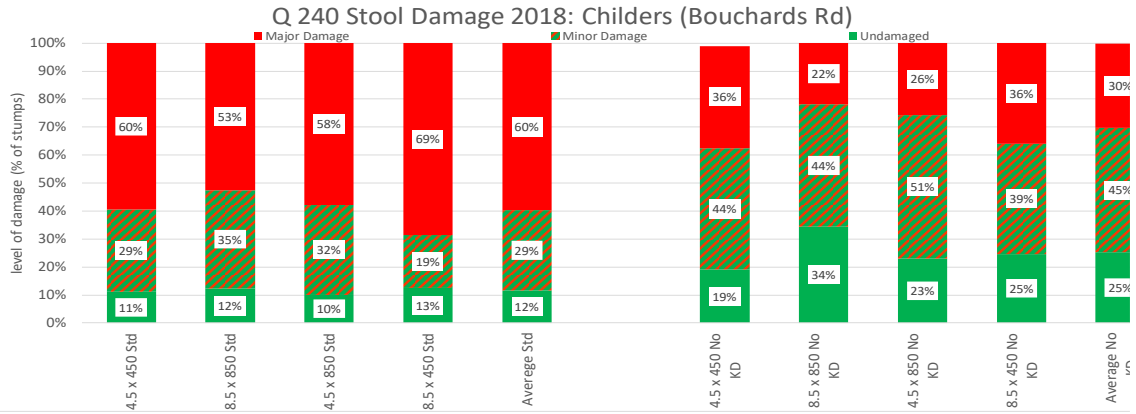

Figure 107: Stool damage percentage Bouchards Rd 2019

The level of major damage is also substantially lower in the no KD treatments.

Emerged plant counts and plant height assessments conducted 67 days after harvest are presented in Figure 108. This indicates that plant numbers were lower in the no-KD treatments, however assessed plant height was higher.

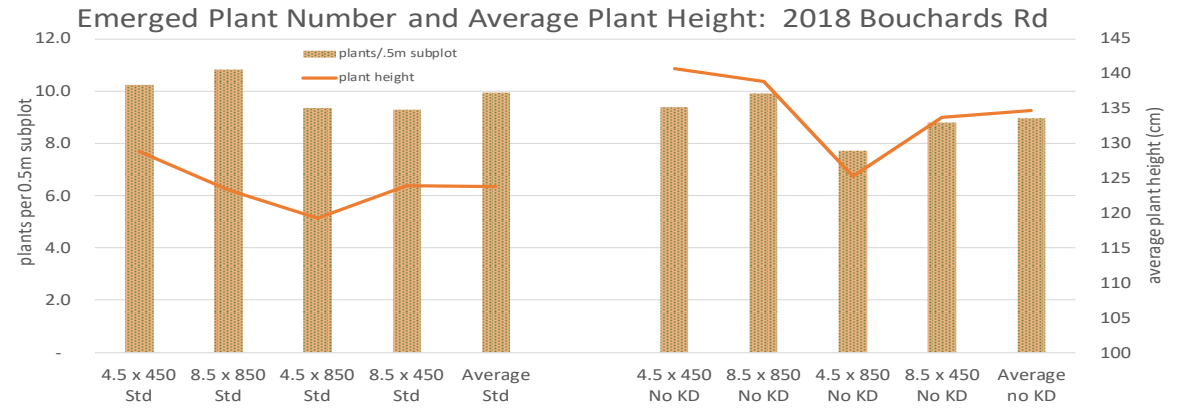

Figure 108: Emerged plant number and average plant height for the Bouchards Rd trial.

On the basis of the plant weight v's plant height relationships gathered, the biomass for the different treatments were derived. This is presented in Figure 109. This indicates higher biomass in the no-KD treatments, despite the lower plant numbers.

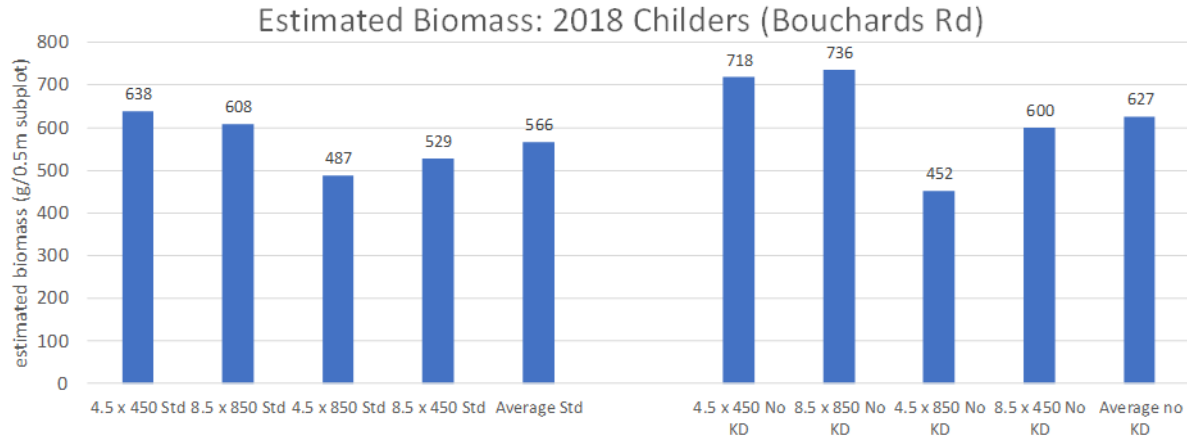

Figure 109: Derived biomass 67 days after harvest for the different treatments.

The trial was harvested on 31/9/2019, with the subplots being manually harvested.

The yield of the sub-plots is presented in Figure 110. This indicates that the average yield of the standard treatments was 97 t/ha, and the no-KD treatments averaged 108 t/ha, an increase of 11%.

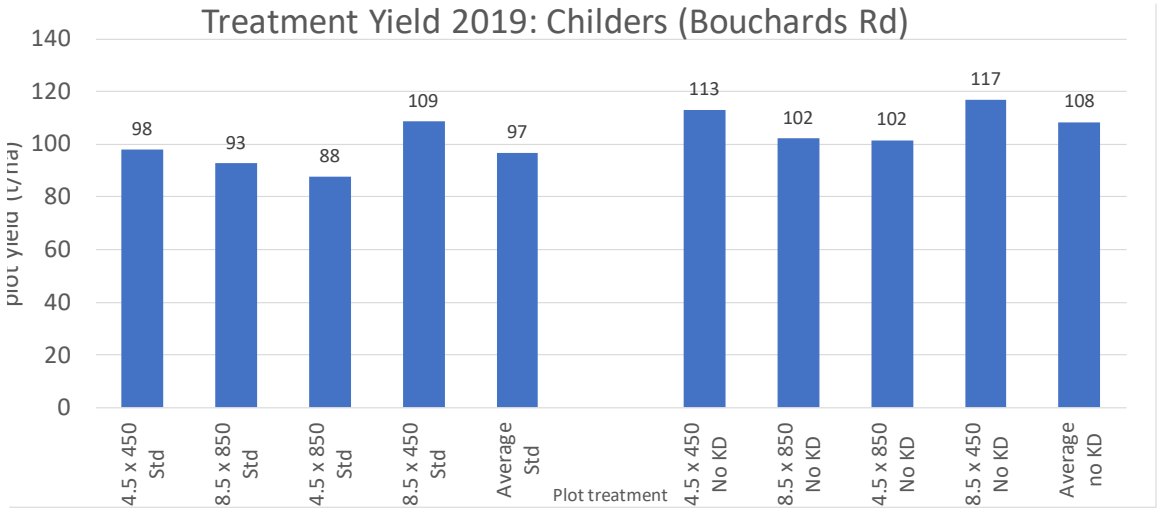

Figure 110: Treatment yield for the sub plots at the Bouchards Rd trial.

Of interest also was the highest yielding treatments were associated with lower component speeds.

The machine-harvested yields of the full plots is presented in Figure 111. This indicates little difference between the main treatments.

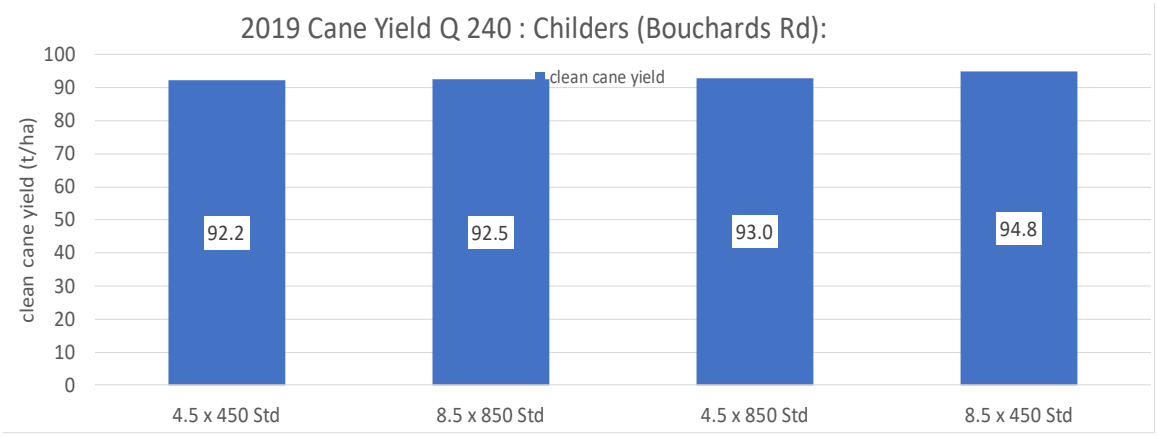

Figure 111: Machine harvested yields of main plots.

Figure 112 presents the average stool population (stumps/0.5m for the treatments) and the variability of this population measure, presented as the mean of the Standard deviations in each of the three replicates.

Again, the data indicates a drop in stump numbers from an average of 5.5stumps/0.5m section to 4.1 stumps/0.5m, statistically different at 99% level. The average variability in stool numbers actually deceased from 36% to 26%, and this was also significant at the 99% level. The difference in the mean x Std Deviation was not significant.

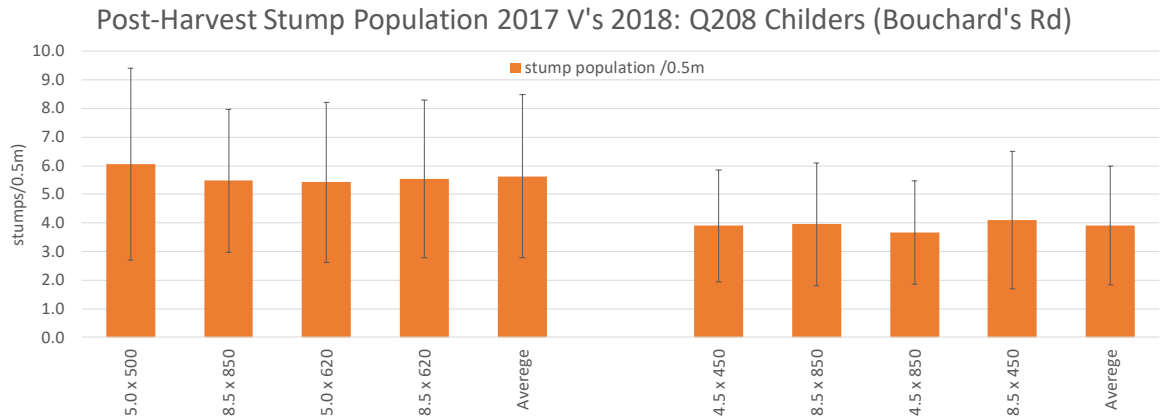

Figure 112: Post harvest stump populations after 2017 (Left data) and 2018 (Right data) harvests.

Whilst the population decreased between 2017 harvest and 2017 harvest, the percentage probability of a gap did not increase however the percentage of plots with less than two stumps/0.5m increased. The viability of these stumps would then be questionable. Stump counts were not undertaken after the 2019 harvest.

Trial 3: Condong Colonial Drive

The data on number of stumps and stump damage rating for the 2018 harvest is presented in Figure 113. This indicates the average number of stumps which could be identified for assessment was approximately 9.5 in the standard treatment and 10 in the no-KD treatments.

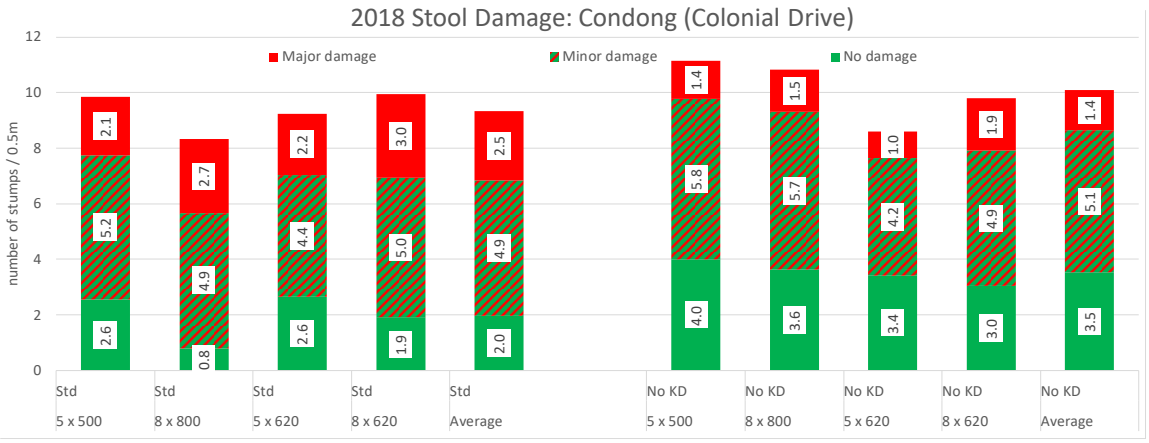

Figure 113: stump damage assessment and numbers, Colonial Drv.

Analysis of the damage presented as a percentage in each category in Figure 114. This indicates the percentage of stumps with major damage averaged 27% in the standard harvester configuration, and this reduction in damage by the removal of the KD effect is maintained.

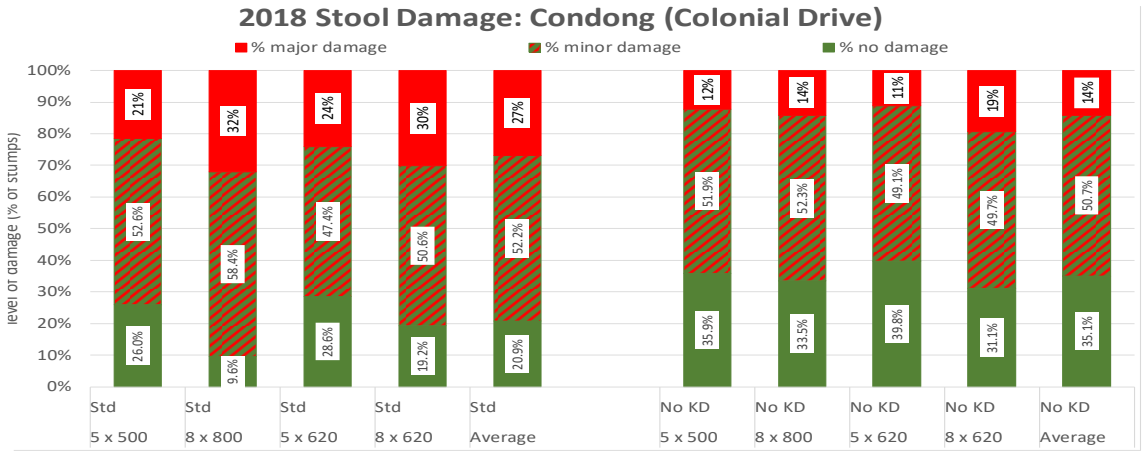

Figure 114: Stump damage data for the Colonial Drive site after the 2018 harvest.

There is no strong trend with respect to damage associated with the harvester treatments.

Early Growth, as determined by the count of emerged shoots 76 days after harvest is presented in Figure 115. The average number of shoots for the standard treatment was 24 /50 cm, and for the no-KD treatment 23 shoots/.5m. This is consistent with other datasets, with little difference in shoot numbers, however overall shoot numbers are comparatively very high.

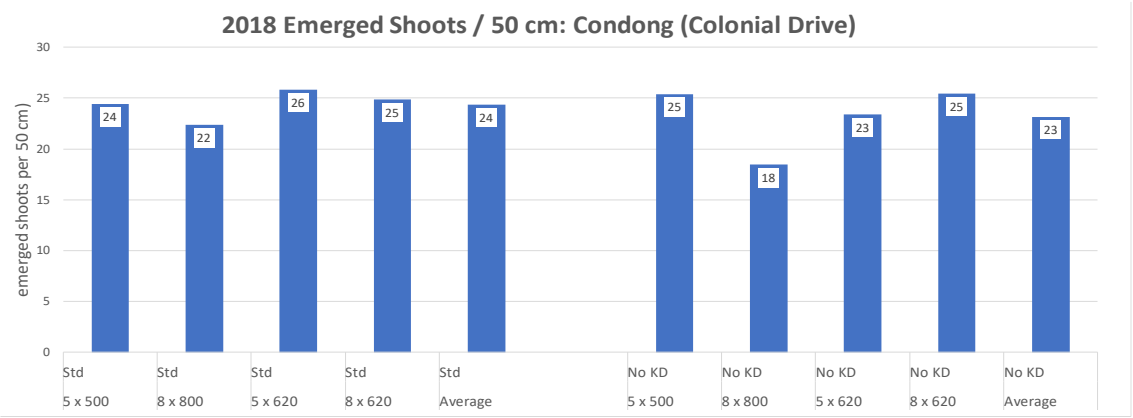

Figure 115: Emerged plants per 0.5m of each dual row at the Colonial Drv trial.

The hand-cut yield data of the sub-plots is presented in Figure 116. The average yield of the hand-cut plots harvested with the standard harvester configuration in 2018 was 102 t/ha, and the average yield for the plots in which the KD effect was removed was 115 t/ha.

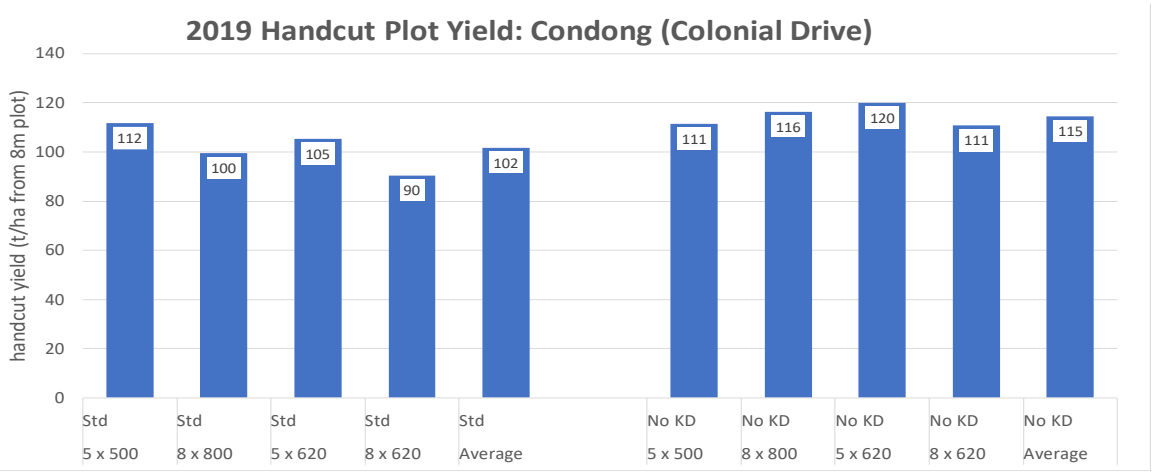

Figure 116: Hand-cut sub-plot yield, Colonial Drv.

Patterns of response between harvester settings and the KD / no KD treatments were not consistent, with benefits associated with lower forward speed and matched components speed in the standard harvesting configuration, but less differences between treatments when the KD effect was removed. Again, this is consistent with other trial plots. The harvested yield for the main trial plots is presented in Figure 117, with yields of these main treatment plots ranging from 124 t/ha to 132 t/ha.

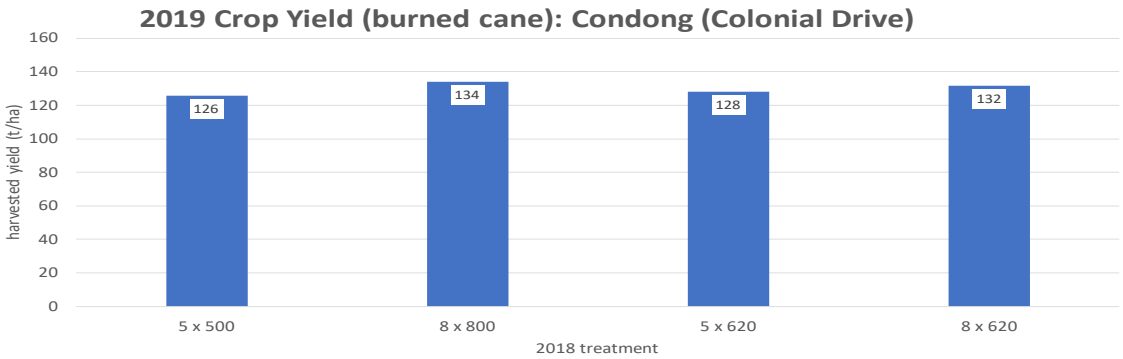

Figure 117: Harvester Yield, Colonial Drv.

As noted with other trials, the highest (but not significantly different) yields were associated with the high groundspeed and matched component speeds. The reason for this outcome is not fully understood.

The change in stumps visible after the 2017 harvest v's the number after the 2018 harvest are presented in Figure 117. Again, this indicates a reduction in stump numbers, with the difference being significant at the 99% level.

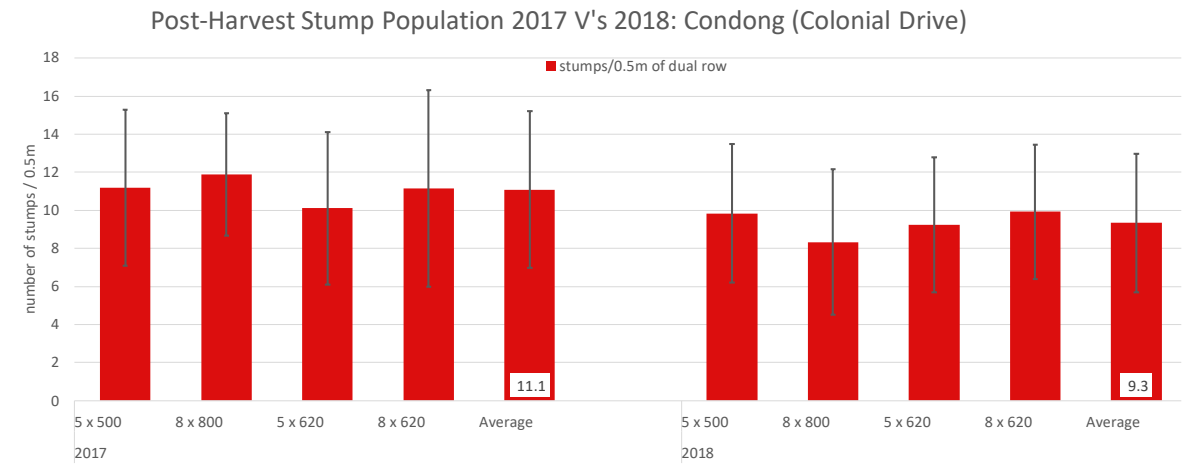

Figure 118: Post-harvest stump count after 2017 and 2018 harvests, Colonial Drive.

The averaged standard deviation, neither raw nor as a percentage of mean population was significantly different. After the 2018 harvest, average stool populations and was still good and the probability of small stools was low.

Trial 4: Childers: Plaths Rd

Numbers of stumps assessed and levels of damage for the different treatments are presented in Figure 119. The average number of stumps which could be identified for assessment averaged 5.8 in the standard treatment, and marginally less at 5.6 in the no-KD treatment. In both treatments, the high harvesting speed and matched component speeds resulted in greater numbers of assessable stumps.

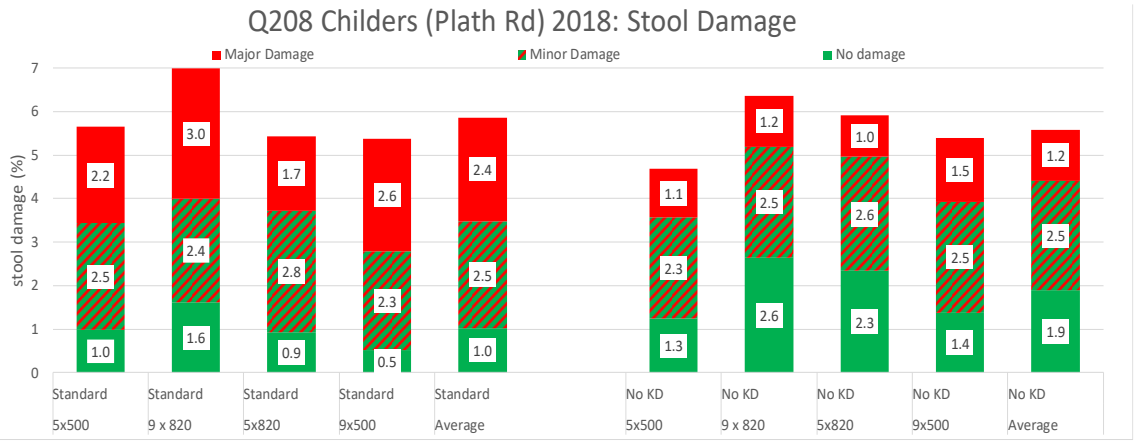

Figure 119: Stump damage assessment, Plath Rd.

Presentation of the damage as relative percentages in Figure 120 again indicates that damage associated with the gathering and feeding processes are very significant.

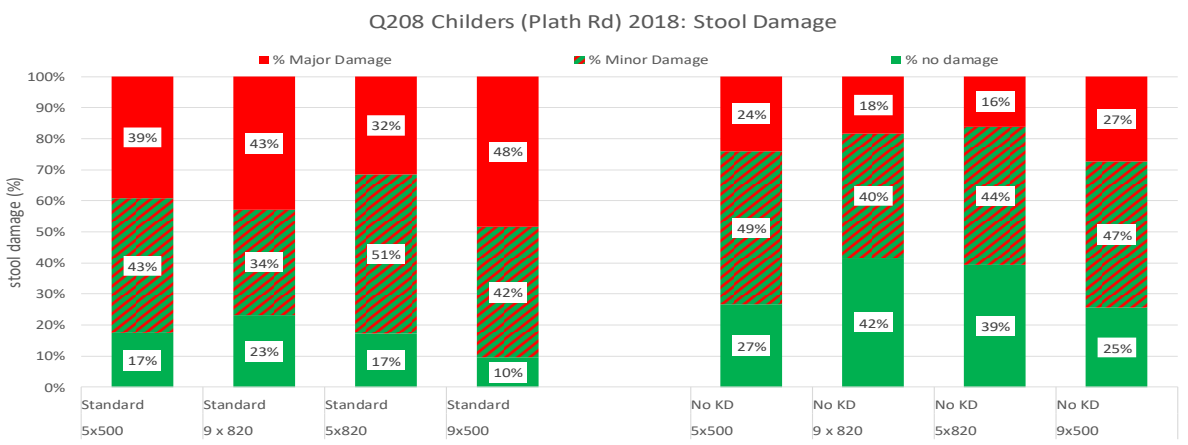

Figure 120: Stool damage observations 2018 harvest.

High levels of damage are also associated with high forward speeds and low basecutter speeds. The standard harvester setup resulted in an average of 17% sound and 40% with major damage compared with 33% sound and 21% with major damage for the no-KD treatments.

Shoot numbers were assessed 71 days after harvest, with the data being presented in Figure 121. Again, the follow through of observed damage to shoot numbers is variable.

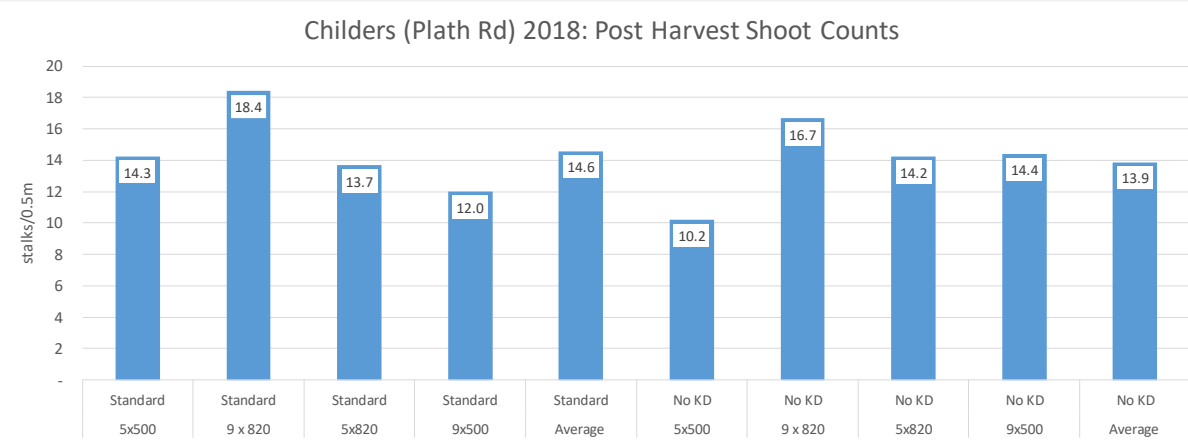

Figure 121: Shoot numbers 71 days after harvest, Plaths Rd.

The Standard harvester configuration achieved an average plant count of 14.6 shoots/0.5m whereas the no-KD treatment resulted in a plant count of 13.9 shoots/0.5m row length.

Yield of the hand-cut plots is presented in Figure 122. The average yield of the hand-cut standard machine configuration was 78 t/ha, whilst the sub plots with no-KD averaged 89 t/ha, an increase of 14%. In the “standard” 2018 harvesting configuration, there was a trend for higher hand-cut yields in the highest groundspeed treatment, however in the “no KD” treatments there was no consistent trends except for higher yield in the low groundspeed x high basecutter speed treatment.

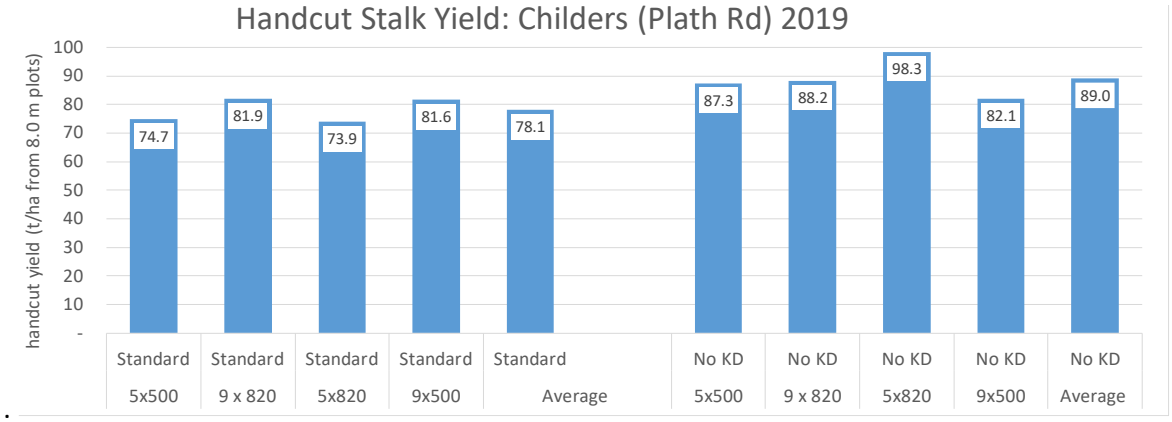

Figure 122: Yields of hand-cut sub-plots at Plath Rd trial.

The machine-harvested plot yield is presented in Figure 123. The variability across the plots meant that differences were not significant.

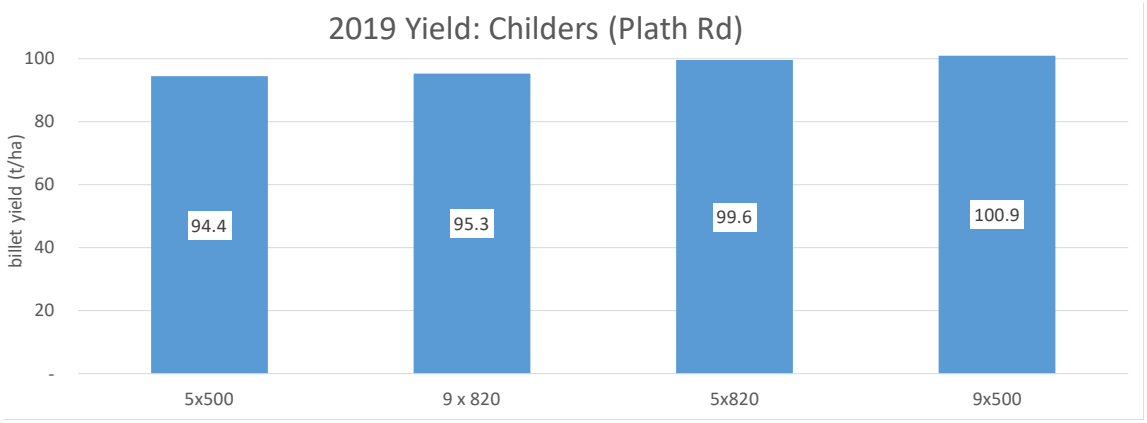

Figure 123: Machine harvested yield for the different treatments, Plath Rd.

The discrepancy between the yield in the hand-cut sub-plots and the yield of the four rows of machine harvested plots was a result of there being a yield gradation along the field. The sub-plots (standard & no KD) were located towards the lower yielding end of the field.

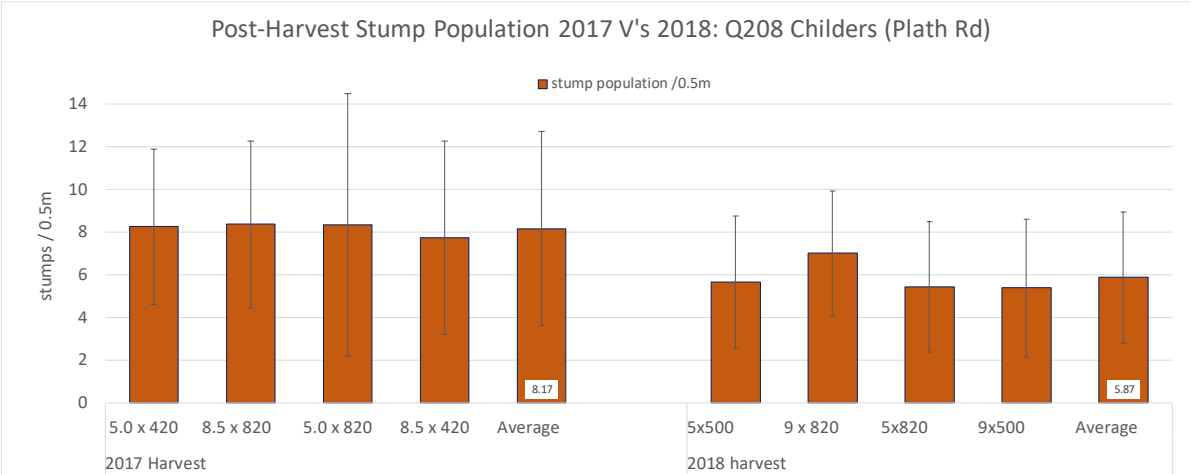

Figure 124: Post harvest stump population 2017 and 2018, Plaths Rd.

Figure 124 presents the data on the post-harvest stump counts after the 2017 and 2018 harvest. The data indicates the mean stump values of 8.2 and 5.9 are statistically highly significantly different. The averaged Standard Deviation between the plots was also statistically significantly different, but the

Standard Deviation as a percentage of average stump number is not statistically different. The data does show that a larger proportion of the 0.5m sections will have very low (<2 per 0.5m section) stump populations, increasing the probability of higher levels of damage and poor ratooning.

Trial 5: Mona Park

Due to issues with the hydraulic configuration on the harvester, the equipment to link component speed to groundspeed was removed. The 2018 trial maintained a high and low operating speed but substituted the "speed matched" treatment for shallow harvesting height, and the "standard" treatment for a deeper (more typical) harvesting depth setting.

Very high stool damage was observed after the 2017 harvest, and even higher damage was observed after the 2018 harvest. The data relating to percentage damage is presented in Figure 125. The average number of stumps found for assessment was 8.31 in the standard treatment and 9.38 in the no-KD treatment.

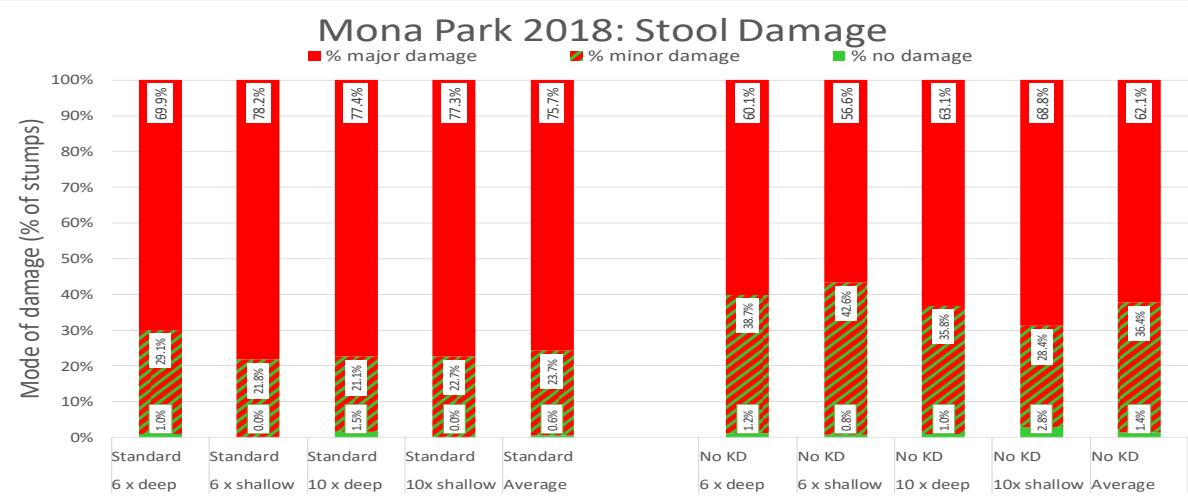

Figure 125: Stool damage ratings after the 2018 harvest at the Mona Park site.

As can be seen, magnitude of damage reduced when the plot was pre-cut to eliminate gathering/KD damage. Averaged major damage rating for the standard harvesting configuration is approx. 76% versus 62% for the treatments with no gathering/knockdown effect. Both these ratings are extreme, however the elimination of knockdown effect does reduce damage. The difference in damage associated with different harvesting treatments is very small and does not give a significant lead as to the primary cause of the issues. One consideration is that the crop was heavily moisture stressed at harvest.

Due to operational difficulties, post-harvest plant counts were not able to be conducted, however millable stalk counts were undertaken at 8 months after harvest. The millable stalk counts are presented in Figure 126. The average stalk diameter was 18.8 mm and no difference was noted in this measurement for the different treatments.

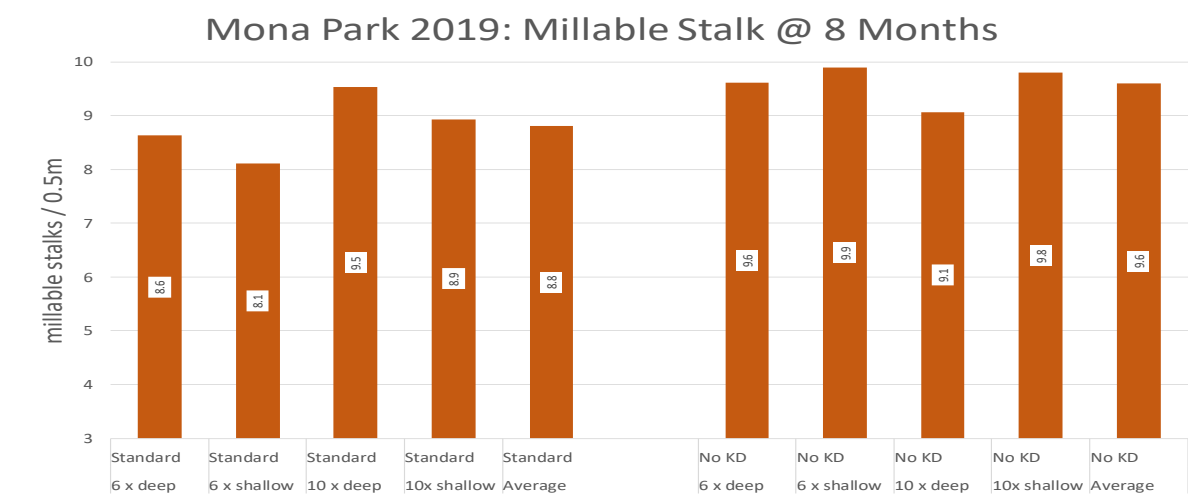

Figure 126: Millable stalk counts at the Mona Park site at app 8 months after harvest.

The millable stalk data presented in Figure 126 is generally inconsistent, with the "deep" treatment having higher stalk counts in the standard harvester configuration, and lower in the "no-KD" treatments. Overall, the no-KD treatments averaged 8.8 stalks/0.5m and the no-KD treatments had 9.6 stalks/0.5m plot.

The yield data for the hand-cut plots is shown in Figure 127.

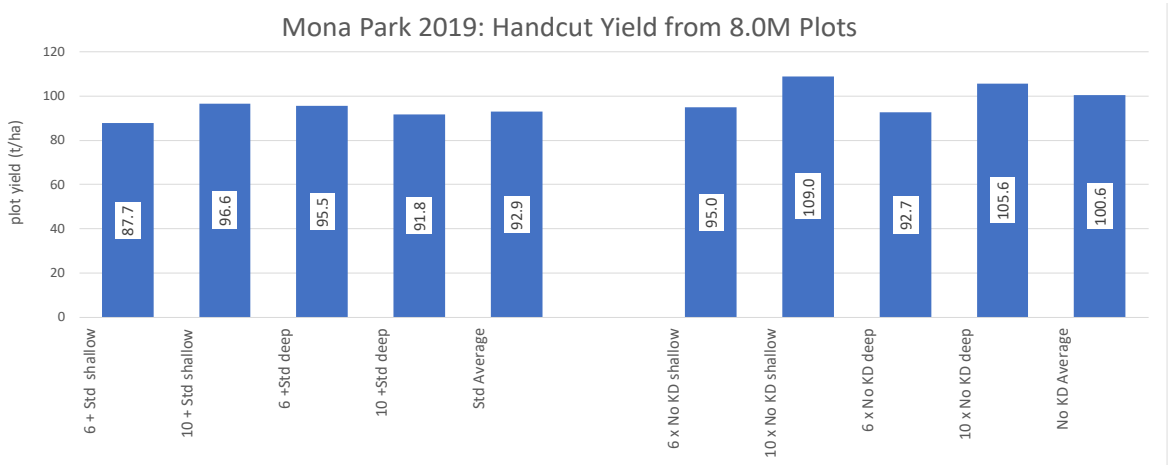

Figure 127: Hand-cut yield from 8m sub-plots at Mona Park.

The average yield from the standard plots was 92.9 t/ha, and the average yield from the no-KD plots was 100.6 t/ha.

Again, the removal of the KD effect impacted on ratoon yield, with the yield increasing by 8.3% in the no-KD treatments. The data comparing stump numbers after the 2017 and 2018 harvests is presented in **Figure 128**.

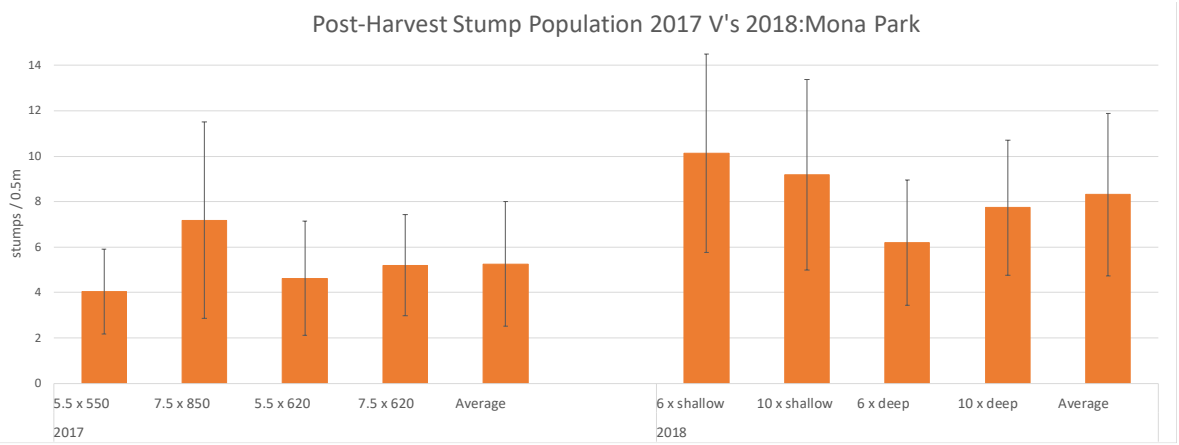

Figure 128: Post harvest stump numbers after the 2017 and 2018 harvests.

The data indicates a statistically significant increase (@ 95%) from 2017 to 2018. There were no significant differences in the Standard Deviation parameters. This trial was irrigated, and appears to illustrate that population recovery is possible if conditions after harvest are suitable.

Trial 6:Ingham (Bambaroo)

The trial at Bambaroo was initiated at the 2018 harvest. The crop was harvested green at low extractor fan speed settings. Site details are shown in Table 41**Error! Reference source not found.**.

Table 41: Details of Bambaroo trial site.

Parameter	Descriptor
Farming Area	Ingham (Bambaroo)
Farm Number	707.6A (Pace Farming)
Block	2-1
Variety and Crop Class	Q 208 2R
Harvest Date	13/09/2018
Yield	70-80 t/ha (heavily sprawled)
Billet Length & Diameter	Billet Length: 165mm. Diameter: 20.7 mm
Row Spacing	1.9m dual row
Row Length	4 x 600 m
Plot Area	.52 ha
GPS Utilisation	Harvester only 2018 & 2019 harvests.

In the post-harvest assessment, the average number of visible stumps able to be assessed was 6.8 in standard treatment and 7.4 in the no-KD treatment. The stool damage assessment data is presented in Figure 129.

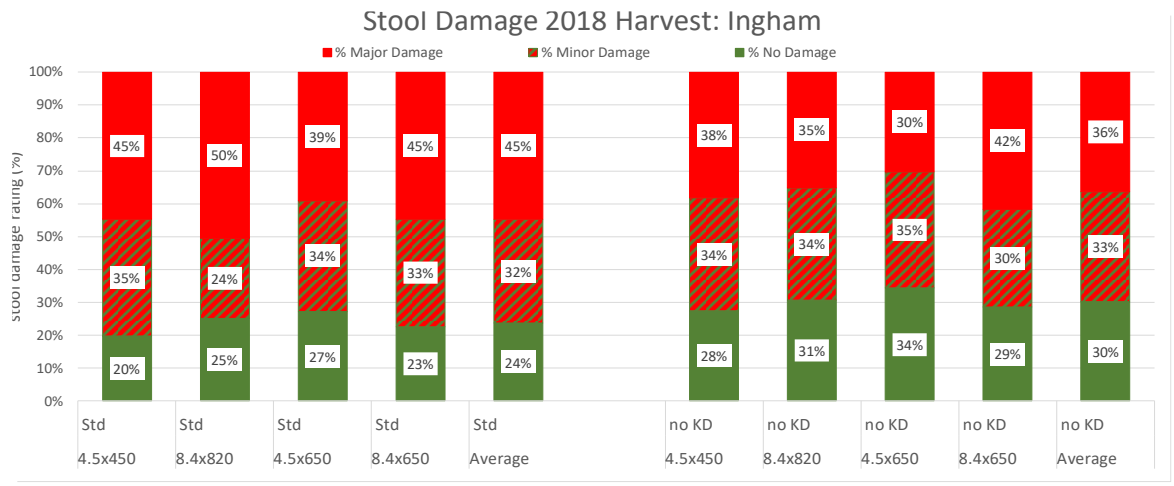

Figure 129: Stool damage assessment data for the Bambaroo site.

As at other sites, the elimination of the KD effect resulted in an increase in undamaged stool of approximately 25%, and a reduction in major damage from 45% to 36%.

Shoot emergence was highly variable, as indicated by the post-harvest plant count undertaken 40 days after harvest, with the data presented in Figure 130. Higher groundspeeds tended to have higher shoot numbers in both the KD and no KD treatments. The overall difference in emerged plant counts between the standard harvesting configuration and no KD is negligible.

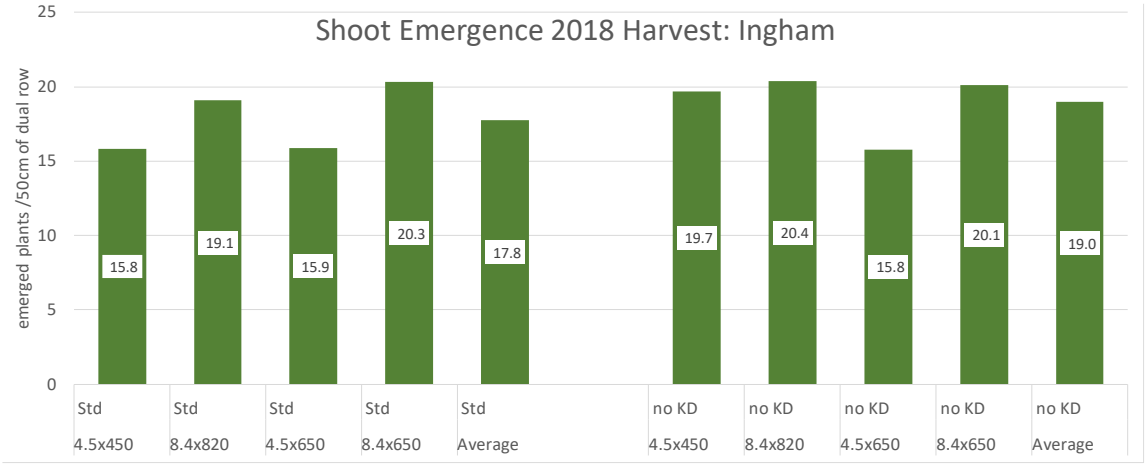

Figure 130: Post-harvest shoot counts, Bambaroo.

Hand-cut yield results from the sub-plots is presented in Figure 131. This indicates the handcut yield for the standard harvesting configuration averaged 65.4 t/ha, whereas the no-KD plots averaged 81.9 t/ha.

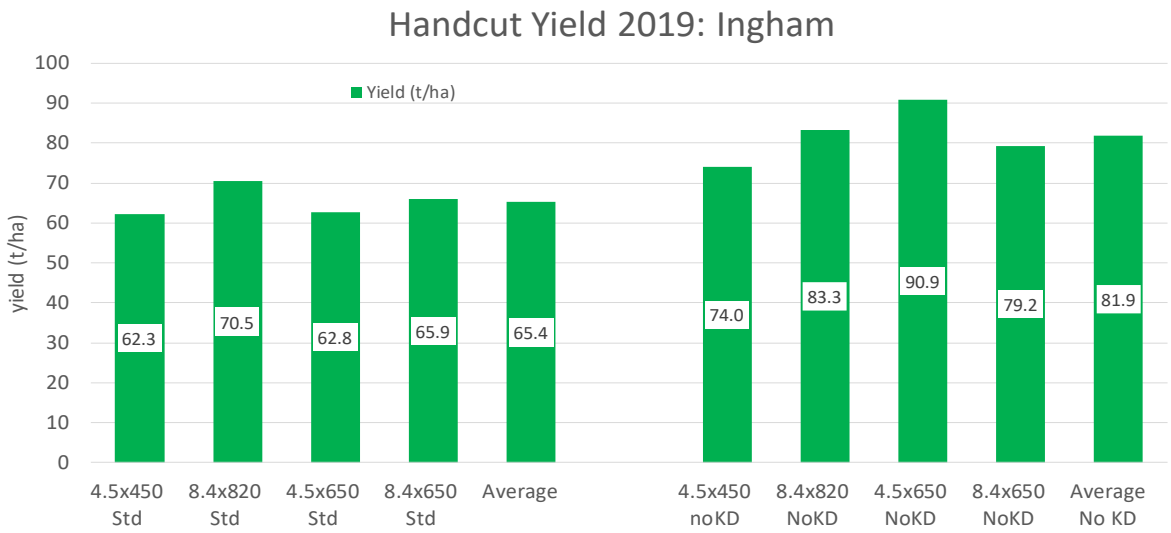

Figure 131: Hand-cut yield from Bambaroo trial.

Again, the very significant reduction in damage across all speed-related treatments indicates the significance of damage associated with the gathering/ Knockdown process of the harvester.

Whilst basecutter damage is still significant, the damage associated with the gathering and/or knockdown/feeding is clearly also very significant. Similar effects have been noted at all trial sites.

Summary of Trial Results:

The most significant outcome from the 2016 and 2017 harvest events was the high levels of damage observed in all treatments. At approximately 30 days and 60 days after harvest, plant counts were undertaken. Additionally, at some sites sample areas were harvested to assess plant weight. A weak trend linking increasing shoot numbers with increasing stool damage, and a general inverse trend linking increasing total shoot biomass with reducing stool damage is apparent. A significant impact of this observation is that shoot biomass rather than shoot number is more significant when evaluating ratoon germination and emergence performance.

The 2017 harvest treatments did give a small and consistent impact on both stool damage. As noted, higher damage tended to give higher shoot numbers, however the inverse effect then followed through to millable stalks and finally yield.

To better assess the causes of damage, handcut sub-plots were introduced at the 2018 harvest, to allow the minimisation of the gathering and knockdown effects, thus allowing comparison of “basecutter only” and “full front-end” damage. The elimination of the gathering and feeding damage resulted in a very significant reduction in observed damage, as well as a small but important increase in the number of stumps which were available for damage assessment. This also then directly equates to a reduction in stump removal. This effect was noted at all sites, and a summary of the averaged damage for each treatment is presented in Table 42.

Table 42: Summary of stump damage with and without the gathering and forward feed effects.

Trial	Standard harvest with knockdown			Pre-cut: No gathering or KD effect		
	Undamaged	Minor damage	Major damage	Undamaged	Minor damage	Major damage
Childers: Bouchards Rd	12%[A]	28%[B]	60%[C]	25%[A]	45%[B]	30%[C]
Childers: Plath Rd	17%[D]	43%	40%[E]	33%[D]	45%	21%[E]
Condong: Colonial Drive	21%[F]	52%	27%[G]	35%[F]	51%	14%[G]
Condong: BZ Farms	10%[H]	34%	56%[I]	29%[H]	32%	39%[I]
Burdekin: Mona Park	1%	24%[J]	75%[K]	1.5%	36.5%[J]	62%[K]
Ingham: Bambaroo	24%[L]	32%	45%[M]	30%[L]	33%	36%[M]
Average	14%	36%	51%	25%	40%	34%

For each category of damage in each trial, the difference between pairs of means sharing a superscript is statistically significant to at least p = 0.05. The differences between pairs with superscripts A, C, E, G, I and K are statistically significant to p= 0.01.

As indicated, the elimination of the gathering/knockdown effect resulted in an increase in undamaged stumps at all sites and a reduction in stumps with major damage (from 51% to 34%) over all sites. The high levels of statistical significance of the reductions in damage levels, despite the small sample sizes and significant variations due to uncontrolled factors, suggest that the knockdown geometry is a very significant contributor to observed damage levels.

Emerged-plant counts generally showed a trend of higher counts with increasing damage, but there was a trend towards greater plant weight and height in plots with less damage. This indicated that shoot counts alone after harvest are not a good indicator of relative damage.

Pre-harvest plant counts were also undertaken. The plant counts in the initial plots and the plots which were pre-cut indicated a positive correlation with reduced levels of damage.

At harvest, the pre-cut sections were hand-cut, stalks counted and weighed. To minimise extraneous effects such as planting rate, direction of previous harvests, and other factors, a section in the same row immediately adjacent to the pre-cut section was also hand-cut, stalks counted and weighed. The impact of the treatments on plot yield is presented in Table 43. The yield response in each pair of sub-plots was primarily driven by stalk number, not stalk weight at all sites. Stalk weight did vary across replicates, particularly at Mona Park, where yield from the highest yielding plot pair was 182% of the yield of from the lowest yielding pair of plots. However, typically, the difference in yield in any pair of plots was driven by stalk number, not difference in stalk weight.

Table 43: 2019 Harvest yield summary - conventional versus no knockdown.

TRIAL	STANDARD CONFIGURATION (T/HA)	NO KNOCKDOWN (T/HA)	YIELD RESPONSE TO NO KNOCKDOWN	P VALUE
Bouchards Rd (Childers)	97	108	12%	0.095
Colonial Drive (Condong)	109	125	14%	0.031
Bambaroo (Ingham)	65	82	25%	0.007
Plath Rd Childers	78.1	89	14%	0.035
Mona Park (Burdekin)	93	101	9%	0.014
Condong (BZ) (126 t/ha avg)	13.2 stalks/m	16.6 stalks/m	25%	0.005
Average			16%	

The highest response to the removal of the knockdown/gathering effects was noted at Bambaroo and at BZ Farms, with the plot yield difference at Bambaroo being 25%, and the post-harvest stool count at BZ Farms indicating 25% higher stalk numbers. These two sites also had the highest level of significance in the difference (P=0.007 and P=0.005, respectively). Both crops had been sprawled at the 2018 harvest, and as such higher levels of damage anticipated. Both crops were the thin-diameter variety Q208[Φ].

The Plath Rd site and the Colonial Drive site both indicated a 14% increase in plot yield with the knockdown effect removed, with significances of P=0.035 and P=0.031. The variety at Colonial Drive was Q240[Φ], a thicker variety where higher levels of damage were anticipated. Whilst a significant effect, as previously discussed it is thought that stalk breakage above ground tends to protect the stool during harvest.

The Bouchards Rd site indicated a 12% increase in yield from the removal of the gathering/KD effect. The P=0.095 means that this was not statistically significant, however it can still be considered to be a trend which is consistent with the results of the other trials.

The Mona Park trial indicated a yield response of 8% to the elimination of gathering and KD effects, but the P=0.137 indicates the response was not significant. As previously indicated, the yield of the highest yielding pair of plots was 182% of the lowest yielding pair of plots. This variation overwhelmed the treatment differences, despite the no-KD treatment having a higher yield in 10 of the 12 plots. Post-harvest EM soil mapping of the field indicated that large differences in yield across the plot area could be anticipated.

The trial data demonstrates that, whilst damage associated with the basecutters is significant (given also that new-or near new basecutter blades were utilised during the trials), the issue of damage during the gathering and knockdown process is also a very significant contributor to damage, and that this can be directly associated with yield depression. Damage reduction from developments in basecutter configuration will be constrained because of the high level of damage prior to the basecutting process.

Observations during the trials also indicated that loss of stool is a major issue, as indicated by an increase in the "gappiness" of the remaining plant stand. At all sites except the Mona Park site (irrigated), there was a significant reduction in what were considered viable stools, as indicated by the increase in proportion of 0.5m row sub-sections which had two or less stumps. The effect is illustrated in Photograph 25 and Photograph 26. This effect is consistent with the findings of Chapman (1988), who noted that the decline in yield was primarily associated with loss of population. Evenness of emerged plant spacing would be a primary driver of this effect.

Photograph 25: As the ratoon cycle progresses, the most noticeable effect was the increase in gappiness, derived by the removal of small stools and increase in the size of remaining stools.

Photograph 26: Another example of high levels of gappiness associated with progression of the ratoon cycle.

6.3.5.2018-19 Related Issues.

Despite the fact that five of the six trial sites were specifically chosen with a crop row spacing that nominally matched the field equipment wheel spacing, machine placement error remains a major issue, even with highly committed and competent operators. This has two direct effects:

- The harvester basecutters are no longer aligned with the centre of the crop bed/row, and
- Encroachment of harvester and haulout wheels on the crop row.

An example of the harvester alignment issue is well indicated by Photograph 27 and Photograph 28, which were taken at the Mona Park site during harvesting of trials. The GPS on the harvester was not operating. The marker on the left (Photograph 27) aligns with the true centre of the crop row/bed, and the marker on the right is the alignment of the centre of the harvester basecutters, determined from the basecutter blade pattern in the undisturbed soil. As can be seen, the typical placement error of the harvester is consistently >250 mm. Typical error when the harvester is operated on GPS is < +/-25mm. Placement error of haulout units can be substantially greater than the harvester placement error, resulting in damage to the crop stool and compaction of the sides of the crop beds

Photograph 27: Typical error in the placement of the harvester without GPS Autosteer. The marker on the left aligns with the true row/bed centre, the marker on the right aligns with the centre of the basecutters.

Photograph 28: The harvester placement error across a section of the field.

The offset of the harvester adversely impacts on gathering and feeding performance of the machine.

More significantly, given the distance between the centres of the basecutter discs is 600 mm, that level of placement error means that the crop row is being harvested by one basecutter disc. This is illustrated in Figure 132.

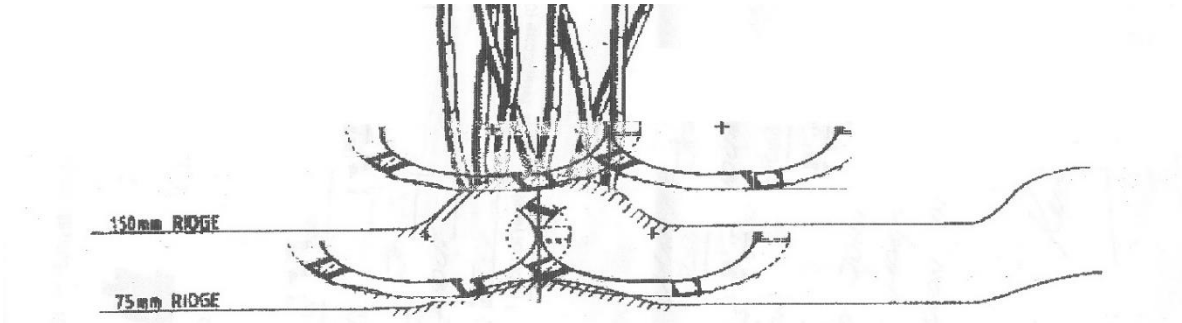

Figure 132: Illustration of the interaction between the swept path of the basecutter blades when the harvester is aligned on the row (bottom sketch) and when the harvester is "off the row" (top sketch).

The effect of this is clearly evident in in Photograph 29. Because the harvester is offset:

- The gathering boards are less effective in lifting the cane to above the basecutters.
- The lowest part of the blade sweep is effectively over the centre of the crop row, and as such this is where the deepest cutting is occurring. The blades are cutting shallower towards the edges of the crop bed.

- The blades do not effectively “sweep” the sides of the crop bed.

These factors combine to induce the operator to set the basecutter operating depth deeper, causing more damage to the stool.

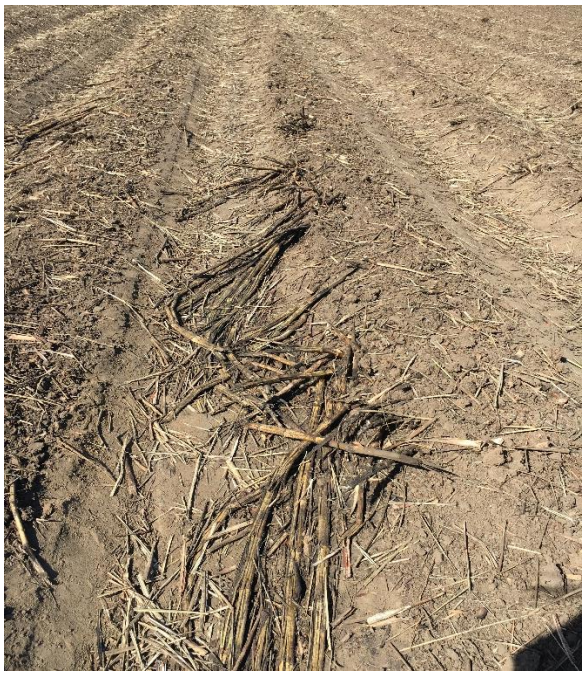

Photograph 29: Offset of the harvester off the row results in difficulty in gathering the cane stalk and inability of the basecutter blades to “sweep” the sides of the bed.

Photograph 30: Despite matching crop row spacing with machine width, machine placement error results in major compaction damage to the sides of the crop beds and reduces the potential of the crop ratoon.

The encroachment of the harvester and haulout units on the adjacent crop beds is also a major issue. The combination of these effects is well demonstrated in Photograph 30.

Photograph 31: Control of traffic in the traffic lanes is seen in this field in Guatemala where the harvester and all haulage equipment is operated on GPS, and all machines are set to match the crop 1.9m bed spacing.

The converse of this effect is noted in photo Photograph 31, where the harvester and haulage units are all operated on GPS guidance at all times and the crop row spacing and machine track spacings match. This photograph was taken at an estate in Guatemala. Experience in Australia has been that

attention to these factors result in increased ratoon cycle productivity (Photograph 32). The harvesting equipment operated by Central Tweed Harvesting all operates on GPS Autosteer, however adoption in the Australian Industry of this technology has been very low.

Photograph 32 Matched row spacing and GPS on all equipment have increased ratoon cycle length on this farm, with this photograph being of a 6th ratoon crop.

6.4. Harvester Modifications

Gathering Damage

The process of gathering and aligning lodged cane stalks by the gathering spirals causes some damage to both the cane stalk and also to the cane stool. The damage to the cane stool is associated with tension in the cane stalks during the gathering process and to the bending and rotation associated with the re-alignment of the stalks. The more "difficulty" encountered by the gathering spirals in achieving the alignment of the cane stalks, the greater the anticipated level of damage. As harvesting speeds increase, the forces and associated damage can be anticipated to increase because of the reduced time available for the re-alignment process and associated increases in component accelerations.

To minimize forces associated with the gathering process requires the gathering spirals to be of appropriate design and be operating at the correct relationship with groundspeed. To date, the relationship between billet damage and groundspeed, in matched or un-matched configurations has been limited. Key points include:

- On all machines except the Rocky Point machine, the speed control of the spirals and forward feed rollers has been "achieved" by an open loop control system. The data available indicate that this system is not achieving the targeted control of component speeds, particularly under variable field conditions.
- The Rocky Point harvester is fitted with a "closed loop" control system on the spirals and uses speed feedback from this circuit to control the oil flow to the forward feed rollers. This machine is also fitted with spirals with modified wrap with a design ratio of 16 rpm/km hr^{-1} (Photograph 1 and Photograph 2).
- The performance of the Rocky Point harvester, particularly with respect to performance in large heavily lodged cane, is clearly superior to the standard machines with only open loop speed control. These machines are also considered superior to unmodified machines.

Billet quality analysis was undertaken on product from this this machine as part of an SRA cane loss trial. The data is presented in Table 44. The crop was being harvested was a high yielding sprawled crop, and "Sound" billet proportions of 60-70% would have been considered good under the conditions. The very high levels of sound billets in the trial indicate that the gathering and feeding functions were being achieved with very low stalk damage.

Table 44: Billet quality analysis on the Rocky Point machine which is fitted with modified fronts.

Row Labels	*Sound Billets*	*Damaged Billets*	*Mutilated*
Aggressive	81.9 %	14.1 %	4.0 %
Low Loss	85 %	11.6 %	3.4 %
Nominal	85.6 %	13.1 %	1.3%
Recommended	88 %	8.3 %	3.7 %
Average	**85.1 %**	**11.8 %**	**3.1 %**

Billet quality data from samples taken from the JD 3520 harvester utilised in the Condong trial at BZ Farms in the 2017 trial is presented in Figure 133. The average data indicates approximately 51% sound billets.

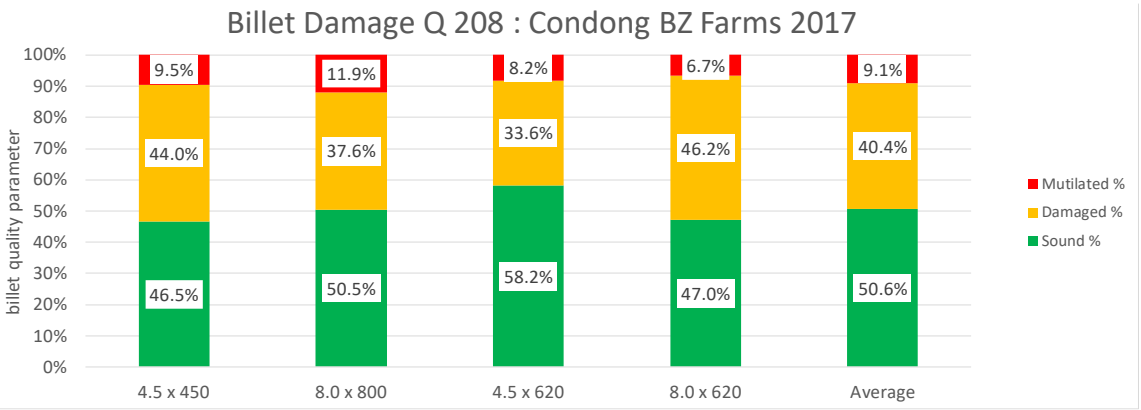

Figure 133: Billet quality data for the JD 3520 harvester in 2017 at BZ Farms.

Prior to the 2018 harvest, the machine was "optimised" and a new design of chopper drum fitted. The billet quality observed in the trial is presented in Figure 134. This indicates an improvement in billet quality in this field to approximately 60% sound billets.

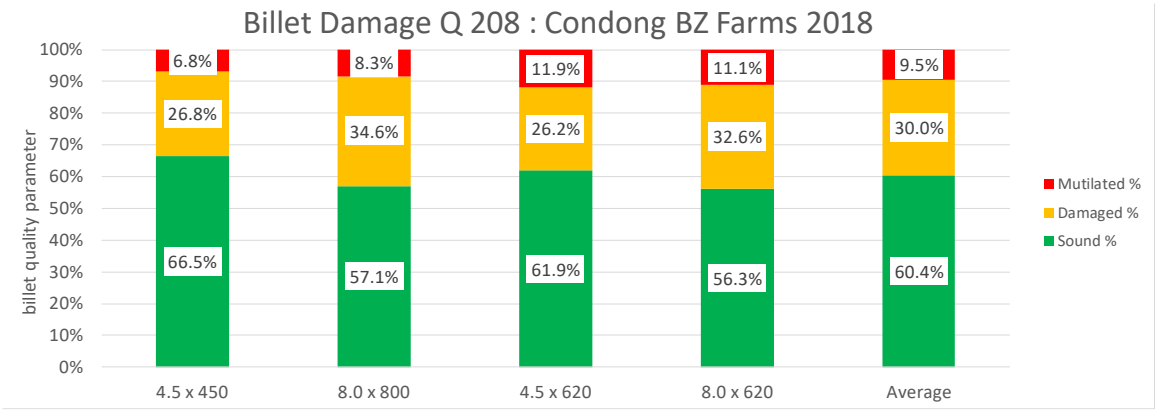

Figure 134: Billet quality data for the 2018 harvest.

For the 2019 harvest, the 3520 had the modifications to the gathering and feeding components completed, including linking of component RPM to groundspeed.

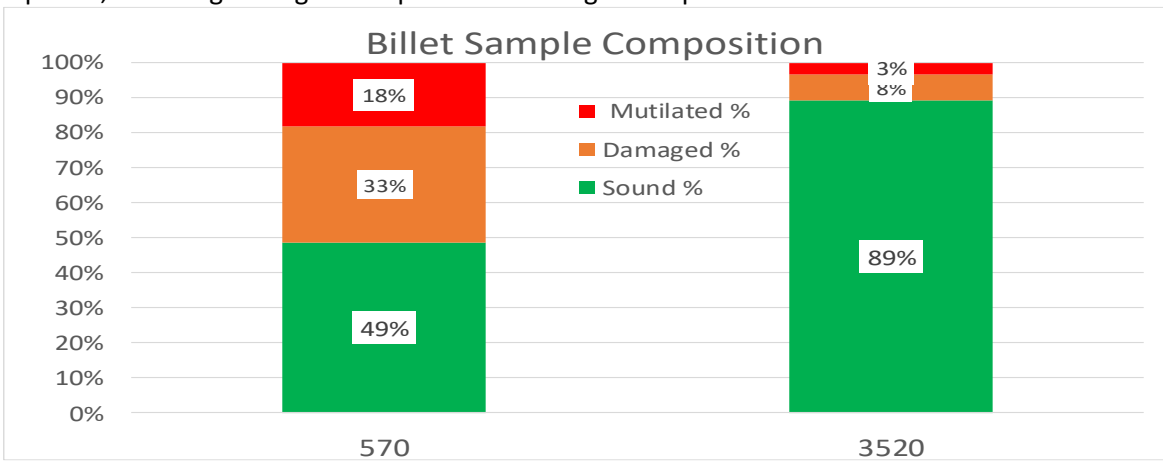

Figure 135: Billet quality composition for the modified 3520 and a standard CH570 harvester in the same field conditions.

The comparative billet quality of the modified 3520 and the standard CH 570 are presented in Figure 135. The improvement of billet quality associated with machine modification is highly evident:

- The standard harvester produced a billet sample with approximately 50% sound billets in the 2017 harvest.
- This level of sound billets is consistent with the standard new harvester working in the same field and under similar crop conditions in the 2019 harvest.
- The billet quality produced by the machine after modifications and with all components operating linked to groundspeed achieved a sound billet rating of 89%.
- The Rocky Point harvester, with front end component speeds linked to groundspeed (Table 44), also achieved billet quality significantly higher than Industry standards.

6.5. Stream 2

6.5.1. Modelling initial qualitative conclusions

The model is capable of predicting cane damage (as indicated by cane loss) in broad agreement with the results of the field trials undertaken at Childers. The predictions confirm that higher cane loss and therefore damage occur at relatively lower basecutter speeds regardless of forward harvester speed. These relatively larger losses are caused by the acoustic forces incurred by the impact of the

blade rather than multiple cuts. The significance of the knockdown roller as a cause of cane loss also confirms the findings of the 'pre-cut' field trials although this significance is lessened at higher basecutter speeds.

A more nuanced understanding of basecutter damage would be gained if the soil and cane models were further improved such that the effects of non-homogenous cane material properties and more realistic soil/ root sub-models were developed.

6.5.2.Simulating Cutting Behaviour by modelling basecutter blade geometry and condition

The Kroes (1996) bending and cutting geometry described in Cutting Behaviour section starting on page 67 of this document, and shown in Figure 31, Figure 32 and Figure 33 was adopted to test different blade geometries and blade conditions.

Kroes (1996) tested experimentally the basecutter incline (the angle achieved with the ground by the basecutters in the harvester direction). The angles tested by Kroes (1996) were 0 degrees (blade perpendicular to stalk during the impact), 7.5, 15 and 22.5 degrees. The experimental field trials carried out in Stream 1 of this project have shown that if the stalk is not bent at all, there is significantly less damage to the stalk during cutting. That means that, if the stalk was bent less while still being able to feed, there would most likely be less damage at the cutting site. The mechanism is further complicated because some stalks will be impacted in the compression side, while others will be impacted on the tension side, and some on the side (where the compression and tension are relatively balanced).

The basecutter blade geometry and condition were modelled. Since it is likely that the basecutter blades would soon lose a sharp edge, two geometries were modelled:

1. A 5 mm blade thickness with a 1 mm blunt edge.
2. A 3 mm blade thickness with a 0.5 mm blunt edge (for example, a higher quality slower wearing blade material).

The approach taken was to model the combinations shown in Table 45. The performance was judged by the measured cut force, and more importantly, the predicted damage to the stalk. In this case, the number of removed slices was counted by visual inspection of the predictions. The predictions are shown in Figure 136 to Figure 141.

Table 45: Modelled blade geometries and predicted results.

BLADE INCLINE (°)	BLADE THICKNESS (MM)	BLADE EDGE (MM)	MAXIMUM BENDING STRESS BEFORE CUT (MPA)	MAXIMUM CUT FORCE (N)	NO. OF REMOVED SLICES
0	5	1	17	840	3
0	3	0.5	19	1180	2
15	5	1	23	1150	8
15	3	0.5	19	1210	4
22.5	5	1	19	990	10
22.5	3	0.5	19	980	9

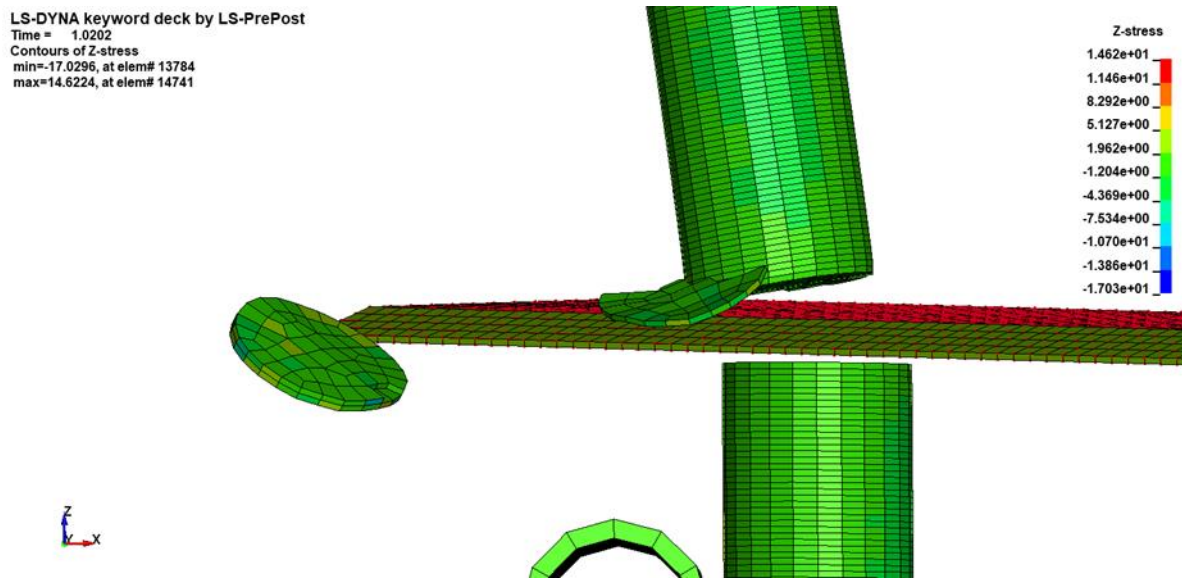

Figure 136: Predicted cut for blade incline 0°, blade thickness 5 mm, blade edge 1.0 mm.

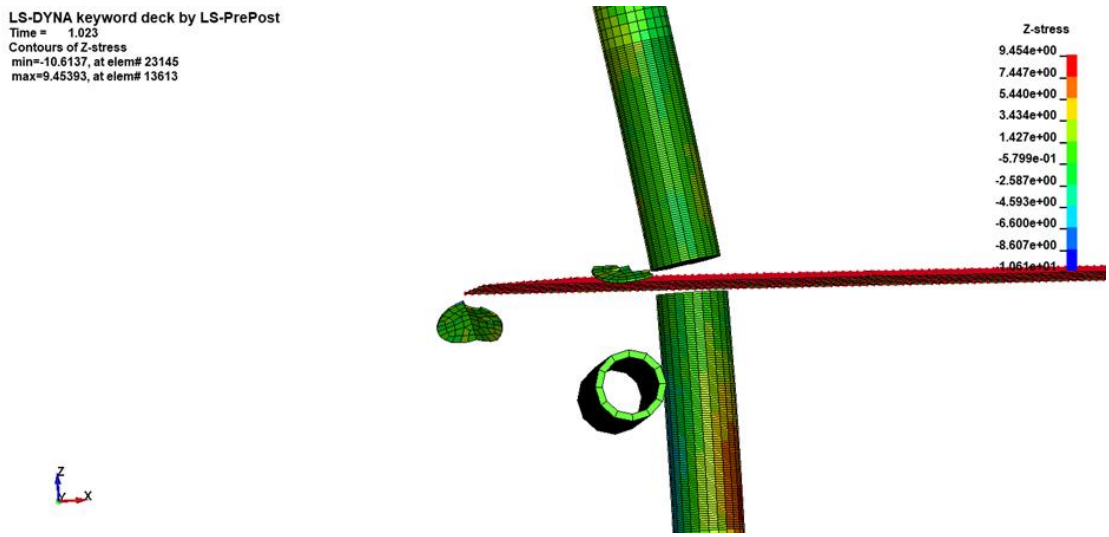

Figure 137: Predicted cut for blade incline 0°, blade thickness 3 mm, blade edge 0.5 mm.

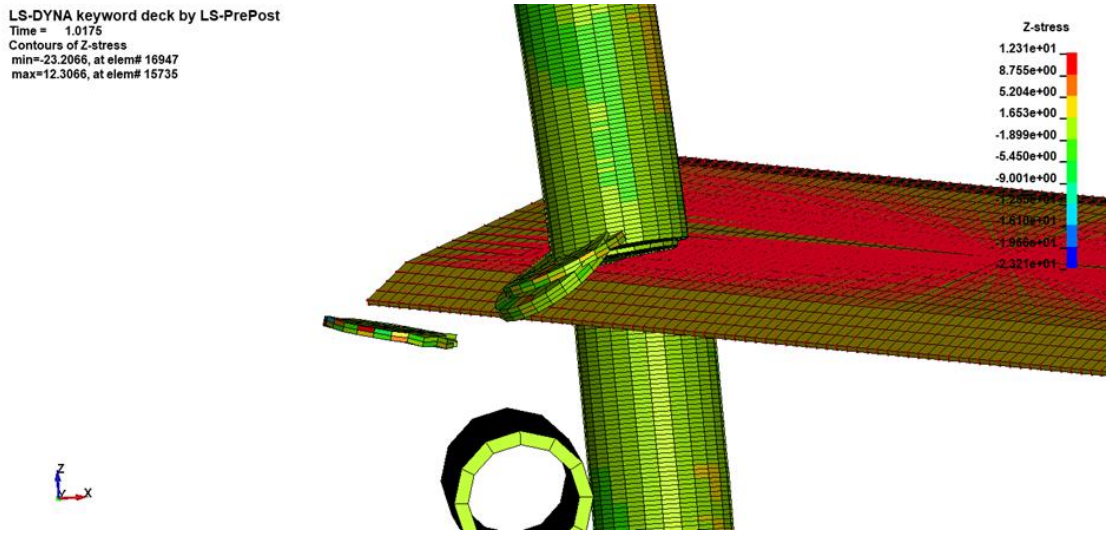

Figure 138: Model A, predicted cut for blade incline 15°, blade thickness 5 mm, blade edge 1.0 mm.

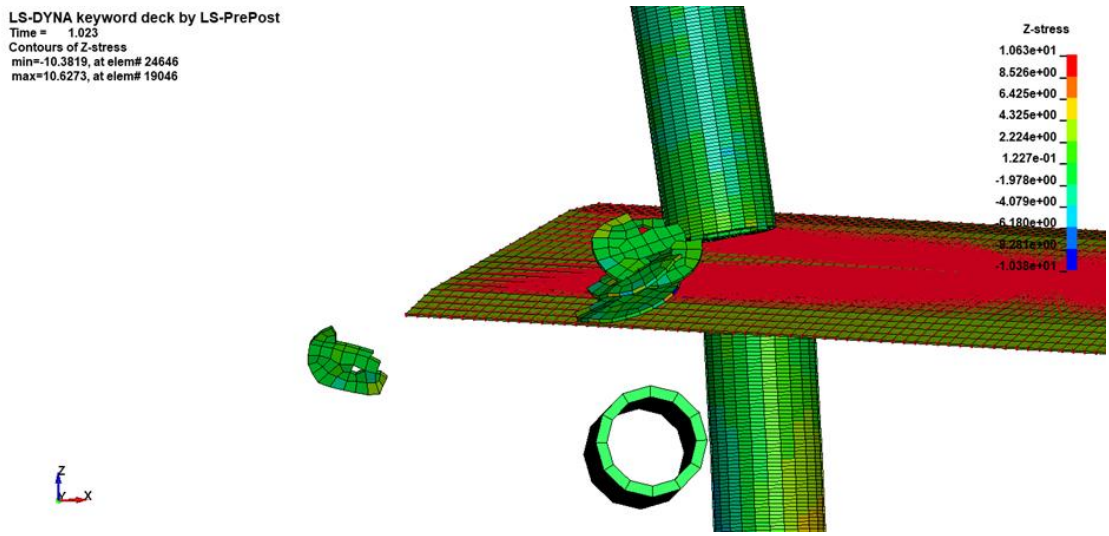

Figure 139: Model A, predicted cut for blade incline 15°, blade thickness 3 mm, blade edge 0.5 mm.

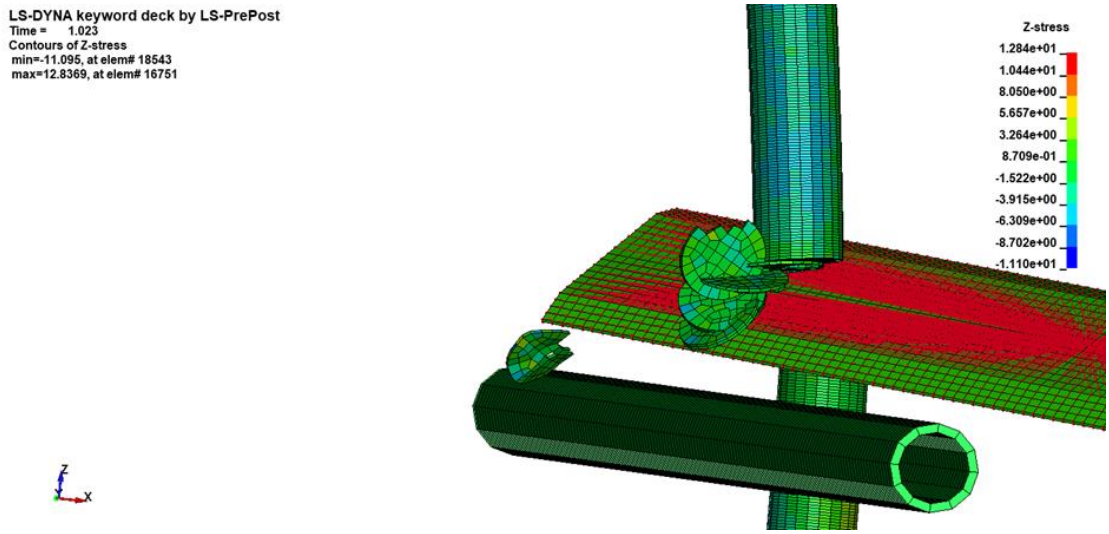

Figure 140: Model A, predicted cut for blade incline 22.5°, blade thickness 5 mm, blade edge 1.0 mm.

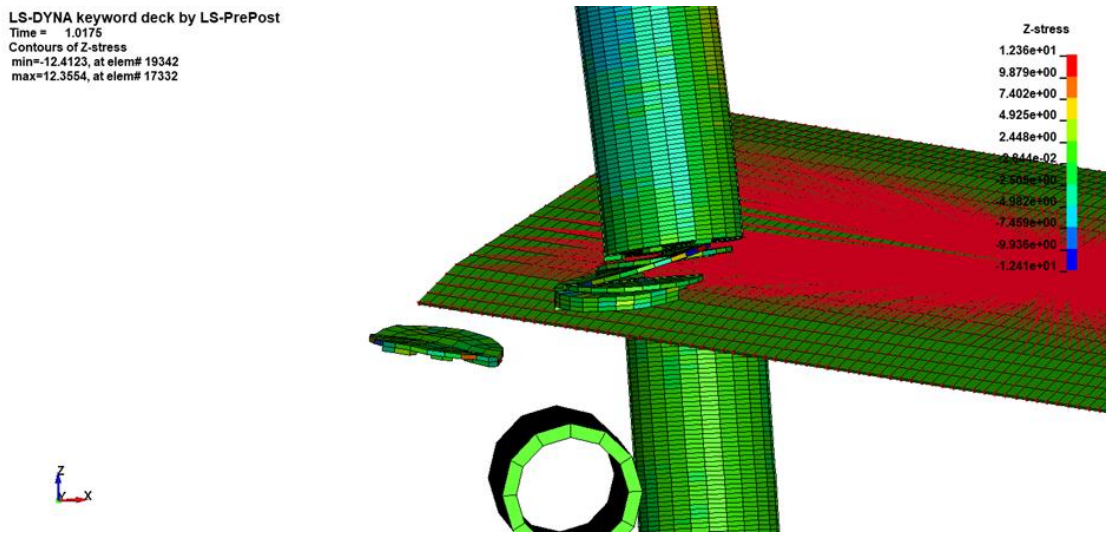

Figure 141: Model A, predicted cut for blade incline 22.5°, blade thickness 3 mm, blade edge 0.5 mm.

Inspection of Table 45 shows that the 3 mm thick blade with a sharper edge of 0.5 mm was predicted to consistently cause less damage to the stalk. This is expected: a larger impact area of the blade should cause more damage. It is also consistent with the conclusion by Kroes (1996) that 'a blunt blade increased the cutting force and energy, hence, increased the damage'. However, it is interesting to note that the predictions did not show a consistent reduction in cutting force for the thinner, sharper blade. This may be because prediction of the cutting force requires a finer mesh for both the stalk and the blade.

Table 45 also shows that a smaller incline angle is consistently predicted to cause less damage to the cane. Again, this would be expected: as the angle increases, the area that the stalk is impacted by increases. However, this prediction is contrary to the conclusions of the experimental results by Kroes (1996) in section 11.9, who stated that 'increasing the incline, however, did reduce the overall damage for both varieties'. Kroes also stated that 'the incline angle did not appear to effect damage to the stalks of the Q123 varieties. The minor splitting in both the stool and stalk of the vertical 82C-954 samples was reduced to major edge damage at 15° and then minor edge at 22.5°. The results by Kroes suggest that:

1. The stalk damage due to the basecutter blade incline is cane variety dependent, and
2. The current predicted failure mechanism of the stalk when impacted by the blade (the removal of slices) may not be correct for some cane varieties.

It is noted that, during the improvement of bending predictions, there was a combination of values of material parameters that resulted in the prediction of axial splitting of the cane stalk during bending failure. That predicted failure mechanism is shown in Figure 142. This behaviour was predicted when the values of parallel shear strength and perpendicular shear strength in Table 15**Error! Reference source not found.** in the cutting prediction section were changed to 5.0 MPa and 2.0 MPa while retaining the other values in the table. Follow up and adjustment of the magnitudes of these parameters while retaining the ratio may result in an improved prediction of the cutting mechanism for some cane varieties, while retaining an adequate prediction of bending. This is reinforced by observations made by Kroes (1996) of splits forming in the stalk perpendicular to the direction of impact of the basecutter blade, for example on page 11-32.

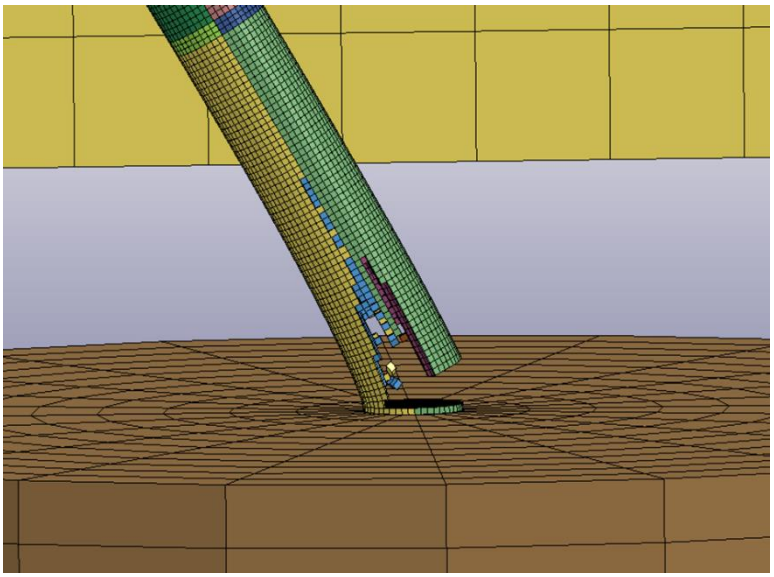

Figure 142: Model A, predicted axial splitting of the cane stalk during bending failure.

6.5.3. Simulation of entire total harvester interaction

The series Figure 143 through Figure 150 shows the modelled progress of a stalk of cane from first contact with the harvester until the stalk enters the feed train. This simulation has the geometry shown in Model A in the procedure section 5.6.7.

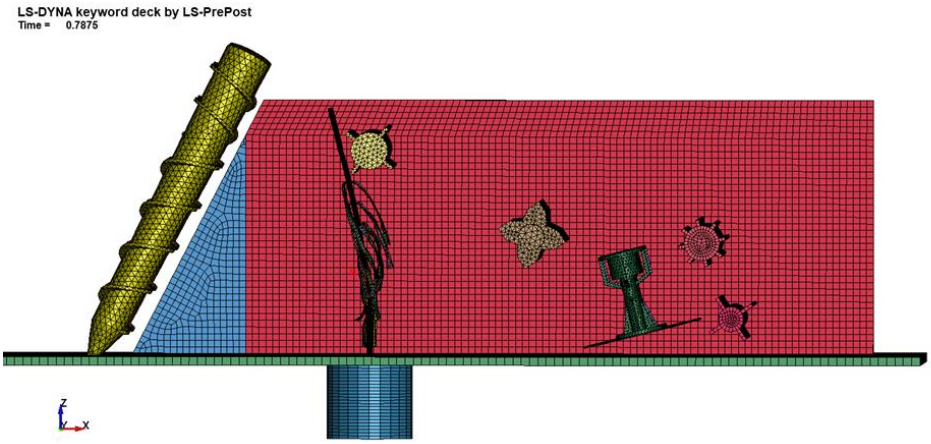

Figure 143: Model A results: stalk contacting knockdown roller.

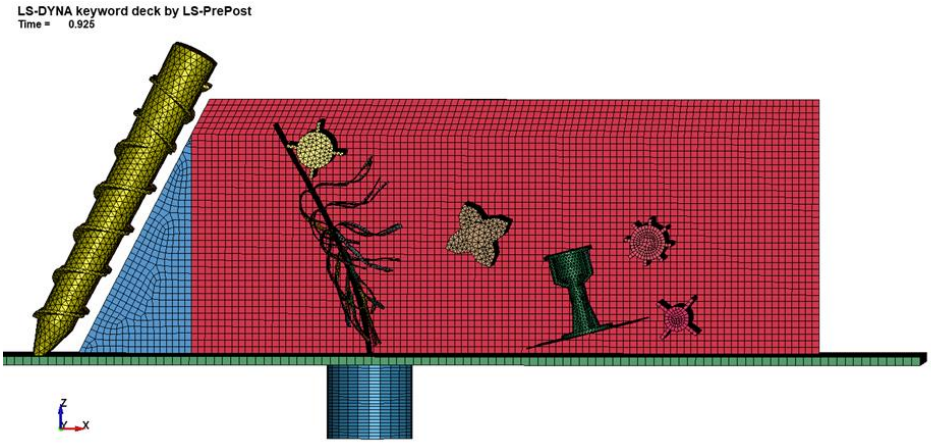

Figure 144: Model A results: stalk being pushed over by knockdown roller.

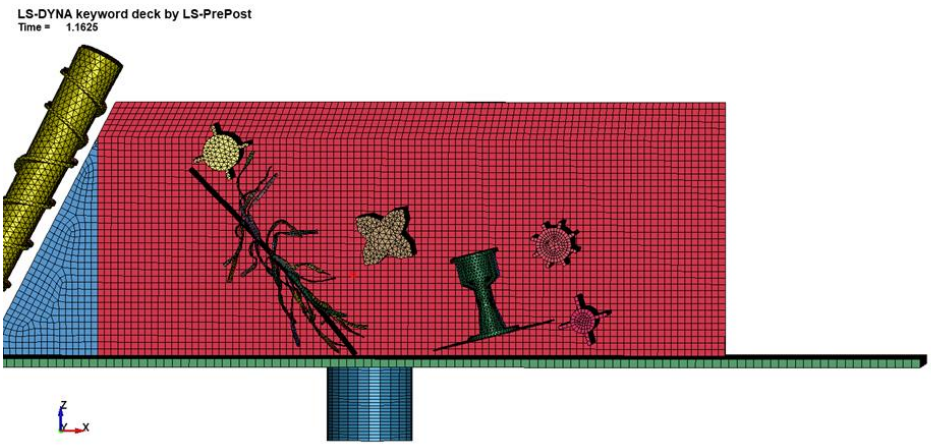

Figure 145: Model A results: stalk being broken by knockdown roller.

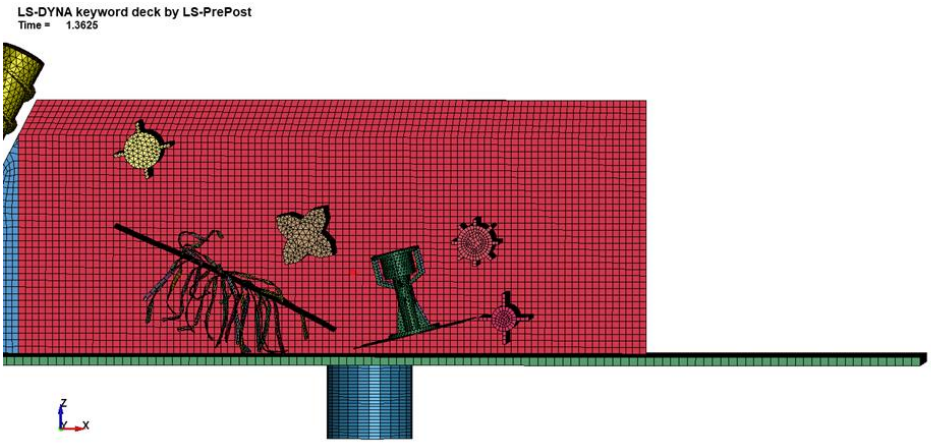

Figure 146: Model A results: stalk falling.

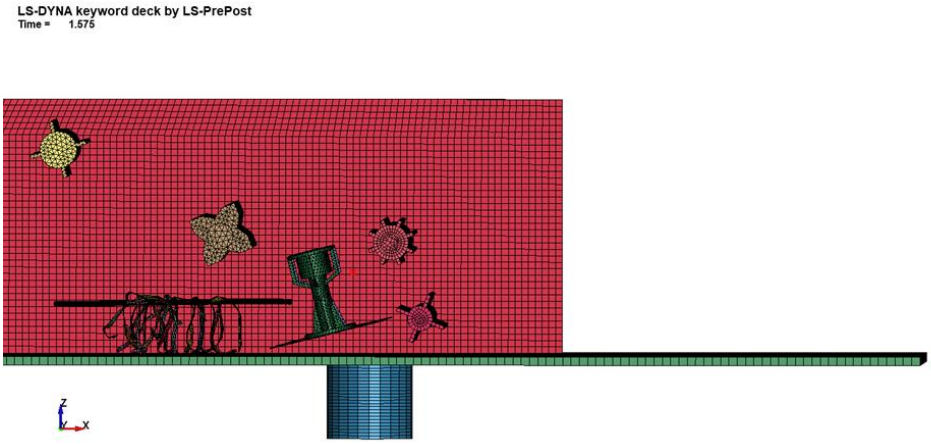

Figure 147: Model A results: stalk falling and rotating.

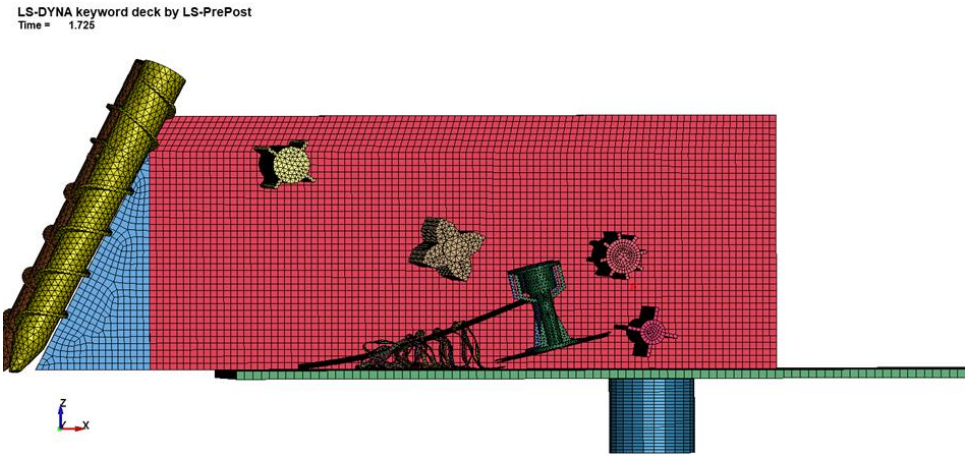

Figure 148: Model A results: stalk contacting top frame of basecutter frame.

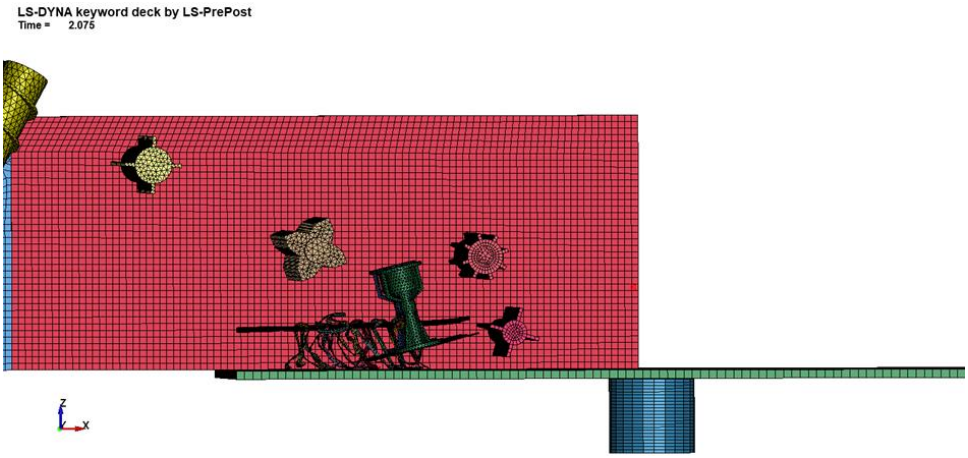

Figure 149: Model A results: stalk moving through basecutter opening.

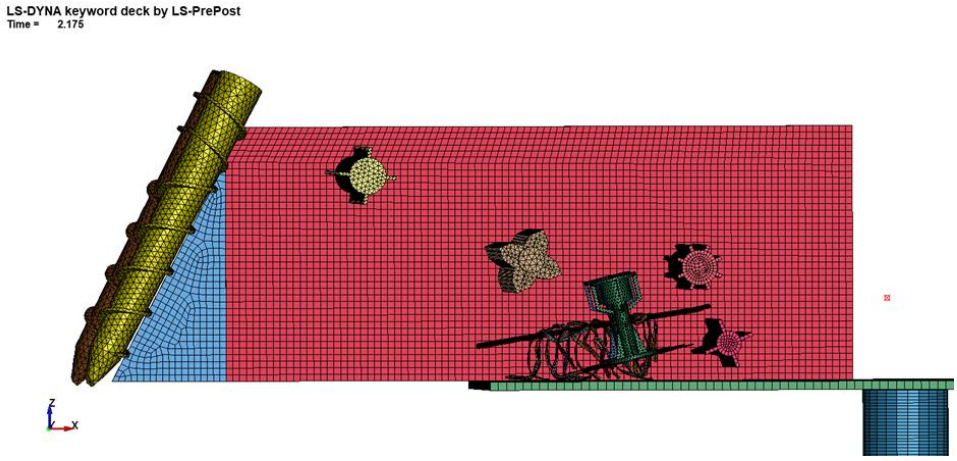

Figure 150: Model A results: stalk reaching gap between butt lifter and top feed roller.

The predictions look quite realistic and a good start. The spirals take little part in the simulation as the stalk and its leaves are in the middle between the spirals and there is little contact. The cane stalk is pushed, bent and broken at its base with the ground by the knockdown roller, as noted by Kroes (1996) and observed in Stream 1 field trials. The momentum of the cane stalk and the forward movement of the harvester allow the cane stalk to orientate with the basecutter opening and be fed through, reaching the butt lifter roller and the top feed roller. The finned roller is predicted to take little part in the feeding of this single stalk and leaves. In reality, the cane stalk and leaves will be supported and held back by the other stalks and leaves around it as the harvester moves through the location.

The current simulation shows that there is a significant horizontal distance between the spirals and the knockdown roller, and particularly between the knockdown roller and the finned roller, which seems to be significantly underutilized. The preliminary results provide a guide as to modifications that could be carried out to the geometry.

6.5.4. Simulation of spiral geometries with 45° and 63.5° sideways angle with the ground

The prediction of the stalks and leaves for the five stalk model traversing the spirals was carried out for two spiral geometries, 45° (Model C) and 63.5° (Model A) sideways angle with the ground. Figure 151 and Figure 152 and Figure 156 and Figure 157 show the stalk and leaves partway through the spirals for the 45° and 63.5° angles respectively. Figure 153 to Figure 155 and Figure 158 to Figure

160 show the predicted forces on the spirals for the 45° and 63.5° angles respectively, for three directions:

1. The harvester direction.
2. Force parallel to harvester width.
3. Force in the vertical direction.

The forces are difficult to interpret without comparison to other harvester speeds and spiral speeds. Overall, the 45° spirals are predicted to provide higher positive forces in the harvester direction, and interestingly in the vertical direction. If it is assumed that higher positive forces will feed the cane better into the harvester, and also lift any cane lying down, then the 45° spirals' angle with the ground is predicted to provide better performance. Interestingly, both simulations show that the stalks and leaves in contact with the spirals are held back compared to the inner stalks, implying that the spirals are rotating too slowly for the current speed of the harvester.

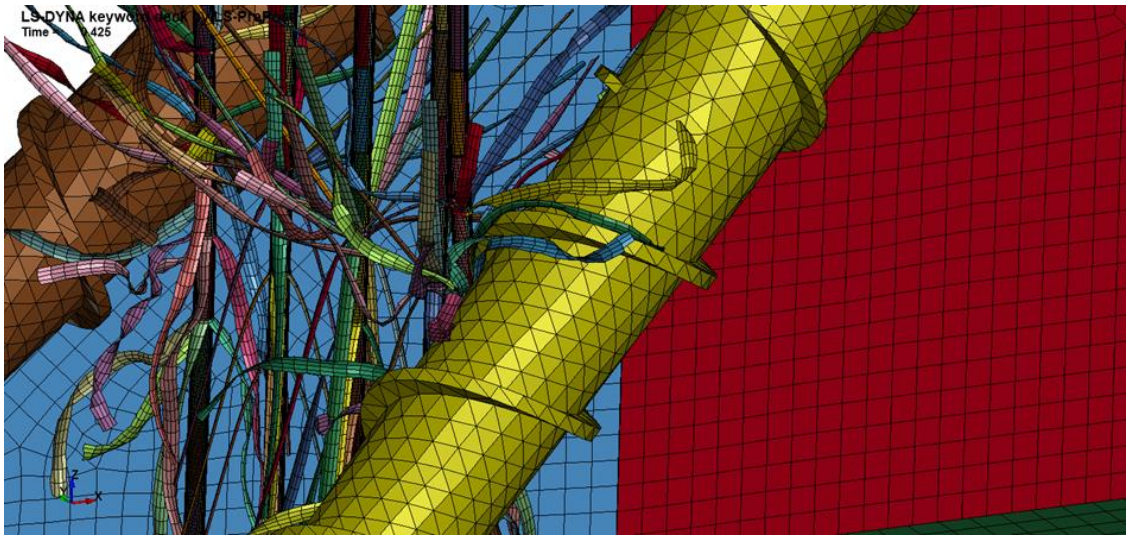

Figure 151: Model C - sideways spiral angle with ground of 45°– stalk and leaves along mid spirals.

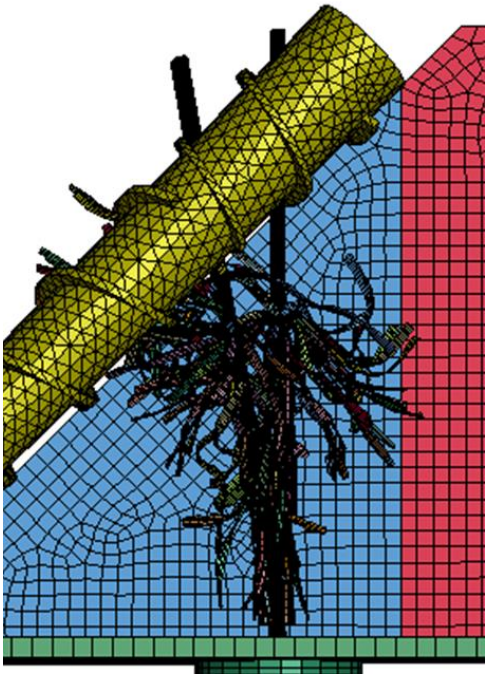

Figure 152: Model C- sideways spiral angle with ground of 45°– stalk and leaves passed spirals

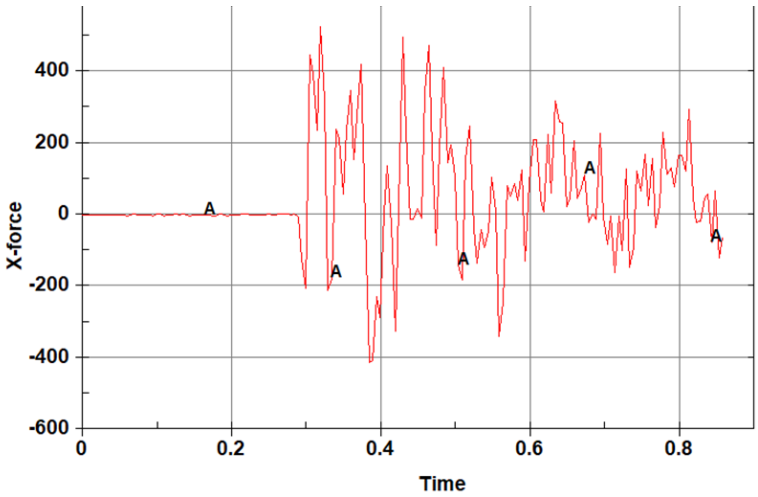

Figure 153: Model C- sideways spiral angle with ground of 45°– force (N) in harvester direction.

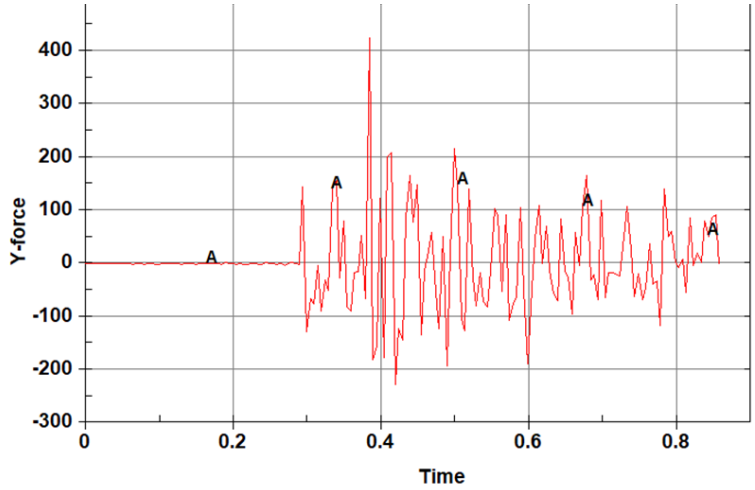

Figure 154: Model C – sideways spiral angle with ground of 45° - force (N) parallel to harvester width.

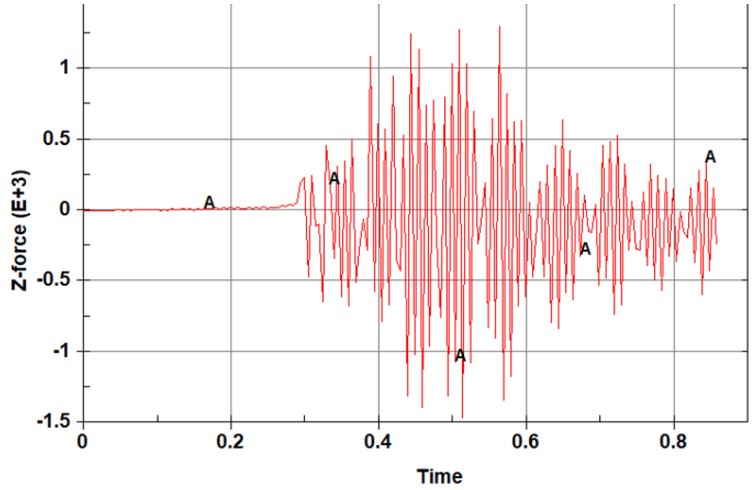

Figure 155: Model C – sideways spiral angle with ground of 45° - force (N) in the vertical direction.

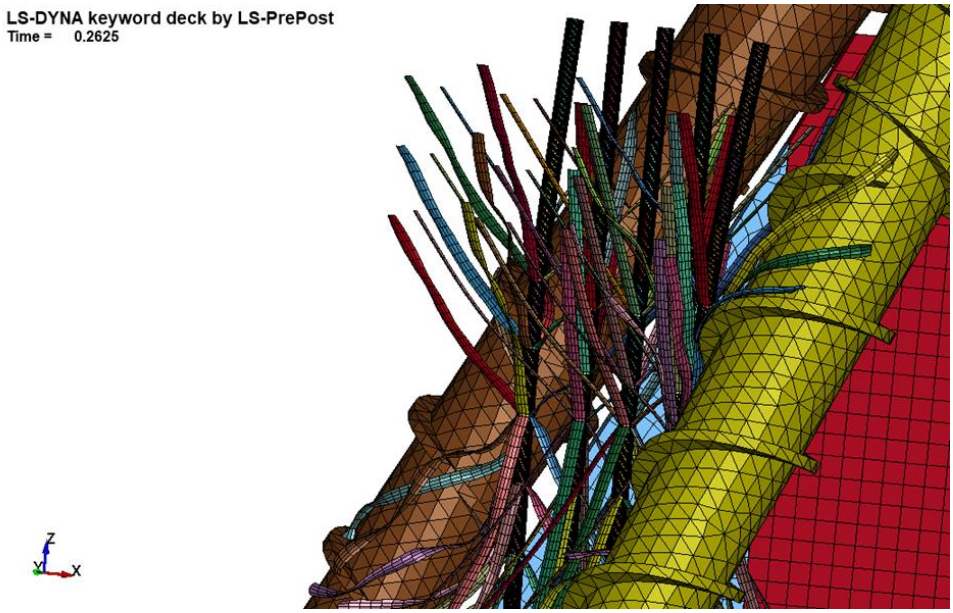

Figure 156: Model A - sideways spiral angle with ground of 63.5°– stalk and leaves along mid spirals.

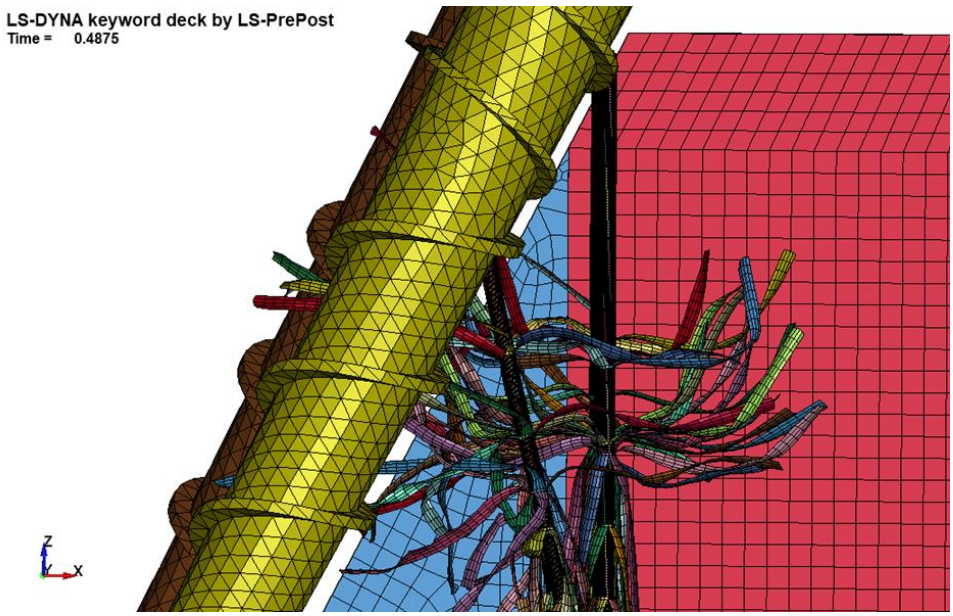

Figure 157: Model A - sideways spiral angle with ground of 63.5°– stalk and leaves passed spirals.

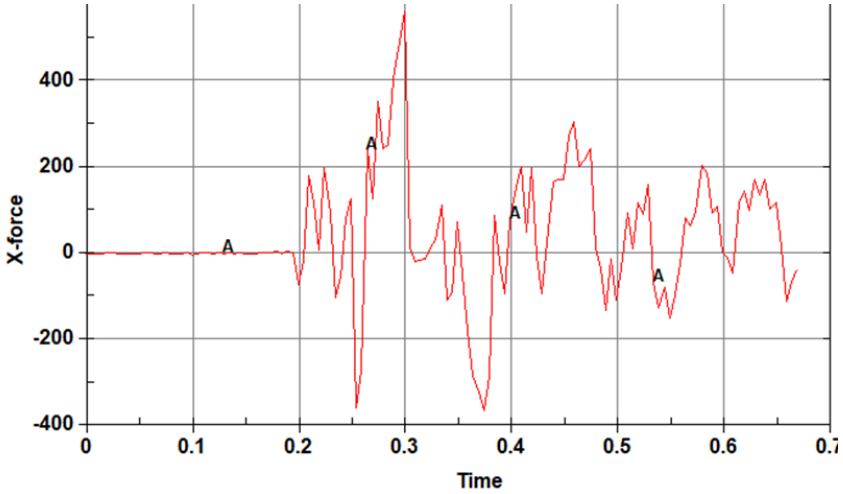

Figure 158: Model A - sideways spiral angle with ground of 63.5°– force (N) in harvester direction.

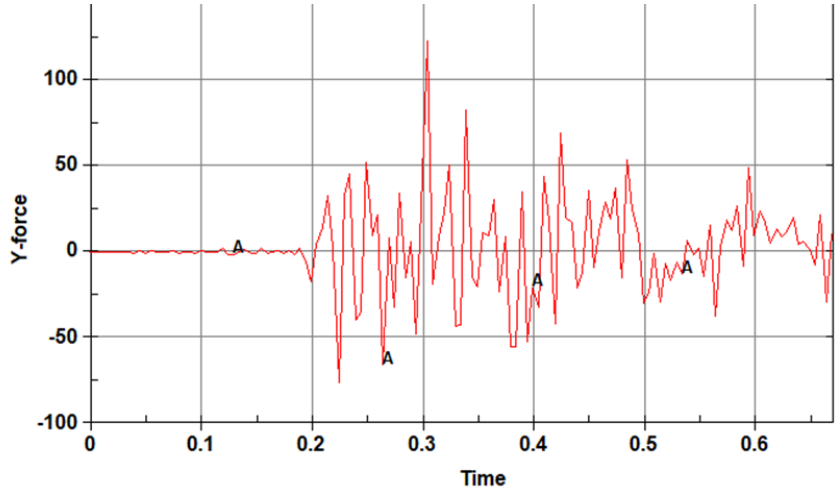

Figure 159: Model A – sideways spiral angle with ground of 63.5° - force (N) parallel to harvester width.

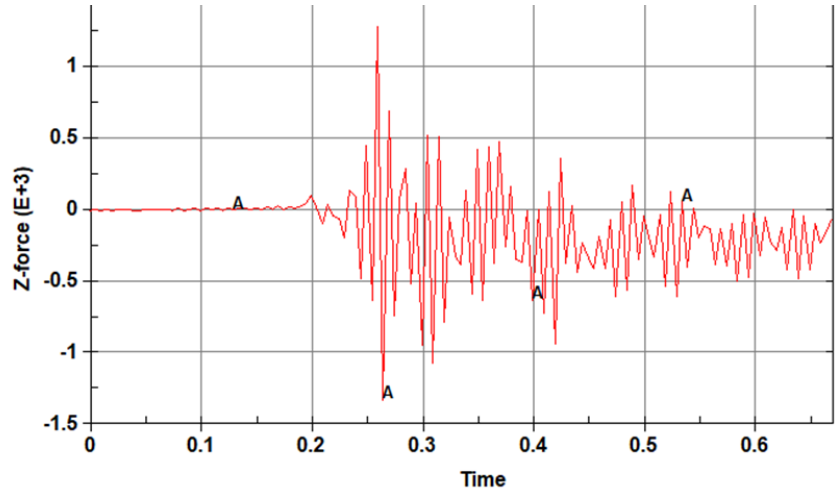

Figure 160: Model A – sideways spiral angle with ground of 63.5° - force (N) in the vertical direction.

6.5.5. Simulation of single stalk with harvester geometry F

Predictions for the simulation with a single stalk and geometry F, which has an spiral angle with the ground at 45°, the knockdown roller moved horizontally towards the finned roller, and the harvester shortened in the horizontal direction, are described in this section.

The series Figure 161 through Figure 167 shows the modelled progress of a stalk of cane from first contact with the harvester until the stalk enters the feed train.

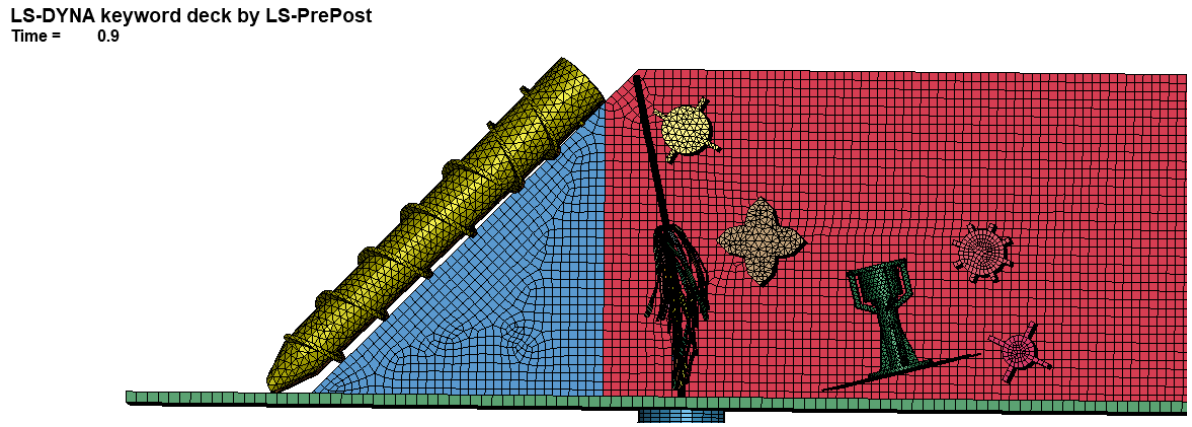

Figure 161: Geometry Model F: stalk contacting knockdown roller.

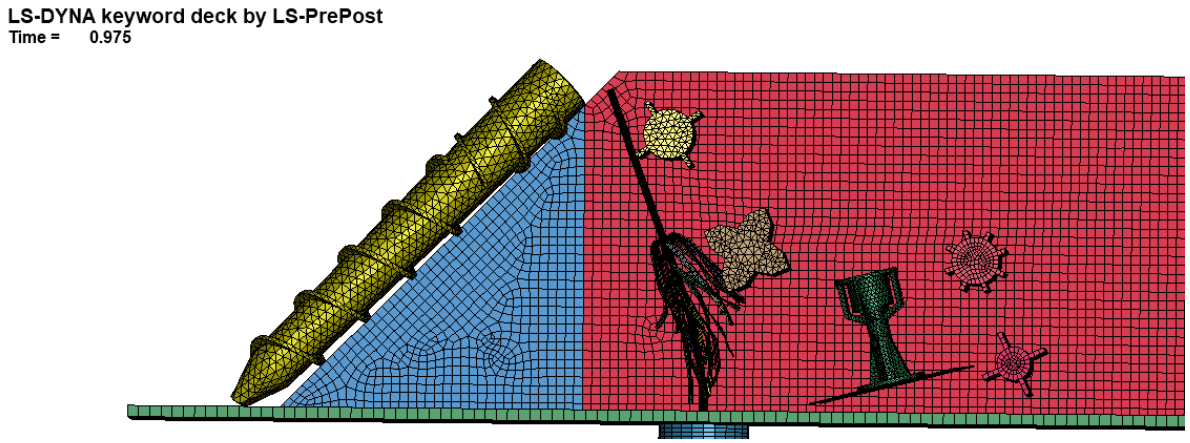

Figure 162: Geometry Model F: stalk being pushed over by knockdown roller, leaves contacting finned roller.

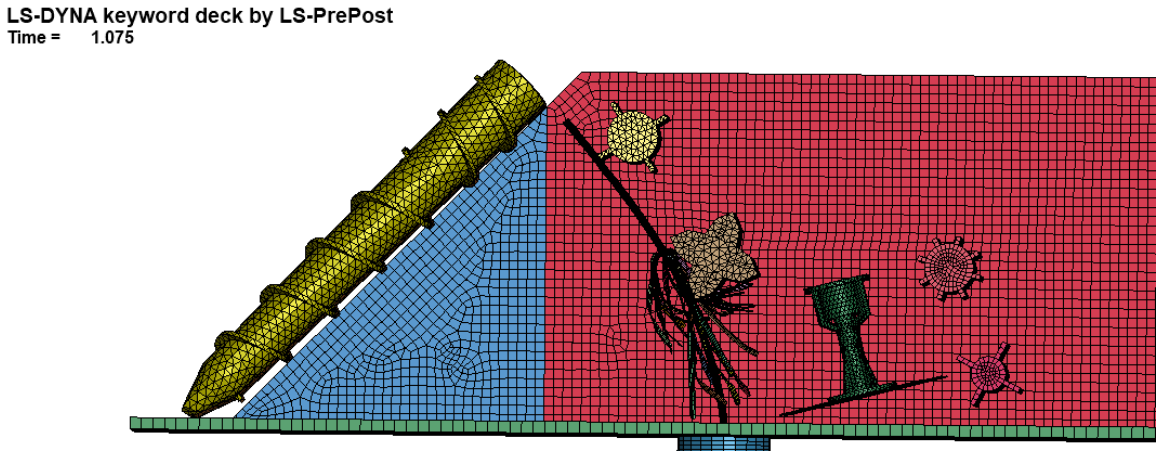

Figure 163: Geometry Model F: stalk being broken at bottom by knockdown roller and finned roller.

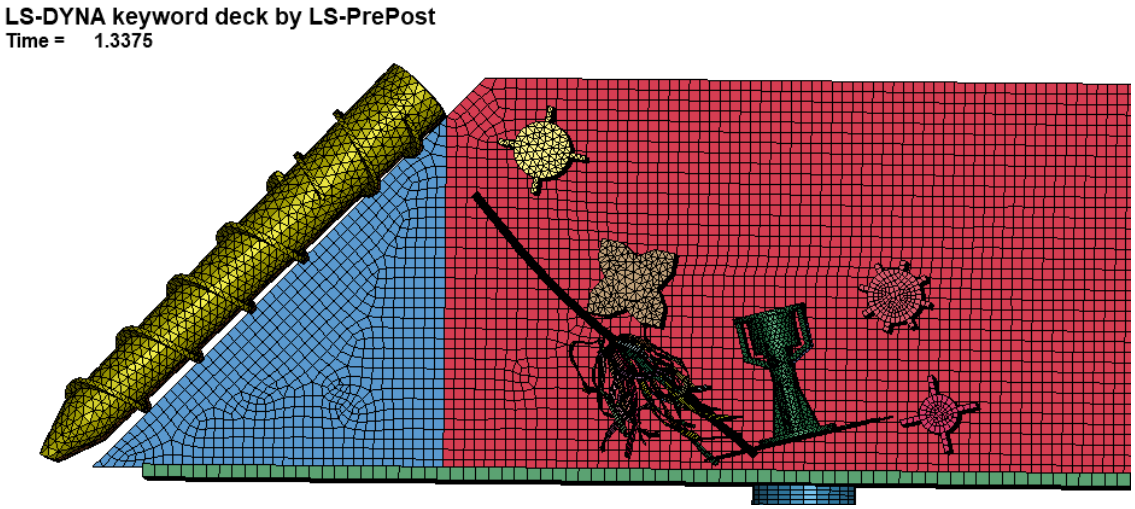

Figure 164: Geometry Model F: stalk falling and rotating, still in contact with finned roller, with bottom part of stalk entering basecutter area.

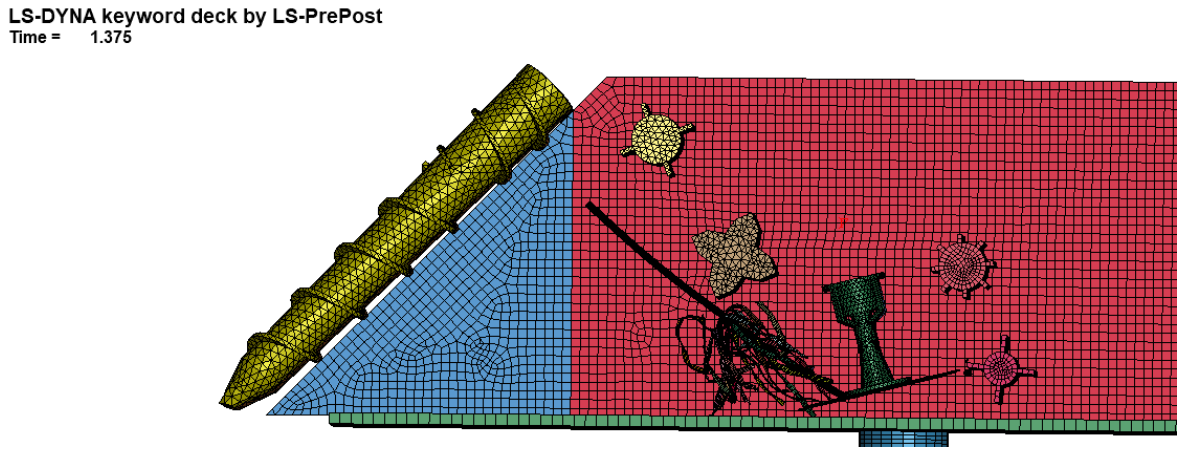

Figure 165: Geometry Model F: stalk continuing to fall and rotate, feeding through basecutter area, with a small part of the bottom stalk being cut off and bouncing just underneath butt lifter roller.

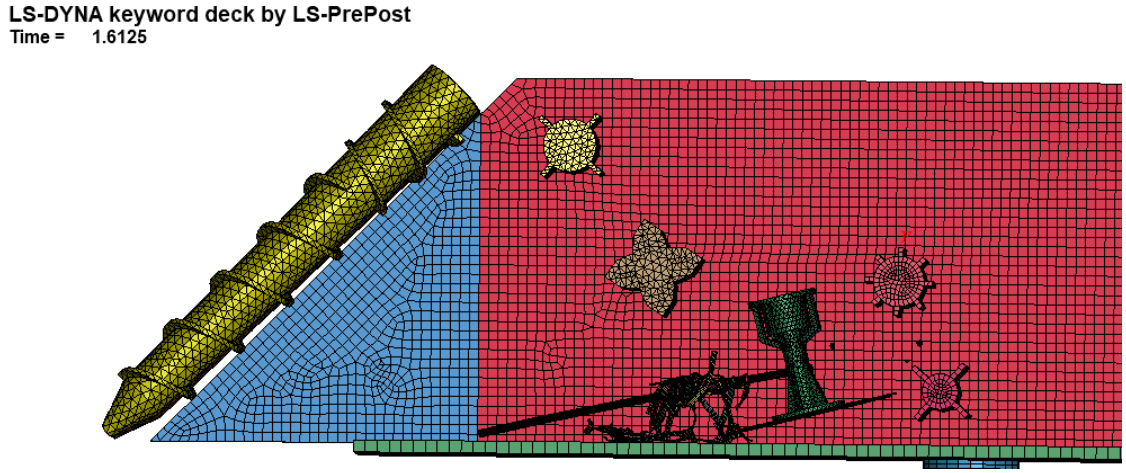

Figure 166: Geometry Model F: stalk continuing to fall and rotate, feeding through basecutter throat area.

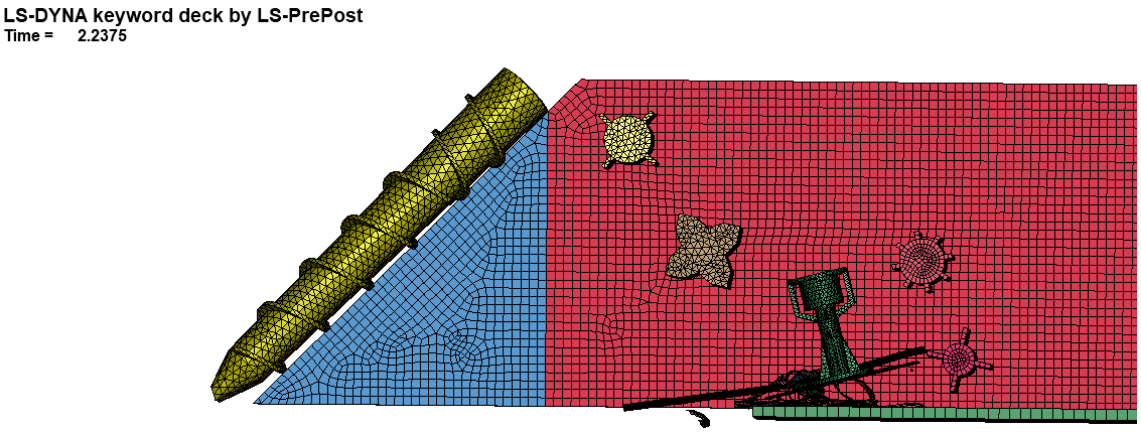

Figure 167: Geometry Model F: stalk continuing to fall and rotate, feeding through basecutter area and contacting butt lifter roller.

It is shown that, compared with the starting geometry (geometry model A), the geometry of model F allows the knockdown roller and the finned roller to work more interactively in feeding the stalk through into the basecutter area. The reduced length of the harvester in this location should reduce the friction of the cane stalks and leaves on the sidewalls as the contact area is reduced. The cane stalk is still predicted to break at the bottom before the basecutter blades reach it, therefore there is further scope to improve the geometry and operating parameters for the knockdown roller, finned roller and basecutters to achieve bending without breaking, cutting of the stalks by the basecutter blades and subsequent feeding through the basecutter's throat. It is also concluded that the harvester described in model A can be shortened by approximately 1.2 m.

7. CONCLUSIONS

The primary finding from the research program is that very high levels of damage to the cane stool are associated with current harvesting technology and practices. This is clearly reducing the economic ratoon cycle length at very significant industry cost.

Assuming no indirect damage from wheel traffic and similar sources, the primary sources of damage to the cane stool are associated with:

- The gathering and feeding processes involved in aligning and feeding the cane crop into the harvester (tension and rotation of the stalk);
- The pre-loading (knockdown) of the cane stalks to achieve feed across the basecutters and into the harvester feedtrain; and
- The damage associated with the severing of the cane stalk (basecutting).

The relative damage caused by each of these functions relates to both crop and field characteristics and the way the cane stalk is manipulated by the front end of the harvester. One issue is that whilst the operating speed of the harvester can vary by up to a factor of five, all the gathering and feeding components as well as the stalk severing system (basecutters) operate at constant speed.

Based on previous research and the changes in harvesting practices since then, the initial hypothesis of the project was that, by linking the tip speed of the forward feed components of the harvester to groundspeed in some optimal relationship, damage to the cane stalk and stool should be able to be minimised. Similarly, based on the research by Kroes, it should be possible to minimise stalk damage during basecutting by optimising basecutter speed.

It was further hypothesised that improved understanding of machine-cane interactions would then allow significant further advances in component design and, therefore, machine performance.

The trials at the six project trial sites identified that typically fewer than 25% of the stumps remaining after harvest have minimal or low levels of damage, and typically over 50% have severe damage. In some situations, average damage levels exceeded 95%.

Reducing harvesting speed in isolation had no repeatable beneficial effect, which was consistent with the results of other recent research. Some advantage was initially achieved by modulating the speed of forward-feed components in conjunction with lower groundspeeds, and it was believed that this effect was achieved because the high contact speeds of the forward-feed rollers were “driving” the stalks into the machine throat, probably causing compression or buckling failure of stalks close to the ground just prior to basecutting. The lack of response to reducing groundspeed alone is, as noted, consistent with other recent research. The research conducted by Hurney *et al.* (2005) where responses to groundspeed were quantified was conducted with “earlier generation” harvesters. These machines had less aggressive “front end” setup, and as such inherent damage caused by the feeding process was probably lower. Results presented by Hurney on basecutter blade sharpness trials indicated “undamaged” stumps as typically around 50% with sharp blades. In no trials in this program, with the standard harvester configuration (and sharp blades), were levels of damage this low recorded.

Early results did, however, indicate that shoot counts alone are a poor indicator of ratoon performance, and that shoot vigour and biomass is a much better determinant.

To better understand the causes of the very high levels of damage being suffered by the crop during harvest, a strategy was adopted of manually pre-cutting sub-plots at a height which allowed full

interaction between the basecutters and the cane stalk but eliminated potential for contact with the forward feed components. This was achieved by hand-cutting the sub-plots at a height of approximately 200-250mm above ground level prior to machine harvesting.

The trials then demonstrated an approximate halving of major damage to the plant stumps. These plots registered lower emerged plant shoot counts but higher average plant biomass. This followed through to yield, where the average increase in yield achieved by the pre-hand-cut plots averaged 16%.

Clearly, whilst very significant damage to the stool is inflicted by the gathering and knockdown functions, damage by the basecutters is still substantial. It appears that it is possible to model the complex interactions between the plant and the harvester components and functions to a usable degree of representivity.

Key observations hold over the wide range of trial conditions, however there is significant variation in magnitude. It is considered likely that a large part of this variability could be explained by field/crop conditions with further work. Understanding the causes of this variation may allow some mitigation of the observed losses (farming systems) while waiting for longer term measures to develop (harvester design).

8. RECOMMENDATIONS FOR FURTHER RD&A

The project established that both that the gathering and knockdown functions of the harvester are responsible for large but variable negative impacts on subsequent ratoon growth and yield, and that the changes in harvesting speed or relative speed of “front end” harvester components did not appear to have a consistent or large impact on ratoon yield. As such, while modest improvements in ratoon yield may be achievable under some conditions by altering harvester speed and forward feed component speeds, much greater gains stand to be achieved by altering machine design to enhance the machine-crop interactions and reduce damage to both the cane stalk being harvested and to the ratooning stool. Such modifications, in conjunction with speed control on key components could also be anticipated to enhance machine functional performance under a wider range of harvesting conditions. The synergy of modifications to the design of the gathering system and linking speeds to groundspeed has been well demonstrated on an operational scale.

Given the potential gains achievable by overcoming the observed negative impact on ratoon yield by the current harvester design, it is suggested that overcoming this challenge is worthy of significant further investment.

The two primary areas thought to give greatest potential benefit are:

- Developing a better understanding of the factors behind the wide variation in observed yield reduction between trial sites, with the goal of identifying strategies to minimise ratoon yield reduction through farming system changes; and
- Further work on harvester design to minimise the aggressiveness of the knockdown geometry, whilst maintaining or enhancing ability to gather and feed difficult crops.

There is not yet sufficient data to explain the variation in ratoon yield reduction with any certainty, however some degree of the variation could plausibly be explained by observed differences between the trial sites and varieties. Of relevance also was the finding that Q 240, a nominally brittle variety which was expected to suffer major damage generally suffered lower damage than the thinner

varieties. If this hypothesis stands, it is likely that harvester-induced yield reduction could be reduced with farming system changes.

Promising reductions in knockdown damage were achieved with relatively minor modifications to an existing harvester, and while significant further work would be required to develop a robust and reliable retrofittable solution, there are no foreseeable impediments to the development of a modification kit that can be commercialised within the Australian industry. This could be anticipated to very positively impact on ratoon performance relative to the results with modern harvesters.

9. PUBLICATIONS

Two publications have arisen from this work to date:

- Norris CP, Whiteing C, Norris SC (2020) Machine-cane interactions: what is the impact of 'front-end' design and harvester operation on product quality and crop ratooning? Proc. Aust. Soc. Sugar Cane Technol. (in press)
- https://sugarresearch.com.au/caneclip/caneclip-front-end-harvester-components/

10. ACKNOWLEDGEMENTS

The success of the project was made possible by the generous assistance of a number of people outside the immediate project team. Both NorrisECT and QUT would firstly like to acknowledge the key roles of Sugar Research Australia, the Queensland University of Technology and the Commonwealth Department of Agriculture, Water and the Environment for their key roles in funding the project.

On an operational level, NorrisECT would like to acknowledge the following groups and people whose assistance made the project possible:

- Mr Mark North of Jaistand Pty Ltd (North Farms),
- Mr Dave Bartlett, Mr Matt Cattrell and the team at Tweed Valley Harvesting and Citifarms in NSW,
- Mr Pat Halpin and the team at Central Harvesting, Isis,
- Mr Mark Mammino of Isis,
- Mr Bruce Petersen of Isis,
- Mr Greg Chiesa and the team at SJC Harvesting, Ingham,
- The team at Pace Farming, Bambaroo, Ingham,
- Mr Josh Keith and team of Rocky Point Harvesting
- The team at Wilmar Mona Park.

QUT would like to acknowledge the contribution of Phil Hobson as one of the original chief investigators, the assistance of Jindong Yang from LEAP Australia for crucial information and assistance with LS-DYNA modelling tasks, and the Queensland University of Technology eResearch Office for computational resources and services.

11. REFERENCES

Anon., 2004. *Manual for LS_Dyna: Soil Material Model 147. Publication No. FHWA-HRT-04-095.* s.l.:USDepartment of Transportation.

Anon., 2005. *Evaluation of LS_Dyna Wood material model 143. Publication No FHWA-HRT-04-096.* s.l.:US Department of Transportation.

Anon., 2007. *Manual for LS_Dyna: Wood Material Model 143. Publication No FHWA-HRT-04-097.* s.l.:US Department of Transportation.

Anon., 2017. *LS-Dyna Keywords user's manual Volume II: Material Models..* s.l.:Livermore Software Technology Corporation.

Anon, 2014. *Harvesting Best Practice Manual.* Brisbane: Sugar Research Australia, Limited; Technical Publication MN14001.

Caldere Dominguez, M. A. & Norris, C. P., 2018. Measuring and Managing the Losses Associated with Machine Harvesting: The experience at San Antonio. *South American Sugar Technologists Association Conference.*

Chapman, L. S., 1988. Constraints to production in ratoon crops. *Proc. Aust. Soc. Sugar Cane Technol. 10, 189-192.*

Davis, R. J. & Norris, C. P., 2000. *Improved feeding of green cane by harvesters. Final Report Project BSS165,* s.l.: BSES.

Davis, R. J. & Norris, C. P., 2002. Harvester front end performance: Is aggressive feeding essential for reliable operation?. *Proc. Aust. Soc. Sugar Cane Technol. 24, 190-198.*

Davis, R. J. & Schembri, M. G., 2004. Enhancing harvester forward-feeding performance: An exercisein optimising machine-cop interactions.. *Proc. Aust. Soc. Sugar Cane Technol. 26.*

Di Bella, L., Thiedeke, C. & Norris, C. P., 1997. *Report on extension and filed research program to reduce soil in the cane supply. BSES Internal report.,* s.l.: BSES.

Fuelling, T. G., 1980. Performance testing of chopper cane harcesters for cane quality. *ISSCT Conference Proceedings,* pp. 825-836.

Handong, H. et al., 2011. Finite element simulation of sugaecane cutting process. *Transactions od the CSAE,* Volume 161.

Harris, H. & da Cunah Mello, R., 1999. Kinematics, blade shapes and edges for alternative basecutter configurations. *Proc. Aust. Soc. Sugar Cane Technol. 11, 185-190.*

Hurney, A. P., Croft, B. J., Grace, D. & Richards, D. R., 2005. *Influence od harvester basecutters on ratooning of sugarcane. Final report BS81S,* s.l.: BSES.

Kroes, S., 1996. Cane loss due to basecutter and knockdown damage. *Proc. Aust. Soc. Sugar Cane Technol. 19, 155-161.*

Kroes, S., 1996. *The cutting of sugarcane. PhD Thesis.,* Toowoomba: University of Southern Qld.

Kroes, S., 1997. *The cutting of sugarcane,* Toowomba: University of Southern Qld.

Kroes, S. & Harris, H., 1994. Effects of harvester basecutter parameters on the quality of cut.. *Proc. Aust. Soc. Sugar Cane Technol. 16, 169-177.*

Kroes, S. & Harris, H., 1996. Knockdown causes major damage to cane during harvesting.. *Proc. Aust. Soc. Sugar Cane Technol. 18, 137-144.*

Kroes, S. & Harris, H. D., 1997. The optimum harvester forward speed.. *Proc. Aust. Soc. Sugar Cane Technol. 19, 147-154.*

Larsen, P. L., Patane, P. A. & Asamoah, I., 2017. Benchmarking Cane Supply Quality in the Herbert, Burdekin, Proserpine and Plane Creek Regions.. *Proc. Aust. Soc. Sugar Cane Technol. 39, 77-88.*

Larsson, J., Domanti, S. A. & Loghran, J. G., 1997. Numerical modelling of the communition of sugar cane billets.. *Proc. Aust. Soc. Sugar Cane Technol. 19, 350-359.*

Lenarts, B. et al., 2014. Simulation of grain-straw separation vy Discrete Element Modelling with bendable straw particles.. *Computers and Electronics in Agriculture, 101, 24-33..*

MacAdam, J. W. & Mayland, H. F., 2003. *The relationship of leaf strength to cattle preference in tall fescue cultivars.,* s.l.: Forages.

McBean, I. & Rose, P., 2017. *Improving idustry returns through harvest best practice: Sugar Research Australia, Final Report 2014/091,* s.l.: Sugar Research Australia.

Milla, R., 2017. *Understanding the effects od harvester speed on subsequent ratoon performance in the Burdekin: final report project 2014/092,* Brisbane: Sugar Research Australia, Limited.

Norris, C. P., Davis, R. H. & Poulsen, L. S., 1998. An investigation into the feeding of lodged green cane by harvesters.. *Proc. Aust. Soc. Sugar Cane Technol. 20, 224-231.*

Norris, C. P., Landers, G. L. & Norris, S. C., 2015. Successful adoptionod machine harvesting: Managing the challenges. *Presentation to ISSCT Agricultural Engineering and Agronomy Workshop, Durban, South Africa.*

Plaza, F. & Hobson, P. A., 2011. *Evaluation of EDEM software for modelling pneumatic cane cleaning. Project No 5878-3886-04 Technical Report 2/11,* s.l.: s.n.

Popov, E. P., 1978. *Mechanics of materials.* 2nd ed. s.l.:Prentice-Hall Inc.

Schembri, M. & Garson, C. A., 1996. Gathering of green cane by harvesters: a first study.. *Proc. Aust. Soc. Sugar Cane Technol. 18, 145-151.*

Schembri, M. G. & Harris, H. D., 1998. Examining the effectiveness of smashing cane by impact loading in the shredder.. *Proc. Aust. Soc. Sugar Cane Technol. 20, 340-348.*

Spargo, R. F. & Baxter, S. W. D., 1974. The development of the Australian chopped cane sugar cane harvester.. *Proc of American Society of Agricultural Engineers (Winter Meeting) Paper 74-15-25.*

Tijskens, E., Ramon, H. & De Baerdemaeker, J., 2003. Discrete elemnt modellingfor process simulation in agriculture.. *Journal of Sound and Vibration,* Volume 266, pp. 493-514.

Ucgul, M., Fielke, J. M. & Saunders, C., 2015. *Defining the effect of sweep tillage tool cutting edge.,* s.l.: s.n.

Whiteing, C. & Kingston, G., 2008. *Regional adoption of alternative harvester confiugrations for sustinable harvesting efficiency. Final Report SRD Project BSS270,* s.l.: Sugar Research Australia..

12. APPENDIX

12.1. Appendix 1 METADATA DISCLOSURE

Table 46 Metadata disclosure 1

Data	Project data
Stored Location	QUT – RDSS (Research Data Storage Service) in the Projects\sef\ctcb\sri\Projects folder for Project 4306, or Projects\sef\cab\sri\Projects folder for Project 4306
Access	Restricted; QUT's CAB Bioprocessing staff with access to the Projects folder
Contact	Floren Plaza – Senior Research Fellow

Table 47 Metadata disclosure 2

Data	Project data
Stored Location	NorrisECT Sharepoint common document library
Access	Internal only.
Contact	Stuart Norris